

Abstract book



16th Biometal
25-30 August, 2024

FOREST HOTEL • KRAKÓW, POLAND



16th Biometal

25-30 August, 2024

FOREST HOTEL • KRAKÓW, POLAND



Symposium Co – chairs:

Diego Mantovani
Laval University, Canada

Frank Witte
Berlin Charité, Germany

Magdalena Bieda – Niemiec
Polish Academy of Sciences, Poland

Abstract book committee:

Vinicius Sales
Laval University, Canada

Alexis Levasseur
Conferium

Abdelhakim Cherqaoui
Laval University, Canada

Carlos Henrique Michelin Beraldo
Laval University, Canada



北京大学
PEKING UNIVERSITY





**medical
magnesium**



UNIPRESS EXTRUSION
Sp. z o. o.

innosys

Medical and Smart Solution

Cooperating Organizations



Institute of Metallurgy and Materials Science
Polish Academy of Sciences



| 주 | 아 이 메 디 텍
International Medical Technology



UNIVERSITÉ
LAVAL



北京大學
PEKING UNIVERSITY



Metals

Monday, August 26th, 2024



Moments of Inertia

B. Wiese¹, F. Witte², P. Maier^{3,4}, N. Hort^{1,5}

¹Helmholtz-Zentrum Hereon, Geesthacht, Germany; ²Charité Universitätsmedizin, Berlin, Germany;

³University of Applied Sciences Stralsund, Stralsund, Germany; ⁴Lund University, Lund, Sweden;

⁵Leuphana University Lüneburg, Lüneburg, Germany

INTRODUCTION: While developing materials for degradable implants based on magnesium, we have given a special regard to mechanical properties (incl. Young's modulus E) and degradation rates over decades. These are indeed crucial and important properties. They are influenced by chemical composition, microstructural features like intermetallic phases, grain size etc. Additionally, the different processing steps (casting / solidification, heat treatments, wrought processing, machining etc.) also have impact. However, numerous implants and medical devices are rods with a high aspect ratio (length l to area of cross section A) like needles, nails, K-wires, clips, cannulas etc.

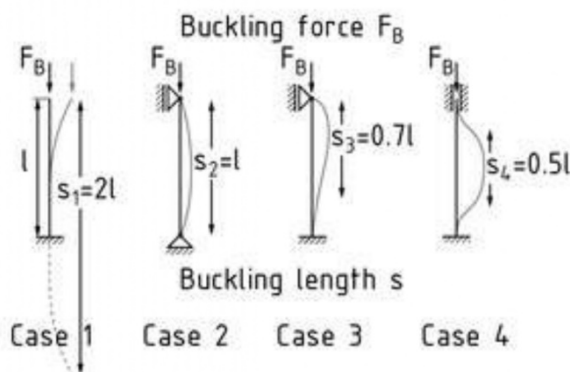


Figure 1: The Euler cases^{1,2}

For these types of devices, it is also about geometry and therefore about moments of inertia as reported by Euler and standard textbooks regarding civil engineering^{1,2}. The four Euler cases (figure 1) describe the buckling behaviour of a straight, slim rod with a length l which is under vertical compressive load F_B . The buckling length s is the length under which catastrophic fracture can occur when the fracture force F_B exceeds the strength of the material.

$$F_B = \frac{\pi^2 EI}{s^2} = \frac{\pi^3 E r^4}{r^4} \quad I = \frac{\pi r^4}{4}$$

Equation 1: buckling force F_B

Equation 2: moment of inertia I of a round rod²

$$\sigma_B = \frac{F_B}{A} = \frac{\pi^2 E r^2}{l^4}$$

Equation 3: buckling strength σ_B of a round rod²

Application: As an example, let us take a nail. Compressive strength, Young's modulus E and the length l (25 mm) of the nail are known. We also

assume a round cross section area with a radius r of 2.5 mm as well as the nail is straight and not bent. In this case we can easily calculate the buckling force F_B (equation 1) by using the moment of inertia I (equation 2)². If needed the buckling strength σ_B can also easily be determined (equation 3). A surgeon most likely grasps the nail at the end and the nail touches the bone at the other end. The nail is inserted into the bone and slightly fixed by the bone. For a straight nail this is described by the Euler case 4 (figure 1).

We can now compare a steel nail with a Mg nail. For steel (316L³) we assume $E = 190$ GPa and a compressive strength of 170 MPa and for Mg (WE43⁴) $E = 45$ GPa and a compressive strength of 250 MPa. However, for this calculation (see table 1 for buckling force and strength) the knowledge of the compressive strengths of the materials is not really necessary but still useful.

Table 1: Buckling force & strength of steel and Mg

Material	F_B	σ_B
Steel (316L ³)	3.68 kN	187.5 MPa
Mg (WE43 ⁴)	0.87 kN	44.4 MPa

SUMMARY: For achieving the same fracture force, it would be necessary to increase the diameter of the Mg nail drastically. If this is acceptable, ok. If still a small diameter is needed it is impossible to use Mg and its alloys for this type of application. This consideration should come latest at the time when it is clear which application is planned. Moreover, similar considerations can be made for almost any type of application, maybe using FEM approaches for more complex load cases⁵.

REFERENCES: ¹L. Euler (1744) Methodus inveniendi lineas curvas maximi minimive proprietate gaudentes, sive, Solutio problematis isoperimetrici latissimo sensu accepti, Apud Marcum-Michaellem Bousquet & Socios, Geneva. ²W.F. Chen, J.Y.R. Chen (2003), *The Civil Engineering Handbook – 2nd edition*, CRC Press. ³<https://www.farnell.com/datasheets/26035.pdf>. ⁴D. Dvorsky et al. (2021) Microstructure, Mechanical, Corrosion, and Ignition Properties of WE43 Alloy Prepared by Different Processes, *Metals*, 11(5), 728. ⁵G.S. Nayak et al. (2024) Influence of implant base material on secondary bone healing: an in silico study, *Comput Methods Biomech Biomed Engin* 13 (2024) 1-9, 10.1080/10255842.2024.2338121.



Hall-Petch effect in ultrafine-grained bioresorbable Zn

M Balog¹, P Križik¹, A Školáková², P Švec Jr³, J Kubásek⁴, J Pinc², M Takáčová⁵, M M de Castro¹, R Figueiredo⁶

¹Institute of Materials and Machine Mechanics, SAS, Slovakia. ²Institute of Physics, ASCR, Czech Rep. ³Institute of Physics, Slovak Academy of Sciences, Slovakia. ⁴University of Chemistry and Technology, Czech Rep. ⁵Biomedical Research Center, Institute of Virology, SAS, Slovakia. ⁶Universidade Federal de Minas Gerais, Brazil.

INTRODUCTION: The selected Zn alloys meet rather challenging standards for applications of endovascular stents (ES) and orthopedic internal fixators (OIF). However, presence of the alloying elements may lead to numerous problems e.g., the natural overaging of precipitates, heterogeneous corrosion, detrimental *in-vitro* response e.g., an increase in inflammation, a decrease in biocompatibility, etc. The problems associated with a presence of the alloying elements are omitted for pure Zn. Refinement of Zn grain structure by cold/hot working leads to increased strength accompanied with reasonably high ductility by the grain boundary (GB) mediated, so-called Hall-Petch (H-P), strengthening. Though, as a result of a low recrystallization temperature of Zn, highly strained Zn structures experience dynamic (and static) recrystallization (DRX) followed by extensive grain growth. It prevents formation of severely refined ultrafine-grained (UFG) Zn, which could benefit more significantly from H-P strengthening. Additionally, refined Zn structures undergo changes related to grain structure regeneration at the room (RT) or human body temperatures, accompanied with a strength decrease. Therefore, refined pure Zn reaches relatively low, substandard strengths. In our leading study we proposed an efficient GB stabilization in UFG Zn by *in-situ* nano ZnO by Zener pinning action [1]. The model Zn+4.75vol% ZnO composite showed the superior and stable mechanical properties than those reported for pure Zn materials. The utilized stabilization concept didn't compromise corrosion and biological responses. In the present work H-P relation was assessed experimentally for UFG Zn in the strength-grain size region, which has remained unexplored up to now. The effect of the intercept grain size (d_i) and ZnO content on the corrosion and *in-vitro* biological responses was elaborated.

METHODS: Three Zn bulk materials with d_i ranging from 0.61 to 1.11 μm , stabilized with 4.83-9.62vol% of nanoscale ZnO dispersoids were fabricated by powder metallurgy. HR-TEM, SEM, EDS and EBSD were used to describe the microstructure of the composites. A relation between 0.2% strain offset yield stress ($YS_{0.2}$) and

d_i was evaluated experimentally by tensile tests at RT. The experimental data were compared to a theoretical model for the deformation behaviour of UFG metals based on grain boundary sliding (GBS) through dislocation glide [2].

RESULTS&DISCUSSION&CONCLUSIONS:

The finest d_i of 0.61 μm , ever reported for unalloyed bulk Zn, was achieved. The highest $YS_{0.2}$ of 187.4 MPa, ever reported for unalloyed Zn, accompanied with a reasonable ductility of 8.5% was measured. The conventional linear H-P relation following $YS_{0.2} = 40.8 + 104.8 d_i^{-0.5}$ was confirmed in the d_i range of ~400–0.6 μm . A grain refinement softening in UFG region predicted by the theoretical GBS model was disproved by experimental data. This was attributed to stabilization of GB by nano-metric ZnO. The corrosion and *in-vitro* biological responses were not compromised by fine d_i and ZnO content, with advantage of uniform corrosion behaviour and a small bacteriostatic activity. From a practical point of view, the obtained data will be of help to design of new high-strength, especially bioresorbable, Zn-based materials.

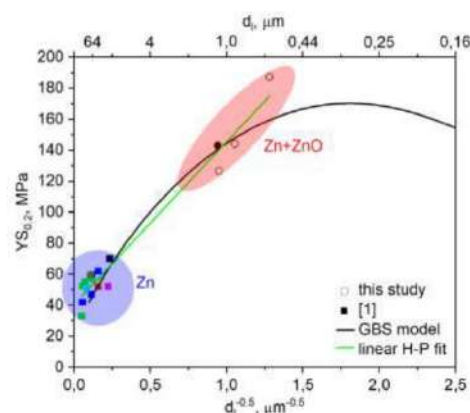


Fig. 1 H-P relation for pure Zn and Zn+ZnO materials compared to GBS theoretical model.

REFERENCES: ¹M Balog et al. (2023) *J. Mater. Res. Technol.* **25**: 4510. ²R B Figueiredo et al. (2023) *Prog. Mater. Sci.* **137**: 101131.

ACKNOWLEDGEMENTS: Supported by the APVV-20-0417, VEGA 2/0157/24 and ITMS 313021T081 projects and the Stefan Schwarz Support Fund.



Unique microstructural transformations during laser processing of a dual-phase Mg-Li alloy

F D'Elia¹, G Szakács², N Hort^{2,3}, C Persson¹

¹ *Division of Biomedical Engineering, Department of Materials Science and Engineering, Uppsala University, Uppsala, Sweden.* ² *Institute of Metallic Biomaterials, Department of Functional Magnesium Materials, Helmholtz-Zentrum Hereon, Geesthacht, Germany.* ³ *Institute of Product Technology and Systems, Leuphana University Lüneburg.*

INTRODUCTION: Magnesium-lithium (Mg-Li) alloys are unique given their dual-phase structure (HCP α -Mg, BCC β -Li), with formation of a BCC at Li contents above 11.7wt.%. This enables improved formability, and as such, much of the focus on these alloys has been on component design for structural applications. Of late, however, there is a growing interest in Mg-Li alloys for degradable implants. This is spurred by improved corrosion resistance through formation of a Li_2O_3 protective film¹, good biocompatibility², and potential for Li to lower the elastic modulus of Mg, which further reduces the risk for stress shielding. Central to these properties is the design of microstructure, primarily dictated by alloy chemistry and process conditions. In this research, we investigate the underlying effect of rapid solidification on microstructure formation in a dual-phase ($\alpha+\beta$) Mg-Li alloy. We hypothesize that the combination of dual crystal structure and controlled processing will allow for unprecedented tailoring of microstructure, ultimately leading to improved control of material properties.

METHODS: An $\alpha+\beta$ Mg-6(wt.%)Li alloy was prepared by mixing pure Mg and a Mg-12wt.% Li master alloy in a vacuum furnace prior to casting into a steel mould. Cylindrical plates were then sectioned from the cast ingots and used as substrates in an EOS M100 laser-powder bed fusion (L-PBF) machine (EOS GmbH, Germany), where laser tracks were deposited at a constant speed of 80 mm/s and at powers ranging from 15 to 100W. In-depth microscopy (i.e., SEM, TEM) and nano-hardness measurements were carried out along the laser tracks to determine the potential for tailoring both microstructure and mechanical properties through cooling rate (i.e., laser power).

RESULTS: Microscopy along the melt pools revealed the prevalence of epitaxial nucleation at melt pool boundaries, followed by distinct microstructural transformations profoundly dependent on laser power. At 15W, a planar-cellular transition was observed (Fig. 1a), followed by a transformation to a cellular/dendritic morphology at 50W (Fig. 1b) and fine nano-lamellae at 65W (Fig.

1c). Further increase in laser power refined the lamellae thickness, which enabled an increase in nano-hardness. Characterisation of nano-lamellae by TEM confirmed the presence of amorphous Li (Fig. 1d) coupled with that of α -Mg.

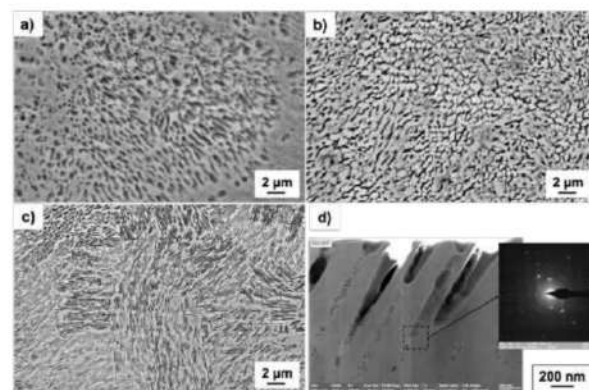


Fig. 1: Micrographs depicting melt pool microstructure at laser powers of a) 15W, b) 50W, and c) 65W, as well as d) the presence of amorphous Li in nano-lamellae microstructure.

DISCUSSION & CONCLUSIONS: Controlled rapid solidification demonstrates the ability to tailor microstructure in Mg-6Li alloy. Most significant is the formation of nano-scale lamellae consisting of layered HCP α -Mg and amorphous Li. Amorphous structure was likely induced by the high growth rate of α -Mg during coupled growth. The significance of such nano-lamellae for degradable implants is attributed to the potential for enhanced mechanical strength, as confirmed by the increase in nano-hardness, along with improved corrosion resistance due to amorphous Li structure. Future work seeks to characterise the corrosion properties and fabricate bulk microstructures using L-PBF.

REFERENCES: ¹ C.Q. Li, et al., (2018) *Electrochim. Acta* **260**:55-64. ² W.R. Zhou, et al. (2013) *Acta Biomater* **9**(10):8488-98.

ACKNOWLEDGEMENTS: The authors thank Dr. Olivier Donzel-Gargand of Uppsala University for TEM, and the EU (Marie Curie – 101110609), the Swedish Research Council (2021-04708), and VINNOVA (2019-00029; AM4Life) for funding.



Microstructure design strategy for biodegradable magnesium alloys based on mechanical and corrosion properties

Guangyin Yuan

School of Materials Science & Engineering, Shanghai Jiao Tong University, Shanghai China

E-mail: gyyuan@sjtu.edu.cn

INTRODUCTION: Simultaneously improving the strength, plasticity and corrosion properties has become the key to the wider clinical applications of Bio-Mg alloys. Besides the alloying technology, the microstructure optimization design is an effective method to improve the comprehensive properties of Mg alloys. However, it is not clear that what kind of microstructure can simultaneously improve the strength and corrosion properties of biomedical Mg alloys.

METHODS: Mg-Nd-Zn-Zr alloy (denoted as JDBM) was chosen as one candidate of the biodegradable vascular stent materials. The samples with three typical microstructures were prepared successfully, i.e., fine equiaxed grains, coarse equiaxed grains and bimodal microstructure. Mechanical properties and corrosion behaviors of these samples were studied to uncover the best microstructure design strategy, including grain size, distribution and orientation relationship.

RESULTS: As shown in Fig.1: 1) Compared with the samples with uniform fine or coarse grains, samples with bimodal microstructure exhibit the best mechanical properties (YS \approx 264 MPa, UTS \approx 274 MPa, EL \approx 17.93%) thanks to the combined effects of fine grains and coarse grains. However, the corrosion resistance is the worst due to the micro-galvanic corrosion between coarse and fine grains of the bimodal structure. 2) Samples with coarse equiaxed grains show a medium corrosion resistance of 0.30 mm/year and a strength-ductility of about 175 MPa (YS), 221 MPa (UTS), and 21.53% (EL). 3) Samples with fine equiaxed grains show the best corrosion resistance properties (0.17 mm/year) mainly due to the high-density grain boundaries. Besides, this sample shows a good strength-ductility balance (YS \approx 256 MPa, UTS \approx 266 MPa, and EL \approx 13.45%) based on grain refinement.

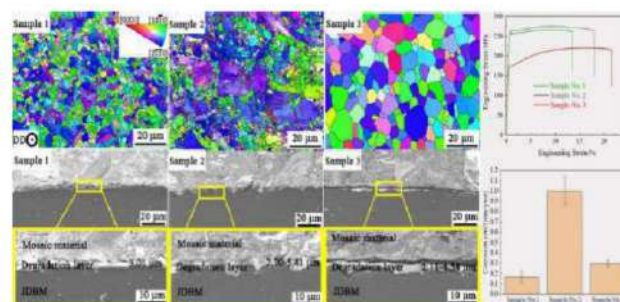


Fig.1: Three typical samples with different microstructure characteristic and their mechanical and corrosion properties.

DISCUSSION & CONCLUSIONS: The present findings will facilitate the researchers in optimizing their study strategy and achieving a better combination of mechanical and corrosion properties when designing and processing biodegradable Mg-based alloys. Samples with fine and uniform equiaxed grains are recommended in most cases for the application of biodegradable Mg alloys, which will provide excellent mechanical properties and corrosion resistance simultaneously.

REFERENCES: ¹X Wang, C Chen, LY Li, et al (2023), Corrosion Science, **221**:111366. ²X Wang, C Chen, BZ Miao, et al (2024), J.Mater.Sci.Technol.,**183**:165-174.

ACKNOWLEDGEMENTS: This work was supported by the National Natural Science Foundation of China (No. 52130104).



Additive manufacturing of a biodegradable MgZnCa alloy using Powder bed fusion – laser beam

Giulio Pietro Cavaliere^{1*}, Francesco D'Elia¹, Cecilia Persson¹

¹ Division of Biomedical Engineering, Department of Materials Science and Engineering, Uppsala University, Uppsala, Sweden

INTRODUCTION: Processing magnesium (Mg) alloys by additive manufacturing (AM) has the potential to fabricate patient-specific implants for healing large bone defects. However, AM-fabricated Mg alloys still continue to display increased corrosion rates that can severely compromise the mechanical integrity of the implant during the healing process. Additionally, the presence of rare earth elements (REEs) in e.g., biomedical WE43 Mg alloy, raises further concerns regarding both environmental and clinical aspects¹. To address these limitations, we aim to develop process parameters suitable for powder bed fusion – laser beam (PBF-LB), a metal AM technology, of a REE-free MgZnCa alloy, with the ultimate goal of understanding the effect of processing on microstructure.

METHODS: Gas atomized Mg₆₅Zn₃₀Ca₅ (at.%) powder (Nanoval GmbH) was used for printing on an Aconity Midi PBF-LB machine (Aconity 3D GmbH). Process parameter optimization included variations of laser power, scan speed, hatch distance, and scan strategy. Density measurements were conducted via image analysis and used to gauge optimal printing parameters. Microstructural characterization of the as-printed parts was performed using Back-Scattered Scanning Electron Microscopy (BS-SEM). Additionally, single laser tracks were investigated to understand the formation of microstructure in the melt pool as a function of processing and thermal history.

RESULTS: Parameter optimization enabled reduced porosity, achieving a density above 98%. Increasing the hatch spacing had a clear detrimental effect on density, as did using a no-rotation scan strategy. The microstructure was refined, but non-uniform due to variations in local thermal gradients along the specimen. A region with a slower cooling rate was identified in the sections of the melt pools that were subjected to multiple rescanning during the process. In these areas, the microstructure was composed of equiaxed MgCaZn grains, α -Mg dendrites, and a lamellar structure of eutectic composition (Figure 1). In contrast, the higher cooling rate regions, not rescanned during the process, were composed of

Mg- and Zn-dendrites. The melt pool analysis revealed predominantly keyhole mode melting for all investigated process parameters.

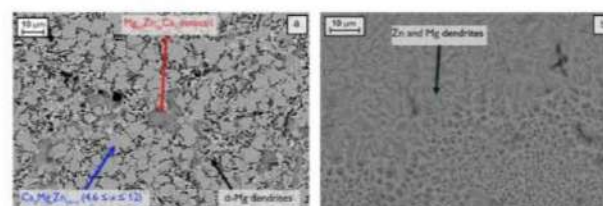


Figure 1: BS-SEM image, sample printed at 75W, 400 mm/s, hatch spacing of 0.04 mm, and 67° rotation, showing the microstructure formed in areas with lower cooling rates (a) and faster cooling rate (b).

DISCUSSION & CONCLUSIONS: In this work, we optimized the density of a MgCaZn alloy produced by PBF-LB and characterized the microstructure in different areas, relating them to the local thermal history. The hatch spacing and scanning strategy had a similar effect on density as that previously reported for other Mg alloys produced by PBF-LB². The microstructure in regions of slow cooling was similar to that previously reported for samples cast with similar compositions³. Meanwhile, a different microstructure, composed mostly of Mg and Zn dendrites, was found in areas subjected to faster cooling rates. Future work aims to characterize corrosion properties to determine the underlying influence of such distinct microstructures, as a first step towards the fabrication of specimens with improved corrosion resistance.

REFERENCES: ¹Feyerabend, Acta Biomaterials, 2010; Julmi, Materials, 2021; ³ Roche, Journal of alloys and compounds, 2019.

ACKNOWLEDGEMENTS: This Project has received funding from the EU Marie Skłodowska-Curie grant agreement No. 956004, BioTrib, as well as VINNOVA (Grant no: 2019-00029, AM4Life Competence Centre), as well as the Swedish Research Council (2021-04708).



16th Biometal

25-30 August, 2024

FOREST HOTEL • KRAKÓW, POLAND



Controversies and challenges of long standing biological and physiological dogmas

Yannis Missirlis

Professor (ret'd) , University of Patras, Greece

There is never so far, and probably never will be, an end of history in sociological, but also, in scientific affairs. Although the developments in biomaterials, artificial organs, and all interventions creating biointerphases are relatively recent, the quest is focused mainly on the inert material and less on the bio part (after making sure that toxicity and serious negative responses are dealt with).

My proposal is that every improvement in stable or degradable biomaterials should humbly serve the biological entity. Consequently, the refinements in the materials/engineering processes should go hand-in-hand with deeper understanding of the physiological processes in the compromised biological subject.

Utilizing several cases, both related to biomaterial science and to human physiology, in general, challenges to “established” ideas will be put forward for discussion.



Electroformed Fe-Mn alloys for biodegradable implant application

V.F. Sales^{1,2}, C. Paternoster^{1,2}, G. Kolliopoulos², D. Mantovani^{1,2}

¹ Lab Biomaterials and Bioengineering, CRC-I, Dept Min-Met-Mater Eng. & CHU de Quebec Research Center, Division of Regenerative Medicine, Laval University, Quebec City, G1L 3L5, Canada.

² Department of Mining, Metallurgical and Materials Engineering, Université Laval, Quebec City, G1V 0A6, Canada.

INTRODUCTION: Fe-Mn alloys have been proven a suitable candidate for temporary implants (i.e., coronary stents).¹ Currently, these alloys are fabricated by casting. This method is generally used as the primary fabrication technique and is usually followed by thermo-mechanical processes. Despite being an established production chain for most metallic materials, this form of manufacturing makes the production of biomedical devices time and energy-consuming.² Based on that, a sustainable alternative for producing thin metallic devices is required, like electroforming. This technique allows the production of thin pieces (μm scale) with complex geometries.³ Deep eutectic solvents (DESs), often consisting of an ammonium salt or a metal salt, are a class of ionic liquids, proposed as a promising and sustainable alternative to replace water for the electrodeposition of metals.⁴ This work aimed to produce Fe-Mn alloys using a DES-based on ethylene glycol, iron, and manganese chloride salts, with glycine as a complexing agent (0.2 M, 0.4 M, and 0.6 M), improving the deposition of Mn. Electroformed Fe-Mn alloys (Figure 1) with a thickness from 50 to 85 μm were successfully obtained.

METHODS: The electrolyte was obtained by mixing ethylene glycol, FeCl_2 and MnCl_2 with H_3BO_3 and CaCl_2 as additives to reduce internal stress. The samples were produced and chronopotentiometry analysis were performed in a 100 mL cell equipped with three-electrodes setup at $T=80^\circ\text{C}$. Scanning electron microscopy (SEM) and energy-dispersive X-ray (EDS) assessed the surface morphology and chemical composition. Electrochemical experiments (potentiodynamic polarization, electric impedance spectroscopy) were performed to study the corrosion behavior.

RESULTS: Figure 1 shows the upper part of the selected electroformed Fe ($C_{\text{gly}} = 0\text{ M}$ for G00) and Fe-Mn ($C_{\text{gly}} = 0.6\text{ M}$ for G06) alloy using electrolytes with different glycine concentration. The SEM micrographs showed a decrease in the size of the particles with increasing addition of glycine. Also, the efficiency of the electroforming process improved from 73% to 87%. Corrosion

rate also increased, from 0.4 mm/y to 1.7 mm/y. The concentration of Mn at G06 was 4% at.

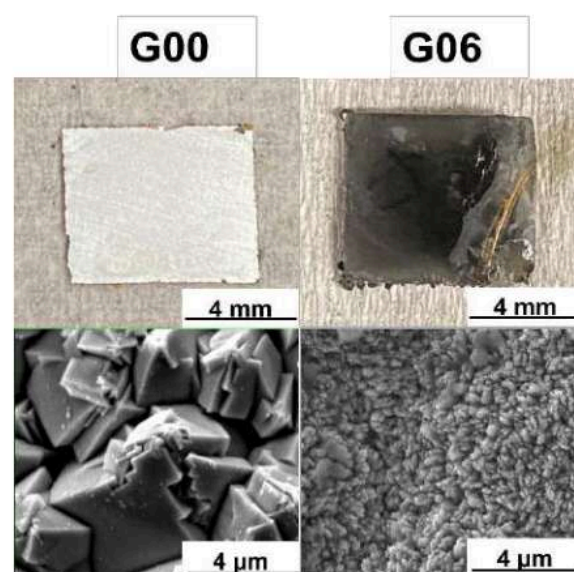


Fig. 1: Scanning electron microscopies of electroformed Fe-Mn samples produced with different concentrations of glycine ($C_{\text{gly}} = 0\text{ M}$ for G00, and $C_{\text{gly}} = 0.6\text{ M}$ for G06).

DISCUSSION & CONCLUSIONS: Glycine concentration affected the morphology of the electroformed Fe-Mn alloys. From a cubic shape (pure Fe) to a needle form at high glycine concentration (0.6 M). The presence of glycine in the DES inhibited the reduction of Fe^{2+} allowing the deposition of Mn.

REFERENCES: 1. H. Hermawan, et al., *J Biomed Mater Res A*, 2010, **93**, 1–11. 2. D. Hong, et al. *Acta Biomater*, 2016, **45**, 375–386. 3. J. M. Yang et al., *Int J Mach Tools Manuf*, 2008, **48**, 329–337. 4. E. Smith et al *Chem Rev*, 2014 **114**, 11060–11082.

ACKNOWLEDGEMENTS: This work was mainly funded by NSERC-Canada under the CU-I2I and Alliance programs and PRIMA Quebec. DM was supported by NSERC-Canada and holds a Canada Research Chair Tier I. GK was supported by NSERC-Canada and FRQNT (ERA-MIN2). The financial support of the Canada Foundation for Innovation (CFI) is also acknowledged.



Machine-Learning driven accelerated determination of structure-property relationship in Mg alloys

Sreenivas Raguraman¹, Maitreyee Sharma Priyadarshini¹, Adam Griebel², Paulette Clancy¹, Timothy P. Weihs¹

¹Johns Hopkins University, ²Fort Wayne Metals

INTRODUCTION: Mg-Zn-Ca alloys are increasingly used for implants due to their excellent biocompatibility, although they face challenges like deformation and rapid corrosion.¹ Balancing their microstructure, mechanical strength, and corrosion resistance is essential, especially since alloying often reduces corrosion resistance.² With recent FDA approval³ highlighting their potential, understanding the effects of processing on these properties is crucial for biomedical applications. Here we rapidly identify the effects of thermal processing on microstructure and properties using machine learning techniques.

METHODS: Figure 1 details the experimental methodology. In summary, we performed a solution heat treatment study on a dilute Mg-Zn-Ca-Mn alloy (ZX10) processed by ECAP at 200°C. We tracked the microstructure and properties using X-ray diffraction, optical microscopy, hardness tests, and 1-day immersion corrosion studies, validating results with SEM, EBSD, and EDS. Due to the high correlation and evolution of microstructural features during heat treatment, we applied machine learning techniques like LASSO regression⁴ and Pearson R Correlation⁵, combined with existing physical relations, to understand the complex interplay between microstructure and properties.

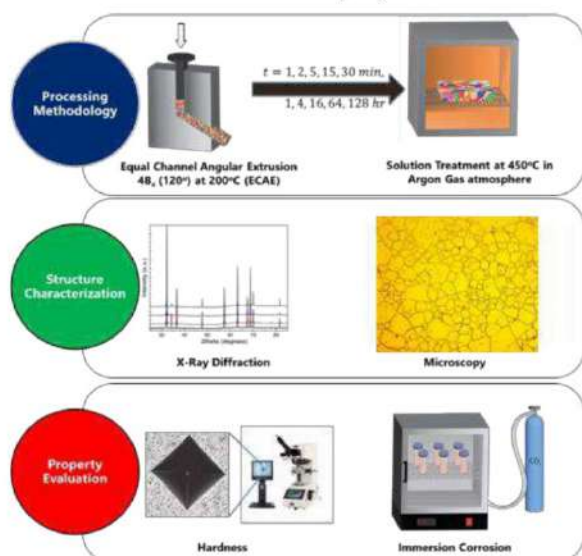


Figure 1. Graphical Schematic illustrating the experimental work carried out in this study.

RESULTS: As heat treatment progressed, both hardness and corrosion resistance decreased. Tracking microstructural features showed that dislocation density and precipitate fraction decreased, while grain size increased. Physics-informed machine learning helped us understand the relationships and dominance of these features as seen in Figure 2. Our analysis revealed that grain size, through the Hall-Petch mechanism, most significantly influenced hardness. Meanwhile, $\text{Ca}_2\text{Mg}_6\text{Zn}_3$ and Mg_2Ca precipitates dominated corrosion behaviour due to their electrochemical potential differences.

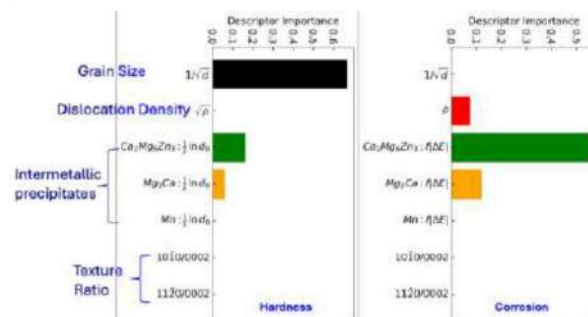


Figure 2. Physics informed LASSO plots showing the influence of microstructural features on the hardness and corrosion rate.

DISCUSSION & CONCLUSIONS: Combining accelerated characterization, testing, and machine learning allowed us to quickly identify relationships between microstructural features and their effects on properties. Our analysis showed that small grain size and lower intermetallic concentration provide the best combination of high hardness and low corrosion.

REFERENCES: ¹ Raguraman, Sreenivas, et al. *TMS Annual Meeting & Exhibition*. Cham: Springer Nature Switzerland, 2024. ² <https://bioretec.com> ³ Raguraman, Sreenivas, et al. *arXiv:2404.13022* (2024). ⁴ D Freedman, R Pisani, and R Purves, “Statistics (international student edition)” (2007). ⁵ R Tibshirani, *Journal of the Royal Statistical Society*.

ACKNOWLEDGEMENTS: The authors like to thank National Science Foundation and Department of Energy for supporting the personnel involved in this study.



Electroforming Fe-Co binary alloys for biodegradable tiny implants

C H M Beraldo¹, C Paternoster¹ and D Mantovani¹

¹ [Laboratory for Biomaterials and Bioengineering](#), CRC-I, Department of Min-Met-Materials Eng., & University Hospital Research Center, Regenerative Medicine, Laval University, QC, Canada.

INTRODUCTION: Processing implants made of biodegradable metals constitute a research hotspot, especially for tiny Fe-based implants. First, biocompatibility and mechanical properties elect Fe to the range of a promising biodegradable metal. Second, electroforming processes constitute a very interesting approach for fabricating tiny implants made of pure Fe. However, electroforming Fe-based binary and ternary alloys constitute a challenge. Moreover, the low degradation rate of Fe-based implants must be accelerated. Alloying Fe with elements that will increase its corrosion rate, such as Zn, Mn, Mg and phosphorous, have already been reported [1]. Cobalt also constitutes an interesting alloying element, especially from an electrochemical point of view. Besides its toxicity at concentrations $> 8 \mu\text{g day}^{-1}$, Co is present as trace element in the human body, and inherently present antibacterial features [2-3]. In addition, Fe and Co present close standard electrode potential (-0.44 V and -0.28 V , respectively) which turns the co-electrodeposition effective. In this study, the potential of effectively electroforming binary Fe-Co alloys was investigated.

METHODS: Pure electroformed Fe was deposited using a modified version of the Fischer–Langbier solution. The Fe-Co samples were produced in an electrolytic bath composed of a fixed amount of Fe chloride, and a variable amount of CoCl_2 , 4.5 g L^{-1} (sample Fe-12Co) and 20 g L^{-1} (sample Fe-20Co), ascorbic acid and H_3BO_4 . The deposition took place under pH 1, and at $T = 85^\circ\text{C}$, using current density $j = 2 \text{ A dm}^{-2}$, for $t = 120 \text{ min}$. Deposition took place using a three-electrode cell, containing an Ag/AgCl reference electrode, a carbon rod as counter-electrode and a square Ti sample ($2.0 \text{ cm} \times 2.0 \text{ cm}$) as working electrode. The obtained samples were characterized using profilometry and optical microscopy (OM), and the corrosion rate calculated from the potentiodynamic polarization in modified Hanks' balanced salts solution.

RESULTS: Fig. 1 shows the morphological aspects of the electroformed samples. One can see that the low addition of Co refined the grains. In contrast, for higher Co addition, coarser grains were observed, as in the Co-Fe alloy proposed by Rozlin and Alfantazi [4]. In addition, the

refinement observed in the Fe-12Co alloy caused reduction of its surface's roughness, as well as discussed by Wang *et al.* [5]. As a result, this sample also presented higher corrosion rate ($0.26 \text{ mm year}^{-1}$) than the other ones (pure Fe = $0.15 \text{ mm year}^{-1}$ and Fe-20Co = $0.01 \text{ mm year}^{-1}$), since refined grains increase the grain boundaries that are more susceptible to corrosion.

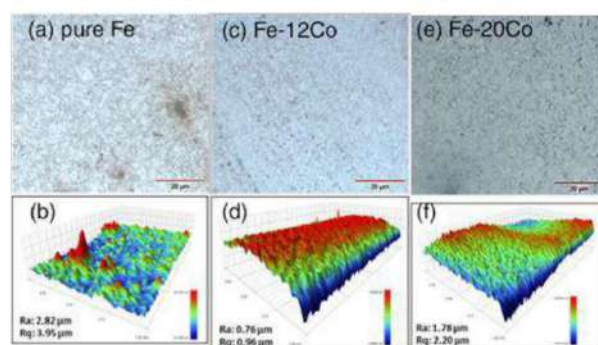


Fig. 1: Optical microscopy (top line) and roughness profiles (bottom line) of Fe, Fe-12Co, and Fe-20Co samples.

DISCUSSION & CONCLUSIONS: Low Co addition was responsible for the refinement of the grains in the Fe-based alloys, which also decreased the surface roughness. In contrast, for the highest Co content, the roughness of the surface increased and the morphology showed similar aspect to that of the pure Fe. In terms of corrosion resistance, low Co decreases the corrosion resistance, while high Co amount produced a passive layer resistant to corrosion. Future investigation using lower Co amount is of interest, as well as *in vitro* analysis.

REFERENCES: ¹G. Gąsior, J. Szczepański, A. Radtke (2021) *Materials* **14**:3381; ²L. Leyssens, B. Vinck, C. Vand Der Straeten, et al (2017) *Toxicology* **387**:43-56; ³E.L. Chang, C. Simmers, D.A. Knight (2010) *Pharmaceuticals (Basel)* **3**:1711-28; ⁴N.M.N. Rozlin, A. M. Alfantazi (2012) *Mater Sci and Eng A* **550**:388-94; ⁵G. Wang, J. Han, Y. Lin, et al (2021) *Mater Today Commun* **27**:102279.

ACKNOWLEDGEMENTS: This project was partially supported by NSERC-Canada, PRIMA-Quebec, and the Quebec University Research Hospital.



Development of Mg-2Y-1Zn(Gd, Ag, Ca) alloys with LPSO phase for degradable implant applications

D Tolnai¹, DCF Wieland¹, B Wiese¹, H Helmholz¹, J Bohlen², M Nienaber², G Garcés³

¹ Institute of Metallic Biomaterials, Helmholtz-Zentrum Hereon, Max-Planck Strasse 1, 21502 Geesthacht, DE, ² Institute of Material and Process Design, Helmholtz-Zentrum Hereon, Max-Planck Strasse 1, 21502 Geesthacht, DE, ³ Departament of Physical Metallurgy, National Center for Metallurgical Research, CENIM-CSIC, Avda. Gregorio del Amo 8, Madrid, 28040, SP

INTRODUCTION: The similar Young's modulus to cortical bone allows Mg-based implants to provide optimal support, while the degradation under physiological conditions renders the removal surgery obsolete, thus increasing patient comfort and reducing risks and medical costs¹. The addition of Y and Zn can substantially improve the mechanical properties. Favourable processing conditions promote the formation of a Long Periodic Stacking Ordered Structure (LPSO) that provides superior strength without deteriorating the ductility², while the biocompatibility of Mg-Y-Zn (WZ) alloys makes them suitable as biodegradable implant materials³.

METHODS: The material was produced by permanent mould indirect chill casting⁴. Four alloys were cast with the compositions of Mg-1.8Y-0.6Zn in pure form and with the addition of 1.6 wt. % of Gd, 1 wt.% of Ag and 0.4 wt.% of Ca, respectively. The ingots were homogenized at 400 °C for 24 h and subsequently quenched in water. The indirect extrusion to extrude 10 mm bars was performed at 400 °C with a speed of 1 mm·s⁻¹ at an extrusion ratio of 1:25. The electron microscopic characterization was performed using a TESCAN Vega SB-U III scanning electron microscope (SEM) and a JEOL JEM 2010 transmission electron microscope (TEM). The mechanical testing was conducted on a Zwick Z050 universal testing machine at RT at a constant initial strain rate of 10⁻³s⁻¹. The degradation characteristics were investigated in SBF (simulated body fluid), and cell viability of SCP-1 mesenchymal stem cells tests were carried out to determine biocompatibility.

RESULTS: The microscopic characterization (Fig. 1a) has shown that the microstructure of the alloys consists of Mg grains and the 18R (1.6 nm lamella distance) type LPSO structure forming during solidification. During the homogenization treatment the 14H type LPSO structure (1.8 nm lamella distance) precipitates and the existing 18R structure also transform partially to 14H. The addition of Gd and Ag promotes the formation of 14H, while Ca stabilises the 18R structure. The results of the mechanical testing (Fig. 1b) indicate that the

unmodified WZ alloy exhibits the highest yield strength 157±2 MPa, but the alloying additions increase the UTS and the ductility as well. The degradation rate of the alloys measured in SBF ranges between 0.11±0.3 mm/y (Mg-1.8Y-0.6Zn-1Ag) and 0.17±0.5 mm/y (Mg-1.8Y-0.6Zn-1Gd). The alloys show a good biocompatibility as shown in Fig 1.c, where the viable cells appear in green and the dead cell in red.

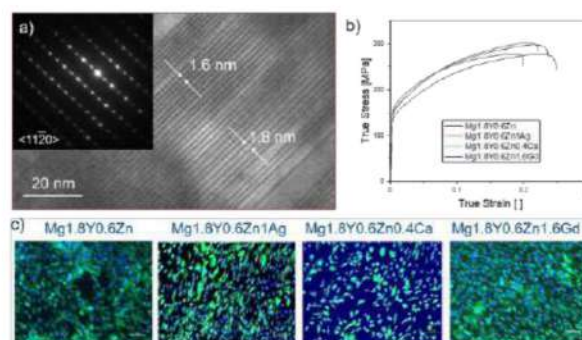


Fig. 1. a) TEM of Mg1.8Y0.6Zn showing the coexistence of the 18R and 14H LPSO phase b) Stress-strain curves of the alloys under tensile load and c) cell viability tests live/dead staining 7d incubation green-vital; red-dead, blue-nucleus.

DISCUSSION & CONCLUSIONS: Mg-Y-Zn based alloys with low concentrations of alloying elements show sufficient mechanical properties low degradation rates and good *in vitro* biocompatibility. The additional alloying elements broaden the functionality with antibacterial properties (Ag) or better sintering behaviour (Ca). These characteristics render the use of the alloys as degradable implants in orthopaedic or traumatic surgery applications feasible.

REFERENCES: ¹H. Hermawan, D. Dubé, D. Mantovani, (2010) *Acta Biomater.* **6**:1693-1697. ²K. Horváth et al., (2017) *Magnesium Technology 2017. The Minerals, Metals & Materials Series.* Springer, Cham. https://doi.org/10.1007/978-3-319-52392-7_8. ³T. Kraus et al., (2018) *Acta Biomater.* **66**:109-117. ⁴F.R. Elsayed et al., (2011) *Mater. Sci. Forum* **690**:65-68.



Additively manufactured Zn-2Mg alloy porous scaffolds with customizable biodegradable performance and enhanced osteogenic ability

Aobo Liu¹, Peng Wen¹

¹ *State Key Laboratory of Clean and Efficient Turbomachinery Power Equipment, Department of Mechanical Engineering, Tsinghua University, Beijing, China*

INTRODUCTION: Ideal Zn-based biodegradable metal bone implants necessitate customizable biodegradable behaviours and improved osteogenic ability, conforming to the individual requirements of specific patients. Although design of implant material composition is a prevalent strategy, its efficacy in modulating the implant's performance is notably restricted [1]. Structure design has shown efficacy in regulating the performance of bio-inert metal implants, like Ti alloy scaffolds [2]. However, no study has been systematically conducted on the impact of structure design on the performance of biodegradable Zn-based metal scaffolds. The mechanism that how structure design controls the biodegradable performance and osteogenic ability of scaffolds remains unclear. Hence, in this study, Zn-2Mg alloy scaffolds with different porosities and different unit sizes were designed and fabricated to study the influence and the underlying influencing mechanism of structure design on the in vitro and in vivo behaviour of Zn alloy scaffolds.

METHODS: Gyroid unit cells were generated with different unit sizes and porosities. Scaffolds with a unit size of 2 mm and porosities of 40%, 60%, and 80% were denoted as G-40-2, G-60-2, and G-80-2. Scaffolds with a porosity of 60% and unit sizes of 1.5 mm, 2 mm, and 2.5 mm were denoted as G-60-1.5, G-60-2, and G-60-2.5 (Fig. 1).

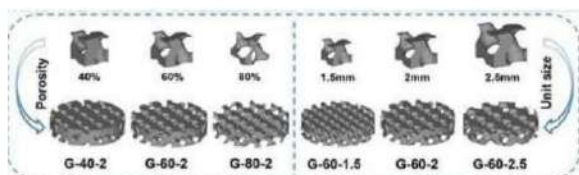


Fig. 1: Structure design of Zn-2Mg scaffolds.

RESULTS: Compressive strength (CS) and elastic modulus (EM) of scaffolds substantially decreased with increasing porosities. CS and EM just slightly decreased with increasing unit sizes (Fig. 2). Weight loss after degradation increased with increasing porosities and decreasing unit sizes (Fig. 3). Scaffolds with lower porosities and smaller unit sizes had better osteogenesis (Fig. 4).

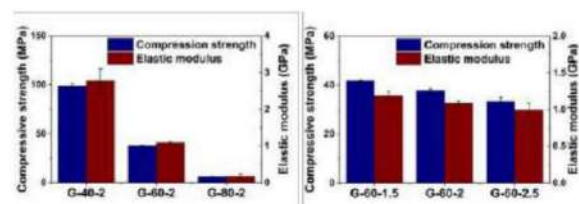


Fig. 2: Compressive properties of scaffolds.

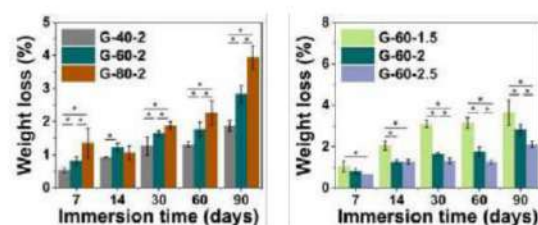


Fig. 3: Weight loss of scaffolds after immersion.

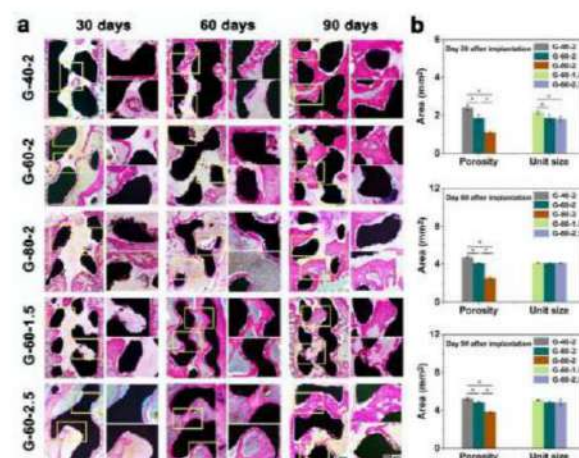


Fig. 4: In vivo osteogenic ability analysis.

DISCUSSION & CONCLUSIONS: The biodegradable performance of scaffolds can be accurately regulated on a large scale by structure design and the additively manufactured Zn-2Mg alloy scaffolds have improved osteogenic ability for treating bone defects.

REFERENCES: ¹ Y. Qin, H. Yang, A. Liu, et al. (2022) *Acta Biomater.* **142**: 388-401. ² Y. Zhang, N. Sun, M. Zhu, et al. (2022) *Biomater. Adv.* **133**: 112651.

ACKNOWLEDGEMENTS: This template was modified with kind permission from eCM Journal.



3D-printing of bioresorbable Zinc-Magnesium for critical-size bone defects

M. Voshage¹, F. Fischer¹, L. Jauer¹, S. Pöstges², A. Kopp², J.H. Schleifenbaum¹

¹Chair for Digital Additive Production DAP, RWTH University, Aachen, Germany,

²Meotec GmbH, Aachen, Germany

INTRODUCTION: In this work, bioresorbable zinc-magnesium alloys are 3D-printed by Powder Bed Fusion of Metals using a Laser Beam (PBF-LB/M). The goal is to manufacture load-bearing, implants (e.g. patient-specific scaffolds or cages) with suitable degradation properties without damage to the surrounding tissue.

METHODS: For the experiments, Zn0.5Mg and Zn1Mg powder-mixes from *Nanoval* are used. Test specimens are manufactured using a modified PBF-LB/M machine from *Aconity3D*. Scaffold structures are designed with respect to size and load capacity depending on the medical indication using *Rhino 7.3* and *Grasshopper* plugin. Compression tests are conducted according to DIN 50134. Test specimens are based on f_{2ccz} unit cells with 10x10x15 cells in XYZ and a strut diameter of 200 μm with a pore width of 800 μm . EBSD analyses are carried out to determine the phase constituents as well as grain size and grain orientation in the manufactured test specimens.

RESULTS: Scaffold structures with a strut diameter of 200 μm are manufactured as shown in fig. 1-top. By combining a tailored exposure strategy with abrasive post-processing, sintered particles are removed, achieving dimensional accuracy of approx. $\pm 20 \mu\text{m}$ in the scaffold structures. Mechanical properties are analysed using compression tests (fig. 1-center). The max. compressive force for Zn0.5Mg is 2046 N, while for Zn1Mg it is 1927 N. The compressive stress Re_H can be calculated as 19.57 MPa for Zn0.5Mg and 18.26 MPa for Zn1Mg. The strain at this point is $\epsilon_{\text{max}} = 8.42\%$ for Zn0.5Mg and $\epsilon_{\text{max}} = 6.57\%$ for Zn1Mg. Decreased strength with increased ductility is demonstrated for Zn0.5Mg compared to Zn1Mg and can be explained by different microstructures. Fig. 1-bottom shows the results of EBSD analyses of Zn1Mg and Zn0.5Mg specimen. The mean area-weighted α -Zn grain size of the Zn1Mg specimens is $3.39 \pm 1.58 \mu\text{m}$ and $6.00 \pm 3.38 \mu\text{m}$ for Zn0.5Mg.

DISCUSSION & CONCLUSIONS: A decrease in grain size with increasing Mg content is consistent with the results from the literature¹. According to the Hall-Petch relation, grain refinement is expected to increase strength. Furthermore, a decrease in strain and compression

is attributed to rise in intermetallic $\text{Mg}_2\text{Zn}_{11}$ phases. The compressive stress depends not only on the material properties but also on geometry and porosity. Additive manufacturing of complex structures made from bioresorbable ZnMg with load-bearing properties suitable for bone replacement has been demonstrated. The process chain for tailored implants includes a customized design with data preparation, a tailored PBF-LB/M process, and abrasive post-processing.

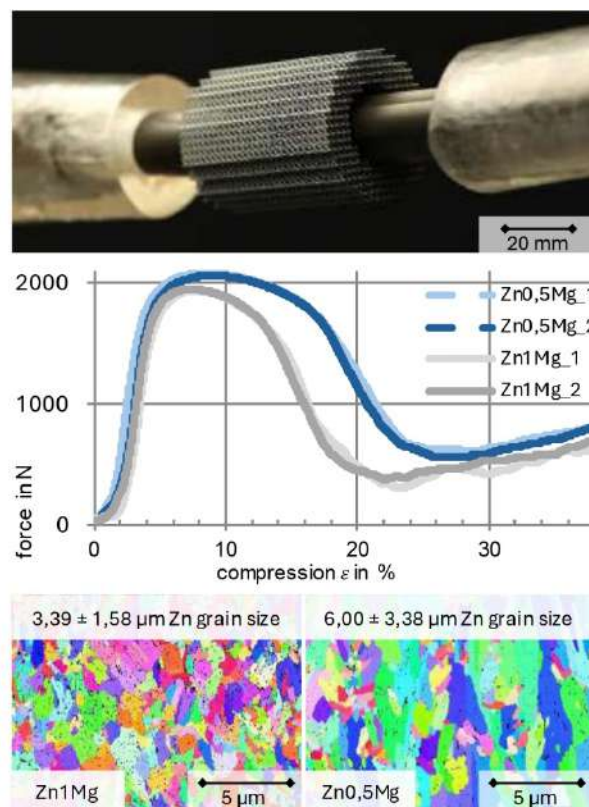


Fig. 1: (top) PBF-LB/M manufactured scaffold², (center) Results of compression tests according to DIN 50134, (bottom) EBSD analysis²

REFERENCES: ¹Y. Yang et al. (2018) *A combined strategy to enhance the properties of Zn by laser rapid solidification and laser alloying*, doi.org/10.1016/j.jmbbm.2018.03.018

²M. Voshage (2024) *Additive manufacturing of Zinc Magnesium alloys*, ISBN 978-3-98555-199-6

ACKNOWLEDGEMENTS: Parts of this work were funded by the German Federal Ministry of Education (13GW0404D & 03RU1U173C)



Combination of biodegradable Zn- and Mg-based alloys using multi-material Additive Manufacturing: challenges and opportunities

S Pöstges¹, T Poel¹, J Molina², J Llorca², A Kopp¹

¹ Meotec GmbH, Aachen, Germany.

² IMDEA Materials Institute, Getafe, Spain.

INTRODUCTION: Biodegradable metals, particularly zinc (Zn) and magnesium (Mg) alloys, offer significant potential for biomedical applications, especially in temporary implants that gradually degrade within the body. Recent studies demonstrate the feasibility of additive manufacturing (AM) of both materials to address patient-specific solutions with high geometric complexity^{1,2}. This study explores the innovative combination of Zn- and Mg-based alloys using multi-material AM techniques, aiming to synergize the unique properties of these materials for optimized performance in medical devices.

METHODS: Gas atomized, pre-alloyed Zn1Mg and WE43MEO powder is used to carry out the tests. All specimens are manufactured using a modified Laser Powder Bed Fusion system from Aconity 3D GmbH with the option to integrate a drum-based recoating module from Schaeffler Aerosint SA allowing a layer wise combination of two different powder materials. To identify the optimum build plate material a total of 48 cuboid specimens with different volume energy density as well as support structure geometries are fabricated. In a next step, both materials are printed on top of each other by variation of the bonding parameters between both materials targeting to produce samples with a crack free interface. Additionally, the deposition accuracy of the recoating module is studied by varying the parameters of the recoating unit.

RESULTS: In the context of this study, Zn1Mg cuboid test specimens are reproducibly manufactured on a WE43 build plate with a relative density greater than 99.5 % and a support structure geometry of 300 μm . Additionally, a crack free interface between Zn1Mg and WE43MEO is achieved when combining the materials in printing direction as shown in Fig. 1 exemplary. For the layer wise multi-material 3D printing, parameters for the ejection and suction pressure of the drum-based recoating module are found to obtain a layer thickness of 30 μm for both materials.

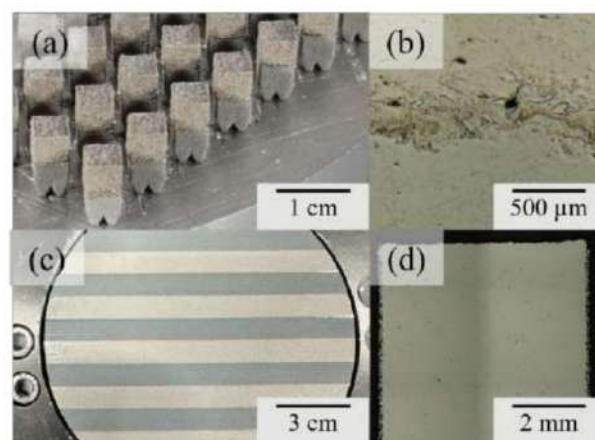


Fig. 1: (a) Multi-material cuboid specimens with Zn1Mg base part and WE43MEO top part, (b) cross section image of the fusion zone with crack free interface, (c) layer-wise combination of both powder materials with optimized parameters of the recoating unit, (d) exemplary cross section image of Zn1Mg cuboid specimen printed on a WE43 build plate with a relative density of 99.74 %

DISCUSSION & CONCLUSIONS: A sufficient build plate material was found as both materials were manufactured with a reproducible relative density > 99.5 % on a WE43 plate. Moreover, the general feasibility of combining both powder materials in printing direction was shown. In further investigations the mechanical and degradation properties will be determined. The parameter optimization of the drum-based recoating unit led to a layer wise combination of both powders representing the basis of the processing within one layer which will be studied.

REFERENCES: ¹M. Li et al (2021) Microstructure, mechanical properties, corrosion resistance and cytocompatibility of WE43 Mg alloy scaffolds fabricated by laser powder bed fusion for biomedical applications, *Materials Science & Engineering C* **119**: 1-17. ²M Voshage et al (2022) Additive Manufacturing of biodegradable Zn-xMg alloys: Effect of Mg content on manufacturability, microstructure and mechanical properties, *Materials Today Communications* **32**: 1-9.



Effect of PEO-coatings in hybrid Zn-Mg alloys processed through high-pressure torsion

J Salinas¹, N Mollae², C.J. Boehlert¹, J Llorca, *M Echeverry-Rendón*²

¹Michigan State University, USA; ²IMDEA Materials Institute, Spain

INTRODUCTION: Metals such as Fe, Mg, and Zn are the most reported for degradable metallic implants¹. All of them are considered essential elements for the human body and are necessary to perform the basic systemic functions of cells, tissues, and organs. Zn shows intermediate corrosion rates between Fe and Mg (≈ 0.1 mm/year), but it is the least studied to date, and the *in vivo* effects in the medium/long term are not yet fully understood. Studies so far have shown that Zn has good corrosion resistance and acceptable biocompatibility. Still, significant concerns have been raised due to its poor mechanical strength, aging at room temperature, creep effects, and high sensitivity to strain rate.

Consequently, there are currently numerous studies aimed at improving the mechanical properties of Zn alloys by adding other biodegradable metals, such as Mg, Ca, Sr, etc.² Conversely, plasma electrolytic oxidation (PEO) is an electrochemical surface treatment that results in a natural ceramic-like coating that can improve the corrosion resistance and biological behavior of Zn³. This study aims to determine if the quantity of Mg of Zn-Mg-based alloys in hybrid samples processed through high-pressure torsion alters the effectiveness of PEO. The goal is to achieve a suitable product to implement as a biodegradable orthopedic implant.

RESULTS: Hybrid samples of Zn-3Mg, Zn-10Mg, and Zn-30Mg processed through high-pressure torsion were successfully coated using PEO treatment in a phosphate-based electrolyte. The optimum voltage for the coating in the different materials was defined between 250 and 270 V, and the current density was in the range of 600 and 650 mA/cm². The thickness of the coatings obtained was in the order of 40-50 μ m. Samples were characterized from the surface and cross-section using SEM and EDS. The porous-like coating was obtained with a uniform distribution. Degradation results and cytocompatibility through indirect and direct test experiments showed an increase in the improvement of the PEO-treated Zn.

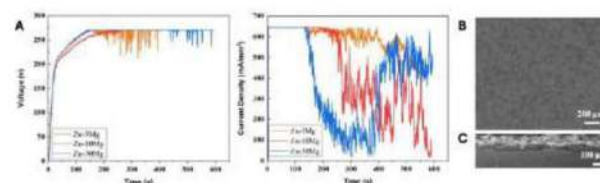


Fig.1: Curves of PEO coatings obtained for continuous voltage (A) PEO surface of the Zn-Mg coating (B). The rest of the parameters (C) Cross-section of the sample

DISCUSSION & CONCLUSIONS: Through the PEO technique, it was possible to obtain uniform and optimized coatings based on ZnO and Zn(OH) to improve the biological properties of Zn mainly. The Mg content in Zn alloys has a direct relationship with the microstructure and the formation process of the coating, which defines critical characteristics of the material, such as corrosion resistance and biocompatibility. This study concluded that aspects such as the techniques for obtaining the alloy, composition, and coatings could synergistically promote the degradation behavior and biocompatibility of materials used as biodegradable implants.

REFERENCES: ¹ M Heide, E Walker, L Stanciu (2015) Mg, Fe and Zn Alloys, the Trifecta of Bioresorbable Orthopaedic and Vascular Implantation. *J Biotechnol Biomater* 5:178. ² X. Liu, J Sun, K Qiu, Y Yang, Z Pu, L Li, Y Zheng (2016). Effects of alloying elements (Ca and Sr) on microstructure, mechanical property and *in vitro* corrosion behavior of biodegradable Zn-1.5Mg alloy. *J. Alloys Compd.* 664, 444-452. ³ J. Joseph, S. Corrujeira, R. Catubig, K. Wang, A. Sommers, P. Howlett, D. Fabijanic (2020) Formation of a corrosion-resistant coating by a duplex PEO and conversion surface treatment, *Surface & Coatings Technology*, 395 125918.

ACKNOWLEDGEMENTS: The National Science Foundation Division of Material Research (Grant No. DMR2153316), and the "Ayudas de atracción de talento investigador "César Nombela" 2023" of the Regional Government of Madrid (2023-T1/TEC-29099).

Corrosion

Tuesday, August 27th, 2024



cryo-atom probe tomography; quasi-'in situ' analysis of the reactive liquid-solid interface during Mg corrosion

Tim M. Schwarz¹, Leonardo S. Aota¹, Eric Woods¹, Xuyang Zhou¹, Ingrid McCarroll¹, Baptiste Gault^{1,2}

¹ Max-Planck-Institute for Sustainable Materials, Germany, ² Imperial College London, UK

INTRODUCTION: Corrosion reactions at liquid-solid interfaces critically impact infrastructure degradation and sustainability¹, and in medicine for biodegradable body implants². For the latter, Mg, is a promising candidate thanks to its biocompatibility and biodegradability, making it an excellent replacement for temporary implants made of Ti or steel³. However Mg alloys corrode rapidly and uncontrollably, through mechanisms not fully understood, i.e. there remain open questions regarding the influence of different alloying elements, their distribution, as well as different electrolytes, on the corrosion processes.

Understanding the corrosion processes at the reactive liquid-solid interface requires analytical methods with high local and chemical analysis capability and ideally to measure these reactions *in-situ*, on an atomic length scale, which is currently lacking. Atom probe tomography (APT) provides analytical imaging in 3D with equal chemical sensitivity across the periodic table even for light elements such as hydrogen and with comparable spatial resolution⁴ and can therefore close the gap.

transferred into a cryo-FIB using an ultrahigh-vacuum, cryo-transfer shuttle. A newly developed cryo-lift-out method was used to prepare APT specimens⁶.

RESULTS: By correlating cryo-APT and TEM, we observed outward growth of Mg hydroxide and inward growth of an intermediate corrosion layer of hydr/-oxides with different compositions. The high chemical sensitivity of APT revealed that instead of a MgO layer between the hydroxide and MgCa alloy, a Mg(OH) layer was formed, into which Ca partitions.

DISCUSSION & CONCLUSIONS: With the demonstrated approach it is possible to quasi-"in-situ" analyse the reactive solid-liquid interface by cryo-APT and investigate the early corrosion mechanisms of a Mg0.1Ca alloy. These metastable defect phases at the reactive interface could only be observed by quasi- "in-situ" cryo-APT analyses of the corrosion process, yet these early reaction products are highly reactive and must play a critical role in accelerating the corrosion. However, a better understanding of these early stages of corrosion and their products is necessary to advance the understanding of corrosion processes and their modeling, and consequently for higher level of control over the biodegradation rate of future implant material.

REFERENCES: ¹Bender, R. *et al.* Corrosion challenges towards a sustainable society. *Mater. Corros.* **73**, 1730–1751 (2022). ²Witte, F. The history of biodegradable magnesium implants: A review☆. *Acta Biomater.* **6**, 1680–1692 (2010). ³Niranjan, C. A. *et al.* Magnesium alloys as extremely promising alternatives for temporary orthopedic implants – A review. *J. Magnes. Alloys* **11**, 2688–2718 (2023) ⁴Gault, B. *et al.* Atom probe tomography. *Nat. Rev. Methods Primer* **1**, 51 (2021) ⁵Schwarz *et al.* Quasi-"in-situ" analysis of the reactive liquid-solid interface during magnesium corrosion using cryo-atom probe tomography submitted (2024) ⁶Woods, E. V. *et al.* A Versatile and Reproducible Cryo-sample Preparation Methodology for Atom Probe Studies. *Microsc. Microanal.* **ozad120** (2023).

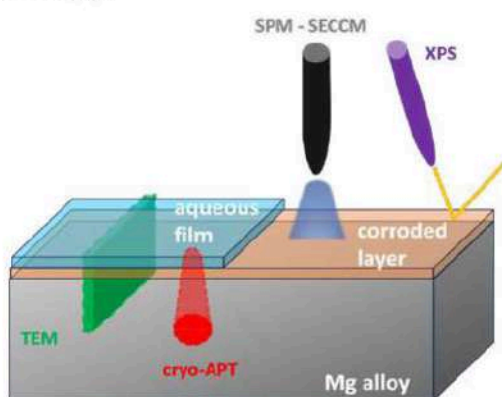


Fig. 1: Schematic overview of different methods to analyze the liquid-solid interface⁵.

METHODS: A binary Mg0.1Ca alloy was corroded using Deionized (DI) water in a glove box under an N₂ atmosphere. The corrosion process was started by pipetting a droplet of 20µl DI water on a polished surface. Afterwards, the corrosion state was fixed by plunge-freezing the sample in liq. N₂ and solidifies the aqueous phase within a porous network. The frozen sample was



Determination of an In-Vitro-In-Vivo-Correlation-Factor (IVIVC) for Biodegradable Magnesium Implants Based on Outcomes of a Tibial Plate System Trial in Sheep

JM Seitz¹, S Habicht¹, M Behbahani², A Kopp¹, R Correa Schragen¹

¹ [Medical Magnesium GmbH](#), Medical Magnesium GmbH, Aachen, Germany

² Aachen University of Applied Sciences, Jülich Campus, Medical Engineering and Technomathematics, Aachen, Germany

INTRODUCTION: Degradable polymer-based biomaterials have been introduced in daily clinical practice decades ago, taking their material associated limitations into account.¹ With the emerging of biodegradable metal-based devices - to overcome these limitations - various in vitro degradation and conditioning test approaches have been introduced to shorten development time and decrease development costs.^{2,3} As metal based biodegradable materials have their own and more complex nature of degradation thorough testing and correct translation of in vitro derived results and findings into in vivo systems gained enormous relevance.⁴ This study presents on the approach to calculate a proper correlation factor for Magnesium alloy WE43MEO by comparing in vivo study results with in vitro degradation derived data.

METHODS: Screw shaped implants made of magnesium alloy WE43MEO (Meotec GmbH, Aachen, Germany) with adherend PEO surface modification were in vitro degraded in phosphate buffered saline (PBS) at 37 °C for periods ranging from 1 to 14 days while the pH was kept between 7.4 and 7.6 following ASTM F3268. Subsequently, the corrosion rate was calculated based on mass loss and ion concentrations according to ASTM G31-12a in an orthogonal approach.

Histologically stained cross-sectional images of WE43MEO-based and PEO-surface modified screw implants that resulted from a prior animal trial in the tibiae of sheep (AZ 81-02.04.2020.A251) with durations of 4 weeks and 6 months until extraction were analyzed regarding their loss in material thickness. The material reduction was determined two-dimensionally within intramedullary sections in six areas per sample (Fig. 1).

The corresponding degradation rates were calculated for each approach and compared to finally determine the test and material dependent IVIVC.

RESULTS: In dependence of the method, in vitro degradation rates were determined to range from

approximately 8 mm/year at day 1 to approximately 2 mm/year at 14 days of in vitro degradation (n=5 for each group). The in vivo degradation rate was determined to be significantly lower based on 4 weeks and 6 months data compared to the in-vitro-based calculations.

The resulting calculated IVIVC ranges from approximately 2 to 7.5 depending on in vivo follow up durations.

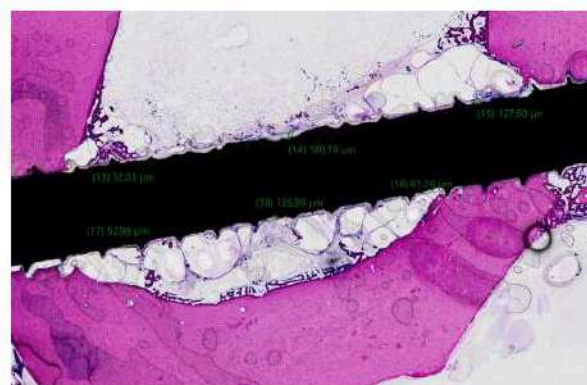


Fig. 1: Histologically stained cross-sectional image of an in vivo degraded screw shaft in a sheep's tibia 4 weeks post-surgery. The loss in thickness was determined in 6 different sections.

DISCUSSION & CONCLUSIONS: Calculation of the IVIVC for a WE43MEO magnesium-alloy was conducted following a reproducible and well-defined approach. Following the herein established route, it is possible to pre-condition magnesium samples in vitro and to link the resulting implant state and data to a corresponding in vivo condition. This may allow reduction of in vivo conditioning and testing of samples and adequate reasoning for potential regulatory purposes. The study-specific parameters must be considered.

REFERENCES: ¹ C. Li, C. Guo, V. Fitzpatrick, et al. (2020) *Nat Rev Mater* **5**:61-81. ² N.T. Kirkland, N. Birbilis (2014) *Magnesium Biomaterials - Design, Testing and Best Practice*. Springer International Publishing ³ N.T. Kirkland, N. Birbilis, M.P. Staiger (2012) *Acta Biomater* **8**:925-936. ⁴ J.M. Seitz, R. Eifler, F.W.



Hybrid coatings to improve corrosion and tribological properties of Mg alloys

AM Rich¹, J Cossu¹, W Rubin¹, T Akhmetshina¹, L Berger¹, JF Löffler¹

¹Laboratory of Metal Physics and Technology, Department of Materials, ETH Zurich, Switzerland

INTRODUCTION: While Mg alloys for clinical use have been continuously improved over the past decades, they often still exhibit a too high degradation rate *in vivo*. This can lead to excess hydrogen gas development, potentially affecting the surrounding tissues.¹ Applying specialized coatings to Mg alloys may improve their degradation profile and enhance functionality.^{1,2} Plasma electrolytic oxidation (PEO) coating is often used to improve Mg degradation and osseointegration, but its thin, porous microstructure is susceptible to intraoperative damage and may not provide full protection from corrosive media. We take advantage of this porous structure by using it as an intermediate layer for polymeric coatings,³ producing hybrid-coated Mg alloys with enhanced tribological and degradation properties.

METHODS: Parylene-C coating was tested on extruded Mg-alloy (X0, Mg0.45Ca, in wt.%) bars with and without PEO coating. Single (10 μ m parylene) and hybrid coatings (PEO + 10 μ m parylene) were examined using scratch and linear reciprocating ball-on-flat sliding wear tests ($n = 9$ per group). Hybrid-coated samples were also tested after immersion in simulated body fluid (SBF) for 4 weeks. Scratch testing was done with a linear increasing force (0.1 to 5 N) along a 5 mm length scratch track to identify the cohesive and adhesive coating failure loads with an optical microscope (Leica VS700C). Wear testing was done by applying a 5 N load to a 2 mm alumina sphere that was oscillated for 10 minutes over a 4 mm wear track, then analyzing the wear track with a profilometer (DektakXT, Bruker).

RESULTS: The hybrid-coated samples had higher critical loads at failure than only parylene-coated samples (2.6 ± 0.3 N vs 1.4 ± 0.4 N), which slightly decreased after immersion in SBF (2.1 ± 0.2 N). The parylene-coated samples had higher wear volume (0.04 ± 0.01 mm³) than the hybrid samples (0.005 ± 0.001 mm³); the wear volume of hybrid-coated samples did not change significantly after immersion (0.008 ± 0.001 mm³). Only PEO-coated samples exhibited a wear volume similar to parylene-coated X0 (0.06 ± 0.8 mm³). Fig. 1a shows cohesive (LC1) and adhesive (LC2) failure loads as well as the calculated wear volumes (Fig. 1b).

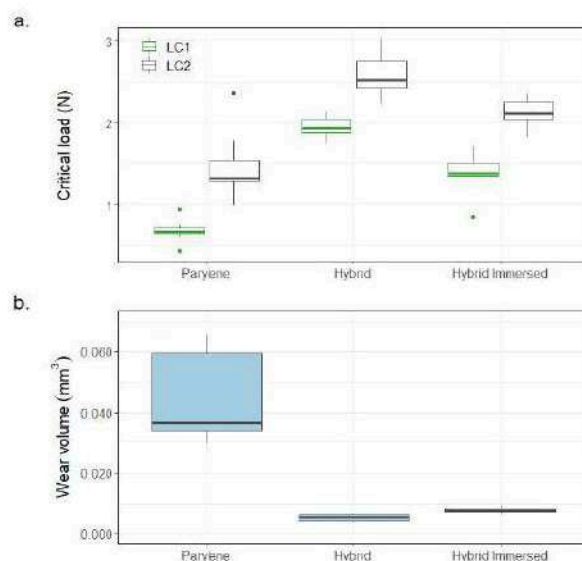


Fig. 1. (a) Cohesive (LC1) and adhesive (LC2) failure loads and (b) wear volumes for parylene-coated, hybrid-coated (PEO + parylene), and hybrid samples immersed four weeks in simulated body fluid.

DISCUSSION & CONCLUSIONS: Critical failure loads were increased for the hybrid samples, even after immersion in SBF, indicating that the parylene coating has stronger adhesion to the PEO surface than the untreated Mg surface. The adhesion is maintained after exposure to a corrosive media similar to the *in vivo* environment. The wear properties of the PEO-coated Mg were improved by the parylene coating, evidenced by the lower wear volume, and this improvement was not diminished by SBF immersion. The improved adhesion of the hybrid samples could be explained by the parylene impregnating the porous PEO substrate, promoting adhesion and sealing pores to improve corrosion resistance. The hybrid-coating technique with biodegradable polymers may be used to reduce Mg degradation and improve tribological properties of implants.

REFERENCES: ¹L. Berger, *et al.*, 14th Biometal Conf. (Aug. 2022), Europ. Cells and Materials (2022), in press. ²W. Rubin, *et al.*, 15th Biometal Conf. (Aug. 2023), Europ. Cells and Materials (2023), in press. ³S. Stauffert *et al.*, *ACS Appl. Nano Mater.* **1** (2018) 1586.

ACKNOWLEDGEMENTS: The authors gratefully acknowledge the Swiss National Science Foundation for funding this research (SNF Sinergia, Grant number CRSII5-180367).



Mechanical properties, biodegradation and biocompatibility of Mg scaffolds treated by high temperature oxidation and hydrotalcite coating

Bo Peng¹, Zehui Lv², Xisheng Weng², Peng Wen¹

¹*State Key Laboratory of Clean and Efficient Turbomachinery Power Equipment, Department of Mechanical Engineering, Tsinghua University, Beijing, China.* ²*Department of Orthopedic Surgery, Chinese Academy of Medical Science and Peking Union Medical College, Beijing, China.*

INTRODUCTION: Mg scaffolds featuring intricate internal pores not only increase surface area but also pose challenges in achieving reliable coating quality. Previous research has demonstrated that high-temperature oxidation (HTO) can generate a uniform rare earth oxide film on the surface of WE43 alloy, significantly impeding degradation and enhancing biocompatibility [1]. However, animal studies suggest that the passivation effect of HTO alone may be insufficient for scaffolds [2]. Layered double hydroxides (LDHs) [3] have been shown to create a chemically converted film with excellent biocompatibility on Mg alloys, further regulating scaffold degradation. In this study, we applied a combination of high-temperature oxidation and hydrotalcite coating to Mg scaffolds to improve mechanical integrity, degradation behavior, and biocompatibility.

METHODS: Mg scaffolds were fabricated via laser powder bed fusion and then chemically etched to achieve the as-polished (AP) state. Subsequently, a dual-layer coating, consisting of an oxide film and a hydrotalcite film, was applied to the scaffold surface using a combination of high-temperature oxidation (HTO) treatment and hydrothermal processing, resulting in HTO and HTO-LDH scaffolds (Fig. 1).

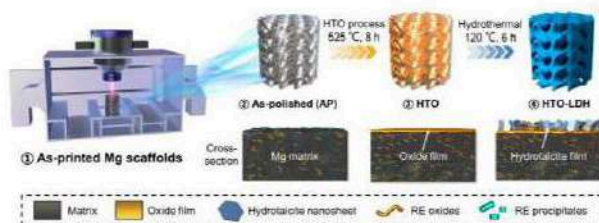


Fig. 1: Synthesis process of HTO-LDH Mg scaffold

RESULTS: The Mg scaffolds with the dual-layer coating exhibited significantly reduced weight loss ratio and hydrogen release rate upon immersion in r-SBF solution (Fig. 2). Furthermore, they displayed improved mechanical integrity (Fig. 3) and enhanced compatibility (Fig. 4) due to a noticeable decrease in degradation rate.

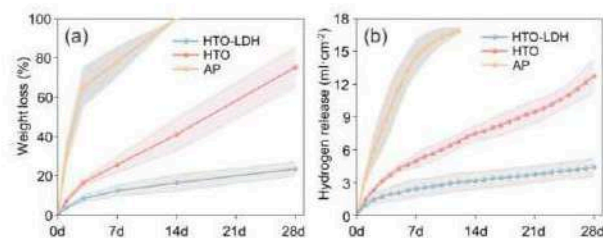


Fig. 2: Weight loss ratio and hydrogen release of Mg scaffolds after immersion.

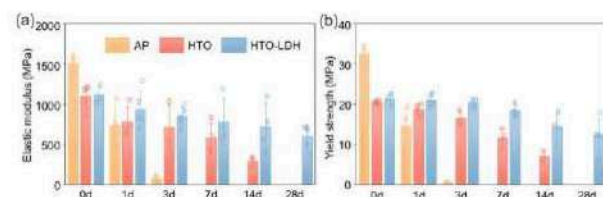


Fig. 3: Compressive elastic modulus and yield strength of Mg scaffolds after immersion.

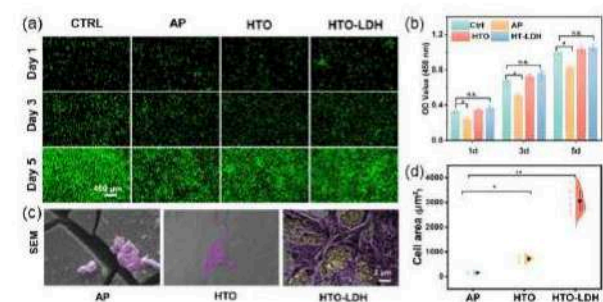


Fig. 4: (a) Live/dead staining. (b) CCK-8 assay. (c, d) In vitro cell adhesion of BMSCs.

DISCUSSION & CONCLUSIONS: High-temperature oxidation and hydrotalcite coating can significantly modify the biodegradation behavior and surface condition of Mg scaffolds, thereby improving their mechanical integrity and biocompatibility.

REFERENCES: ¹ J. Liu, B. Song, F. Song, et al (2022) *J Magnesium Alloy*. ² B. Liu, J. Liu, C. Wang, et al (2005) *Bioact Mater* **4**: 518-524. ³ Z. Lv, T. Hu, Y. Bian (2023) *Adv Mater* **35**: 2206545.

ACKNOWLEDGEMENTS: This template was modified with kind permission from eCM Journal.



Stress corrosion cracking testing as an assessment tool for novel biodegradable Mg alloys

Sochima S. Ezenwajiaku¹, Michele V. Manuel¹

¹ [Department of Materials Science and Engineering](#), University of Florida, Gainesville, USA

INTRODUCTION: Despite breakthroughs and advances in research of novel magnesium (Mg) biodegradable implants there is still a misalignment of *in vitro* and *in vivo* material performance. This is partially due to the limitations of current evaluation methods. There are few *in vitro* strategies and experimental frameworks that can mimic the complex dynamic process in the body. Mechanical properties, particularly during the degradation process, are a performance parameter that requires an improved assessment technique. As our field expands, it is appropriate to review and propose enhanced testing techniques for novel biodegradable metals.

CURRENT STATE OF ART: The majority of studies assessing new Mg biodegradable materials (BMs) tend to concentrate on mechanical properties before implantation/degradation and corrosion resistance as distinct factors¹. Ideal samples with tensile, yield, and elongations of > 300 MPa, 230MPa, and 15-18% respectively, are acceptable for orthopaedic fixation applications². However, when evaluating the effectiveness and applicability of BMs, sustaining mechanical support during the tissue healing process is critical. The change of residual strength during degradation has been coined as mechanical integrity. Recent shifts in the field have begun to add mechanical integrity as an evaluation criterion, currently *pseudo in-situ* mechanical testing is commonly employed as a standard practice. Nonetheless, there is a lack of standardization, and this method is subject to several limitations. However, an alternative approach to assessing mechanical properties during degradation is through stress corrosion cracking (SCC) testing. The evaluation of SCC has the potential to become a more reliable indicator of *in vivo* mechanical performance³.

STRESS CORROSION CRACKING TESTING: Magnesium (Mg) based alloys have shown significant promise among the various BMs, however, its poor chemical stability in corrosive environments, like the human body, is a challenge. This poor stability can lead to SCC, a failure mechanism that combines a harsh corrosive environment and applied stress, potentially leading to premature catastrophic failure. Factors such as, microstructure, alloy composition, pH, solution

constituents, temperature, and test conditions significantly affect the SC sensitivity of Mg alloys. The alloys' structural and compositional characteristics can mitigate the cracking sensitivity. It is widely recognized that robust passivation, which is the capability to form a protective layer on the surface, can decrease the susceptibility to SCC, but very few studies focus on the SCC resistance. Utilizing SCC test techniques like slow strain rate testing (SSRT) enables the extraction of both qualitative and quantitative data, including SC susceptibility indices for ultimate tensile strength and elongation to failure, critical stress intensity factor, as well as crack propagation patterns. These test methods can provide extensive information for evaluating mechanical properties/integrity during degradation in a shortened experimental timeframe.

DISCUSSION & CONCLUSIONS: Overall, effectiveness of biodegradable metals relies heavily on sustained mechanical support during tissue healing. However, current evaluation methods are primarily limited to corrosion resistance and pre-implantation mechanical testing. SSRT and other SCC testing methods have the potential to serve as a more reliable indicator of the mechanical performance of materials *in vivo*. Furthermore, these methods can aid in the establishment of new metrics and evaluation standards for the design of novel biodegradable materials and prediction of failure mechanisms.

REFERENCES: 1. Mei D, Zhang Q, Li Y, et al. The misalignment between degradation rate and mechanical integrity of Mg-Zn-Y-Nd alloy during the degradation evaluation in modified Hanks' solutions. *J Magnes Alloys*. Published online May 20, 2023. doi:10.1016/j.jma.2023.04.006
2. Khan AR, Grewal NS, Zhou C, Yuan K, Zhang HJ, Jun Z. Recent advances in biodegradable metals for implant applications: Exploring *in vivo* and *in vitro* responses. *Results Eng*. 2023;20:101526.doi:10.1016/j.rineng.2023.101526
3. Jiang J, Geng X, Zhang X. Stress corrosion cracking of magnesium alloys: A review. *J Magnes Alloys*. 2023;11(6):1906-1930. doi:10.1016/j.jma.2023.05.011



Microstructural characterisation and evaluation of mechanical properties of additively manufactured biodegradable Zn-xMg alloys

H Abenayake¹, C Persson¹, F D'Elia¹

¹ Division of Biomedical Engineering, Department of Materials Science and Engineering, Uppsala University, Sweden

INTRODUCTION: Among the three main families of biodegradable metals (Fe, Mg, and Zn)¹, biomedical Zn-alloys have recently garnered significant attention as promising materials for biodegradable implants. Compared to Mg-alloys that degrade too fast and Fe-alloys that degrade too slow, Zn-alloys have an intermediate biodegradation rate, resulting in optimal biocompatibility². However, numerous mechanical aspects of Zn-alloys such as strength, ductility, and static recrystallisation do not yet meet the required mechanical characteristics of natural bone structures, hindering their implementation as biodegradable implants². Due to the favourable mechanical properties induced by Mg alloying, Zn-Mg alloys have attracted increased interest in recent years³. Based on experimental evaluations in the literature³ and thermodynamic calculations, a Mg alloying content of less than 1 wt.% has been identified as ideal for improving tensile strength while minimally compromising ductility. Furthermore, the complexity of natural bone makes Additive Manufacturing (AM) a promising method for bone replacement due to its superior design flexibility, along with its unique ability to tailor microstructure and mechanical properties. Thus, the purpose of this study was to evaluate the mechanical behaviour of three additively manufactured Zn-xMg alloys (x=0.06, 0.5, and 1 wt.%) in relation to their microstructure, influenced by Mg content.

METHODS: Alloys were prepared by mixing powders of pure Zn and pure Mg. Laser powder bed fusion (L-PBF), a metal AM technology, was employed. As a measure of print quality, bulk density of as-printed samples was primarily quantified using image analysis of light optical microscopy (LOM) images. Phase analysis was performed using a combination of X-ray diffraction and energy dispersive X-ray spectroscopy. The microstructure was characterised using scanning electron microscopy and LOM. Mechanical properties were preliminarily assessed through microhardness measurements.

RESULTS: Relative densities > 99.5% were achieved for all three alloys under different processing windows (laser power, scanning speed, and hatch distance). As shown in Fig 1a, a

hierarchical microstructure featuring melt pool boundaries (dashed white lines), columnar (dashed red circle), dendritic (dashed yellow square), or combined structures (dashed green circle) was observed. Homogeneous distribution of Mg₂Zn₁₁ intermetallic (framed image) was identified as one of the primary strengthening mechanisms. This is evidenced by gradual increase in microhardness with increasing Mg content (due to increased amount of intermetallic) as depicted in Fig 1b.

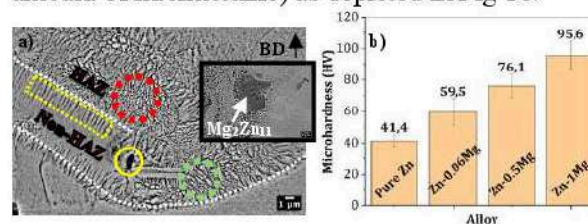


Fig. 1. a) An SEM image of as-printed Zn-0.5Mg, framed SEM image showing Mg₂Zn₁₁ intermetallic; b) Microhardness w.r.t Mg content

DISCUSSION & CONCLUSIONS: Although dense parts could be produced, porosity (Fig. 1a - yellow circle) originating from MgO-rich regions was observed, attributed to oxidised Mg powder particles. Heat-affected zones (HAZ) subjected to thermal cycling mainly consist of columnar structures due to the reduced net cooling rate, while non-HAZ consist of dendritic microstructures. Besides intermetallic strengthening, solid solution strengthening also contributes to the increased microhardness with higher Mg content. In conclusion, Mg alloying is a promising approach to addressing the poor mechanical properties of Zn, and future works aims to characterise tensile properties and recrystallisation effects.

REFERENCES: ¹H. Hermawan, Prog Biomater, 2018, 7, 93–110. ²G. Li et al., Acta Biomater, 2019, 97, 23–45. ³M. Voshage et al., Mater Today Commun, 2022, 32, 103805.

ACKNOWLEDGEMENTS: This work is conducted within the Additive Manufacturing for the Life Sciences Competence Centre (AM4Life). The authors acknowledge financial support from Sweden's VINNOVA (Grant no: 2019-00029), as well as the Swedish Research Council (2021-04708) and EU (grant no. 101110609; AMMagScaff).



The effect of powder preparation on mechanical properties and degradation behavior of biodegradable Fe-Mn-C sintered alloys for biomedical applications

Abdelhakim Cherqaoui¹, Carlo Paternoster¹, Simon Gélinas², Carl Blais², Diego Mantovani¹

¹: Laboratory for Biomaterials and Bioengineering, Research Center of CHU de Québec, Québec City, G1L 3L5, Canada;

²: Department of Min-Met-Materials Engineering, Laval University, Québec City, G1V 0A6, Canada.

INTRODUCTION: Fe-Mn-C alloys have recently raised interest for temporary biodegradable implants, thanks to their outstanding mechanical properties and good biocompatibility [1]. However, the control of their degradation rate could open their applicability to several applications [2]. Therefore, this study aims to develop a powder metallurgy Fe-Mn-C steel with porosity features suitable for a range of biomedical applications. The effects of powder preparation on the microstructure, the degradation rate, and the mechanical performances of Fe-Mn-C were investigated.

METHODS: Mixed (MX) and mechanically milled (MM) FeMnC powders were used to produce four groups of sintered FeMnC samples. The number in the condition name specifies the weight amount of milled powder. Particle size, chemical composition, and powder morphology were investigated using a laser particle size analyzer, microwave plasma atomic emission spectroscopy (MP-AES), energy dispersive spectroscopy (EDS), and scanning electron microscopy (SEM). Mixtures of MX and MM powders ranging from 55 μm to 75 μm were compacted in a uniaxial press (600 MPa) to obtain green compacts. They were sintered later at 1200 °C under an Ar-10%H₂ atmosphere for 3 h, followed by furnace cooling. Microstructural and mechanical characterization of sintered samples were carried out using SEM, x-ray diffraction (XRD), and transverse rupture tests. The degradation behavior was investigated through static immersion tests (up to 14 days) in Hanks' solution (pH 7.4) at 37 °C.

RESULTS: Chemical analysis of the starting powders and the sintered samples revealed variations in the amounts of Mn, C, and O. The MM powder exhibited a higher oxygen content of approximately 0.85 ± 0.04 wt.% compared to the MX powder, which had 0.06 ± 0.01 wt.%. In the final sintered samples, the amounts of Mn, C, and O were approximately 17 wt.%, 0.4 wt.%, and 0.15 wt.%, respectively. *Fig. 1* shows that a network of interconnected pores was successfully formed especially for MX, 25MX, and 50MX. Porosity decreased with increasing amount of MM powder. The highest density was achieved with the 75MM sample, which had a relative density of $RD_{75MM} = 81.18 \pm 0.52$ %. This later exhibited a

tensile rupture strength of 777 ± 23 MPa. Degradation rates (DRs) were in the range 0.04 ± 0.01 (MX) to 0.12 ± 0.02 mm/year (25MM). SEM/EDS analysis carried out on degraded surfaces revealed the presence of degradation product layers containing mainly Fe, Mn, C, and O. This result suggests that the degradation products formed on the sample surfaces during the static immersion degradation tests were mainly in the form of Fe and Mn carbonates.

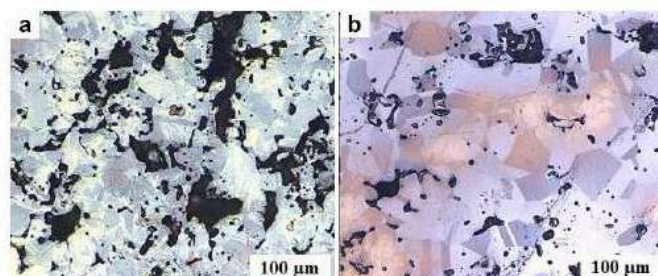


Figure 1. Nitral 2% OM images of sintered samples for a) MX, b) 75MM conditions.

DISCUSSION & CONCLUSION: The preparation method of the starting powder significantly influenced the final microstructure, mechanical performance, and degradation behavior of the sintered alloy. The addition of MM powder up to 50 wt. % resulted in complex microstructures composed of ferrite, austenite, and martensite. In contrast, 75MM exhibited a dual-phase microstructure with 61 wt.% austenite and 39 wt.% martensite. These microstructural variations, along with the densification levels of each sample group, led to differences in DRs and mechanical properties. Notably, the 75MM sample exhibited the highest mechanical performances ($TRS_{75MM} = 777 \pm 23$ MPa) but had low degradability ($DR_{75MM} = 0.06$ mm/year). In contrast, the 25MM sample demonstrated an optimal balance of improved DR ($DR_{25MM} = 0.12$ mm/year) and satisfactory mechanical strength ($TRS_{25MM} = 691 \pm 34$ MPa), making it suitable for biodegradable implant applications such as suture anchors [3].

REFERENCES: [1] Gambaro S. et al., *Mat Tod Comm* 27 (2021) 102250, [2] Schinhammer M. et al., *Acta Bio* 6 (2010) 1705, [3] Nagra N. et al., *Bone Joint Res* 6 (2017) 82

ACKNOWLEDGEMENTS: This work was funded by NSERC-Canada under the Alliance program.



Corrosion morphology influencing residual mechanical performance characterised by μ CT and digital image correlation

P Maier^{1,2}, B Clausius¹, M Brand¹, TS Tegtmeier¹, B Wiese³, N Hort^{3,4}

¹University of Applied Sciences Stralsund, School of Mechanical Engineering, Stralsund, Germany, ²Lund University, Department of Mechanical Engineering Sciences, Sweden, ³Helmholtz-Zentrum Hereon, Geesthacht, Germany, ⁴Leuphana University Lüneburg, Germany

INTRODUCTION: At severe corrosion, the loss of cross-sectional area is a suitable parameter for determining the residual mechanical performance¹. At the beginning of corrosion, pitting, if present, may be responsible for premature failure^{2,3}.

METHODS: Mg10Gd (extruded) tensile samples were corroded at 37 ± 1 °C for 24 h in Ringer's acetate solution at half the circumference of the gauge length. μ CT analysis (SkyScan 2214) was performed before (after corrosion) and after the tensile test. The tensile tests were done by applying Digital Image Correlation (DIC), using a GOM Aramis system. By the μ CT scans it is possible to correlate the corrosion morphology with the fracture area and the surrounding corroded region. By analysing DIC strain and correlated stress maps the increased stress intensity could be identified and correlated with the corrosion morphology.

RESULTS: Fig. 1 shows the changes in the DIC stress maps in the top view of the corroded part of the gauge length during the tensile test and the overlap with the speckle pattern shortly before fracture. The stress peaks correlate with the final fracture area. The 3D- μ CT scan in Fig. 2 shows the corrosion morphology of the tensile sample, its fractured area and the critical corrosion pit. This pit is expected to be responsible for the pit-to-crack transition since it is located within the fractured area, see also red part of the curve in Fig. 3.

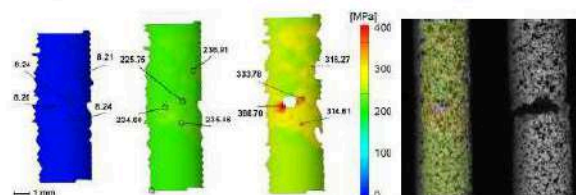


Fig. 1: DIC stress maps: separated & overlapping the sample, values shown are stress values calculated from the strain field.

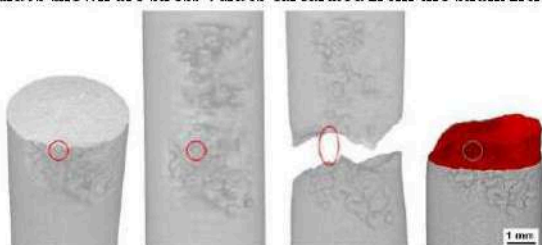


Fig. 2: 3D- μ CT scan of corroded tensile sample, gauge length: cross-section of critical area for crack initiation, tensile sample before and after fracture and highlighted fracture area (left to right), red circle: responsible pit (Fig. 3, z-position 9.63 mm).

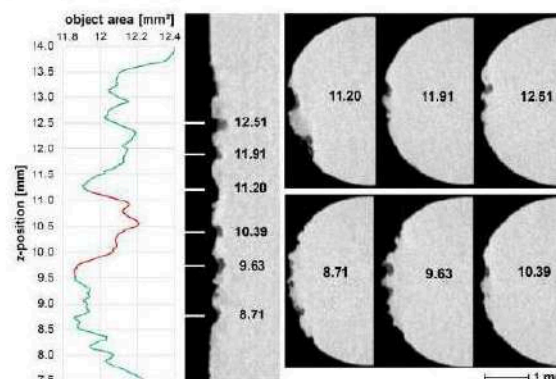


Fig. 3: 2D- μ CT scans: cross-sectional area (object area) along the gauge length (left), longitudinal sections with z-position and their corresponding cross-sections (right).

According to the object area curve in Fig. 3 there are 2 regions of small cross-section, at z-positions 8.71 and 9.63 mm. The red part of the curve shows the fractured area. At 9.63 mm a corrosion pit appears of critical shape (undercutting) and depth (291 μ m), and it surrounded by other pits. The crack propagates to z-position 11.20 mm, where also large pits are found, however of less critical shape (wide). The undercutting pit at 12.51 mm is not part of the fracture, the larger object area at this cross-section shows less pits than at 9.63 mm. According to Fig. 1, the stress map shows only increased stresses up to 400 MPa at final fracture.

DISCUSSION and CONCLUSIONS: This study makes clear that crack initiation can be independent of the smallest cross-section of the sample when pitting of critical shape, size and quantity occurs. It has been shown that the longitudinal planes in the direction of loading have to be also evaluated. The stress maps of the investigated samples clearly show with values up to 400 MPa and a TYS of 183 MPa and UTS of 238 MPa, that the corrosion pits have a notch effect and can be responsible for crack initiation when the alloy has a high pitting sensitivity. Interesting is, that the strength values were hardly influenced by corrosion of this extent, but the ductility was reduced to 63%. These results have the character of preliminary tests, statistically verified data will now be evaluated, with the focus on shape, size and accumulation of corrosion pits.

REFERENCES: ¹K. Van Gaalen et al. (2022) *Bioactive Materials*, 8, 545-558. ²B. Clausius et al. (2023) *Magnesium Technology 2023*, The Minerals, Metals & Materials Series, Springer, Cham, 95-98. ³P. Maier (2023) *5th International Conference on Biomedical Technology*, Abstractbook, 131-132.



Mitigating poor corrosion resistance of WE43 Mg alloy lattice structures through optimized structural design

Z Alomar¹, P Minárik², C Persson¹, D Drozdenko², F D'Elia¹

¹ Department of Materials Science and Engineering, Division of Biomedical Engineering, Uppsala University, Uppsala, Sweden. ² Faculty of Mathematics and Physics, Charles University, Prague, Czech Republic.

INTRODUCTION: WE43 Mg alloy is one of the few biodegradable alloys currently used in clinical applications. However, most WE-based implants in use today are bulk forms (e.g., bone screws) and are conventionally manufactured (e.g., casting, extrusion). With the advancement of 3D printing technologies, such as Laser Powder Bed Fusion (LPBF), the fabrication of more intricate and porous implants has become feasible. The main challenge with Mg-based lattice implants though, is their excessive degradation rate. Literature reports varying results for WE43, with some lattices losing structural integrity within a day, and others maintaining it for up to 28 days [1-2]. This study aims to understand the underlying mechanisms for such discrepancies, primarily by investigating the influence of structure geometry, including unit cell configuration and relative density, as well as that of alloy microstructure.

METHODS: LPBF process optimization was first performed through variation of the laser power and scanning speed. Various structures, including Triply Periodic Minimal Surfaces (TPMS) and strut-based lattices, were designed and fabricated alongside bulk samples. These designs were chosen to explore the influence of geometry on both microstructure and corrosion behavior. Bulk corrosion testing was performed through hydrogen evolution measurements in phosphate-buffered saline (PBS) for two distinct durations: an initial short-term test of 2 hours, and a longer-term test of 3 days. Furthermore, potentiodynamic polarization (PDP) and novel acoustic emission (AE) measurements were performed to identify underlying corrosion mechanisms at localized regions, including those attributed to the complex geometrical features of lattice structures.

RESULTS: High quality samples with densities as high as 99.6% were achieved. Short-term corrosion measurements on various samples indicated that strut-based lattice structures lost their structural integrity within the initial 2-hour period. In contrast, both the TPMS and bulk samples maintained their structural integrity after 3 days. AE measurements showed good correlation to PDP curves, clearly indicating the instance of surface

breakdown and re-passivation, as shown in Fig. 1 for a bulk WE43 sample (black circles). Moreover, the AE amplitude remained at a constant level until the end of the test, indicating minimal cracking and structural damage; in agreement with immersion tests, where bulk-samples maintained integrity. In contrast, a higher occurrence of surface breakdown was seen in the case of strut-based lattices due to sharper edges compared to TPMS. This is also consistent with the increase in surface exposure to the medium and enhanced electrochemical pitting observed within the microstructure.

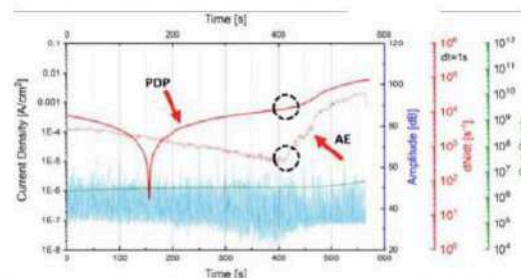


Fig. 1: AE short-term measurement of bulk WE43 sample showing the corrosion initiation (circled).

DISCUSSION & CONCLUSIONS: Structural geometry has a profound effect on the corrosion behavior of LPBF-fabricated WE43 Mg alloy. Both TPMS and bulk samples exhibit superior corrosion resistance compared to strut-based lattices whose inherent sharp edges and corners act as initiation sites for localized corrosion. AE and PDP measurements, together with microscopy, provide insight into the localized corrosion mechanisms and highlight the importance of optimizing strut thickness and orientation in lattices. Future investigations seek to design optimized lattice structures capable of striking a balance between mechanical performance and corrosion resistance.

REFERENCES: ¹ M. Li, et al. (2021) *Mater Sci Eng C* 119:111623. ² Y. Li, et al. (2018) *Acta Biomater* 67:378–392.

ACKNOWLEDGEMENTS: This project has received funding from the EU under Marie Curie grant no 101110609, as well as the Swedish Research Council (2021-04708), and Sweden's VINNOVA (2019-00029; AM4Life).



Tuning magnesium degradation by bipolar Plasma Electrolytic Oxidation

M Pavarini¹, C Alecci¹, M Castiglioni¹, M Moscatelli¹, R Chiesa¹

¹ *BioSurf lab, Department of Chemistry, Materials and Chemical Engineering "G. Natta", Politecnico di Milano, Milan, Italy*

INTRODUCTION: Magnesium and its alloys have significant potential as bone substitutes due to their bone-like mechanical properties and intrinsic biodegradability¹. However, their typically low corrosion resistance can impair their load-bearing capacity and interfere with the healing process by inducing an undesirable inflammatory response². In this context, electrochemical surface modification processes such as Plasma Electrolytic Oxidation (PEO) offer a promising way to control Mg corrosion by forming protective ceramic coatings that facilitate bone regeneration at the implant site³. In this work, we focused on the tuning of novel pulsed bipolar PEO processes for the treatment of magnesium alloys in order to improve the protective effect of the coatings, with the aim of enhancing the suitability of the technique for prospective clinical applications.

METHODS: The novel PEO treatments were carried out on Mg samples in a simple alkaline bath consisting of sodium hydroxide and metasilicate. Several pulsed bipolar treatment conditions were applied by tuning both the anodic and cathodic components in terms of relative amplitude and duty cycle, and their effect on the cross-sectional morphology and chemical properties of the coatings was evaluated by SEM-EDS. The corrosion properties of the samples and the adhesion of the coatings were then evaluated by potentiodynamic polarization under physiological-like conditions and by scratch tests, respectively.

RESULTS: The cross-sectional structure of PEO coatings formed under bipolar conditions is strongly dependent on the intensity and duration of the cathodic duty cycle. Although all coatings show a significant increase in thickness compared to those formed under unipolar conditions, a short cathodic phase produces a clear bilayer oxide with a thin, porous outer layer coupled to a thicker (up to 50 μm) inner one (Fig. 1). Conversely, coatings formed with longer cathodic phases have a coarser and more porous structure.

The potentiodynamic polarization tests (Fig. 2) showed a significantly attenuated corrosion behavior for the bipolar PEO coated specimens with a thicker compact oxide layer compared to both the unipolar PEO and untreated Mg specimens. In addition, the adhesion of the coatings appears to

benefit from such high compactness at the oxide-metal interface, as evidenced by the absence of delamination zones around the applied scratches.

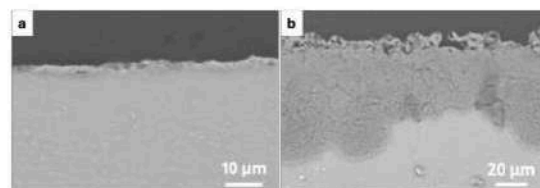


Fig. 1: Representative cross-sectional morphology of coatings formed in unipolar (SQ50, a) and bipolar (ACSQ10, b) PEO conditions.

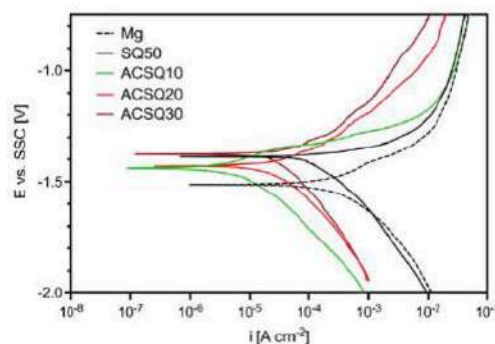


Fig. 2: Potentiodynamic polarization curves of PEO coatings formed in various bipolar conditions.

DISCUSSION & CONCLUSIONS: All bipolar PEO films show a pronounced bilayer structure, suggesting a differential formation mechanism between oxide outgrowth and ingrowth. Overall, the best balance of oxide thickness and compaction was achieved by applying short cathodic duty cycles. Such a balance proved promising in terms of corrosion control and could potentially be beneficial for longer-term retention of the base material's mechanical properties.

The preliminary results of this work emphasize the value of PEO coatings to significantly improve the corrosion resistance of Mg alloys, particularly by increasing the thickness and compaction of the oxide through pulsed bipolar treatments, while providing suitable surface stability for *in vivo* applications.

REFERENCES: ¹ P.C. Banerjee et al (2019) *Materials (Basel)* **12**:1–21. ² M.D. Costantino et al (2020) *Acta Biomater* **101**:598–608. ³ G.P. Wirtz et al (1991) *Mater Manuf Process* **6**:87–115.



Assessment of magnesium wire coatings for absorbable medical devices

Adam J. Griebel¹, Cody J. David¹, Jeremy E. Schaffer¹, Weilue He², Roger Guillory II³

¹Fort Wayne Metals Research Products Corp., Fort Wayne, IN, USA ²Michigan Technological University

³Medical College of Wisconsin, Milwaukee, WI

INTRODUCTION: Magnesium wire has the potential to serve as the backbone of many medical devices including stents, staples, and sutures. In certain cases, the relatively rapid degradation could necessitate surface treatments or coatings to prolong functionality¹. This study sought to evaluate the feasibility and effectiveness of such coatings. A promising Mg alloy candidate, LZ21^{2,3}, possesses excellent ductility and moderate strength, properties suitable for said devices. In this study, LZ21 underwent anodization and coating with polycaprolactone (PCL). The study's aims were to assess how anodization and polymer coating affect the degradation process of LZ21 wire, measure the in vivo degradation rate of LZ21, and obtain an in vitro - in vivo correlation factor (IVIVC).

METHODS: LZ21 wire was drawn by conventional cold drawing to 300 μm diameter, at which size it was annealed to impart high ductility. A portion of the wire was anodized in a proprietary process, imparting a thin layer containing Mg, F, O, and P. A portion of the anodized wire was then coated with an 80k M_n (number average molecular weight) PCL via extrusion to a total diameter of 340 μm . Corrosion of bare and coated wire was assessed in vitro (Hank's solution) and in vivo (subcutaneous mouse model). After corrosion, in vitro samples were tensile tested and serially sectioned to assess residual strength and area. In vivo samples were sectioned, and residual area was compared to the in vitro study to establish an in vitro - in vivo correlation (IVIVC).

RESULTS: Sections of wires after degradation are shown in Fig. 1. Residual areas over time are shown in Fig. 2. After 7 days in Hank's, bare wire retained 18% of its original strength, while anodized wire retained 60% over the same period and PCL wire had >90% out to 14 days. Residual strength and area values correlated well with each other ($R^2 = 0.945$). Degradation in vitro was more rapid than in vivo; at 7 days, the bare wire IVIVC was calculated at 8.1.

DISCUSSION: Bare LZ21 wire demonstrates reasonable corrosion rates in vivo, and anodization and PCL are effective and commercially scalable methods for slowing corrosion of Mg wire.



Figure 1. Representative transverse cross-sections of bare and coated wires after degradation in the indicated environment and duration.

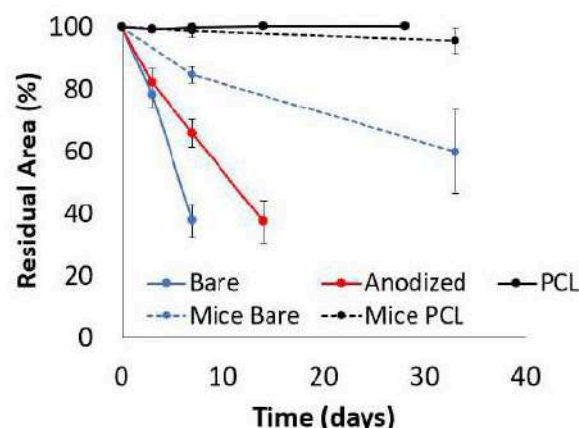


Figure 2. Residual areas of wire over time.

REFERENCES: ¹W. Ali, M. Li, L. Tillmann, et al (2023), *Biomaterials Advances* 146:213314. ²A.J. Griebel, J.E. Schaffer (2022) US20220251688A1 ³A.J. Griebel, C. David, J.E. Schaffer, et al (2024) *Magnesium Technology 2024*, 187-191.

ACKNOWLEDGEMENTS: U.S. NIH, NHBLI (Grant 1R15HL167221-01 to RJG) provided partial funding. The assistance of Dale Herndon, Lane Bailey, Sean Telley and Harold Perez in wire preparation and testing is gratefully acknowledged.



Towards an accurate prediction of magnesium biocorrosion by closer mimicking the in-vivo environment

M Yalcinkaya, A Bruinink, M Cihova, P Schmutz

Laboratory for Joining Technologies and Corrosion, Empa - Swiss Federal Laboratories for Materials Science and Technology, Dübendorf CH-8600, Switzerland

INTRODUCTION: Magnesium (Mg) has attracted great interest as a biodegradable metallic implant due to the formation of bioresorbable corrosion products during its degradation in the body. Yet, a challenge in the reliable prediction of degradation mechanism is that currently performed in-vitro experiments typically induce the formation of corrosion products with different chemical structures and transport properties than those observed in animal studies (in-vivo) [1].

From a materials perspective, another complexity level is generated by the low solubility of alloying and impurity elements in magnesium, resulting in the formation of cathodic secondary phases [2]. As the majority of published in-vitro studies involved such heterogeneous Mg surfaces, it remains unclear, if the corrosion product layer actually limits magnesium's anodic oxidation or decreases the cathodic reactivity of secondary phases.

To investigate the influence of these cathodic secondary phases on the Mg corrosion behavior in a physiological mimicking environment, an experimental setup was developed to include often overlooked in-vivo aspects such as solution flow, physiological pH buffering on the implant surface. Two very different materials were compared: low-purity Mg (99.9 wt% Mg; Fe >200 ppm), which contains a high amount of Fe-rich intermetallic phases, and ultra-high purity magnesium (XHP) (>99.999 wt% Mg; Fe <1 ppm) as a homogenous substrate without any secondary phase.

METHODS: Samples were exposed to our new formulation of a simulated interstitial body fluid (SIBF) that mimics the composition of human interstitial body fluid, based on an extensive literature review of the real measured values of inorganic ions and organic species [3]. The pH of SIBF is regulated with dynamic bicarbonate buffering and flown over Mg. The electrochemical reactivity of Mg samples was then evaluated by performing Electrochemical Impedance Spectroscopy (EIS). The samples were subsequently characterized using Scanning Electron Microscopy/Energy Dispersive X-ray Spectroscopy (SEM/EDS).

RESULTS: Fig.1 shows that the precipitation of corrosion products forms a porous intermediate layer on the Mg matrix and intermetallic phases.

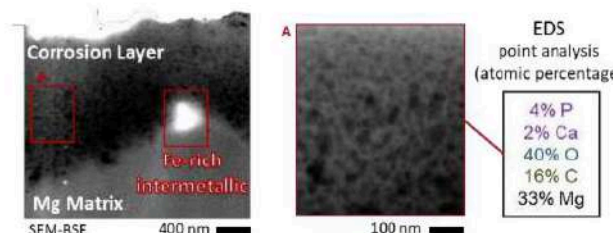


Fig. 1: Ion-milled cross-section of low-purity Mg, after 24 in SIBF (37 °C, 1 µl/sec, pH 7.4)

EIS and SEM/EDS results indicated significantly reduced cathodic reactivity of the intermetallic phases, where the obtained values became comparable to those of ultra-high purity Mg.

Furthermore, corrosion products formed in solutions with different ions were studied on both purity degrees to assess the ionic diffusion barrier effect of Mg-hydroxide, Mg-phosphate, and Ca-phosphate formed on a heterogeneous or homogeneous surface.

DISCUSSION & CONCLUSIONS:

The levels of free Ca^{2+} , PO_4^{3-} and CO_3^{2-} ions have completely opposite effects on the electrochemical reactivity of Mg depending on the presence of Fe-rich intermetallic phases. Non-physiological concentrations of these ions in test solutions might be responsible for microstructure-dependent variations seen between in-vivo and in-vitro studies. We further aim to understand how organic compounds and inflammatory pH levels affect specific corrosion products to provide a more accurate Mg biocorrosion mechanism.

REFERENCES: ¹ J Walker, S Shadanbaz, N Kirkland, et al (2012) *J Biomed Mater Res B Appl Biomater* 100:1134-41. ² D Höche, C Blawert, S V.Lamaka, et al (2016) *Phys. Chem. Chem. Phys.* 18:1279-91. ³ A Bruinink, *Handbook of Biomaterials* RSC (in press)

ACKNOWLEDGEMENTS: The authors would like to acknowledge the Metrohm Foundation for the financial support of this research.



Investigation of the ultra-structure of bone around Mg implant alloys and the connection to the mechanical properties

D.C.F. Wieland¹, K. Ishkakova^{1,2}, B. Zeller-Plumhoff¹, R. Willumeit-Römer¹

¹*Institute of Metallic Biomaterials, Helmholtz-Zentrum Hereon, Geesthacht, DE*

²*Institute of Catalysis Research and Technology, Karlsruhe Institute of Technology, Karlsruhe, DE*

INTRODUCTION: The potential of biodegradable magnesium implants for treating bone fractures is gaining attention due to their excellent biocompatibility and mechanical properties. However, despite the increasing importance of understanding the regeneration process and bone tissue response, there are limited studies on the ultrastructure reaction in bone. As the implant degrades, its by-products form, potentially affecting the ultrastructure [1-3]. We aimed to analyze how the ultra-structure changes might affect the mechanical properties of bone.

METHODS: Sheep bone explants with Ti and ZX00 Mg alloy screws (3.5 mm diameter, 16 mm length) were examined after 6, 12, and 24 weeks. high-resolution SAXS/WAXS experiments and nanoindentation to reveal differences in the strain distribution in the bone tissue were conducted at the P03 beamline at PETRA III, Hamburg. We investigated the ultrastructure (lattice spacing, crystallinity, orientation and the HAP platelet thickness) of the bone surrounding the implants, see Figure 1. Additionally, bone maturity and osteon density were studied using histology.

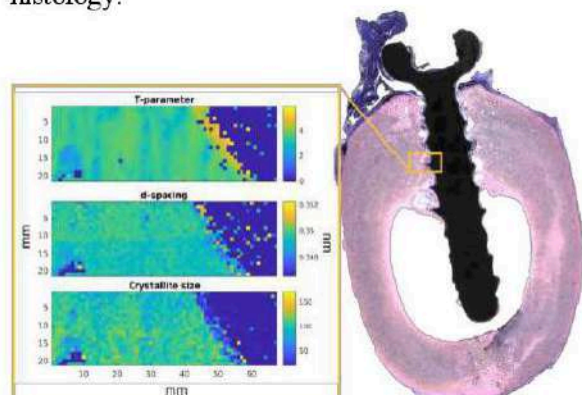


Figure 1: The example of the histological image of the ZX00 sample after 24 weeks of healing. The yellow box represents the scanned region of 0.3 by 1 mm². The exemplary maps showing T-parameter, d-spacing, and crystallite size calculated based on (002) Bragg's reflection distribution are displayed in the yellow frame.

RESULTS: The analysis revealed a significant decrease in the lattice spacing of the (002) Bragg's peak closer to the ZX00 implant compared to Ti.

The crystallite size showed no significant difference. The hydroxyapatite platelet thickness and osteon density decreased near the ZX00 implant interface. Correlative indentation and strain maps indicated higher stiffness and quicker mechanical adaptation for the bone surrounding Ti implants compared to Mg, see Figure 2.

DISCUSSION & CONCLUSIONS: The HAP (002) plane's d-spacing and platelet thickness decrease in the presence of the of ZX00 implants, with crystallinity and platelet thickness correlating to the bone remodeling and maturity. This is further supported by larger strains and lower stiffness observed in the bone surrounding ZX00 implants. Histological findings, such as lower osteon density in the presence of ZX00 implants, align with the hypothesis that bone maturation is slower around ZX00 than Ti implants.

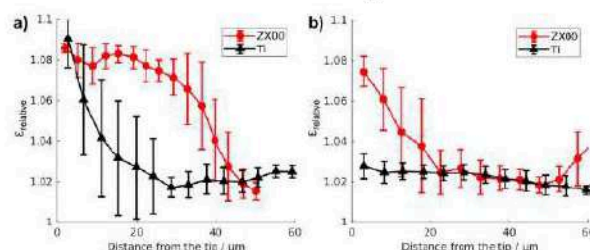


Figure 2 Relative strain ϵ in the bone tissue at the ZX00 or Ti implant interface after 6 (a) or 24 (b) weeks after the implantation, depending on the distance from the indenter tip at 150 and 200 mN, respectively.

REFERENCES: [1] T.A. Grünwald, et al. Acta biomaterialia 31, 448-457 (2016), [2] T.A. Grünwald, et al. Biomaterials 76, 250-60 (2016) [3] B. Zeller-Plumhoff, et al. Acta Biomaterialia 101, 637-645 (2020) [4] T.A. Grünwald, et al., Biomaterials 76, 250-260 (2016)

ACKNOWLEDGEMENTS: We would like to thank also thank Andrew Smith for the support at the I22 beamline and Benedikt Sochor for the support at the P03 beamline (proposals I-20210635 and I-20211088).



Towards a Standardized Magnesium Corrosion Method

Herb Radisch^{1,3}, Adam J. Griebel^{2,3}

¹ Pulmair Medical Inc., San Diego, CA, USA. ² Fort Wayne Metals Research Products Corp., Fort Wayne, IN, USA. ³ ASTM F04.15.03

INTRODUCTION: A critical property of absorbable metals is that they corrode in biological media. Accurately measuring and quantifying this property for magnesium alloys is far from straightforward in an *in vitro* setting, as the measured corrosion rate of a single specimen will depend on a host of factors, including media type, temperature, pH, test duration, buffering mechanisms, surface-to-volume ratio, corrosion metric (e.g. mass loss, volume loss, H₂ evolution, etc.), fluid mechanics, and corrosion product removal method. Variations in any of these can lead to differing measured corrosion rates and can complicate correlation with *in vivo* testing.

Due to the wide variety of possible *in vitro* corrosion tests, it is difficult to directly compare reported corrosion rates for various materials across the literature. The entire field would benefit from a single, repeatable method which can allow for direct comparison of different materials in different laboratories.

Recent work by the ASTM F04.15.03 task group has sought to establish such a test method. Three interlaboratory studies have taken place over the past 6 years, with substantial refinements to the method between each study. These data have been collected in support of a revision to ASTM F3268¹ which will likely include this method and data.

METHODS: A Degradation Control Material (DCM) was used by all labs in each study. The material was a wrought EK20 Mg alloy (Mg-1.1Nd-0.5Ho-0.25Zr (wt%)) alloy with a diameter of 6 mm and length of 8 mm. Luxfer provided DCM samples for the first two studies and Fort Wayne Metals prepared the DCM for the third.

In the first study, 10 specimens each at 8 sites were corroded in a modified Hank's solution for 3-5 days. At the end the study, corrosion products were removed by one of several methods specified in ASTM G1, and overall mass loss per day was reported. In the second study, participants at the 5 sites were required to use ASTM G1 solution C.5.2 (chromate) for corrosion product removal and report a calculated corrosion rate. In the third study, participants at 7 sites prepared the Hank's solution in a more tightly controlled sequence, and the duration was extended to 14 days. Mass loss

after chromate corrosion product removal was used to calculate a corrosion rate for each sample.

RESULTS: In the first study, measured mass loss varied widely by laboratory, with some even reporting mass gain. This large variability was attributed to the various permitted methods of corrosion product removal (e.g. chromate, mechanical brushing, etc.). In the second study, only the C.5.2 chromate solution was permitted for corrosion product removal. This made this step more consistent, but overall corrosion rates still varied widely between groups. In the third study, 1 of the 7 sites used inadequate resolution for mass measurement and their data was discarded, leaving 6 sites. The remaining corrosion rate results are shown in Figure 1 below. The average corrosion rate was 0.494 mm/yr. Standard deviation within a site was 0.069 and across sites was 0.151 mm/yr.

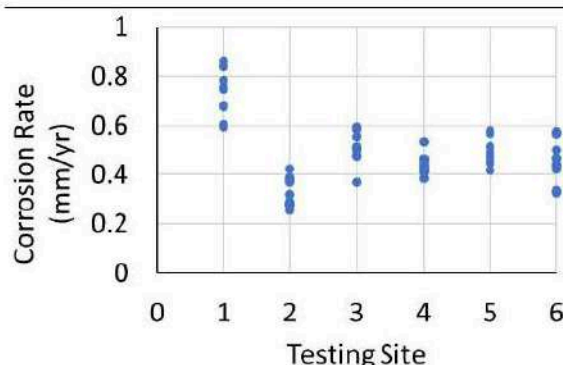


Figure 1. Corrosion rates for the DCM reported by the 6 sites testing 10 samples each for the third study.

DISCUSSION & CONCLUSIONS: Though the method has room for optimization, this effort will provide a common language for corrosion measurement of magnesium alloys intended for medical applications.

REFERENCES: ¹ASTM F3268: Standard Guide for *in vitro* Degradation Testing of Absorbable Metals. ²ASTM G1: Standard Practice for Preparing, Cleaning, and Evaluating Corrosion Test Specimens.

ACKNOWLEDGEMENTS: The efforts of the many individuals and organizations who have contributed to the method and collected and analyzed data are gratefully acknowledged.



Effect of medium renewal mode on the degradation behavior of Mg alloys for biomedical applications during the long-term in vitro test

MY Liu^{1,2}, QY Zhang¹, XH Tang¹, CX Liu¹, D Mei¹, LG Wang¹, SJ Zhu¹, ML Zheludkevich², SV Lamaka², SK Guan¹

¹ School of Materials Science and Engineering & Henan Key Laboratory of Advanced Light Alloys, Zhengzhou University, China. ² Institute of Surface Science, Helmholtz-Zentrum Hereon, Germany.

INTRODUCTION: In vitro testing environment closely mimicking in vivo condition and representative of degradation behavior of magnesium alloy is yet to be achieved. For example, the effects of medium renewal mode are still vague. In this study, we investigated the influence of the specific ratio of medium volume to surface area and the disposable medium real-time renewal mode (flow-through) on Mg corrosion based on three representative test protocols. It is found that in flow-through medium renewal mode, the composition of the medium is maintained quasi-constant which is essential for corrosion tests. This work is beneficial for ultimately establishing the representative in vitro testing protocols for Mg bioabsorbable materials.

METHODS: The immersion tests were performed at 37°C, either in HBSS (pH=7.42 ± 0.02) or isotonic 0.9 wt.% aqueous NaCl (pH=6.8). Three medium renewal modes were selected in this work: a) According to ISO 10993-121, 1.25 mL of stagnant medium per 1 cm² of sample surface area was used, called 1:1.25 in the following text; b) According to ASTM-G31-722, 20 mL of stagnant medium per 1 cm² of sample surface area was used, called 1:20 in the following text; c) Referring to the new test approach, the initial volume of 20 mL per 1 cm² sample surface area and the disposable media was renewed with the rate of 1 mL·min⁻¹, which is provided by a peristaltic pump.

RESULTS: (a) In the HBSS medium, the morphology and thickness of corrosion products on the Mg surface are affected by medium renewal modes, which influence the corrosion rate of both Mg materials. (b) The weight loss results of pure Mg in the NaCl solution under the three medium renewal modes are significantly different from the trends when tested in the HBSS solution. Moreover, the corrosion rates also show the difference between ZE21B alloy and pure Mg at the early stage of corrosion.

DISCUSSION & CONCLUSIONS: Compared with the 1:1.25 and 1:20 renewal modes, the flow-

through medium renewal provides the most stable ionic and pH environment, which is similar to the in vivo service environment of Mg implants. By comparing the corrosion behavior of Mg-based materials under the three medium renewal modes, it is found that the influence of medium renewal modes on the corrosion behavior of Mg can be weakened by using the large ratio of medium volume to surface area.

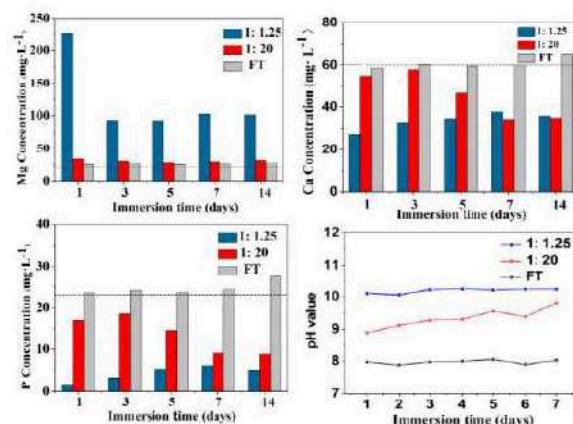


Fig. 1: The main ion concentration and pH value change under various HBSS renewal modes.

REFERENCES: ¹ International Organization for Standardization (2012), ISO 10993-12:2012, Biological evaluation of medical devices—Part 12: sample preparation and reference materials. ISO, Geneva, Switzerland. ² ASTM International (2004), ASTM-G31-72: standard practice for laboratory immersion corrosion testing of metals, Annual book of ASTM standards. American Society for Testing and Materials, Philadelphia, PA, USA. ³ C. Wang, C. Song, D. Mei, et al. (2022), Corros. Sci. 197 (2022) 110059.

ACKNOWLEDGEMENTS: The authors thank the Henan Province High-end Foreign Experts Introduction Program (HNGD2022037), the financial support from the National Key Research and Development Program of China (2021YFC2400703), and the National Natural Science Foundation of China (52301107).



Micro-Arc Oxidation of NiTi and Mg_{1.2}Zn_{0.5}Ca_{0.5}Mn Skeletal Fixation Device

LH Olivas-Alanis¹, D Cho¹, B Panton¹, T Avey¹, Chmielewska², M Sanguedolce⁴, A Luo¹, David Dean^{1,4}

¹ Department of Material Science and Engineering, The Ohio State University, Columbus, OH, US

² Multidisciplinary Research Center, Cardinal Stefan Wyszyński University, Warsaw, Poland

³ Department of Mechanical, Energy and Management Engineering, University of Calabria, Rende, CS, Italy

⁴ Department of Plastic and Reconstructive Surgery, The Ohio State University, Columbus, OH, US

INTRODUCTION: Stress shielding-induced bone loss is often attributed to the high stiffness of Ti6Al4V, the standard-of-care material used in skeletal fixation and replacement devices [1]. Hence, the development and application of stiffness-matched devices is of great importance. In addition to “debulking” strategies, the use of new, safe materials may improve device performance. We present here a test of a multimaterial mandibular graft fixation device. The two materials are a Mg alloy we developed and have studied Mg_{1.2}Zn_{0.5}Ca_{0.5}Mn; and a Ni-rich Nickel-Titanium (NiTi) alloy. Both materials are less than half as stiff as Ti6Al4V in their dense forms. The Mg alloy will degrade. At that point, the device will be incapable of stress-shielding. We have developed a coating strategy that uses Micro-Arc Oxidation (MAO) and sol-gel deposition of CaP. The surface treatment and coating is designed to ensure that the Mg alloy component will not begin to degrade until after bone healing is sufficiently complete.

METHODS: Our multi-material device comprises a Laser Based (PBF-LB) 3D printed NiTi shell and a cast-heat treated Mg_{1.2}Zn_{0.5}Ca_{0.5}Mn machined and solid insert (Fig. 1). The cylindrical Mg alloy insert is cut via electro-discharge machining (EDM). To prohibit accelerated galvanic corrosion, a Zn interlayer is placed between the two components. Once joined, the MAO of the Mg alloy surface is conducted under a current-controlled process with 2.5 A current for 15 minutes. A Stainless-Steel bucket, containing the electrolyte, acted as a counter-electrode. The alkaline phosphate electrolyte composition is 3g/L (NaPO₃)₆ + 8g/L KF·2H₂O [2]. The sample was connected to the power source with a Ti wire fitted to the NiTi shell and exposed to the electrolyte. A polymeric coating was placed over the NiTi surface, to direct the current toward the Mg insert, and removed with acetone after the MAO process is complete. The resulting surface was evaluated via SEM and EDS (Fig. 2). The newly treated Mg alloy surface was subsequently deep coated, with

several layers, with a CaP via a previously published sol-gel process [2].

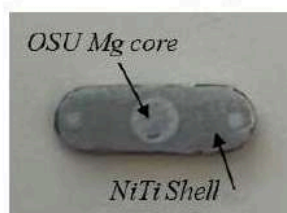


Fig. 1. MAO-treated multimaterial device showing the NiTi shell and Mg core.

RESULTS: Fig. 2 shows the resulting MAO-coated surface on the Mg insert. The process was conducted with a maximum current of 2.5A, and the output process voltage varied between 66 to 160V. The SEM image and EDS analysis show a dense, porous MAO surface layer on the Mg insert with a thickness of up to 50 μm. This porous surface is needed to strongly bind the CaP layer to the Mg alloy surface.

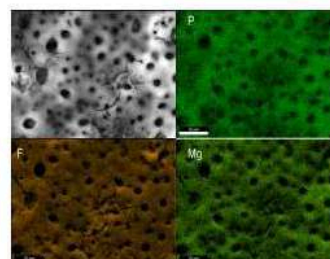


Fig. 2: SEM images Showing the presence of P, F, and Mg in the coating (MAO electrolyte).

DISCUSSION & CONCLUSIONS: This is the first attempt that we are aware of to achieve an MAO treatment on a Mg surface when joined to a NiTi component. This is a significant achievement given the conductivity difference between the materials. Moreover, the current tends to flow through more conductive NiTi rather than through Mg alloy. Hence, treating the Mg surface is challenging, but achievable. The next steps consider the application of this coating to highly complex surfaces.

REFERENCES: ¹ A. Chmielewska and D. Dean (2024) *Acta Biomaterialia* 173(1):51-65. ² H. Ibrahim et al., (2019) *Thin Solid Films* 687, 137456.

ACKNOWLEDGEMENTS: Partial funding was provided by OSU James Comprehensive Cancer Center Biomedical Device Initiative.



New insights into the microstructure of Mg-0.6Ca alloys using electron microscopy and Raman spectroscopy - A correlative characterization.

E Nidadavolu¹, M Mikulics², M Wolff¹, T Ebel¹, R Willumeit-Römer¹, J Mayer^{2,3}, H. Hardtdegen²

¹ Institute Metallic Biomaterials, Helmholtz-Zentrum Hereon, Geesthacht, Germany

² Ernst-Ruska-Centre (ER-C-2), Forschungszentrum Jülich, Jülich, Germany

³ Central Facility for Electron Microscopy (GFE), RWTH Aachen University, Aachen, Germany

INTRODUCTION: Powder processed Mg-Ca alloys are often reported to show homogeneous degradation due to their homogeneous microstructures [1].

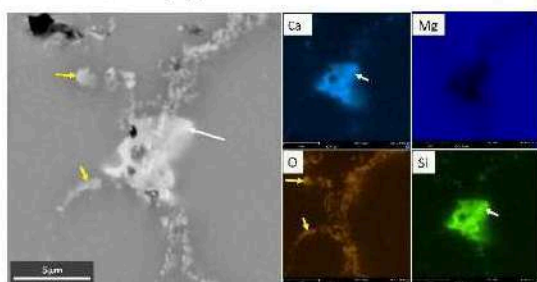


Fig. 1: Representative EDX map of MIM Mg-0.6Ca at a grain boundary.

However, ambiguity in the preliminary cell adhesion studies indicate the necessity to check surface contaminations due to carbon (C) residuals. This is probable as polymeric binders are used in additive manufacturing (AM) technologies like metal injection molding (MIM) and 3D printing [2]. In this regard, Raman spectroscopy was utilized to reveal carbonaceous residuals in the MIM Mg-0.6Ca microstructures.

METHODS: Mg-0.6Ca alloy feedstock was produced by mixing polymeric binder materials (waxes and backbone polymer) with the Mg-0.6Ca powder. Sintering was carried out under argon at 635 °C for 64 h. Later, a specimen of dimensions 6 mm x 6 mm (diameter x height) was machined for both SEM (coupled with EDX detector) and Raman spectroscopy. Raman spectra were collected with a confocal Raman microscope between 100 and 4000 cm⁻¹ wavenumbers.

RESULTS: EDX analysis revealed the presence of numerous fine precipitates located adjacent to each other along the grain boundaries (Fig.1). Predominantly, oxygen (O), calcium (Ca) and silicon (Si) intensities were observed. Certain precipitates comprised only O intensities whereas Ca and Si intensities coexist at random. In the range where carbon related Raman modes are detected (between ~1200 and ~2000 cm⁻¹), modes at nearly

1370 cm⁻¹ and 1560 cm⁻¹ are present which are ascribed to the presence of elemental C and a mode at 1865 cm⁻¹ is probably due to the C=C stretching mode. Grain interiors are mostly free of any precipitation giving rise to noisy signal in Raman due to the specimen's metallic nature (Fig.2 green spectra).

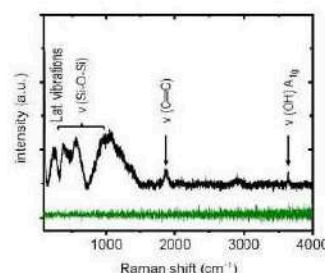


Fig. 2: Representative Raman spectra of MIM Mg-0.6Ca at a grain boundary (black spectra) and grain interior (green spectra).

DISCUSSION & CONCLUSIONS: The results indicate that Raman is a viable option to characterize carbon impurities on metallic biomaterial surfaces. The hydrocarbon cracking during the thermal debinding process (400-550 °C) releases C that might interact with Mg to form metastable carbides. The C=C in Fig. 2 can therefore be related to MgC₂ type carbides. Additionally, free C radicals are probable due to accelerated vacuum thermal decomposition of the hydrocarbons seen at wavenumbers 1370 cm⁻¹ and 1560 cm⁻¹ [2]. The exact nature of the stoichiometry with respect to Ca and Si still needs evaluation, however, the presence of C impurities might be important for future cell culture studies.

REFERENCES: ¹ E. Nidadavolu et al (2021), *Journal of Magnesium and Alloys* 9(2):686-703. ² J.G. Schaper et al (2018), *Advanced Engineering Materials* 26(11):1-9.

ACKNOWLEDGEMENTS: This research was funded by BMBF under the VIP+ project BioMag3D (Code: 03VP09852) and by the Joint Lab for Integrated Model and Data Driven Material Characterization (MDMC) of the Helmholtz Association.



Corrosion study of Fe20Mn0.5C parts obtained through additive manufacturing

I. Limón¹, D. Valdés¹, C. Paternoster², M. Multigner¹, M.D. Escalera¹, M. Muñoz¹, B. Torres^{1,3}, D. Mantovani², J. Rams^{1,3}

¹ Dpto. Ciencia e Ing. de Materiales, ESCET, Universidad Rey Juan Carlos, Madrid, Spain

² Laboratory for Biomaterials and Bioengineering, CRC-I, Dept Min-Met-Materials Eng. & CHU de Quebec Research Center, Regenerative Medicine, Laval University, Canada

³ Inst. de Inv. en Tecnologías para la Sostenibilidad, Universidad Rey Juan Carlos, Madrid, Spain

INTRODUCTION: Additive manufacturing (AM) offers unique opportunities to satisfy the complex design requirements of implants like stents. On the other hand, research on Fe-based biodegradable alloys for stent applications has increased considerably over the past decade due to their suitable mechanical properties like ductility and high ultimate strength¹. In this work, the effect of Laser Powder Bed Fusion (LPBF) parameters on the corrosion of Fe20Mn0.5C has been studied using potentiodynamic polarisation and Electrochemical Impedance Spectroscopy (EIS).

METHODS: An optimization of LPBF parameters (7×14×3 mm) was carried out varying the laser power (160-240 W) and the scan speed (340-640mm/s) (Fig. 1) in Renishaw equipment attending to the volumetric energy density (VED), which allows for quantitative comparison between parts manufactured by different laser parameters, and porosity of the samples. Three conditions were selected for the electrochemical tests: P160V640, P200V440 and P240V340. The electrochemical tests were carried out on at least three samples (15×15×3 mm) for each condition (one sample in each test) to guarantee the reproducibility of the results. The corrosion tests were performed using Hanks' modified solution. An Autolab PGSTAT 302N potentiostat was employed for electrochemical measurements. These measurements were conducted at room temperature in a three-electrode inert polymeric cell. The working electrode was the Fe20Mn0.5C sample, while the reference and counter electrodes were silver/silver chloride (Ag/AgCl) and graphite, respectively. Anodic polarization measurements were carried out at a 0.00166 V/s scan rate from -10 to 10 mV around the open circuit potential (OCP). The EIS tests were conducted at a frequency range from 10⁶ Hz to 1 mHz with 10 points per decade and a sinusoidal power amplitude of 0.01 V, after 1, 24, 48, 72, 96 and 168 hours immersion times.

RESULTS: The OCP values (Fig. 2) showed an increase from 1 hour to 24 hours of immersion,

with all three specimens reaching very similar OCP values (~ -0.73 V), after which they stabilized for all three conditions. The R_p values at the first 24 hours of the immersion period) were very similar for all conditions, around ~ 500 $\Omega \cdot \text{cm}^2$. After 24 hours, the P240V340 specimen gradually increased its resistance until 96 hours of immersion, reaching a value of ~ 16900 $\Omega \cdot \text{cm}^2$. The differences observed could be related to the different porosity of the samples.



Fig. 1. Additively manufactured samples still attached to the building platform.

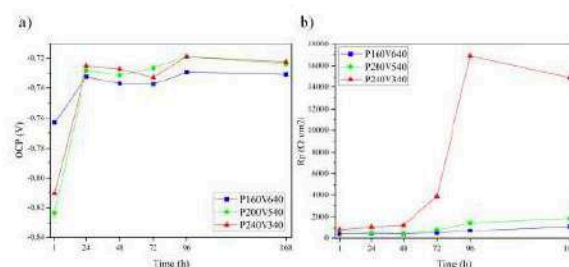


Fig. 2: Polarization results: a) open circuit potential (OCP), b) polarization resistance (R_p).

DISCUSSION & CONCLUSIONS: The corrosion rate strongly correlates with the porosity which in turn depends on the VED of the LPBF system during the manufacturing process.

REFERENCES: ¹ M. Schinhammer, C. M. Pecnik, F. Rechberger, A. C. Hänzli, J. F. Löffler, and P. J. Uggowitzer, "Acta Mater.", vol. 60, no. 6–7, pp. 2746–2756, Apr. 2012.

ACKNOWLEDGEMENTS: Financial support (AEI) PID2021-123891OB-I00, PID2021-124341OB-C21 and URJC -C1PREDOC2020.



Partially bioresorbable Ti-Mg composite dental implant (BIACOM[®])

M Balog¹, P Krížik¹, A M H Ibrahim¹, M Takáčová², M M de Castro¹, M Stamborska¹, A Catic³, Z Schauperl⁴, J Skiba⁵

¹*Institute of Materials and Machine Mechanics, SAS, Slovakia.* ²*Biomedical Research Center, Institute of Virology, SAS, Slovakia.* ³*School of dental medicine, University of Zagreb, Croatia.*

⁴*Faculty of mechanical engineering and naval architecture, University of Zagreb, Croatia.*

⁵*Institute of High Pressure Physics, PAS, Poland.*

INTRODUCTION: A high rate of adentia along with growing demand for cosmetic dentistry drive the dental implant (DI) market. Owing to their excellent biocompatibility, mechanical properties and corrosion resistance the commercial purity TiGr4, and TiGr5 alloy, are widely preferred in orthopedics and dentistry. Although Ti-based implants show good clinical performance, there are two issues that have not been fully addressed: i) the stress-shielding effect of implant over underlying bone structure, and ii) the insufficient bioactivity of the implants with surrounding bone in as-processed condition. We introduced a novel Ti-Mg composite, named BIACOM[®], tailored for the application of DI [1]. BIACOM[®] features highly strained ultrafine-grained pure Ti matrix embedded with interconnected Mg filaments skeleton. BIACOM[®] exploits the advantages of both biometals: a permanent Ti matrix provides the requested mechanical properties, a bioresorbable Mg component acts as beneficiary modulator for generating an osseointegrative surface via spontaneous dilution in body environment as well as bone formation stimulant. Mg, which has Young's modulus (E) much lower to that of Ti, gives rise to a reduction of the stress-shielding effect and has very good biodegradation potential. Owing to the porosity, which forms as a result of the selective Mg dilution, E of BIACOM[®] decreases and the bonding interface strength improves further. Concurrently BIACOM[®] maintains the mechanical performance and fatigue endurance, which complies with the minimum values specified in the ISO 22674 standard for the Type 4 biomedical material [2]. The BIACOM[®] specimens with the optimized surface yield acceptable corrosion rates of Mg [3]. Furthermore, they show a desirable *in-vitro* response, that is comparable to that of the TiGr4 reference. Preliminary implantation assays, which utilized large animal models and Ti12vol%Mg specimens, resulted in a positive response *in vivo* [4].

METHODS: The raw BIACOM[®] material rods, with Ti17vol%Mg composition, were produced from a plasma atomized TiGr1 and a gas atomized Mg99.8wt.% powders by a powder metallurgy

hydro-extrusion compaction. Two different DI designs: conventional and integrated, and two surface finishes: as-machined and HBSS prewashed were evaluated. The DI were CNC machined from as-extruded BIACOM[®]. Mechanical performance was modelled by FEA and experimentally verified in compliance with the ISO14801 standard for the fatigue testing of endosseous DI. The corrosion of Mg from the surface of the implants was evaluated by H₂ evolution volumetric method. *In-vitro* cytotoxicity biological response was assessed by the indirect contact MTT assay using DMEM extracts of DI and L929 cell line according to the ISO 10993-5. The TiGr4 DI were used as a reference.

RESULTS&DISCUSSION&CONCLUSIONS:

The present paper concisely reports the development of BIACOM[®] DI, which were designed in a way to reflect the peculiar properties of this novel partially bioresorbable material. The results confirmed that the integrated design BIACOM[®] DI with a prewashed surface meets the relevant mechanical and biological standards requested for endosseous DI, with an advantage of reduced stress-shielding effect and osseointegrative surface.

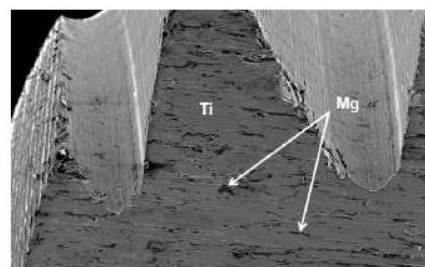


Fig. 1 The tip of the integrated BIACOM[®] DI.

REFERENCES: ¹ M Balog et al. (2019) *J. Mech. Behav. Biomed. Mater.* **90**: 45. ² A M H Ibrahim et al. (2020) *J. All. Compd.* **839**: 155663. ³ A M H Ibrahim et al. (2021) *Mater. Sci. Eng., C.* **127**: 112259. ⁴ A Catic et al. (2019) *Clin. Oral Implants Res.* **30**(S19): 163.

ACKNOWLEDGEMENTS: Supported by the APVV-20-0417, VEGA-2-0157-24 and ITMS 313021T081 projects and the Stefan Schwarz Fund.



Extruding Low-Profile Semi-Finished Products from Bioabsorbable Magnesium Alloys for Cardiovascular Implants – Influence of Process Parameters

N Hoevelmann¹, Prof. Dr.-Ing. Kristian Arntz², A Kopp¹, M Muether¹

¹Meotec GmbH, Aachen DE; ²Univ. of Applied Science Aachen, DE

INTRODUCTION: The use of biodegradable magnesium alloys in cardiovascular applications is highly attractive to follow the “leave nothing behind” strategy, that is widely followed by industry and clinics. [1] Therefore is necessary to form tubes or wires with high tensile strength, high elongation and small grain sizes.

METHODS: Three biodegradable magnesium alloys (WE43, ZX00, and AZ31) were casted, extruded to a diameter of 9.5 mm and heat treated to form billets for succeeding low-profile extrusion. Wires of a diameter 1.5 - 2.5 mm from 9 mm billets were pressed in a custom vertical low-profile extrusion line. Input variables for the low-profile extrusion process were temperature, speed, method (direct/indirect) and extrusion-ratio. The investigated influence on mechanical properties, microstructure, and surface quality were analysed by tensile testing, sectioning, etching and laser-microscopy.

RESULTS: Press speed and press temperature are interconnected, as the block temperature increases with rising press speed. A strong interaction between these parameters was expected but not confirmed. The lack of significance in speed could be due to the narrow range of speed values used in the experiments. At lower process temperatures, higher forces are required for forming, as shown in the process window diagram. The WE43 experiments demonstrate this, with three out of four presses at 460°C requiring maximum force. Temperature and speed are closely linked, increasing press speed raises forming temperature due to increased friction and adiabatic heating. Comparing the results from this study with those from literature on various magnesium alloys, there is no clear indication that higher temperatures or speeds result in lower tensile strengths. For WE43 samples, the highest tensile strength of 415 MPa was achieved at low temperature and high speed. No clear trend is observed for elongation; higher tensile strengths often correspond to lower ductility, but higher elongations are also seen with high strengths. Recrystallization mechanisms result in a finer grain structure during and after forming. Higher deformation degrees lead to smaller newly formed grains. This relationship is confirmed by comparing the grain sizes of 1.5 mm and 2.5 mm

wires across all alloys. The pressing method significantly impacts the target properties in the experiments conducted. Contrary to Zhang et al.'s [2] thesis that higher temperatures negatively affect tensile strength, higher tensile strengths were achieved with direct pressing for all alloys. Direct pressing likely involves higher forming temperatures due to increased friction heating the material. The advantages of indirect pressing, such as faster pressing with lower temperature development, were not utilized in this study for direct comparison.

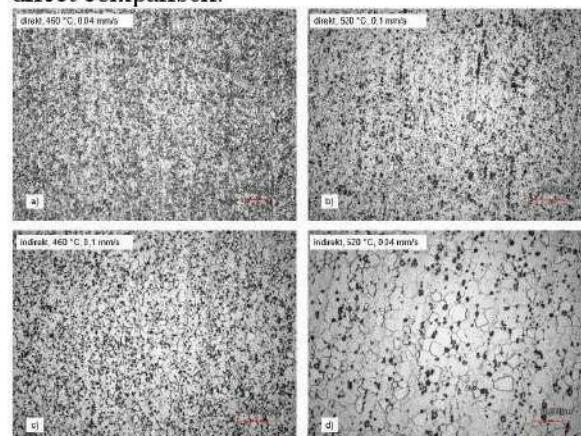


Fig. 1: Micrographs of the Ø 1.5 mm WE43 longitudinal samples at 1500x magnification.

DISCUSSION & CONCLUSIONS: The results indicate that in alloys WE43 and ZX00, only tensile strength is significantly influenced by the process parameters, with press method having a positive effect and temperature having a negative effect. Moreover, the interaction between press method and temperature negatively impacts tensile strength in ZX00 with increased process settings. Maximum tensile strengths exceeding 400 MPa, maximum elongations of 20%, grain sizes below 1 µm, and surface roughness depths smaller than 2 µm can be achieved.

REFERENCES:

- ¹ Gregory A. Stanley, MD *A Tale of Two Legs: Putting Patients Ahead by Leaving Nothing Behind* Endovascular today, April 2017
- ² Zhang, B. P.; Geng, L., et al. *Enhanced mechanical properties in finegrained Mg–1.0Zn–0.5Ca alloys prepared by extrusion at different temperatures* Scripta Materialia (Bd. 63), H. 10, S. 1024–1027



Influence of laser power and scanning speed on performances of LPBF Fe-16Mn-0.7C for bioabsorbable stent applications

Maria Laura Gatto¹, Paolo Mengucci¹, Marcello Cabibbo¹, Carlo Paternoster², Diego Mantovani²

¹ *Università Politecnica delle Marche, Ancona, Italy.* ² *Laval University, Quebec City, Canada;*

INTRODUCTION: Fe-Mn-C alloys have significant applications in developing temporary implants like bioabsorbable stents [1]. Laser powder bed fusion (LPBF), a promising additive-manufacturing technique, allows tailoring the microstructure by adjusting laser process parameters, expected to improve the degradation rate and mechanical properties of Fe-Mn alloys [2].

METHODS: In this study, we produced Fe-16Mn-0.7C bulk samples by varying laser power (50÷70 W) and scanning speed (700÷1000 mm/s), while maintaining a constant volumetric energy density (VED) of approximately 88 J/mm³ (Table 1), to understand the effect of printing parameters on the alloy's performances.

Table 1. Printing parameters used for producing Fe-16Mn-0.7C samples by LPBF technology.

Sample	Laser power [W]	Scanning speed [mm/s]	VED [J/mm ³]
P70v1000	70	1000	87.5
P60v855	60	855	87.7
P50v715	50	715	87.6

RESULTS: Fully austenitic microstructure, Fe and Mn amount in wt.%, and mechanical properties (microhardness approximately of 300 HV) appear comparable among the samples fabricated with different conditions. However, the defect analysis via X-ray micro-computed tomography (Fig. 1) allows to identify an operational window for producing fully dense Fe-16Mn-0.7C bulk samples using LPBF. Ongoing corrosion tests are being conducted to validate the obtained results further.

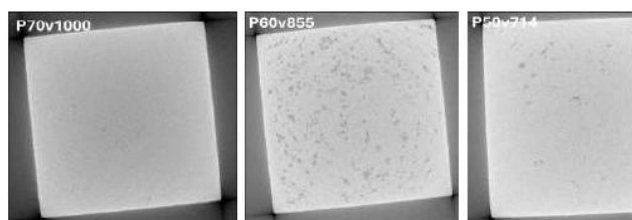


Fig. 1: 2D Cros- sectional slices of Fe-Mn-C samples produced by LPBF.

DISCUSSION & CONCLUSIONS: This operational window resulted in laser parameters (power and scanning speed) much lower than those reported in the literature [2].

REFERENCES:

- [1] Schinhammer, M., Hânzi, A. C., Löffler, J. F., & Uggowitzer, P. J. (2010). Design strategy for biodegradable Fe-based alloys for medical applications. *Acta biomaterialia*, 6(5), 1705-1713.
- [2] Liu, P., Wu, H., Liang, L., Song, D., Liu, J., Ma, X., & Baker, I. (2022). Microstructure, mechanical properties and corrosion behavior of additively-manufactured Fe-Mn alloys. *Materials Science and Engineering: A*, 852, 143585.

In Vitro

Wednesday, August 28th, 2024



Revisiting oxygen reduction during magnesium degradation

C. Wang^{1,2}, M. L. Zheludkevich^{1,3}, S. V. Lamaka¹

¹ *Institute of Surface Science, Helmholtz-Zentrum Hereon, Geesthacht, Germany.* ² *School of Materials Science and Engineering & Jiangsu Key Laboratory for Advanced Metallic Materials, Southeast University, Nanjing, China.* ³ *Institute of Materials Science, Faculty of Engineering, Kiel University, Germany*

INTRODUCTION: We have previously shown that the contribution of oxygen reduction reaction (ORR) to the total cathodic process during magnesium corrosion depends on the accessibility of metallic surface for molecular oxygen diffusing through the electrolyte layer [1-2]. The transport properties of the surface film in limiting oxygen diffusion have been shown to play a major role. For example, a higher contribution (16.5%) of ORR to the total cathodic process in case of slowly degrading ultra-high purity Mg compared to that of 35 times faster corroding pure Mg (1.3%) was explained by faster growing thick layer of Mg(OH)₂ on pure Mg (280 nm vs 70 nm on ultra-high purity Mg) [1]. However, we have recently uncovered a particular case when high-rate ORR occurs even in presence of a thick layer of corrosion products [3].

METHODS: Scanning micro-probe technique was used for measuring the local concentrations (50 μm above the metal surface) of dissolved gaseous O₂ and H₂ in mapping mode. The vertical approach curves were also recorded at different immersion time-points enabling calculation of local ORR currents (*i*_{ORR}). Clark-type amperometric O₂ or H₂ micro-sensors with a tip diameter of 10 μm were used, along with a fiber-optic O₂ micro-optode with a tip diameter of 50 μm. Traditional weight loss and hydrogen collection were also performed. SEM/EDS were used to reveal the comparative thickness and elemental composition of deposited Mg(OH)₂-rich layers of corrosion products.

RESULTS: Compared to high purity Mg (HP-Mg) and Mg-1Y alloy, ORR occurs at a fast rate on Mg-4Ag alloy even with a thick corrosion product layer, contributing significantly to the corrosion process (up to 28.3% of total cathodic process within 72 hours), Table 1. Re-deposition of Ag-containing products within the Mg(OH)₂ film decreases the transport limitation of O₂, significantly facilitating ORR and greatly contributing to the high degradation rate of Mg-4Ag. Superimposing spatial distribution of concentration of dissolved O₂ and H₂ (maps) indicates that the locations generating higher H₂ concentration (due to hydrogen evolution reaction HER) are often, but not always, aligned with the

areas of higher ORR. This suggests that in many cases, the same active cathodic sites are fed by two types of cathodic processes: HER and ORR.

Table 1: The ORR current densities calculated from approach curves of O₂-sensitive micro-probe and contribution of ORR to the cathodic current.

Sample	Weight loss from evolved hydrogen (mg cm ⁻² day ⁻¹) after 72h	Weight loss total (mg cm ⁻² day ⁻¹) after 72h	<i>i</i> _{ORR} (A cm ⁻²) from local O ₂ after 1h	<i>i</i> _{ORR} (A cm ⁻²) from local O ₂ after 24h	Contribution of ORR (%), after 72h
HP-Mg	2.87 ± 0.44	3.31 ± 0.51	1.31 × 10 ⁻⁵	3.38 × 10 ⁻⁶	13.3
Mg-1Y	2.66 ± 0.05	2.77 ± 0.09	4.99 × 10 ⁻⁶	1.99 × 10 ⁻⁷	4.0
Mg-4Ag	7.38 ± 0.33	10.29 ± 0.84	3.07 × 10 ⁻⁵	2.46 × 10 ⁻⁵	28.3

DISCUSSION & CONCLUSIONS: The ORR contributes to the total cathodic process during Mg corrosion, being secondary process, compared to HER. Previous finding suggested that the contribution of ORR decreases with time due to thickening of corrosion product layer, impeding O₂ diffusion to Mg interface where ORR can take place. Recent findings indicate that high electronic conductivity of the layer, e.g. due to re-deposition of metallic Ag, can support ORR on thick film (5-20 μm) for extended periods of time (at least up to 72h). The talk will present an overview of the recent publications [1-3] to demonstrate the contribution of oxygen reduction to the total cathodic process on degrading Mg and explain the factors influencing the extent of oxygen reduction for different alloys and testing media. The role of transport properties of the surface film in limiting oxygen diffusion will be considered. The advantages and downsides of using surface scanning micro-probes will be explained. Unravelling the mechanisms of Mg corrosion is vital for establishing reliable research methodologies, developing new alloys, and predicting Mg degradation behavior.

REFERENCES: ¹ C. Wang, D. Mei, G. Wiese, L.Q. Wang, M. Deng, S.V. Lamaka, M.L. Zheludkevich, *NPJ Mater. Degrad.* (2020) <https://doi.org/10.1038/s41529-020-00146-1>.
² C. Wang, W. Xu, D. Hêche, M.L. Zheludkevich, S.V. Lamaka, *J. Magnesium Alloys* (2023) <https://doi.org/10.1016/j.jma.2022.09.031>.
³ C. Wang, K. Qian, Y. Wu, D. Mei, C. Chu, F. Xue, J. Bai, M.L. Zheludkevich, S.V. Lamaka, *Corros. Sci.* (2024) <https://doi.org/10.1016/j.corsci.2024.111893>



Construction of Cell Sheet In Vitro Evaluation Model for Magnesium Alloy

Liangwei Chen

Department of Oral and Maxillofacial Surgery
Peking University School and Hospital of Stomatology
Beijing, China
chenliangwei@bjmu.edu.cn

Chuanbin Guo

Department of Oral and Maxillofacial Surgery
Peking University School and Hospital of Stomatology
Beijing, China
guodazuo@sina.com

Abstract—Biodegradable metals have shown great pro-osteogenic effects but lack an effective in vitro evaluation model. The cell sheet technique is an effective way to evaluate the toxicity and osteogenesis effect of biomaterials in vitro. In this study, we successfully constructed the cell sheet-magnesium model and proved its excellent resistance to toxicity in vitro. Magnesium alloy showed pro-osteogenic ability in the CS-Mg model, which is similar to that in the in vivo model. The RNA-sequencing assay showed the similarity of the differential gene expression of Mg alloy vs. control between the in vivo and the in vitro model. In conclusion, the cell sheet model can effectively evaluate the osteogenesis effect of magnesium alloy and show great potential in the evaluation of biodegradable metals.

Keywords—biodegradable metals; in vitro evaluation; cell sheet; biocompatibility; osteogenesis effect; direct method.

I. INTRODUCTION

Various degradable metals have shown great potential in tissue regeneration, but it is hard to evaluate the biocompatibility and osteogenesis ability in an in-vitro model, which impedes the clinical transition. Traditional in vitro evaluation models usually use an indirect way by employing metal extract. However, this can not fully reflect the in-vivo situation of biodegradable metals. So, it is urgent to explore a more effective in-vitro method.

The cell sheet (CS) technique involves the construction of a periosteum-like tissue stacked by multilayer cells, which has always been used in bone and cartilage regeneration. Recently, some studies have utilized the cell sheet in vitro 3-D model to evaluate the bone repair biomaterials because it better mimics the in vivo situation compared with the monolayer cell. The cell sheet has shown better resistance to toxicity and osteogenesis ability. This study aims to explore the feasibility of using the CS model to evaluate magnesium alloy in vitro.

II. RESULTS

A. The cell-sheet model shows better osteogenesis ability than the monolayer cell model

First, we assembled two layers and three layers of hBMSCs cell sheet (CS) respectively, and evaluated their osteogenesis ability. The ARS staining result showed that three layers of CS have the most mineralized nodules staining. RT-qPCR was consistent with the previous results. Therefore, we chose three-layer CS to assemble the Mg alloy-CS complex (CS-Mg) for

further study, with Mg alloy-monolayer cell (NC-Mg) as the control.

B. Mg alloy promotes osteogenesis in the cell-sheet model

First, we evaluated the models' resistance to toxicity. In CCK-8 assays, CS-Mg exhibited enhanced proliferation abilities, and flow cytometry showed lower apoptosis levels compared to NC-Mg. Then we drilled a 5 mm circle defect in the cell sheet and monolayer model to mimic the in vivo bone defect and tested osteogenesis ability. The immunofluorescent staining showed more osteogenesis-related proteins including RUNX2, BMP2, and OCN in the CS-Mg group than others. Furthermore, the RNA-sequencing results also showed that the osteogenesis-related genes including *RUNX2* and *BGLAP* in the CS-Mg group were higher than those in the NC-Mg group.

C. The gene expression in the CS-Mg model is similar to that in the in vivo model by RNA-sequencing

We constructed the in vivo mouse bone defect model with Mg alloy membranes as the treatment group. Then we used the RNA-sequencing to evaluate the gene expression difference between the Mg and Mg-free groups. A large number of osteogenesis-related genes were upgraded and the differential gene expression was similar to that in the in vitro model.

III. DISCUSSION

In this study, we proposed a cell sheet-based in vitro bone defect model for the evaluation of the efficacy of MgZnYNd alloy. The CS model had better osteogenesis ability compared with monolayer cells, so it can effectively shorten the time of in vitro evaluation. Traditional indirect in vitro evaluation models can be affected by many factors such as the dilution ratio of extract. In contrast, this CS-Mg model used a direct co-culture approach and showed better toxicity-resistant ability. The pro-osteogenic ability of Mg alloy in the CS-Mg model is similar to that when it is used in vivo. The gene expression evaluation results of this in vitro model correspond to in vivo experiments, indicating that it may be used as a useful tool for exploring the osteogenesis mechanism in vitro.

Furthermore, we used BMSCs to evaluate the osteogenesis effect of magnesium alloy. More types of cells and biodegradable metals can be explored in the future to evaluate the reaction of biomaterials to various kinds of tissues, such as soft tissue and nerve tissue.

National Key Research and Development Program of China (2021YFC2400703), the National Natural Science Foundation of China (NSFC) (52171234).



in-silico studies on the early bone healing potential of Mg based alloys

Gargi Shankar Nayak¹, Michael Roland¹, Björn Wiese², Norbert Hort^{2,3} and Stefan Diebels¹

¹ Chair of Applied Mechanics, Saarland University, Germany, ² Institute of Metallic Biomaterials, Helmholtz-Zentrum Hereon, Germany ³ Leuphana University Lüneburg, Institute of Product and Process Innovation, Universitätsallee 1, D-21335 Lüneburg, Germany

INTRODUCTION: The choice of implant material at the fracture site has an influence on the fracture healing from biological perspective as well as mechanical perspective. Biodegradable implants such as magnesium (Mg), zinc (Zn) have shown to fasten the secondary bone healing process as compared to that of bioinert implants such as titanium (Ti) ¹. Generally, this benefit of Mg was seen mostly only from biocompatibility perspectives ². However, the advantage of Mg is also there in terms of mechanical perspectives. Thus, in this work an *in silico* study was performed to visualize the effect of Ti and Mg as base materials for implants from mechanical perspectives in the initial phase of bone healing.

METHODS: A tibia fracture model was developed with the help of CT-scan data of a cadaveric specimen. The influence of implant material (Ti or Mg) on the interfragmentary strain (IFM) distribution at the fracture site was calculated via FEM. Abaqus was used for this purpose. The loading conditions were taken from the Gait cycle data from Orthoload. Claes tissue differentiation theory was applied to measure the conditions for secondary healing at the callus ³. Moreover, the stress distribution in the implant was also measured to observe the *stress shielding* conditions.

RESULTS: It was found out that in comparison to Ti, Mg implants have minimal *stress shielding* problem, which led to better mechanical stimulus at the fracture site. The conditions for secondary bone healing were better when Mg implants were used.

DISCUSSION & CONCLUSIONS: The influence of the implant base material on IFM required for development of callus into bone was investigated, where Mg was compared with Ti. The lower stiffness of Mg implant led to a better mechanical stimulus for bone formation in callus. As Ti implant took major amount of load, the callus was seen to have little lower IFM which can delay healing.

However, given Mg is a biodegradable implant, this study only confirms the initial phase of bone healing. In the next phase of this study, the biodegradability of the Mg will also be coupled to provide a better overview about the possibility of

applying Mg implant to repair tibia fracture in a long term.

REFERENCES:

- 1 K. Jähn, H. Saito, H. Taipaleenmäki, A. Gasser, N. Hort, F. Feyerabend, H. Schlüter, J. M. Rueger, W. Lehmann, R. Willumeit-Römer, E. Hesse, *Acta Biomater* **2016**, 36, 350.
- 2 H. Y. López, D. A. Cortés-Hernández, S. Escobedo, D. Mantovani, *Key Eng Mater* **2006**, 309–311, 453.
- 3 L. E. Claes, C. A. Heigele, Magnitudes of local stress and strain along bony surfaces predict the course and type of fracture healing, **1999**.



Exploring the biocompatibility and corrosion properties of a novel Mg-Ca-Zn-Y-Mn alloy for orthopedic implant materials

DC. Martinez¹, A Dobkowska¹, A Paradiso¹, D Drozdenko², A Farkas², K Mathis², K Pucia³, A Kaminski³, Y Kawamura⁴, W Swieszkowski¹

¹*Biomaterials Group, Faculty of Materials Science and Engineering, Warsaw University of Technology, Poland*

²*Department of Physics of Materials, Faculty of Mathematics and Physics, Charles University, Czech Republic.*

³*Laboratory of Experimental Animals, Medical University of Warsaw, Poland.* ⁴*Magnesium Research Center, Kumamoto University, Japan.*

INTRODUCTION: Mg-1Ca-0.5Zn-0.1Y-0.03Mn (at.%) alloy containing the long-period stacking ordered (LPSO) phases are characterized by high mechanical properties when compared to traditional Mg-based alloys [1]. This allows for considering it as temporary material for their potential use in biomedical applications. The present study investigates the biocompatibility and resistance to corrosion of the Mg-1Ca-0.5Zn-0.1Y-0.03Mn (at.%) alloy under physiological conditions.

METHODS: Rapidly solidified (RS) ribbons made of the Mg-1Ca-0.5Zn-0.1Y-0.03Mn (at.%) alloy were manufactured by single-roller melt-spinning, consolidated, and extruded [1]. SEM/EDX and EBSD were used to characterize the microstructure. The corrosion behavior was assessed using both *in vitro* and *in vivo* tests. Under cell culture conditions, electrochemical measurements and immersion tests were performed in supplemented Dulbecco's modified eagle medium. EDX and FTIR were used to determine the chemical composition of the corrosion products. The Mg-Ca-Zn-Y-Mn alloy's cytotoxicity and biocorrosion behavior was assessed through indirect and direct cell culture using murine fibroblast (L929) and osteosarcoma MG-63 cells. Finally, Mg-1Ca-0.5Zn-0.1Y-0.03Mn (at.%) (and pure Mg as a control) in the form of discs were surgically implanted in a calvaria bone defect on male Wistar rats (Permission nr. WAW2/031/2024) for 7 and 28 days. The *in vivo* corrosion rate from the Mg retrieved implants will be calculated, and the corroded surfaces will be characterized by SEM/FIB/EDX.

RESULTS: When analyzing *in vitro* findings, the pH rose after 3d from ~7.9 to ~8.3 was observed, with a decrease after 7d to ~8.1. The osmolality of the supernatants increased (0.331 ± 0.01 Osmol/Kg) compared to the control medium (0.304 ± 0.001 Osmol/Kg) after 3 d of immersion. It was stabilized after 5 d to 0.384 ± 0.02 Osmol/Kg. The calculated corrosion rate by the mass loss method was 0.38 ± 0.21 mm/year. L929 cells were over 90% viable in 100%, 50%, and 25% Mg extracts in indirect cell culture (Fig 1a, b). Similarly, viable MG63 cells were observed on the Mg alloy surface after 7d of cell culture (Fig1b, c), where the filopodia and cytoplasmic prolongations of the MG63 cells denoted the cell attachment and cell-cell communication. In addition, higher P and Ca content were observed in the

corrosion layer near the cells. These results allowed us to move forward with *in vivo* implantation to assess the Mg alloy using multimodal analysis (OCT, μ CT, and qualitative histology) when it encounters soft and bone structures (Fig. 1e).

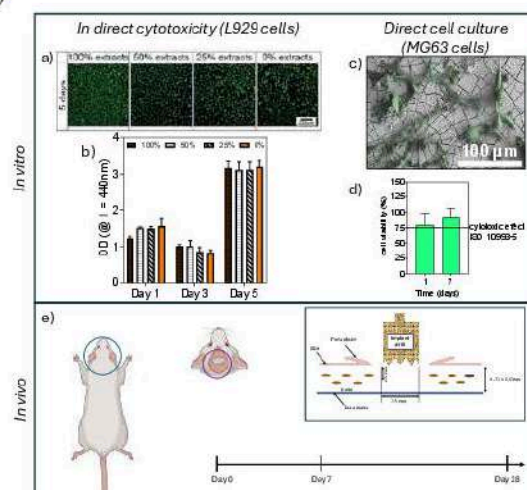


Figure 1: Representative images of the *in vitro* assessment (a-d) and the *in vivo* experimental design (e) to investigate the corrosion behavior of the Mg-1Ca-0.5Zn-0.1Y-0.03Mn (at.%) alloy.

DISCUSSION & CONCLUSIONS: The Mg-1Ca-0.5Zn-0.1Y-0.03Mn (at.%) alloy exhibited promising biocompatibility and corrosion resistance, with L929 and MG63 cells showing high viability and cell attachment. These properties, combined with the corrosion rate lower than 0.5 mm/year, indicate the alloy's potential for use as orthopedic implant material.

REFERENCES: [1] Y. Kawamura, F. Shimada, K. Hamada, S. Ueno, S. Inoue, Development of Biomedical Mg-1.0Ca-0.5Zn-0.1Y-0.03Mn (at.%) Alloy by Rapidly Solidified Powder Metallurgy Processing, *Mater. Trans.* 64 (2023) 2333–2336.

ACKNOWLEDGEMENTS: This research was conducted under the project "Development of Advanced Magnesium Alloys for Multifunctional Applications in Extreme Environments" No. V4-JAPAN/2/15/MagMAX/2022 financed by the National Centre for Research and Development in Poland in the framework of Visegrad Group (V4)-Japan Joint Research Program—AdvancedMaterials.



In vitro degradation analysis of 3D printed Mg-5Gd alloy scaffolds

K Pérez Zapata¹, E Nidadavolu¹, M Wolff¹, T Ebel¹, R Willumeit-Römer¹

¹*Institute of Metallic Biomaterials, Helmholtz-Zentrum Hereon GmbH, Germany*

INTRODUCTION: Magnesium (Mg) alloys have been potentially classified as candidates for use as tissue implants due to their biocompatibility, biodegradability, and mechanical properties. These alloys have been extensively investigated in orthopedic implants, and additive manufacturing (AM) of scaffolds has been seen as one of the most attractive alternatives for bone repair [1]. Within these emerging areas, tissue engineering enables the customization of porous implants to facilitate patient adaptation and bone growth. This requires scaffolds to have good degradability, interconnected structure to promote bone growth, and degradation control to withstand physical loads during healing [2]. The AM of magnesium alloys allows the production of structures similar to natural bone tissue with pore size ranging from 100 till 1000 μm . In this study, the results of scaffolds produced with different pore sizes and their influence on degradation behavior are reported.

METHODS: Three gyroid structures with different pore sizes and cell wall thickness were generated using Creo 7.0 software. Mg-5Gd feedstock comprised of the raw powder and polymer binder materials. Fused granular fabrication (FGF) technique was used to 3D print these scaffolds (AIM3D, ExAM255, Germany). Green parts were sintered under argon at 648 °C for 32h. *In vitro* degradation was carried out under physiological cell culture conditions (37 °C, 5% CO₂, 20% O₂, 95% rel humidity) using DMEM + Glutamax (Life Technologies, Darmstadt, Germany) supplemented with 10% FBS (PAA Laboratories, Linz, Austria). Scaffolds were characterized using micro-Tomography (μCT) and degraded specimens were analyzed using scanning electron microscopy (SEM) technique.

RESULTS: μCT analysis revealed the cell wall thickness of 650 μm , 790 μm , and 1000 μm , corresponding to 1250 μm , 1080 μm and 720 μm pore sizes, respectively in the produced structures. SEM analysis revealed scaffolds that were completely covered with degradation products (see Fig. 1). A homogeneous layer on the surface containing nodular morphologies and some needle-like crystals were found. Due to the different pore sizes of the scaffolds, different degradation rates were observed. As shown in table 1, the highest DR is associated with the sample with the smallest

pore size, which may be caused by an increase in surface area.

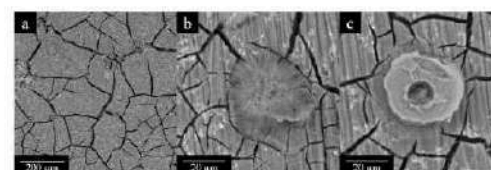


Fig. 1: Degradation products on Mg-5Gd scaffold structures a) homogeneous layer, b) needle, c) nodules. Table 1. DR values of Mg-5Gd scaffolds over a duration of 7 days.

Scaffold	Wall thickness (μm)	DR (mm/year)
P1250	650	5.4
P1080	790	3.9
P720	1000	1

DISCUSSION & CONCLUSIONS: It was found that the smaller pore sized P1000 scaffold showed a lower DR compared to others. With higher surface area a higher release of Mg ions upon contact with the cell culture medium is envisioned. Hence, pore size is significantly influential in modulating degradation behavior. Additionally, to maintain the mechanical stability of the scaffolds during degradation, a thicker strut i.e. smaller pore size can be beneficial. In this regard, compression tests on the produced scaffolds will be carried out. These preliminary results show that sinter-based 3D printing technology is a viable alternative to mass produce tailor-made Mg biomaterials. Using smaller nozzle diameters <200 μm during 3D printing further facilitates production of scaffold pore sizes < 720 μm reported here, which might potentially reduce the DR to <1 mm/year.

REFERENCES: ¹ N. Sezer (2021) *Additive manufacturing of biodegradable magnesium implants and scaffolds: Review of the recent advances and research trends*, JMA. ² I. Marco, (2017) *In vivo and in vitro degradations comparison of pure Mg, Mg-10Gd and Mg-2Ag: a short term study*, European Cells and Materials.

ACKNOWLEDGEMENTS: This research was carried out in the framework of BioMag3D project (code Nr. 03VP09852) financed by the BMBF. The authors acknowledge H Lüneburg, M Luczak and A Schuster for their expertise in methodology and technical assistance.



Advanced biodegradation imaging with novel correlative 3D X-ray and electron microscopy workflow - ZX00 case study

T. Akhmetshina¹, RE. Schäublin^{1,2}, AM. Rich¹, L. Berger¹, P. Zeng², I. Rodriguez-Fernandez^{3,4}, NW. Phillips^{3,7}, JF. Löffler¹

¹Laboratory of Metal Physics and Technology, Department of Materials, ETH Zurich, Switzerland

²Scientific Center for Optical and Electron Microscopy (ScopeM), ETH Zurich, Switzerland

³Paul Scherrer Institute, Villigen PSI, Switzerland

⁴Institute for Biomedical Engineering, University and ETH Zurich, Switzerland

⁷Present address: Mineral Resources, CSIRO, Australia

INTRODUCTION: This work presents a new correlative microscopy workflow that combines quantitative 3D X-ray ptychography (PXCT) with high-resolution electron microscopy. The combination allowed us to successfully investigate corrosion in a medical Mg alloy (ZX00) with minimal damage to the sample while still closely approximating *in situ* conditions.

METHODS: The ZX00 (Mg-0.45Zn-0.45Ca, wt.%) extruded alloy was prepared as described previously¹. A 5- μ m diameter pillar for PXCT was created with a focused ion beam (FIB). The measurements were performed at the cSAXS (X12SA) beamline of the Swiss Light Source (SLS) at the Paul Scherrer Institute. The sample was scanned before and immediately after 1 hour of immersion in simulated body fluid (SBF) at 37 °C and pH 7.4. The same sample was imaged using a FIB-SEM slice-and-view procedure. A lamella was extracted from the middle of the scanned pillar and investigated with scanning transmission electron microscopy (STEM).

RESULTS: The PXCT reconstructions provided 3D electron density maps of the pillar with nanoscale resolution (83 nm for the pristine and 123 nm for the corroded state). The high contrast efficiency of PXCT enabled a clear distinction of nanoscale Mg₂Ca precipitates from the Mg matrix, and their location was further confirmed with FIB-SEM. Moreover, it revealed the complex structure of the corrosion products where four different layers could be distinguished based on their electron density difference (Fig.1a). Electron microscopy with energy dispersive X-ray spectrometry (EDX) mapping allowed correlation of the electron densities to the precise chemical composition of the corrosion products. The results illustrate that the corrosion layer morphology is dense and defect-free, and the corrosion of the material is grain-orientation sensitive (Fig.1b,d). High-resolution STEM-EDX mapping (Fig.1c) revealed Zn redistribution and clustering at the metal-corrosion products interface.

DISCUSSION & CONCLUSIONS: Directly comparing the pristine and corroded states of the same sample enabled us to establish the influence of chemical heterogeneities and microstructure on corrosion resistance. The developed workflow paves the way for more advanced corrosion studies of bioactive materials.

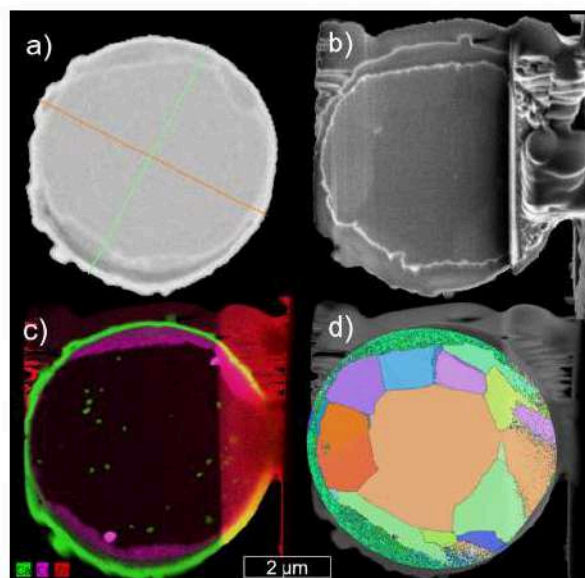


Fig. 1: Same ROI of the corroded pillar (cross-section) imaged with a) PXCT b) SEM c) STEM-EDX and d) TEM grain orientation map.

REFERENCES: ¹P. Holweg, L. Berger, M. Cihova, N. Donohue, B. Clement, U. Schwarze, N. G. Sommer, G. Hohenberger, J. J. J. P. van den Beucken, F. Seibert, A. Leithner, J. F. Löffler, A. M. Weinberg, *Acta Biomater.* 2020, 113, 646.

ACKNOWLEDGEMENTS: The authors gratefully acknowledge financial support from the Swiss National Science Foundation (SNF Sinergia, Grant No. CRSII5-180367). They thank the Paul Scherrer Institute for the allocation of beamtime at the SLS, ScopeM at ETH Zurich and CIME at EPFL, Lausanne for the access to its facilities.



Properties and characterization of magnetron sputtering coatings for biomedical resorbable applications

M Shekargoftar¹, S Ravanbakhsh¹, VS Oliveira¹, G Barucca², P Mengucci², M Cabibbo³, SS Parapari⁴, S Šturm⁴, A Sarkissian⁵, F Witte⁶, C Paternoster¹ and D Mantovani¹

¹ [Laboratory for Biomaterials and Bioengineering](#), CRC-I, Department of Min-Met-Materials Eng., & University Hospital Research Center, Regenerative Medicine, Laval University, QC, Canada; ² Department of Materials, Environmental Sciences and Urban Planning, Università Politecnica delle Marche, Ancona, Italy; ³ Department of Industrial Engineering and Mathematical Sciences, Università Politecnica delle Marche, Ancona, Italy; ⁴ Jozef Stefan Institute, Ljubljana, Slovenia; ⁵ Plasmionique Inc, QC, Canada; ⁶ Department of Prosthodontics, Geriatric Dentistry and Craniofacial Disorders, Charité Universitätsmedizin, Berlin, Germany

INTRODUCTION: Physical vapor deposition (PVD), allowing the condensation of material from the vapor of a solid target, is a widely-used thin film deposition technique already employed in several industries, from microelectronics to biomedical engineering^{1,2}. PVD systems differ according to the way the vapor is produced: one of them is called *magnetron sputtering*. It involves bombarding a target material, ejecting its atoms and directing it toward the substrate through appropriate magnetic fields, that leads to the formation of thin films on the substrate³. Magnetron sputtering (MS) can be used to obtain coatings through a controlled deposition rate, offering a fine tuning of the properties of the condensed material. This is needed especially for those applications in which a strict property control is needed, like for biomedical ones^{4,5}. The technique allows the deposition of pure elements, alloys, ceramic and other compounds, with or without the use of reactive gases. In this work, MS was used for deposition of several biodegradable coatings containing Fe- and Mg- for different applications. The effects of working gases and deposition parameters such as power and substrate temperature on the properties of the coatings were analyzed.

METHODS: The coatings were deposited using a MS system (Plasmionique MS300, QC, Canada). Coatings were deposited on a silicon substrate for preliminary process analysis, and then on functional substrates, for example Mg. The sputtering gas was Ar. The properties of the coatings were characterized using scanning and transmission electron microscopy (SEM and TEM), X-ray diffraction (XRD), X-ray photoelectron spectroscopy (XPS), and other complementary techniques to assess physical, electrochemical and mechanical properties; in particular, the corrosion behavior was studied in Hanks' solution.

RESULTS: Fig. 1 presents the cross-section micrographs of two Fe-Mn-based coatings enriched with W. The chemical composition was related to the different power applied respectively to the Fe-

Mn-C target, and to the W one: for example, the thickness for $P_W = 100$ W was $t = 0.8$ μm , while for $P_W = 400$ W to the thickness was $t = 1.8$ μm , with subsequent W increase, because of the increased sputtering rate of W. The corrosion rates associated with powers of 100 W and 400 W were 0.26 mm/y and 59.06 mm/y, respectively. In addition, it was found that increasing the substrate temperatures produced more homogeneous surfaces, decreased corrosion rates, and increased mechanical properties.

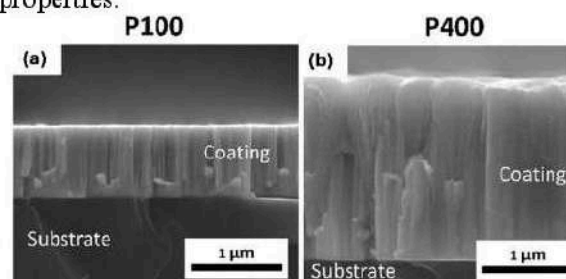


Fig 1. Cross-sections of Fe-Mn-C-W films deposited with a) $P_W = 100$ W and b) $P_W = 400$ W for 1 h

Mg-containing coatings showed a morphology, and corrosion properties related to the microstructure and to the presence of Mg.

DISCUSSION & CONCLUSIONS: Investigating various parameters and working gases in this work provides a template for design and optimization of coatings for diverse applications. Overall, the results contributed to increase the knowledge about magnetron sputtering coatings as a valid technique for deposition of resorbable coatings with controlled properties.

REFERENCES: ¹ Deng Y, *et al.* (2020), *Ceram Int* 46:18373–18390; ² Gupta G, *et al.* (2020). *Mater Today Proc* 38:259–264; ³ Heimann RB (2021), *Surf Coat Tech* 405:126521; ⁴ Li J, *et al.* (2022). *JOM* 74:3069–3081; ⁵ Nilawar S, *et al.* (2021). *Mater Adv* 2:7820–7841.

ACKNOWLEDGEMENTS: This work was supported by NSERC-Canada-Alliance. DM holds a Canada Research Chair Tier I (2012-2026).



Biofunctionalization of metal oxide thin films to promote rapid endothelial progenitor cells recruitment on endovascular implants.

Hugo Level^{1,2}, Diego Mantovani², Corinne Hoesli¹

¹*Stem Cell Bioprocessing Laboratory, Department of Chemical Engineering, McGill University, Canada* ²*Laboratory for Biomaterials and Bioengineering, CRC-I, Dept Min-Met-Materials Eng & Regenerative Medicine, CHU de Quebec Research center, Laval University, Canada*

INTRODUCTION: With the progressive aging of the population, cardiovascular diseases will continue to impose a significant burden on our societies. Consequently, endovascular implants remain crucial tools for treating patients who lack alternative options. Currently, most technologies focus on preventing cell proliferation on the implants' surface to mitigate complications, but this approach limits the long-term integration in the vascular environment¹. With remarkable regenerative properties, endothelial progenitor cells (EPC) represent a promising avenue to develop pro-healing endovascular devices². Here, we propose a surface modification strategy based on metal oxide thin films to promote selective EPC recruitment on metallic implants, including biodegradable alloys.

METHODS: We used biocompatible metal oxide films that served as a platform to covalently graft biomolecules on two different substrates: stainless steel and Hadfield steel (biodegradable iron-manganese alloy). Titanium and zinc oxide thin films were dip-coated on the substrates using a simple and scalable sol-gel process. It was then followed by the formation of a phosphonic acid monolayer containing carboxylic groups for subsequent biomolecule grafting. Different molecules were attached on the surface: biomimetic peptides promoting cell adhesion and antibodies to selectively capture EPC.

The quality of the surface modification was assessed using X-ray photoelectron spectroscopy (XPS) and scanning electron microscopy (SEM). To study the cell-surface interactions, EPC were first isolated from the peripheral blood of several donors. Cells were then seeded onto the modified surfaces for 2h in both static and dynamic conditions, before fixation and staining of the cytoskeleton.

RESULTS: Surface characterization with XPS shows successful modification of the different substrates covered by the oxide films. SEM imaging also supports the homogeneous coating of the surface. Cell adhesion assays yielded two key findings: first, the presence of an integrin-binding

peptide on the metal oxide surface significantly enhances EPC spreading, resulting in a remarkable 380% increase in cell surface area compared to the bare oxide (fig.1). Second, the addition of antibodies allowed for the rapid capture of EPC under dynamic conditions, with nearly 45% of the surface covered after only 2h. Finally, a synergistic effect has been observed between antibodies and biomimetic peptides, leading to both capture and enhanced spreading on our bifunctional surfaces.

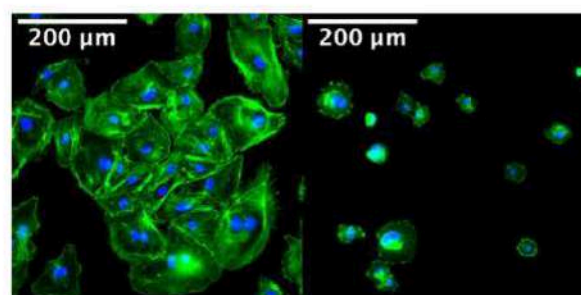


Fig. 1: EPC spreading on metal oxide (actin in green, nuclei in blue). Left: bifunctional surface (peptide+antibodies). Right: bare metal dioxide.

DISCUSSION & CONCLUSIONS: These results suggest that our approach enables the efficient modification of metallic implant surfaces using a metal oxide layer interface. Notably, this work is the first reported attempt to study EPC-surface interactions with metal oxides. In addition, we believe that the presented methods could have a noticeable impact in the field of bioelectronics. In the near future, our goal is to apply our technology on magnesium alloys, where our metal oxide film would serve both as a biofunctionalization platform and a corrosion barrier. Other metal oxides such as iron and molybdenum oxides will be investigated.

REFERENCES: ¹ Mori H., Atmakuri D. R., Torii S., Braumann R., Smith S., Jinnouchi H., et al. (2017). *Jaha* 6, e007244. 10.1161/JAHA.117.

² Aoki, J., Serruys, P. W., Beusekom, H. V., Ong, A. T., Mcfadden (2005). *Journal of the American College of Cardiology*, 45(10), 1574-1579. doi:10.1016/j.jacc.2005.01.048



Composite coatings on magnesium: *in vitro* comparative study

V. Patil¹, B. Williams², A. Amin¹, A. Navarro², T. McGehee², M. Elsaadany² and H. Ibrahim¹

¹College of Engineering and computer science, University of Tennessee at Chattanooga, USA

²Department of Biomedical Engineering, University of Arkansas, USA

INTRODUCTION: The biodegradable nature of Magnesium (Mg) and its alloys in aqueous environments renders them appealing for diverse biomedical applications such as bone fracture repairs [1]. Nevertheless, there are notable challenges that could limit the utilization of Mg and its alloys for this use, primarily stemming from their rapid corrosion rates [2]. Extensive research has been dedicated towards the development of protective coatings that can address this issue. Some of the most investigated coating processes are MAO, sol-gel, and polymer dip coatings. The goal of this study is to formulate various compositions of these promising coatings and provide a comparative assessment of their corrosion, morphological, and biological properties. Some MAO-coated samples were also infused with graphene oxide (GO) particles to investigate their effect on the assessed properties.

METHODS: The different types of coatings were created on the surface of a ZK60 Mg alloy due to its known biocompatibility [3]. A series of *in vitro* tests were conducted including potentiodynamic polarization (PDP), immersion, cytotoxicity study, and a contact angle test. Regarding the cytotoxicity study, the ISO 10993-5 extract method was performed on MC3T3-E1 osteoprogenitor cells. Coupon-leached media was produced by soaking the studied 5 sample groups in complete α MEM media (Thermofisher, USA) supplemented with 10% FBS and 1% penicillin-strep-tomycin for 72h according to the weight ratio of 0.2g/mL where the resulting media was diluted to 6x.

RESULTS: The presence of MgO, MgF₂, Mg(OH)₂ and Ca/P compounds in the MAO coating layers, and the deposited sol-gel and PCL layers were confirmed using EDS and XRD analyses. The MAO/sol-gel group showed the lowest corrosion potential (E_{corr}) and the MAO/GO group showed the lowest corrosion current density (i_{corr}). The MAO/sol-gel group showed almost no weight loss after 14 days of the immersion test. Meanwhile, the MAO/PCL group showed the most weight loss of the coated groups. In general, the results indicated a substantial enhancement in corrosion resistance within the sol-gel coated composite group and superior osseointegration and biocompatibility for the polymer-coated groups, see Fig. 1.

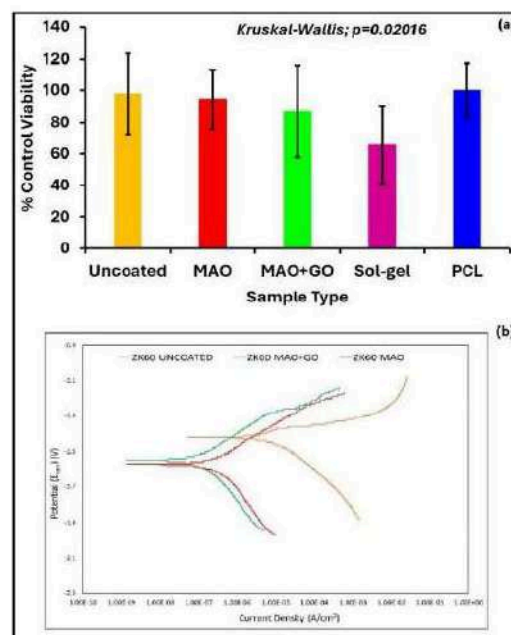


Fig. 1: *in vitro* results of the coated samples (a) cytotoxicity assessment, and (b) PDP corrosion test.

DISCUSSION & CONCLUSIONS: MAO/Sol-gel composite coating demonstrated the highest *in vitro* corrosion resistance, surpassing both the MAO and MAO/PCL coating groups. Also, the addition of GO layered particles to the MAO coating electrolyte improved corrosion resistance and biocompatibility. In addition, the MAO/PCL composite coating exhibited the greatest biocompatibility, evidenced by the highest cell viability and a hydrophilic surface. It is worth mentioning that there are inconsistencies and discrepancies between the corrosion results from immersion tests and electrochemical corrosion tests. Therefore, future studies should incorporate multiple corrosion testing methods to verify their findings. This study underscores the feasibility of producing biocompatible Mg-based implants with controlled corrosion properties through the application of diverse composite coatings.

REFERENCES: ¹Y. Chen, et al (2014) *Acta biomaterialia* 10:4561-4573. ²H. Ibrahim, et al (2017) *Materials Sc. and Eng. C* 70:870-888. ³M. S. Jia, et al (2023) *Bioengineering*: 10 (7), 757.

ACKNOWLEDGEMENTS: The authors acknowledge the support of the National Science Foundation – NSF CAREER Award # 2339911.



Electron microscopy study on WE43 bone explants

T Akhmetshina¹, N Zuberbühler¹, RE Schäublin^{1,2}, L Berger¹, AM Rich¹, W Rubin¹, JF Löffler¹

¹Laboratory of Metal Physics and Technology, Department of Materials, ETH Zurich, Switzerland

²Scientific Center for Optical and Electron Microscopy (ScopeM), ETH Zurich, Switzerland

INTRODUCTION: The medical Mg alloy WE43 remains one of the most extensively studied materials, both *in vitro* and *in vivo*. However, there is still a lack of understanding of how rare-earth elements redistribute after material degradation. In this work, we study *ex vivo* implants after 8 weeks of implantation via high-resolution electron microscopy. Apart from classical scanning electron microscopy (SEM), we employ transmission electron microscopy (TEM) and reveal nano-clusters of neodymium (Nd) in the degradation layer of the implant. We also demonstrate that yttrium (Y) presence in the corrosion products and tissues may be difficult to detect due to the high concentration of phosphorus (P) and the overlapping energies of the Y L-peak and P K-peak.

METHODS: A medical-grade WE43 (Mg-4Y-2.3Nd-0.5Zr, in wt.%) alloy was received from Luxfer MEL Technologies (Manchester, UK) and processed as described in Ref. [1]. Manufactured screws were implanted into adult Swiss Alpine sheep as described in Ref. [2]. After 8 weeks, the implants were extracted and prepared for histological examination using polymethyl methacrylate (PMMA) embedding.³ Chemical analysis was performed on non-stained PMMA-embedded slices ($n=3$) using SEM equipped with energy-dispersive (EDX) and wavelength-dispersive (WDX) X-ray spectroscopy detectors. A lamella was extracted from the explant using a focused ion beam (FIB) and analyzed with scanning TEM (STEM-EDX). Prior to extracting the lamella, EDX analysis was also performed.

RESULTS: We have imaged the non-stained histological slices of the explant screw (Fig.1a) with SEM using backscattered electrons (BSE). This imaging allows us to distinguish the components of the slice (implant, corrosion products and bones) with a contrast connected to the chemical elements (Z-contrast). In addition to the Z-contrast, we used EDX line analysis to distinguish between the metal, corrosion products and bone tissues. High amounts of Y and Nd were found in the corrosion products. In bone tissues located further away from the implant, Y was detected by WDX analysis. We have also observed that in BSE contrast the corroded screw retained its initial shape (Fig. 1b) and different layers of

degradation products could be distinguished. The lamella included three regions with different chemical compositions identified with BSE contrast and confirmed by SEM-EDX. High-resolution chemical mapping of the lamella with STEM-EDX revealed a high density of submicron Nd-rich clusters (Fig. 1d).

DISCUSSION & CONCLUSIONS: *Ex vivo* analytical electron microscopy can help understand the role of rare-earth elements in Mg-alloy biodegradation. Due to the limited energy resolution of EDX (100-150 eV), overlapping P and Y peaks can lead to misleading chemical analysis, and other techniques must be deployed to verify the results. TEM analysis showed an accumulation of Nd clusters at the interface of the corrosion products and bone.

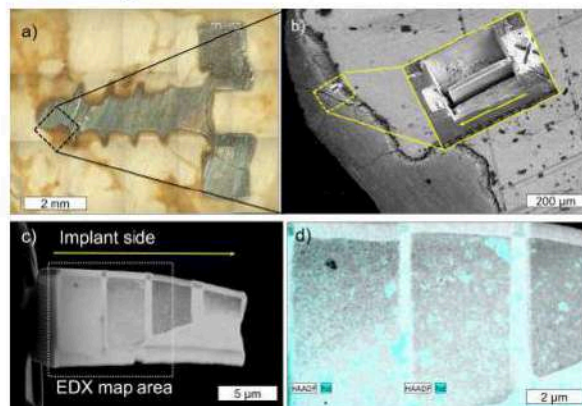


Fig. 1. Overview of the explanted screw (a) by light microscopy and (b) location of the lamella extraction. (c) STEM overview of the lamella and (d) EDX chemical map showing Nd clusters.

REFERENCES: ¹L. Berger, *et al.*, 14th Biometal Conf. (Aug. 2022), Europ. Cells and Materials (2023), in press. ²L. Berger, *et al.*, *Bioact. Mater.* (in review, 2024). ³J. D. Langhoff, *et al.*, *Int J. Oral Maxillofac. Surg.* 37 (2008) 1125-1132.

ACKNOWLEDGEMENTS: The authors gratefully acknowledge financial support by the Swiss National Science Foundation (SNF Sinergia, Grant No. CRSII5-180367). They thank Dr. Julius Ross and Prof. Katja Nuss (University of Zurich, MSRU group) for providing the histological samples. They also thank ScopeM at ETH Zurich for access to its facilities.



Investigating Biocompatibility and Cell Growth on the Surface of additively manufactured Zn1Mg Specimens

F. Fischer¹, Qun Zhao², M. Voshage¹, M. Praster², L. Jauer¹, A. Kopp³, E. Balmayor², J. Greven⁴, J.H. Schleifenbaum¹

¹Chair for Digital Additive Production DAP, RWTH University, Aachen, Germany, ²Experimental Orthopaedics and Trauma Surgery, Department of Orthopaedics, Trauma and Reconstructive Surgery, University Hospital RWTH Aachen, Aachen, Germany, ³Meotec GmbH, Aachen, Germany, ⁴Department of Thoracic and Cardiovascular Surgery, Medical Faculty, RWTH Aachen, University Hospital Aachen, Aachen, Germany

INTRODUCTION: The growing need for alternatives to autologous bone grafts when treating bone defects leads to the development of bioresorbable materials like zinc-magnesium¹. This work investigates the biocompatibility, cytotoxicity, and osteoblast cell growth of additively manufactured (AM) zinc-magnesium specimens to assess this alloy for clinical application (e.g. patient specific, load-bearing implants).

METHODS: Zn1Mg alloy cylinders from *Nanoval GmbH & Co. KG* were fabricated using a modified laser powder bed fusion machine from *Aconity 3D* with a diameter of 6 mm and a thickness of 1 mm. The specimens are “as-manufactured” (i.e. no further post-processing) for all tests. Osteoblasts were cultured in DMEM (Pan Biotech, Aidenbach, Germany, catalog number: P04-05550, 37°C, 5% CO₂) with the cylinders for up to 14 days to determine first aspects of biocompatibility and growth properties of the alloy. Cell viability, cytotoxicity, and proliferation were assessed using Live/Dead staining with calcein, DAPI staining, with subsequent fluorescence microscopy, and flow cytometry (FACS). Additionally, cellular morphology was examined using Phalloidin/DAPI staining and scanning electron microscopy (SEM).

RESULTS: Live/Dead staining shows high osteoblasts viability and proliferation on Zn1Mg after 7 days. FACS analysis confirms a 99.1% survival rate out of 40k cells (fig. 1, top). Fluorescence microscopy of DAPI-stained cells indicates an increase in nuclei over 3, 7, and 14 days. Furthermore, the phalloidin/DAPI staining (fig. 1 (center)) reveals a pronounced development of the cytoskeleton after 14 days. SEM images of the Zn1Mg cylinder surface after contact with the cells for 14 days (fig. 1 (bottom)) display the typical texture of additively manufactured parts, characterized by unmelted particles sintered to the surface. Embedded in this texture, osteoblasts can be seen.

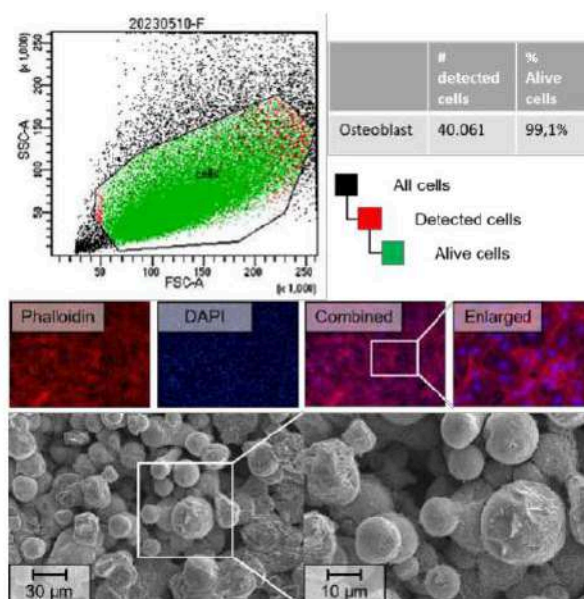


Fig. 1: (top) FACS analysis after contact with Zn1Mg (center) Phalloidin/DAPI staining of osteoblasts after 14 days (bottom) SEM images of cylinder surfaces after 14 days²

DISCUSSION & CONCLUSIONS: The 99.1% survival rate significantly exceeds the 70% minimum requirement of DIN EN ISO 10993-5, classifying Zn1Mg alloy as non-toxic. Cell viability and proliferation show positive responses to the alloy and its degradation products. Surface roughness does not hinder cell attachment, as indicated by observed filopodia suggesting cell migration. These findings support future use of AM Zn1Mg for patient-specific implants and scaffolds enhancing cell ingrowth.

REFERENCES: ¹C. Shuai et al. (2019) Biodegradable metallic bone implants, DOI: 10.1039/C8QM00507A ²M. Voshage (2024) Additive manufacturing of Zink Magnesium alloys, ISBN 978-3-98555-199-6

ACKNOWLEDGEMENTS: Parts of this work were funded by the German Federal Ministry of Education (13GW0404D & 03RU1U173C)



Characterisation and assessment of corrosion rate of HfO₂-PDLGA coated WE43 produced by atomic layer deposition for cardiovascular stent applications

CG Hynes¹, Z Ghaferi², S Malinov¹, A Flanagan², F Buchanan¹, A Lennon¹

¹*School of Mechanical and Aerospace Engineering, Queen's University Belfast, UK.*

²*Boston Scientific Ltd., Galway, Ireland*

INTRODUCTION: Atomic layer deposition (ALD) as a coating technique has several potential advantages for the development of magnesium (Mg) based bioresorbable cardiovascular stents and the control of Mg's rapid corrosion rates: ALD eliminates issues related to line-of-sight coating methods and can produce conformal coatings with tuneable, nanoscale thicknesses¹, that do not deleteriously impact on the overall stent geometry from an overall strut thickness perspective². Hafnium dioxide (HfO₂) is commonly produced by ALD and there is an emerging interest in its use as a suitable biomaterial. This study aims to investigate the potential of HfO₂ coatings, deposited via ALD, in conjunction with poly lactic co glycolic acid (PDLGA) – a common drug eluting polymer employed for cardiovascular stents – to regulate the degradation rates of WE43 magnesium alloy for stent applications.

METHODS: HfO₂ coatings were grown at 150°C by ALD on WE43 Mg coin components to produce HfO₂ layers with a thickness of 5 nm, 50 nm and 100 nm. XPS was conducted to assess coating composition. SEM studies evaluated the structure and morphology of the coating. Degradation studies were conducted in simulated body fluid (SBF) to measure hydrogen (H₂) evolution. Additionally, 0.3 mm dia. WE43 wires were coated with 50 nm HfO₂ and subsequently dip coated with PDLGA. Wires were immersed in SBF to assess the corrosion resistance of the HfO₂-PDLGA coatings and tensile testing was conducted before and after immersion for 40 hrs.

RESULTS: SEM images (Fig. 1a,b) revealed a uniform HfO₂ coating on the Mg surface. XPS analysis revealed an atomic concentration of O and Hf at a ratio of 2:1, indicating an adequate coating process (Fig.1c). H₂ evolution studies (Fig. 1d) revealed a thickness-based reduction in H₂ evolution across HfO₂ coated samples in a 21-day period. Tensile tests (Fig. 2 a,b) of the coated wires demonstrated improved retention of yield strength of HfO₂ coated wire specimens after immersion in SBF.

DISCUSSION & CONCLUSIONS: HfO₂ coatings demonstrated improved corrosion resistance of Mg, which was tuneable with respect to the coating thickness.

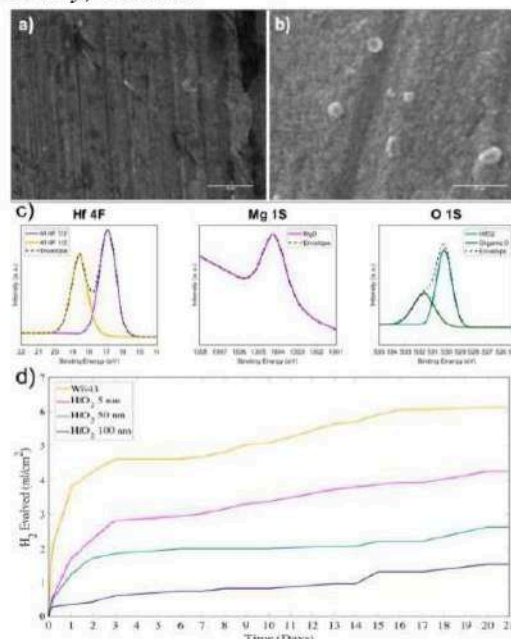


Fig. 1: SEM images of a) WE43 and b) HfO₂ 50 nm coating, c) XPS of 50 nm HfO₂ and d) H₂ evolution measures of WE43, 5 nm, 50 nm and 100 nm HfO₂ coatings.

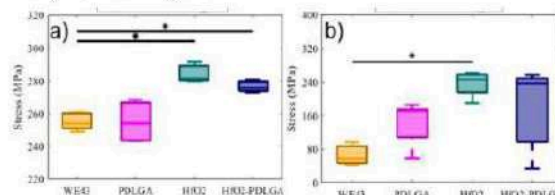


Fig. 2: Yield strength of WE43 wire, PDLGA, HfO₂ and HfO₂-PDLGA coating a) before immersion and b) after immersion in SBF.

Tensile testing of the coated wires demonstrated improved strength retention of the HfO₂ coated wires after immersion in SBF, although the addition of PDLGA-coating increased variability considerably (Fig. 2b). This study provides interesting preliminary insights into the potential role of HfO₂ as a coating material for controlling Mg degradation.

REFERENCES: ¹ Johnson, R. *et al. Materials Today*. 17, 236-246 (2014). ² Basiaga, *et al., Arch. Civil Mech Eng*. 17, 32-42 (2017)

ACKNOWLEDGEMENTS: This project has received funding from the EU's H2020 Research and Innovation Programme under the Marie Skłodowska-Curie grant agreement no 813869.

In Vivo

Thursday, August 29th 2024



Corrosion performance and corrosion rates from *in vitro* to *in humans* – Challenges in transferability and interpretation of results

J Reifenrath

Hannover Medical School, Department of Orthopaedic Surgery, Hannover, Germany

The field of biodegradable metals is fast evolving and expanding to new potential biometal candidates such as various alloying systems, coatings, fabrication processes or usage of new encouraging base materials (e.g. molybdenum). In those research fields the question of biocompatibility is often tried to address with simple and fast cytotoxicity assays, without realizing that the corrosion behavior and the specific environment have a substantial influence on the corrosion of the metal. After receiving the cytotoxicity results there are still many questions how these results represent the performance of the candidate metals *in vivo* in preclinical in animal models or even *in humans*.

Overall, the here presented comparison of *in vitro*, *in vivo*, *in human* and *in silico* methods can help in the choice of methods as well as in the interpretation of obtained results when corrosion performance of new promising biodegradable metals is evaluated, which directly influences *in vivo* or *in human* performance with regard to biocompatibility and functionality.

This lecture is aiming to provide an overview on the corrosion performance of different biodegradable metals (magnesium, zinc and iron) in different environments from atmospheric conditions over *in vitro* and *in vivo* to *in humans*. *In vitro*, choice of corrosion media, pH and/or mechanical stimulation influence corrosion performance and calculation of corrosion rate can additionally vary in dependence of the used test method (e.g. electrochemical measurement or weight/ volume loss). *In vivo*, the surrounding tissue with a huge variance in blood supply, inflammatory processes and the availability of corrosion accelerating elements has an impact on corrosion rate and morphology, which cannot be fully addressed in *in vitro* settings. Additionally, availability and applicability of test systems differ to *in vitro* settings, with mainly μ -computed tomography as tool to calculate corrosion rates. However, in dependence to the used CT-system a differentiation between original material and corrosion layer is not always possible, which limits comparable calculation of *in vivo* corrosion rates. Calculation of corrosion in humans is even more challenging, as radiographic follow ups often are restricted due to ethical issues and the assessment is limited in magnetic tomographic imaging. Finally, the use of *in silico* methods for corrosion prediction will be addressed.



Computational modelling of Mg-based implant degradation and bone healing

B Zeller-Plumhoff^{1,2}, T AlBaraghteh¹, D Priebe¹, N Pohl¹, S Trostorff³, R Köhl^{2,3}, R Willumeit-Römer^{1,2}

¹ Institute of Metallic Biomaterials, Helmholtz-Zentrum Hereon, Germany. ² Kiel, Nano, Surface, and Interface Science – KiNSIS, Kiel University, Germany ³ Department of Mathematics, Faculty of Mathematics and Natural Sciences, Kiel University, Germany

INTRODUCTION: The development and testing of new biodegradable metal implants is a time- and resource-consuming process that can generally be divided into *in vitro* testing and preclinical and clinical *in vivo* testing. For a long time one main objective to accelerate this process has been to enable a correlation between *in vitro* and *in vivo* corrosion rates. *In silico* methods can facilitate this process and, moreover, they can also be applied to predict the bone growth surrounding the implant. While models of varying detail and complexity exist, we are presenting an approach in which ordinary differential equations (ODEs) are used to model the degradation rate of magnesium-based implants, both *in vitro* and *ex vivo*, as well as the bone growth and its mineralization. For comparison, the bone growth surrounding titanium implants is also modelled. With these models, we aim to find a correlation between degradation rates in varying testing scenarios, as well as the degradation and bone growth, such that we may predict *in vivo* degradation and bone growth based solely on *in vitro* degradation rates.

METHODS: We are applying the degradation model presented by Gießgen et al.¹ to model the degradation of Mg-10wt.%Gd, for which both *in vitro* and *ex vivo* data are available. The bone growth model presented by Komarova et al.² is used to predict the bone growth when titanium implants in the shape of M2 screws are implanted into the diaphysis of rat tibia. In order to include the influence of the Mg-based implants on the bone growth, an additional term is inserted into the (ODE) describing the inhibition of bone growth, thus considering the release of Mg²⁺ ions to be inhibiting (or accelerating) the bone growth. We assume that all other parameters stay constant when considering titanium vs. Mg-10Gd and fit only those parameters describing the inhibition. The ODE models of implant degradation and bone growth are thus coupled. The experimental data is taken from Krüger et al.^{3,4} and Ćwieka and Iskhakova et al.⁵

RESULTS: The initial results using ODEs to model the degradation and resulting bone growth *in vivo* are promising. The model Komarova et al.

can be used to model the bone growth around titanium implants with a mean absolute error (MAE) for the bone volume fraction of 4 %. Similarly, the volume loss and bone volume fraction for Mg-10Gd can be simulated with MAEs of 2% and 4%, respectively. Figure 1 shows a comparison of the models with the experimental data for Mg-10Gd and Ti.

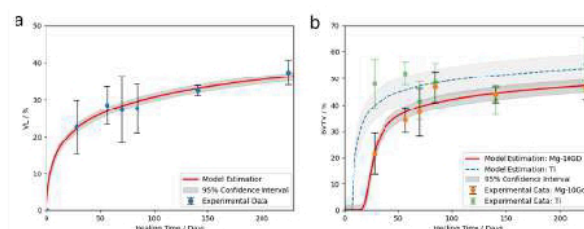


Fig. 1: Comparison of model results and experimental data for (a) volume loss of Mg-10Gd implants and (b) bone volume fraction (BTV) for Mg-10Gd and Ti implants, respectively. The experimental results are given as median \pm standard deviation. Confidence intervals are shown in grey.

DISCUSSION & CONCLUSIONS: Within this presentation, we will outline the correlation between model parameters when calibrated to *in vitro* and *ex vivo* volume loss data and how this may be used to predict the bone growth *in vivo*. To this end, we will validate the models by using data from Mg-5wt.%Gd data and ZX00 data. Additionally, we will compare how other degradation models may enhance the prediction.

REFERENCES: ¹ Gießgen et al. (2019), Mater. Corr. **70**(12). ² Komarova et al. (2015), Front. Cell Dev. Biol. **3** ³ Krüger et al. (2021), J. Mag. Alloys **9**(6) ⁴ Krüger et al. (2022), Bioact. Mat. **13** ⁵ Ćwieka and Iskhakova et al., under revision at Bioact. Mat.

ACKNOWLEDGEMENTS: This work was supported by the German Ministry for Education and Research (16DKWN112C).



How zinc becomes a stent: challenges and technological aspects in the design of new material

A Jarzębska¹, M Gieleciak¹, A Bigos¹, Ł Maj¹, K Trembecka¹, Ł Rogal¹, M Bieda¹, J Kawalko², D Wojtas³, A Mzyk⁴, J Skiba⁵

¹ *Institute of Metallurgy and Materials Science, Polish Academy of Sciences, Krakow, Poland,*

² *Academic Centre for Materials and Nanotechnology AGH University of Science and Technology, Krakow, Poland,* ³ *Department of Pathophysiology, Faculty of Medicine, Masaryk University, Brno, Czechia,* ⁴ *Department of Health Technology, Danish Technical University, Kongens Lyngby, Denmark,* ⁵ *Institute of High Pressure Physics, Polish Academy of Sciences, Warszawa, Poland,*

INTRODUCTION: The growing scientific interest in zinc stems from its optimal degradation rate, which makes it suitable to produce implants intended for temporary presence in the human body. However, zinc suffers from low mechanical properties and its recrystallization temperature is close to room temperature. This is why the immediate application of zinc in medicine is unattainable. Therefore, research focused on enhancing the mechanical properties of zinc-based materials and controlling their microstructural changes during stent manufacturing is of great importance.

METHODS: In this study, pure zinc and two alloys with the additions of magnesium and copper were chosen as candidates for absorbable stent manufacturing. To ensure high mechanical performance of zinc-based materials, plastic deformation in the form of hot extrusion at 250°C followed by three-pass hydrostatic extrusion (HSE) was carried out. The hydrostatically extruded rods were then machined into mini-tubes with a wall thickness of 150 µm using Electro Discharge Machining (EDM). Finally, different methods of shaping into stents, including laser cutting and EDM, were undertaken. At each step of the manufacturing, detailed microstructural examinations were performed using the Electron Backscattered Diffraction (EBSD) technique. Moreover, to establish the effect of the manufacturing on the functional properties of zinc-based materials, static tensile tests, immersion tests, and cytotoxicity assays were conducted on both rod-like material and mini-tubes. The zinc-based material showing the most optimal combination of properties was chosen for stent preparation.

RESULTS: The microstructural investigations revealed that hydrostatic extrusion significantly refined both the grains of zinc and the intermetallic phases, resulting in homogeneous microstructure.

This effect was more pronounced with an increasing number of alloying elements, yielding the average grain size of 1.6 µm for the ZnMgCu alloy. Despite greater grain refinement, the ternary alloy did not exhibit the best mechanical performance. Instead, the ZnMg alloy showed the highest ultimate tensile strength of 375 MPa with an elongation to failure of 35%. Interestingly, regardless of the chemical composition of the hydrostatically extruded materials, the corrosion rate remained comparable i.e., ~ 0.3 mm/year (calculated after a 14-day immersion in c-SBF). However, the degradation mechanisms differed among the materials, with alloys degrading more uniformly than pure zinc.

Based on cytocompatibility evaluation using material extracts, only the ZnMg did not lead to cytotoxicity in HUVECs as indicated by acceptable cell viability and cell morphology.

The studies also indicated that the EDM process required optimization to maintain the original microstructure caused by the hydrostatic extrusion process, and consequently, the properties measured for the rod-like materials. Additionally, the results highlighted the need for careful laser cutting procedures.

DISCUSSION & CONCLUSIONS: The studies have demonstrated that zinc is a viable candidate material for producing absorbable stents. Despite its low recrystallization temperature, careful selection of chemical composition and manufacturing methods can yield high-strength implants with appropriate degradation rates and cell responses.

ACKNOWLEDGEMENTS: This work was financially supported by the National Centre for Research and Development, project no. LIDER/54/0229/L-11/19/NCBR/2020



PROGRESSION OF THE ACUTE IN VIVO INFLAMMATORY RESPONSE TOWARDS ENGINEERED BIOABSORBABLE MG-AL IMPLANTS.

M Connon¹, S Raguraman², TP Weihs², RJ Guillory II¹

¹ *Medical College of Wisconsin & Marquette University, Joint Department of Biomedical Engineering,* ² *Johns Hopkins University, Department of Materials Science and Engineering,*

INTRODUCTION: While the foreign body reaction for traditional implant materials has been thoroughly described, there is a general lack of information regarding the dynamic inflammatory response towards bioabsorbable metals. Complicating the matter further, studies have demonstrated that the microstructure of absorbable metals plays a key role in regulating immune reactions, however emphasis has been mostly placed on the long-term response, without much consideration to the acute phase reaction. The goal of this study is to investigate the impact of microstructurally distinct and clinically relevant magnesium-aluminum (Mg-Al) implants and its impact on acute inflammation in vivo. We describe the corrosion behavior of Mg-Al implants in vitro and in vivo, and describe relationships between inflammation and corrosion behavior.

METHODS: Magnesium – 9% wt. aluminum alloys underwent two different thermal aging procedures. The first solution treatment (ST, 450°C for 168 hrs.) homogenizes the Al-rich phases into the Mg bulk matrix. Following ST, alloys were peak aged (STPA, 150°C for 100 hrs.) to produce secondary Mg₁₇Al₁₂ precipitates throughout the microstructure. Sample dimensions were discs at ST (Ø4.90 mm, t 0.33mm) and STPA (Ø4.91 mm, t 0.5mm). Corrosion progression was described for the implants in vitro in triplicates in DMEM + 10% FBS, and characterized with μ CT, SEM-EDS, and ICP-QQQ. Samples were implanted subcutaneously on either side of a male mouse's supine midline for 1-5 days. Luminol sodium salt saline solution (50mg/ml) was injected intraperitoneally to indirectly detect myeloperoxidase activity (MPO), and imaging was performed using a IVIS Spectrum μ CT system. μ CT acquisition was completed before luminol injection. Images were analyzed and presented in total flux (photon/second) with maximum and minimum thresholds indicated. Histological analysis was performed at endpoints throughout study.

RESULTS: The STPA implant generally experiences faster corrosion than the ST implant (>

2 days immersion), due to its inhomogeneous microstructure which contains Mg₁₇Al₁₂ precipitates, ultimately accelerating the micro galvanic corrosion reaction at the surface. The ST implant is still visualized at day 5 (Fig.1C), while the STPA implant is mostly degraded with some product still visible; this corroborates the previous findings in vitro showing STPA has a faster corrosion rate than ST. Fig. 1A-B shows the MPO activity indirectly measured using the luminol assay at day 1 and 5. At day 5 the highest luminol signal is colocalized with the STPA implant.

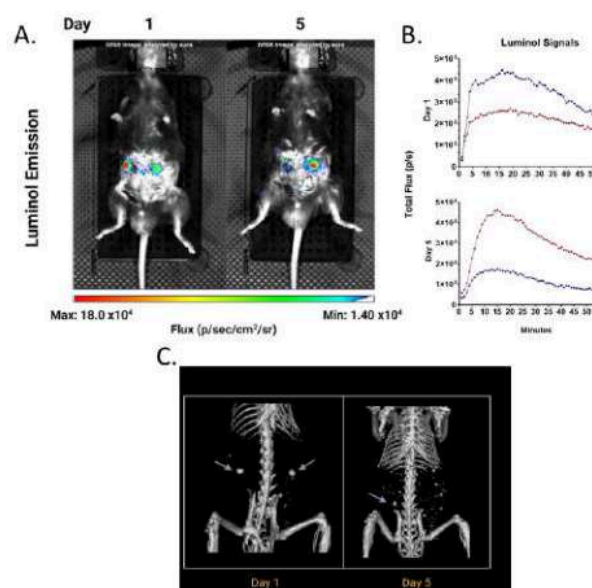


Fig. 1: A. Luminol imaging at days 1 and 5, B. Quantification of luminol imaging and C. μ CT imaging of implants at days 1 and 5.

DISCUSSION & CONCLUSIONS: This work indicates a persistent acute phase inflammatory reaction, possibly exacerbated by residual Mg₁₇Al₁₂ particles which are more noble and likely undegraded. This work will directly aid in future efforts to identify appropriate Mg microstructures not only for manipulating corrosion and mechanical performance, but also for tuning the inflammatory response towards more regenerative reactions.



Understanding the thrombogenicity of magnesium alloys for use in biodegradable cardiovascular stent applications

DEJ Anderson¹, CA Baker¹, J Johnson¹, J Goldman², MT Hinds¹

¹ [Department of Biomedical Engineering](#), Oregon Health & Science University, Portland, OR, USA.

² [Department of Biomedical Engineering](#), Michigan Technological University, Houghton, MI, USA.

INTRODUCTION: Biodegradable cardiovascular stents have the potential to treat vascular occlusion as a temporary device, allowing for the possibility of reintervention. Additionally, these devices reduce the need for long-term antithrombotic therapies, which are known to increase patients' bleeding risk. However, understanding the acute thrombosis response of any vascular devices, is critical. Mg alloys have so far led in the development of biodegradable stents, but preclinical and clinical testing is nearly always completed with antithrombotic and antiplatelet therapies. This work tested the *in vitro* and *ex vivo* responses of a variety of developed Mg alloys in a highly prothrombotic *ex vivo* model to characterize the alloys' responses and identify the mechanism causing these changes occur.

METHODS: Mg alloy wires were obtained from Ft Wayne Metals: WE43 (Mg-4Y-3Nd-0.4Zr), ZX10 (Mg-1Zn-0.3Ca-0.15Mn), and AZ31 (Mg-3Al-1Zn-0.5Mn). CoCr wires (Goodfellow, Inc; Co40-Cr20-Fe15-Ni15-Mo7-Mn2-C-Be) were used as a clinical control. *In vitro* testing was performed to quantify factor (F)XIIa and fibrin generation, indicating early and late ends of the contact pathway of coagulation, respectively.¹ *Ex vivo* testing was completed using a non-human primate model of acute thrombogenesis without antiplatelet therapies.¹ Autologous platelets and homologous fibrin were radiolabelled with ¹¹¹In and ¹²⁵I, respectively, to quantify the thrombus generation over 1hr exposure to flowing, whole blood. Downstream blood samples allowed for testing of the wire microenvironment to quantify myeloperoxidase (MPO), thrombin-antithrombin (TAT), and platelet factor 4 (PF4). Thrombi on the wires were qualitatively characterized with SEM.

RESULTS: The Mg alloys consistently showed lower thrombogenicity compared to the CoCr control. Specifically, they had slower fibrin take off times, decreased quantities of FXIIa generation, and lower platelet and fibrin attachment *ex vivo*. *Ex vivo* results (Fig 1) demonstrated the significantly lower quantities of platelets and fibrin on the wire coils after 1hr of flowing, whole blood for ZX10 and WE43, compared to CoCr.

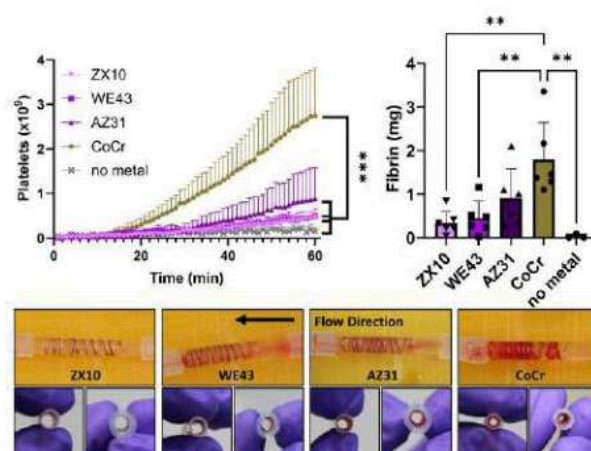


Fig. 1: Platelet (left), fibrin (right), and whole thrombus (bottom) accumulation on metal wires after 1hr of flowing, whole blood exposure. Cross section images are shown for proximal (left) and distal (right) ends for each sample. Platelet data were analyzed with a 1-way repeated measures ANOVA. Fibrin data were analyzed with a 1-way ANOVA. (** $p < 0.01$, *** $p < 0.001$)

DISCUSSION & CONCLUSIONS: The Mg alloy results reflect previous observations of low thrombogenicity for pure Mg, suggesting that alloying did not limit the anti-thrombotic effects of Mg. However, given the observed gas development on the wires, it is unclear whether this reduction in thrombosis is inherent to Mg ions or if it is a biophysical prevention of protein adsorption and therefore thrombosis. Ongoing work is examining a Mg alloy after surface treatment to determine the effects of surface passivation on thrombogenicity.

REFERENCES: ¹ N.M. Keeling, et al. (2024) *J Throm Haemo* 7: 1433-46.

ACKNOWLEDGEMENTS: We appreciate Fort Wayne metals, in particular Adam Griebel, for providing materials for this work. This project was supported by NIH grants R01HL144113, R01HL168696, and R01HL167442. We gratefully acknowledge the veterinary staff at the Oregon National Primate Research Center, supported by P51OD011092.



Pre-Clinical and Early Clinical Experiences on a New Fully Bioabsorbable Magnesium Pin for Dental Applications

A Kopp¹, K Melcher¹, M Mütter¹, L Silva², P Köcher³, S Fuest⁴, L Matthies³, R Smeets³

¹Meotec GmbH, Aachen, DE ²Porto University School of Dentistry, Porto, PT ³University Medical Center Hamburg-Eppendorf, Department of Oral and Maxillofacial Surgery, (⁴Division of Regenerative Orofacial Medicine), Hamburg, DE.

INTRODUCTION: In dentistry, barrier membranes are used for guided tissue or bone regeneration (GTR/GBR). Particularly in guided bone regeneration, the immobilization of bone grafts through membrane fixation is crucial for success. This method limits graft movement, thereby ensuring a stable chamber for bone healing. Fixation is typically achieved using pins. Ideally, these pins are replaced by bone when no longer needed. Nonetheless, to this day dental practitioners have to use non-absorbable Titanium pins to fixate bioabsorbable membranes, which is a contradiction in concept [1,2]. A new bioabsorbable pin system based on Magnesium WE43 was developed and tested (pre-)clinically. Market approval was followed by first-in-patient cases, offering fully resorbable restorations of the oral cavity in different indications for the first time.

METHODS: Bioabsorbable dental pins were manufactured from WE43MEO (Meotec GmbH, Aachen) and tested ex-vivo against commercially available metal and polymer pins for pull-out, insertion force as well as shear strength. Further testing included pre-clinical testing (approval N044/2020) in Aachen mini pigs over periods of 4, 8 and 16 weeks in groups of 4 animals against commercial Titanium pins (Ustomed GmbH & Co. KG, Tuttlingen), followed by μ -CT and histological evaluation. First clinical cases were conducted on male and female patients of different age in cases of ridge augmentation and vertical bone augmentation.

RESULTS: The insertion test showed that all groups reached the forces of ~50 N. The shear test revealed that maximum forces are similar for Mg pins and Ti pins and significantly lower for PLA pins, demonstrating comparable mechanical performance between Mg and Ti pins, with Mg pins outperforming PLA pins in shear strength. In the preclinical model, no signs of inflammatory reactions, allergic symptoms, or toxic effects were observed. Mg pin degradation continued steadily over 4 to 16 weeks, with rates increasing from approx. 50% at 4 weeks to 80% at 16 weeks. Gas accumulation was observed mainly in a circular pattern around the pin head, with pins and

membranes remaining in place (see Figure 1). Mg pins were successfully placed in all patients. Healing was uneventful, with no complications observed. Gas cavities reduced by 3 months, with no functional impact. Mg pins effectively immobilized the membranes and were largely resorbed after 3 months.

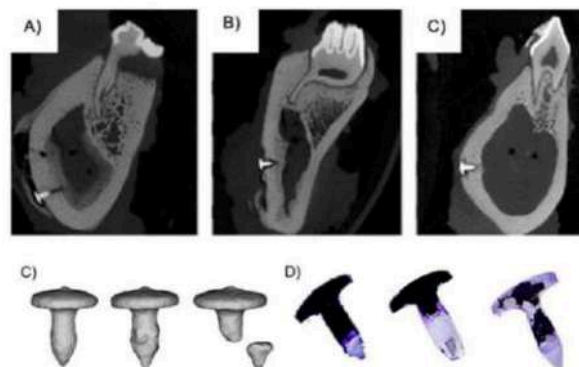


Fig. 1: Radiological degradation of Mg pins after 4 (A), 8 (B) and 16 weeks (C) of healing. Radiological 3D reconstructions (C) and histological images (D) at 4, 8 and 16 weeks of healing (left to right).

DISCUSSION & CONCLUSIONS: Magnesium pins displayed mechanical stability and Biocompatibility in all pre-clinical testing. No wound healing disorders, toxic reactions, or allergic responses were noted. Despite visible gas accumulations, clinical findings showed successful pin fixation and membrane immobilization as well as stable and steady degradation without significant interference with bone healing. Thus, Magnesium pins offer an alternative to traditional Titanium pins, reducing risks like intraoral exposure and radiological artifacts in MRI. Magnesium pins provide adequate mechanical strength for membrane fixation and eliminate the need for pin removal in GTR/GBR procedures.

REFERENCES:

- ¹ Sasaki, J. et al.: Barrier membranes for tissue regeneration in dentistry Biomater. Investig. Dent. 2021; 8(1): 54–63.
- ² Kačarević, Z. P. et. al.: Biodegradable magnesium fixation screw for barrier membranes used in guided bone regeneration Bioactive Materials 2022; Vol.14: 15-30



Biocompatibility behaviour of surface mechanical attrition treated Mg5Zn0.2Ca magnesium alloy

Nilesh Kumbhar¹, Shubham Parihar¹, Santosh S Hosmani¹, Akiko Yamamoto²

¹ Indian Institute of Technology Indore, Indore, 453552, India, ² National Institute for Materials Science, Namiki 1-1, Tsukuba, Ibaraki 305-0044, Japan

INTRODUCTION: The rapid corrosion and limited mechanical integrity in physiological environments pose significant challenges for magnesium alloys, limiting their use in biomedical applications. Surface Mechanical Attrition Treatment (SMAT) addresses these issues by inducing severe plastic deformation and refining the coarse grain structure into a fine-grained structure. This study investigates the effects of SMAT on the biocompatibility of Mg5Zn0.2Ca magnesium alloy, exploring the relationship between grain refinement, corrosion resistance, cytotoxicity, and protein adsorption [1-3].

METHODS: Mg5Zn0.2Ca alloy, consisting of 5 wt.% Zn, 0.2 wt.% Ca and the remaining Mg was selected for this study and divided into three categories, as shown in Table 1.

Table 1. Specimen Nomenclature

Nomenclature	SMAT Parameters		
	Ball Velocity	SMAT Duration	Surface Coverage
SA1	10 m/s	10 min.	2000%
SA2	5 m/s	23 min.	2000%
NSA	Non-SMATed Alloy		

TEM and EBSD were used to analyze grain refinement. The hardness was measured using Vickers Microhardness with a 50 g load and 10 s dwell time. Corrosion resistance was assessed using EIS, Tafel analysis, and immersion tests followed by SEM and XRD to examine passivation behaviour. E-MEM supplemented with 10 vol.% FBS and 5% CO₂-95% air atmosphere was used to perform corrosion and cytotoxicity experiments. Cytotoxicity extract test (performed with L929 cell line) measured relative plating efficiency, while protein (Bovine serum albumin and fibronectin) adsorption tests quantified protein adsorption.

RESULTS: TEM and EBSD analyses revealed significant grain refinement in SMATed samples, with sample SA1 showing the finest grain structure (grain size of 30 ± 12 nm). Microhardness measurement shows the gradient in the microhardness values with maximum hardness values of 120 HV_{0.5} for SA1, 91 HV_{0.5} for SA2 and 56 HV_{0.5} for NSA. EIS and Tafel analysis indicated

that SA1 had the highest corrosion resistance, followed by SA2, with NSA exhibiting the least resistance. SEM and XRD analysis after immersion tests showed a thicker passive layer on SMATed samples. Cytotoxicity tests showed lower cytotoxicity (better relative plating efficiency) for SA1 and SA2. Optical microscopy and SEM confirmed better cell morphology and less corrosion damage in SA1 and SA2 compared to the NSA.

DISCUSSION & CONCLUSIONS: The observed grain refinement in SMATed samples, especially in SA1, directly correlates with improved corrosion resistance and biocompatibility [1,3]. Microhardness gradient values also agree with the degree of grain refinement produced by colliding ball velocities for SA1 and SA2. Reduced corrosion current density, lower weight loss and smaller pitting depths depict better corrosion performance for SA1 and SA2. This can also be attributed to the thicker passive layer identified in SEM and XRD analysis. Enhanced fibronectin protein adsorption on SA1 (0.7456 µg/cm²) and SA2 (0.9038 µg/cm²) further supports its improved biological performance. These findings highlight the potential of SMAT to optimize magnesium alloys for use in biodegradable implants. Future research should explore long-term performance and in vivo applications of SMATed magnesium alloys.

REFERENCES: ¹ Mojtaba Mollayousef et al. (2024) *Effects of grain boundaries on the biocompatibility of the pure magnesium*, J Mater Res Technol., vol. 28, pp 1121-1136. ² Torkian A, Faraji G & Pedram M S (2021) *Mechanical properties and in vivo biodegradability of Mg–Zr–Y–Nd–La magnesium alloy produced by combined severe plastic deformation*. Rare Met. Vol. 40, pp 651–662. ³ Paul S et al. (2020) *New Mg–Ca–Zn amorphous alloys: biocompatibility, wettability and mechanical properties*. Materialia, vol. 12, pp 100799.

ACKNOWLEDGEMENTS: The authors would like to thank the Indian Institute of Technology, Indore, India, and the National Institute for Materials Science, Japan, for the support provided during the work.

Can growth disturbances be avoided?

RL Marek¹, I Mertelseder¹, B Okutan¹, NG Sommer¹, AM Weinberg¹

¹*Department of Orthopaedics and Traumatology, Medical University of Graz, Graz, Austria.*

INTRODUCTION: A crucial aspect of treating pediatric fractures is ensuring that the active physis is not negatively affected by the implantation process and implants themselves. Any negative impact on the physis can result in deviations in longitudinal bone growth and deformations¹. To mitigate this issue, bioresorbable magnesium (Mg)-based implants are used, thereby expanding the options for pediatric fracture treatment². The aim of this study was to investigate the local and systemic responses to trans-epiphyseally implanted Mg-based ZX00 screws (Mg alloyed with <0.5 wt% Zn, <0.5 wt% Ca; l=40 mm; d=3.5 mm) on the active physis in a growing sheep model.

METHODS: Three-month-old female juvenile sheep (n=8) received monocortical ZX00 screw implants through the right tibia epiphysis, whereas the left tibia was implanted with a titanium (Ti) screw or left untreated as a control. *In vivo* clinical computed tomography monitored ZX00 physis defects and longitudinal growth at 3, 6, 12, 24, 52, 104, and 156 weeks post-surgery. All animals were sacrificed at 180 weeks post-surgery, and tibiae, spleen, liver, kidneys and lymph nodes were extracted. *Ex vivo* high-resolution micro-computed tomography (20,3 µm per voxel) assessed limb length differences. Undecalcified tibiae with implants were embedded in Technovit® 9100 for qualitative histology, and organs were collected for histopathological examinations.

RESULTS: Between 3-52 weeks post-surgery ZX00 screw breakage was observed at the level of the physis. Due to continuous longitudinal bone growth, the physis grew away from the distal screw fragment. A decrease in physis defect size was measured following the 12-week time point (Fig. 1). No leg length differences or axial deviation were detected after ZX00 screw implantation until skeletal maturity was reached. Starting 104 weeks post-surgery, Ti-legs were significantly shorter ($p < 0.05$) compared to ZX00 and control (Fig. 2). Bone histology samples showed clearly new bone formation, no signs of foreign body response or screw encapsulation. Histological assessment of stained soft tissues revealed implantation of ZX00 screws had no harmful effects on the architecture of the organs, as well as a lack of systemic response.

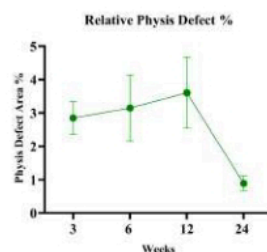


Fig. 1: Physis defect area in relation to whole physis area at 3-, 6-, 12- and 24-weeks after implantation with ZX00 screws.

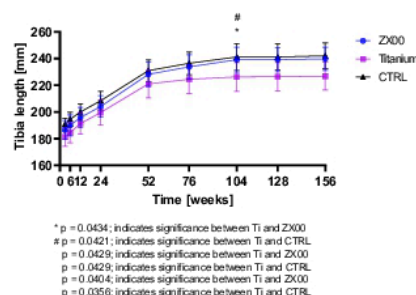


Fig. 2: Leg length differences at 3-, 6- 12- and 24-weeks after implantation.

DISCUSSION & CONCLUSIONS: Our findings highlight the advantages of Mg-based implants for pediatric fracture fixation. Trans-epiphyseally implanted ZX00 screws enabled uncompromised longitudinal bone growth and demonstrated excellent biocompatibility, thus may minimize complications such as growth discrepancies or foreign body reactions. Additionally, Mg-based implants enhance new bone formation around the implant, further strengthening the bone after fracture, which makes them superior for pediatric interventions.

REFERENCES: ¹DM Knapik (2018) *Consequences Following Distal Femoral Growth Plate Violation in an Ovine Model With an Intramedullary Implant: A Pilot Study*, Journal of Pediatric Orthopedics, pp. 640-645

²MH Song (2019) *In Vivo Response of Growth Plate to Biodegradable Mg-Ca-Zn Alloys Depending on the Surface Modification*, J. Mol. Sci, pp. 3761

ACKNOWLEDGEMENTS: Those results are part of a project that has received funding from the European Union's Horizon 2020 research and



Two Years of mm.X in the market – Are there still influences on bioabsorption we do not understand?

K Reuß¹, M Mütther², C Ptock², J Seitz¹, M Gertig¹, C Kösters³, A Kopp¹

¹ Medical Magnesium GmbH, Aachen, ² Meotec GmbH, Aachen, DE,

³ Maria-Josef-Hospital, Greven DE

INTRODUCTION: mm.X implants made from medical grade magnesium alloys have been used in numerous applications for more than 2 years in daily clinical routine in several European markets. Most commonly, the implants are becoming applied in orthopaedic care while surgical treatment traumatic fractures as well as elective deformity correction especially of extremities.

METHODS: The mm.X portfolio is available for surgical centers and distributed through direct sales as well as agents in various CE-marking accepting European markets. Most of the clinical results have been created with the following types of implants:

- **mm.CS:** headless compression screw family (Ø 2.8/3.5/5.0 mm) and length between 10–60 mm
- **mm.PIP:** interphalangeal arthrodesis pin in L 1.7/2.1 mm, W 3.8 mm and 0/10/20° (angle)

Legal manufacturer is Medical Magnesium GmbH (Aachen, Germany). mm.X implants are manufactured from bioabsorbable magnesium alloy WE43MEO (Meotec GmbH, Aachen) and treated by PEO surface modification (Kermasorb®).

RESULTS:

Most commonly the implants were used for -elective forefoot surgery (e.g. HV Correction)

- traumatic joint near fractures including osteochondral fractures and avulsion fractures and
- fractures of the elbow and upper limb.

Patients were surgically treated with mm.X bioabsorbable magnesium implants at clinical centres and underwent postoperative treatment in standard routines with selective imaging control.



Figure 1: Postoperative control at 5-7 months, with different findings and related stages of absorption.

DISCUSSION & CONCLUSIONS: The overall clinical performance of and feedback on applied bioabsorbable magnesium implants under post-market surveillance exhibit very good clinical and functional results, irrespective of the anatomical region or injury pattern. Surgeons are highly satisfied with the results.

Although with a clinically successful result (e.g. fracture consolidation and deformity correction), a very limited number cases revealed prominent radiolucent areas (most likely gas accumulations) in radiographic imaging. These findings did not show any patterns in regards to device related factors (device, material composition, batch, manufacturing time) or time after surgery (varying from 2 weeks to 7 months).

Current research hypotheses is a patient related factor. The following factors (among others) and/or possible comorbidities are evaluated for potential influence on the bioabsorption pattern:

- Treated indication,
- Nicotin or Alcohol abus,
- Diabetes mellitus,
- Age and
- Osteoporosis.

So far the number of these cases with prominent bioabsorption findings is very low and no statistical analysis can be performed.

Based on results to this date, application of mm.X devices is safe and can be marketed consciously for a broad range of indications in orthopaedic care leading to highly satisfactory postoperative results. The education of surgeons, especially in regards to bioabsorption phenomena is crucial.

Extension to further specialities of surgery is already ongoing. First indications in hand surgery (DIP fusion) have been successfully treated. Further devices will enlarge the portfolio in more disciplines in orthopaedic, trauma and sports medicine to broaden the data on mm.X implants and understand possible influences even better.



Preclinical characterization of Mg-Zn-Ca implants biomechanics, by using ovine tibia model

O Suljevic¹, C Stahle², V Weigl^{1,3}, F Warchomicka³, AM Weinberg¹,

¹*Department of Orthopaedics and Traumatology, Medical University of Graz, Graz, Austria.*

²*Bioretec Ltd., Tampere, Finland.* ³*Institute of Material Science, Graz Technical University, Austria*

INTRODUCTION: Magnesium (Mg)-based alloys are promising materials for orthopedic device applications due to its biocompatibility, low elastic modulus, which limits stress shielding, and the fact that the need for a secondary surgical operation to remove the implant can be eliminated [1]. The aim of this study is to compare the biomechanical properties of the test articles, cannulated mono- and bicortical RemeOs™ ZX00 (Mg-0.45Zn-0.45Ca) screws to bone screws of different materials, but similar dimensions. The commercially available comparator articles are cannulated, PLGA (ActivaScrew™) and Titanium (Synthes® Titanium) screws.

METHODS: The three different test articles, ZX00 (RemeOs™), PLGA (ActivaScrew™), and Ti (Synthes®) screws, were implanted into the diaphysis of sheep tibia. The animals were euthanized at the time points 0, 3, 6, 12, 16, and 26 weeks, tibiae were explanted and μ CT imaging, as well as bone mineral density measurements were performed. Furthermore, the specimens were subjected to push- and pullout force testing.

The gathered data was processed to extract the maximal push- and pullout forces. Those values were then normalized to the amount of thread revolutions in contact with the bone (Eq. 1).

$$F_{norm} = \frac{F_{max}}{Rev} \quad (1)$$

The amount of revolutions were calculated by measuring the mean contact length and applying Eq. 2.

$$Rev = \frac{L_{mean}}{P} \quad (2)$$

Rev ... Revolutions per length [-]

L_{mean} ... Implant contact length [mm]

P ... Thread pitch [mm] p=1.25 [mm]

F_{max} ... maximal testing Force [N]

F_{norm} ... Normalized Force [N]

RESULTS:

The ZX00 test object yielded normalized push- and pullout forces higher than the PLGA material and lower than the titanium screws at all tested timepoints. The deviation between cortical thickness and bone to implant contact length can be seen in Figure 1.

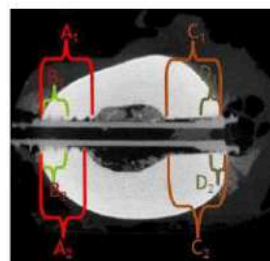


Figure 1: Transverse μ CT cross section view of a bicortically implanted 3.5x24mm ZX00 compression screw in a sheep tibia. Brackets mark the areas where diaphyseal thickness (A&C) and contact length (B&D) were measured.

DISCUSSION & CONCLUSIONS:

In our study we utilized two new approaches:

First by performing pushout tests, we used a new testing method for bone screws.

Second, we partially eliminated measuring inconsistencies due to the differing physiology of the individual bones, by normalizing to the number of thread revolution actually in contact.

Our results suggest that ZX00 screws are a promising bioresorbable alternative, that not only supports bone formation and remodeling [2], but also keeps up with other already marked-approved materials in terms of biomechanical strength.

REFERENCES:

¹ Y Lu, S Deshmukh, I Jones, YL Chiu (2021) *Biodegradable magnesium alloys for orthopaedic applications*, Biomater Transl.

² B Okutan, UY Schwarze, L Berger (2023) *The combined effect of zinc and calcium on the biodegradation of ultrahigh-purity magnesium implants*, Biomaterials Advances (Volume 146)

ACKNOWLEDGEMENTS: This work was supported by MgSafe project and Bioretec Ltd.



In-vivo evaluation of performance and degradation of molybdenum temporary epicardial pacing wires in a rat model

C. Redlich¹, M.-E. Prieto Jarabo², A. Schauer³, C. Guder¹, G. Poehle¹, T. Weissgaerber^{1,4}, V. Adams³, U. Kappert⁵, A. El-Armouche⁶, A. Linke², M. Wagner²

¹ Fraunhofer Institute for Manufacturing Technology and Advanced Materials IFAM, Dresden Branch

² Clinic for Internal Medicine and Cardiology, Heart Center Dresden, Technical University Dresden

³ Laboratory of Experimental and Molecular Cardiology, Heart Center Dresden, Technical University Dresden

⁴ Chair of Powder Metallurgy, Institute of Materials Science, Technical University Dresden

⁵ Clinic for Cardiac Surgery, Heart Center Dresden, Technical University Dresden

⁶ Institute of Pharmacology and Toxicology, Technical University Dresden

INTRODUCTION: Postoperative cardiac arrhythmias are routinely treated with temporary epicardial pacing wires (TEPW) made of stainless steel that are implanted at the time of heart surgery. However, both manually extracting and leaving steel TEPW in the body may cause rare but potentially serious complications. We investigate the novel approach of using bioresorbable molybdenum (Mo) TEPW that can remain in the body and are fully resorbed after a defined time. Degradation, functionality, and biocompatibility in-vitro were already shown in the first part of the study [1]. In the second part of our study, in-vivo performance of the Mo TEPW is investigated.

METHODS: Mo TEPW were manufactured from 40 μm \varnothing Mo wires and electrically insulated by dip-coating with absorbable biopolymers. Two Mo TEPW each were implanted in a rat model by sewing the electrode parts on the anterior heart surface and placed subcutaneously (Figure 1a). Commercial steel TEPW were used in a control group. Electrophysiological parameters were tested in-vivo for up to 4 weeks. Degradation was studied after 1, 2 and 4 weeks, 6 and 12 months post-implantation. Biocompatibility was studied by organ analyses for respective timepoints.

RESULTS: The implantation method was successfully established. Successful pacing was shown for Mo TEPW for up to 14 days, with slightly better stimulation properties than for commercial steel TEPW (Figure 1b). Gradual degradation of Mo TEPW over time was observed with nearly complete degradation of metallic Mo after 12 months in uncoated regions of the TEPW (Figure 1c). Degradation in biopolymer-coated areas was delayed. An increased Mo concentration compared to the steel group was found in skin near the implant, kidney, spleen and urine for the 6- and 12-months cohorts.

DISCUSSION & CONCLUSIONS: Mo TEPW allow for electrical stimulation for up to 14 days with equivalent efficiency to commercial steel TEPW in the in-vivo rat model. This is a good safety margin compared to the usual clinical functional lifetime of 3-4 days. Mo TEPW degraded in a phys-

iologically reasonable time span after their functional lifetime. Mo excretion was largely via urine. The duration of degradation of Mo TEPW may be further modulated by selection and processing of the coating polymers in future developments.

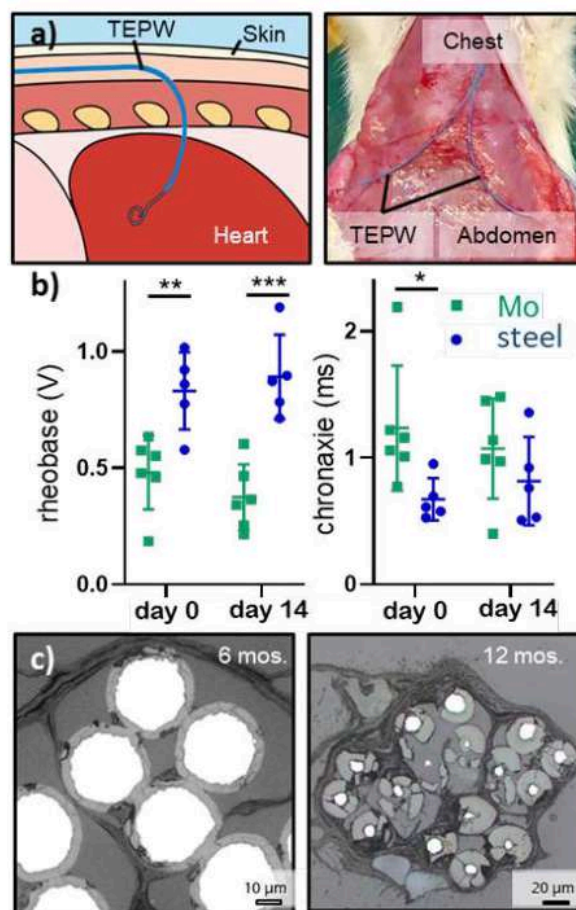


Fig. 1: Schematic and photo of implanted Mo TEPW (a), rheobase and chronaxie for Mo TEPW after implantation (b), in-vivo degradation of Mo TEPW (c).

REFERENCES:

[1] M.-E. Prieto Jarabo et al., *Acta Biomater* **2024**, 1, 178.

ACKNOWLEDGEMENT: This work was funded by the Else Kröner Fresenius Zentrum (EKFZ) for Digital Health.



A review of the resorbable magnesium scaffold program of Biotronik

O. Anopuo¹, A. Krause¹

¹Cortronik GmbH, Rostock Germany.

INTRODUCTION: The desire to improve patient outcome in Percutaneous coronary intervention (PCI), has continued to drive the development of resorbable Magnesium scaffold (RMS). Biotronik has played a leading role in pioneering the development of a competitive RMS for coronary vascular intervention. This work reviews the outcome of the clinical trials carried out on the first, second and third generation RMS in the past, and relates it with the scaffold base material used.

METHODS: For the Biotronik first generation RMS, Absorbable metal stent 1 (AMS-1), the first in Human trial was carried out under the name PROGRESS-AMS. This clinical trial was a non-randomised, consecutive, multicentre trial that assessed the efficacy and safety of an RMS¹. 63 patients were enrolled for this study and the Primary endpoint was cardiac death, non-fatal myocardial infarction, or clinically driven target lesion revascularisation at 4 months¹. In the case of BIOSOLVE I, II, III & IV studies, the same base material was used. BIOSOLVE I scaffolds were coated with the drug Paclitaxel and a copolymer PLGA while those of BIOSOLVE II, III and IV (MAGMARIS®) were coated with BIOLute®, a resorbable Poly-L-Lactide (PLLA) eluting a limus drug. A total of 46 patients were enrolled for the BIOSOLVE I trial, while 123, 61 and 2066 patients were enrolled for the BIOSOLVE II, III and IV respectively²⁻⁴. BIOMAG I is a prospective, multicentre, first-in-human study with clinical and imaging follow-up scheduled at 6 and 12 months for the Biotronik third generation RMS FREESOLVE™. The clinical follow-up will continue for 5 years⁵.

RESULTS: The primary endpoint in-scaffold late lumen loss (LLL) at 4 months for the PROGRESS AMS trial was 1.08±0.49 mm. The target lesion revascularization (TLR) rate was 23.8% at 4 months and 45% after 12 months. No death, no myocardial infarction, subacute or late thrombosis¹. For BIOSOLVE I trial, the LLL at 6 months was 0.65±0.50 mm and target lesion failure (TLF) rate of 4%². After 12 months, LLL was 0.52±0.39 mm with TLF of 7%². No cardiac death or scaffold thrombosis was noted. In the case of BIOSOLVE II & III, a pooled LLL at 12 months was 0.39 ± 0.39 mm and TLF was 3.3% with no definite or probable scaffold thrombosis⁶. For the

BIOMAG I trial with the newly developed FREESOLVE™, the LLL at 6 months was 0.21±0.31 mm. At 12 months, this was 0.24±0.36 mm with TLF of 2.6% and no scaffold thrombosis, no Myocardial Infarction, and no cardiac death⁵. For FREESOLVE™, >99% of the scaffold was fully resorbed at 12 months.

DISCUSSION & CONCLUSIONS: From the reviewed clinical trials, what is obvious is that a huge progress has been made in the last years culminating in the development of a competitive resorbable magnesium scaffold. The emergence of FREESOLVE™ with an improvement of 38% in LLL after 12 months compared to its second-generation RMS Magmaris®, and no definite or probable scaffold thrombosis, is a competitive result compared to its drug eluting permanent stent counterpart.

REFERENCES: ¹R. Erbel et al., *Temporary scaffolding of coronary arteries with bioabsorbable magnesium stents: A prospective, non-randomised multicentre trial*, Lancet 369 (9576) (2007) 1869–1875. ²M. Haude et al., *Safety and performance of the drug-eluting absorbable metal scaffold (DREAMS) in patients with de-novo coronary lesions: 12 month results of the prospective, multicentre, first-in-man BIOSOLVE-I trial*, Lancet 381 (9869) (2013) 836–844. ³M. Haude et al., *Safety and performance of the second-generation drug-eluting absorbable metal scaffold in patients with de-novo coronary artery lesions (BIOSOLVE-II): 6 month results of a prospective, multicentre, non-randomised, first-in-man trial*, Lancet 387 (10013) (2016) 31–39. ⁴Bennett J. *Performance and safety of the resorbable magnesium scaffold, Magmaris in a real-world setting – Primary and secondary endpoint analysis of the full cohort (2,066 subjects) of the BIOSOLVE-IV*, Presented at: TCT 2021, November 2021, Orlando, USA. ⁵M. Haude et al., *A new resorbable magnesium scaffold for de novo coronary lesions (DREAMS 3): One-year results of the BIOMAG-I first-in-human study*, EuroIntervention 19 (5) (2023). ⁶M. Haude, et al., *Safety and clinical performance of a drug eluting absorbable metal scaffold in the treatment of subjects with de novo lesions in native coronary arteries: Pooled 12-month outcomes of BIOSOLVE-II and BIOSOLVE-III*, Catheter Cardiovasc Interv (2018).



Stiffness-matched, Multimaterial (Resorbable and Inert) Skeletal Fixation

D Dean^{1,2}, L Olivas¹, D Cho¹, A Zhang¹, A Chmielewska³, T Snyder⁴, H Emam⁵, J Lozier⁶, K VanKoeveering⁷, R Skoracki², A Luo¹

Departments of: ¹Materials Science & Engineering, ²Plastic & Reconstructive Surgery, ⁵Oral & Maxillofacial Surgery, ⁶Veterinary Clinical Sciences, ⁷Otolaryngology—Head & Neck Surgery, ⁴Center for Design and Manufacturing Excellence, [The Ohio State University](https://www.ohio-state.edu), Columbus, OH USA.
³ Multidisciplinary Research Center, Cardinal Stefan Wyszyński University, Warsaw, Poland

INTRODUCTION: Ti6Al4V, the standard-of-care material graft fixation material, is 4-6 times stiffer than bone. The use of Ti6Al4V devices risks stress shielding, which can lead to bone loss; or stress concentration, which can lead to device failure. We are investigating a stiffness-matched approach to skeletal fixation devices used in reconstructive surgery. Our goal is to improve outcomes through the personalization of fixation device materials, shape, and attachment location so as to recreate the original functional unit and not interrupting the normal loading pattern once healing is complete. [1] We present a novel multi-material skeletal fixation device that incorporates a resorbable Mg1.2Zn0.5Ca0.5Mn core into a personalized, 3D printed, NiTi shell. [2] These devices are designed to bring all healing segments into compression under any load. The fixation plate's site is chosen so as to least interrupt the normal loading pattern once the bone has healed.

METHODS: In our Virtual Surgical Planning (VSP) approach we determine an initial shape for each component, its material, and the location where the overall device will be attached to the patient's skeleton to bring about the fixation of free bone segments and bone grafts and subsequent union (healing) (Fig. 1). Currently we incorporate machined solid Mg alloy inserts inside a 3D printed NiTi shell. Part of that NiTi shell is a porous region which is used to locally modulate stiffness. We report here on our comparison of placing orthogonal struts versus TPMS (Triply Periodic Minimal Surface) gyroid struts in the porous NiTi region. We expected that the orthogonal geometry would fail earlier than the gyroid pore geometry under the cyclic loading ASTM F382 standard [3], requiring the completion of 1,000,000 cycles under 4-point bending condition.

RESULTS: The behavior of the plates under dynamic four-point bending, showed a similar performance as the cycles increases. However, it is clear that the orthogonal structure experiences a structural weakening after 50K cycles (Fig. 2).

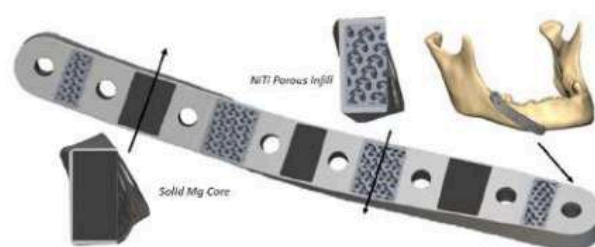


Fig. 1: Personalized Mandibular Graft Fixation: Stiffness is locally modulated by inserting 3D printed, porous Mg alloy core components into a form-fitting, non-porous, 3D printed NiTi shell.

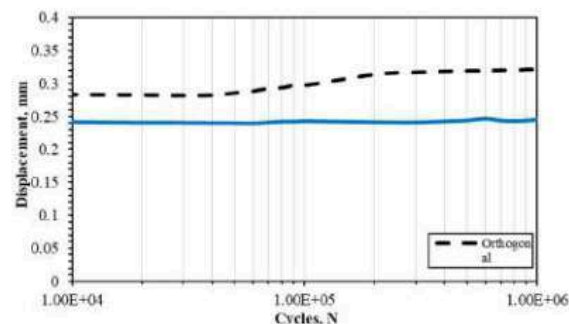


Fig. 2: Displacement-Cycle graph for orthogonal (black non-continuous line) and gyroid (blue continuous line) structures.

DISCUSSION & CONCLUSIONS: Orthogonal struts are more likely to stress concentrate and will thus fail earlier than a gyroid pore geometry. The risk of stress shielding will be dramatically reduced after the Mg alloy component resorbs.

REFERENCES: ¹A. Chmielewska and D. Dean (2024) *Acta Biomaterialia* 173(1):51-65. ²A. Chmielewska, *et al.* (2020) *MRS Communications*, 10(3):467-74. ³ASTM F382-17, 2023.

ACKNOWLEDGEMENTS: Partial support provided by the Biomedical Device Initiative (BDI) at the James Comprehensive Cancer Center, The Ohio State University (Columbus, OH).



Long-term *in vivo* assessment of magnesium-based biodegradable screw-plate implants in a large-animal cranio-maxillofacial defect model

W Rubin¹, T Akhmetshina¹, AM Rich¹, J Ross², D Toneatti³, K Nuss², B Schaller³, JF Löffler¹

¹ *Laboratory of Metal Physics and Technology, Department of Materials, ETH Zurich, Switzerland*

² *Musculoskeletal Research Unit (MSRU), University of Zurich, Switzerland*

³ *Department of Cranio-Maxillofacial Surgery, University Hospital, Inselspital Bern, Switzerland*

INTRODUCTION: Lean magnesium–calcium based biodegradable metallic alloys (BMAs) have been studied in various pre-clinical settings¹⁻³ and present a promising alternative to permanent metallic implant materials for potential clinical use in traumatology. To further explore the efficiency of osteotomy stabilization using BMA-based screw-plate implants, a large-animal study with a cranio-maxillofacial defect model is being conducted over an extended time duration of 42 months. The study covers four different timepoints of sacrifice, ranging from two, six, and 24 months until complete material biodegradation. Initial results for the two- and six-months groups demonstrated promising outcomes for the Mg-based implants⁴. Here, complementary and extending data are presented up to its currently latest observation timepoint of 30 months.

METHODS: As described in Ref. [4], each animal received osteotomies with fully mobilized bone fragments located at the calvarial (CD) and zygomatic arc (ZAD) regions, representing mechanically non- and moderately loaded cranio-maxillofacial areas. The fragments were refixedated by screw-plate implants of (i) specifically designed plasma electrolytic oxidation (PEO)-coated ultra-high-purity Mg–Ca (UHP-X0) alloy implants, and (ii) standard titanium-based implants as a reference. Radiographic data on implant-volume loss, gas-cavity formation, and bone response was evaluated up to the latest time point.

RESULTS: All animals continued to show normal mastication behavior and remained healthy until sacrifice. The implants' volume loss was constant between 6 and 18 months with an average monthly loss of about 3.2% for both implantation sites. Volume-loss rates differed mainly within the first months and at later times for the non-loaded implantation site. Within the Mg group, the gas-cavity volumes peaked initially in weeks two and four and again at six to ten months. Both implantation sites yielded similar gas-cavity volumes when normalized to the implant surfaces. Gas cavities formed near the degrading implants and were also found in later degradation stages up to 30 months. Based on histology, the Mg group yielded bone-implant contact (BIC) at least as high as titanium in both defect areas (*Fig. 1*). Furthermore, new bone formation was higher in the Mg group, which peaked for both materials four weeks after implantation. The

moderately loaded osteotomies exhibited generally higher bone formation. Bone-density reduction near the Mg screws was found radiographically from the second week on and was confirmed by histomorphometry.

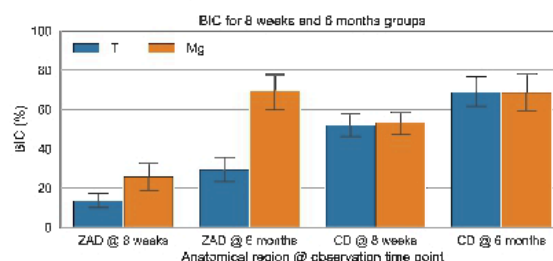


Fig. 1: BIC results for both materials and locations, for the 8-weeks and 6-months animal groups.

DISCUSSION & CONCLUSIONS: Implant volume loss was found to be nearly linear. The gas evolution fluctuations of the PEO-coated Mg samples within the first two months coincided with higher implant-volume losses. In contrast, the later gas-cavity volume increase was not reflected by respective degradation-rate variations. Around the Mg implants, signs of osteostimulative effects were seen, but bone resorption was also observed to some extent. First signs of bone-tissue resorption were observed around the Mg-based material in week two, when increased gas-volume formation was also measured. On the other hand, new bone deposition was found to start equally for both material groups from week four on and was consistently higher for the Mg group. The BIC was considerably higher for the Mg group than for the Ti reference for the moderately loaded osteotomies, possibly due to an induced mechanical stimulus. There are also various indications that the Mg-based material positively affects the local bone metabolism upon continuous implant degradation.

REFERENCES: ¹R. Marek et al. (2023) *Biomater. Adv.* 150:213417. ²L. Berger, et al., 14th Biometal Conf. (Aug. 2022), *Europ. Cells and Materials*, in press. ³P. Holweg et al. (2020) *Acta Biomater.* 113:646-659. ⁴W. Rubin et al., 15th Biometal Conf. (Aug. 2023), *Europ. Cells and Materials*, in press

ACKNOWLEDGEMENTS: The authors gratefully acknowledge financial support by the Swiss National Science Foundation (SNF Sinergia, Grant No. CRSII5-180367), and thank D-HEST at ETH Zurich for its support with the radiography measurements.



Evaluation of iron based bioresorbable flow diverters in the rabbit elastase induced aneurysm model

AA Oliver^{1,2}, C Bilgin¹, J Cortese¹, EA Bayraktar¹, YH Ding¹, D Dai¹, M Connon³, KD Carlson², AJ Griebel⁴, JE Schaffer⁴, D Dragomir-Daescu², R Kadirvel⁵, RJ Guillory II³, DF Kallmes¹

¹Radiology, ²Physiology and Biomedical Engineering, ⁵Neurosurgery, Mayo Clinic, Rochester, MN.

³Biomedical Engineering, Medical College of Wisconsin, Milwaukee, WI. ⁴Fort Wayne Metals, Fort Wayne, IN

INTRODUCTION: Flow diverters (FDs) are miniature braided stents used to treat intracranial aneurysms. Bioresorbable flow diverters (BRFDs) aim to serve their temporary function of occluding and healing the aneurysm before safely absorbing into the body. This may mitigate complications associated with the permanent presence of conventional FDs such as device induced thromboembolism, stenosis, and side branch occlusion [1]. In this work, we evaluate an iron based BRFD in the rabbit elastase induced aneurysm model.

METHODS: BRFDs and control FDs were 4.75mm diameter and 7mm length and were constructed from 48 braided, 25 μ m diameter wires. The BRFDs contained 36 bioresorbable FeMnN alloy (35% Mn, 0.15% N, balance Fe, by wt%) wires and 12 polyimide coated Ta wires to impart radiopacity. The control FDs were composed entirely of permanent 35NLT/Pt DFT wires. All wire components were manufactured by Fort Wayne Metals. BRFDs were deployed for 3 months (n = 7 rabbits) to treat aneurysms induced in the rabbit elastase model [2]. Digital subtraction angiography (DSA) and gross dissection microscopy were used to assess aneurysm occlusion. BRFDs and control FDs were deployed in the abdominal aorta for 3 (n = 7 rabbits) or 6 (n = 3 rabbits) months. MicroCT and hematoxylin & eosin (H&E) staining were used to assess the resorption rate and biological response, respectively, of the aortic implants.

RESULTS: The BRFDs failed to completely occlude the aneurysm in 6 rabbits (Figure 1). The BRFD completely thrombosed in one of the rabbits, resulting in the occlusion of both the parent artery and the aneurysm. MicroCT analysis determined that the volume of FeMnN alloy wires in BRFDs deployed within the aorta lost 61 \pm 14% and 83 \pm 13% (mean \pm standard error) of their initial volume after 3 and 6 months, respectively. H&E staining demonstrated that there was minimal stenosis in the control FDs and BRFDs at 3 and 6 months. No adverse tissue reactions were observed in any of the BRFDs in response to notable corrosion.

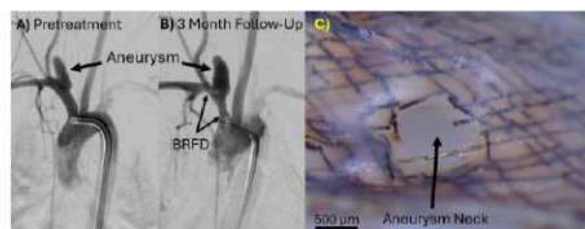


Fig. 1: DSA of the elastase induced aneurysm before (A) and 3 months after (B) BRFD deployment. (C) Gross dissection microscope image of the unoccluded aneurysm neck

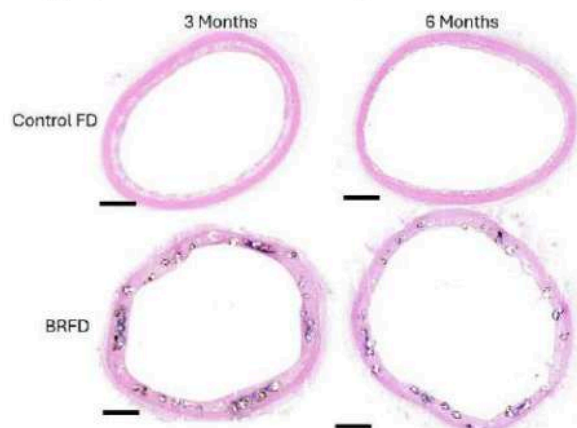


Fig. 2: Representative H&E stains of control FDs and BRFDs implanted in the rabbit aorta for 3 or 6 months. Scale bars are 500 μ m.

DISCUSSION & CONCLUSIONS: We believe rapid and localized corrosion resulted in BRFD wires fragmenting away from the aneurysm neck before they could become covered with neointima and occlude the aneurysm. The FeMnN wires corroded faster than anticipated, but their corrosion did not appear to elicit any adverse tissue responses. In conclusion, the FeMnN alloy appears to be safe in terms of localized toxicity in the arterial environment, but future work should focus on bioresorbable materials with slower, more uniform corrosion for the BRFD application.

REFERENCES: ¹A. Oliver, K. Carlson, C. Bilgin, et al (2023) *J Neurointerv Surg* **15.2**: 178-182. ²T. Altes, H. Cloft, J. Short, et al (2000) *Am J Roentgenol* **174.2**: 349-354.

ACKNOWLEDGEMENTS: Alexander Oliver is supported by the American Heart Association grant # 23PRE1012781.

Posters

Tuesday, August 27th, 2024



Magnetic and thermal characterization of Fe(-Zn)-Mg metastable powders

R G Estrada^{1,3}, M Lieblich¹, P de la Presa², M Multigner³

¹*National Centre for Metallurgical Research, CENIM-CSIC, Madrid, Spain.* ²*Institute of Applied Magnetism-UCM, Spain.* ³*Dept. Ciencia e Ing. de Materiales, URJC, Móstoles (Madrid), Spain.*

INTRODUCTION: The degradation rate of Fe based biomaterials can be accelerated through the incorporation of Mg in the Fe lattice or as nanoparticles [1,2]. Being Fe ferromagnetic, it is expected that Fe-Mg also reacted under magnetic fields. On the other hand, given that Fe and Mg are immiscible, the processed Fe-Mg based alloy is in a metastable state, and thus, it may be especially sensible to thermal treatments. In this work, we present preliminary results on magnetic and thermal behaviour of two Fe-Mg and two Fe-Zn-Mg alloy powders. Fe-Mg based alloys might be used in a variety of applications, such as graft powder, reinforcing particles of biodegradable polymers [3], after consolidation, and as feedstock for the additive manufacture of implants.

METHODS: Powders of Fe-5Mg, Fe-10Mg, Fe-20Zn, (Fe-20Zn)-5Mg and (Fe-20Zn)-10Mg (wt%) were obtained from elemental powders (Fe: 99.7%, dia. $\leq 74 \mu\text{m}$; Mg: 99.8%, dia. $\leq 100 \mu\text{m}$, Zn: $>99.9\%$, dia. $\leq 45 \mu\text{m}$) by attrition milling at 1400 rpm under nitrogen atmosphere. Fe powder was also milled for comparison purposes.

Hysteresis loops at 5 K and 300 K and magnetization versus temperature at 5000 Oe were performed by a Quantum Design SQUID magnetometer.

Differential scanning calorimetry (DSC) studies were conducted using a TA DSC 25 calorimeter. Samples, weighing about 5 mg, were heated from 50 °C to 700 °C at a rate of 10 °C/min.

Transmission electron microscopy (TEM), JEOL JEM 3000F, was employed to measure the lattice parameters of the powders in order to compare them with those of Fe.

RESULTS: Hysteresis loops (Figure 1) show that the addition of Mg or Zn produces an increase of the coercive field and slight changes in the saturation magnetization when compared with pure milled Fe. Magnetic properties of the ternary powder suggest the presence of two magnetic phases.

Preliminary results inferred from DCS curves (not shown) seem to corroborate the presence of metastable states that transform into stable ones with increasing temperature.

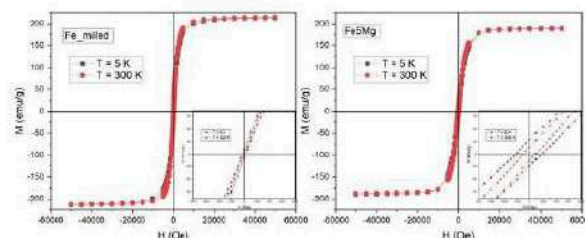


Fig. 1: Hysteresis loops of milled Fe (left) and Fe5Mg alloy (right) at 5 K and 300 K. Inset: low magnetic field magnification.

Lattice parameters obtained from TEM images show a slight increase with respect to Fe for the Fe-Mg alloy powders, Fe-20Zn shows a larger increase, whereas in (Fe-20Zn)-Mg powders the lattice parameters resulted similar to that of Fe, Figure 2.

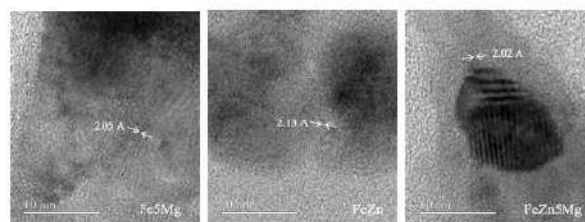


Fig. 2: TEM images: Fe5Mg, FeZn & FeZn10Mg.

DISCUSSION & CONCLUSIONS: Metastable Fe(-Zn)-Mg powders present unique behaviours in terms of magnetic properties and thermal evolution probably because of the change in Fe interplanar distances due to inclusion of Mg and Zn atoms in the Fe lattice. These changes of properties might be used for tailoring degradation rate of Fe-based implants.

REFERENCES: ¹ Y. Guangyin, N. Jialin (2012) *Patent* CN103028148A. ² R.G. Estrada, M. Multigner, M. Lieblich, et al (2022) *Metals*, 12(1). ³ R. G. Estrada, M. Multigner, N. Fagali, et al (2023) *Heliyon*, 9(12) e22552.

ACKNOWLEDGEMENTS: Grants PID2022-139323NB-I00, PID2021-123891OB-I00, PID2021-123112OB-C21 and PRE2020-092118 (R.G.E.) funded by MCIN/AEI/10.13039/501100011033. ICTS-CNME. CAI-Técnicas Geológicas.



A novel microstructural engineering based approach to manufacture biodegradable Mg alloys.

Prithivirajan Sekar^{a,b}, S.K.Panigrahi^{*a,b}

^a Department of Mechanical Engineering, Indian Institute of Technology Madras, Chennai- 600036, India

^b Center of Excellence in Applied Magnesium Research for Futuristic Mobility, Indian Institute of Technology Madras, Chennai- 600036, India

*Corresponding Author: Ph: +91-44-22574742, Email: skpanigrahi@iitm.ac.in

Magnesium based alloys have been extensively researched as biodegradable materials, however, the commercialisation of Mg based implants is still at the infant stage. The present research explores the impact of microstructural engineering on the development of biodegradable Mg alloys. The bio corrosion performance of various thermo-mechanically processed Mg alloy samples are investigated. The research pioneers in understanding the role of microstructural engineering and the corresponding underlying mechanisms on the bio-corrosion behaviour of different sample conditions. The combined effect of grain size (GS), secondary phase and crystallographic orientation on bio-corrosion mechanism of these Mg alloy sample conditions are proposed for the first time. The microstructural engineering increased the bio-corrosion resistance significantly and proved to be a promising technology to develop biodegradable Mg implants.



Hydrothermal processing of metal-ceramic interpenetrating phase composites

C Oliver-Urrutia¹, L Drotárová¹, K Slámečka^{1,2}, M Remešová¹, T Balint³, M Schnitzer³, T. Zikmund¹, L Čelko¹, EB Montufar¹

¹ *Central European Institute of Technology, Brno University of Technology, Brno, CZ.* ² *Faculty of Mechanical Engineering, Brno University of Technology, Brno, CZ.* ³ *Faculty of Mechanical Engineering, Technical University of Košice, Košice, SK.*

INTRODUCTION: Metal-ceramic composites are typically processed at high temperature through sintering metallic-ceramic powder blends [1] or infiltrating liquid metal into a ceramic preform [2]. This work introduces a revolutionary low-temperature method to produce these composites. First, a metallic scaffold is created via additive manufacturing. Next, an alpha tricalcium phosphate (α -TCP) paste is infiltrated into the scaffold, which is then converted into hydroxyapatite through hydrothermal treatment near room temperature. This work shows that hydroxyapatite reinforces the metallic scaffold, and that hydrothermal treatment improves the degradation resistance.

METHODS: Biodegradable Mg scaffolds and stable Ti scaffolds were produced using laser beam powder bed fusion (LB-PBF) and extrusion-based (robocasting) additive manufacturing methods. These scaffolds were then infiltrated with an injectable α -TCP paste, created by mixing α -TCP powder with a 40% Pluronic solution at a liquid-to-powder ratio of 0.50 g/ml. The infiltrated scaffolds underwent hydrothermal treatment in a 100% humid atmosphere, either at 37°C for 7 days or at 190°C for 30 minutes, to transform the α -TCP into hydroxyapatite.

The formation of hydroxyapatite was assessed using X-ray diffraction (XRD) and scanning electron microscopy (SEM). Microstructural changes in the scaffolds during hydrothermal processing were examined through metallographic methods. The infiltration of ceramic into the scaffold was confirmed by X-ray microcomputed tomography (μ CT). Compressive strength was measured using a universal testing machine at a crosshead speed of 1 mm/min ($n = 5$). The degradation rate was determined by immersion testing in Hank's simulated body fluid after 15 days of immersion ($n = 3$).

RESULTS: The hydrothermal treatments successfully converted α -TCP into hydroxyapatite, as confirmed by XRD patterns and the formation of an entangled network of hydroxyapatite crystals (Fig. 1). XRD and SEM also revealed the

formation of a corrosion layer on the Mg surface (Fig. 2), whereas no oxidation signs were observed on Ti. This corrosion layer significantly improved the corrosion resistance of the Mg scaffolds (Fig. 2), with further enhancement from the incorporation of hydroxyapatite. Infiltrating the scaffolds with hydroxyapatite reduced porosity (Fig. 1) and increased compressive strength (Fig. 2), surpassing the strength of the individual components, including the Ti scaffold.

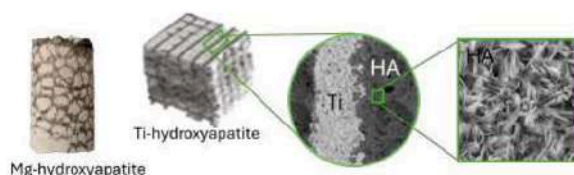


Fig. 1: Mg-hydroxyapatite and Ti-hydroxyapatite composites, Ti-hydroxyapatite interface, and formed hydroxyapatite crystals.

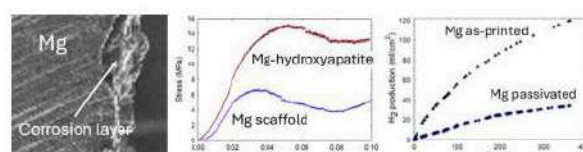


Fig. 2: Passivation layer, stress-strain curves in compression and hydrogen evolution in Mg-based materials.

DISCUSSION & CONCLUSIONS: The hydrothermal treatment improved the degradation resistance of metallic scaffolds by forming a stable, compact passivation layer. Infiltrating hydroxyapatite increased the composites' compressive strength by reducing porosity and delocalizing stress concentration. These new interpenetrating phase composites show promising potential to reduce the metal fraction in bone repair implants without sacrificing mechanical strength.

REFERENCES: ¹ F. Witte, F. Feyerabend, P. Maier, et al (2007) *Biomaterials* 28:2163-74. ² M. Casas-Luna, E.B. Montufar, N. Hort, et al (2022) *J Magnes Alloys* 10:123641-56.

ACKNOWLEDGEMENTS: This work was supported by the Czech Ministry of Health (NW24-10-00195).



Thermodynamic properties of liquid magnesium ternary alloys on the example of Ag-Mg-Ti and Cu-Mg-Ti systems

W. Gozdur¹, M. Pęska², M. Polański², W. Gąsior¹, A. Dębski¹

¹ *Institute of Metallurgy and Materials Science Polish Academy of Sciences, Krakow, Poland.*

² *Military University of Technology, Department of Functional Materials and Hydrogen Technology, Warsaw, Poland.*

Magnesium and its alloys exhibit attractive properties such as an excellent strength-to-weight ratio, good fatigue, or biocompatibility. As a result, Mg-based alloys are widely used in many industries such as aerospace, automotive, and biomedical applications. The last-mentioned use is possible due to biodegradability¹ which is attractive for temporary implants or stents. The corrosion of Mg-based alloys is largely responsible for the formation of galvanic links between the existing phases of the alloy².

For this reason, knowledge of the phase equilibria, occurring between elements forming an alloy and thus between existing intermetallic compounds, phases, and invariant reactions, which describe thermodynamic transformations is an important aspect in designing new material. Such information can be read from the available phase diagrams or can be calculated if appropriate data exists. Therefore, among other considerations, a thorough examination of phase equilibrium systems, from binary to multi-component systems, is essential for developing alloys with potential biomedical applications. Despite being widely studied for various industrial applications, magnesium-based alloys are not always fully understood in terms of their thermodynamic properties. Even after many years of research, some phase diagrams are still either unknown or only exist as theoretical models. Such is the case with Ag-Mg-Ti and Cu-Mg-Ti systems.

This work presents the results of the mixing enthalpy change ($\Delta_{mix}H$) of the liquid Ag-Mg-Ti and Cu-Mg-Ti solutions obtained from the high-temperature drop calorimetric technique. Based on the achieved results and the thermodynamic properties of binary systems, the liquid phase of both systems was described by symmetrical Muggianu³ and asymmetrical Toop⁴ models. To accomplish that, homemade software (TerGexHm) was used.

The presented results of the calorimetric measurements are the first step in the investigation and future evaluation of the thermodynamics of phases and the calculation of the phase diagrams of

the mentioned systems, which may prove useful in the design of new biodegradable alloys.

REFERENCES: ¹M. Mezbahul-Islam, A.O. Mostafa and M. Medraj (2014) *Essential Magnesium Alloys Binary Phase Diagrams and Their Thermochemical Data* Journal of Materials Science 2014, pp. 1-33. ²K. Thekkepat, et. al, (2022) *Computational design of Mg alloys with minimal galvanic corrosion* Journal of Magnesium and Alloys vol. 10, Issue: 7, pp. 1972-1980. ³Y.-M. Muggianu, M. Gambino, and J.-P. Bros (1975) *Enthalpies of Formation of Liquid Bi-Ga-Sn Tin Alloys at 723 K - The Analytical Representation of the Total and Partial Excess Functions of Mixing* Journal de Chimie Physique, vol. 72 pp 83-88. ⁴G. Toop (1965) *Predicting Ternary Activities Using Binary Data*, Transactions of the Metallurgical Society of AIME, vol. 233, pp 850–855.

ACKNOWLEDGEMENTS: This work is supported by the National Science Centre, Poland, for funding project no. 2021/43/O/ST8/01291 entitled “Thermodynamic properties and structure of Cu-Mg-Ti and Ag-Mg-Ti alloys and their potential to interact with hydrogen” in the years 2022–2027.



Assessing magnesium alloys anti-thrombogenicity mechanism using *in vitro* biochemical assays

CA Baker¹, J Goldman², MT Hinds¹, DEJ Anderson¹,

¹ [Department of Biomedical Engineering, Oregon Health & Science University, Portland, OR, USA](#)

² [Department of Biomedical Engineering, Michigan Technological University, Houghton, MI, USA](#)

INTRODUCTION: Bioresorbable metal stents are designed to maintain a vascular lumen for up to 2 years. Complete dissolution of the device results in the elution of beneficial byproducts and allows reintervention at the site of implant. Development of these devices requires a material that is both biodegradable and hemocompatible. Preliminary investigation of magnesium demonstrated reduced activation of the coagulation cascade when compared to other biodegradable metals.¹ The exact mechanism by which magnesium reduces thrombogenicity, particularly as it relates to surface interactions, is unknown. To assess the mechanism, this work tested the role of alloyed materials, pH and Mg²⁺ ion concentration against a clinical control on the *in vitro* activation of the coagulation cascade.

METHODS: Mg alloy wires were obtained from Fort Wayne Metals: WE43 (Mg-4Y-3Nd-0.4Zr), ZX10 (Mg-1Zn-0.3Ca-0.15Mn), AZ31 (Mg-3Al-1Zn-0.5Mn), LZ21 (Mg-2Li-1.2Zn-0.3Ca-0.3Mn), and a Resoloy-like Material (RLM) (Mg-10Dy-1Nd-1Zn-0.2Zr). CoCr wires (Goodfellow, Inc; Co40-Cr20-Fe15-Ni15-Mo7-Mn2-C-Be) were used as a clinical control. Materials were incubated with pooled platelet poor plasma (PPP) from 6 donors (3 male, 3 female). *In vitro* testing assessed FXIIa and fibrin generation, which are the end points of the contact pathway and common pathway of coagulation, respectively.² pH was increased using a NaOH solution to mimic local pH changes. MgSO₄ salts were used to increase the Mg ion concentration to mimic degradation byproduct release.

RESULTS: All alloys had longer fibrin generation times (Fig 1) and lower FXIIa detected compared to CoCr. Specifically, plasma alone generated significantly less FXIIa compared to CoCr, but produced an equivalent amount of FXIIa to any of the alloys. All Mg alloy wires trended towards longer fibrin generation times than CoCr, with AZ31, RLM, and ZX10 having significantly longer times. An increased pH in the PPP abolished detectable FXIIa at a different rate than the magnesium wire. Finally, the Mg ion solution showed a significant difference in clotting time

between ions and the wire, indicating that there is a difference between material and eluted corrosion byproducts.

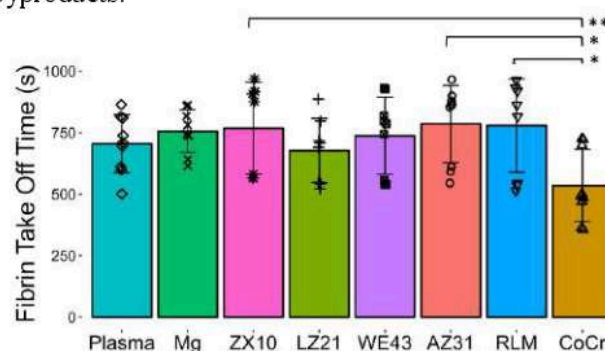


Fig. 1: Fibrin clotting time of different magnesium alloys after 1 hour in platelet poor plasma. Fibrin data analyzed with one-way ANOVA (n=9). (* $p < 0.05$, ** $p < 0.01$).

DISCUSSION & CONCLUSIONS: Mg alloys performed similarly to pure magnesium in the *in vitro* assays. Mg alloys had a reduced level of FXIIa and fibrin generation compared to a CoCr clinical control indicating their value as materials for a bioresorbable stent. pH and ion concentration did not recapitulate the effect of the wire itself, suggesting that the mechanism is tied to the material. Ongoing work with surface modified magnesium alloys seeks to understand the effect of different surface modifications on the anti-thrombogenicity of magnesium alloys. Future work will incorporate platelets and endothelial cell testing to gain a deeper understanding of hemocompatibility and vascular healing.

REFERENCES:

¹ D.E.J. Anderson, et al. (2024) *Bioactive Materials* 38: 411-421

² N.M. Keeling, et al. (2024) *J Throm Haemo* 7: 1433-46.

ACKNOWLEDGEMENTS: We appreciate Fort Wayne metals, especially Adam Griebel, for providing materials for this work. This project is supported by NIH grants R01HL130274, R01HL144113, R01HL101972, R01HL151367, and R01HL168696.



Processing and characterization of biodegradable magnesium alloys containing Zn and Ga

A Komissarov^{1,3}, V Bazhenov², S Rogachev³, A Li³, D Ten³, N Redko¹, A Drobyshev¹, KS Shin^{1,4}

¹ *Laboratory of Bioresorption and Bioresistance, Department of Maxillofacial and Plastic Surgery, Moscow State University of Medicine and Dentistry A.I. Evdokimova, Moscow, Russia* ² *Casting Department, National University of Science and Technology MISIS, Moscow, Russia* ³ *Laboratory of Hybrid Nanostructured Materials, National University of Science and Technology MISIS, Moscow, Russia* ⁴ *Magnesium Technology Innovation Center, Seoul National University, Seoul, Republic of Korea*

INTRODUCTION: Mg alloys are attractive candidates for the manufacture of temporary fixation devices for osteosynthesis. They have good biocompatibility, sufficiently high mechanical strength and acceptable biodegradation rate. The main objective of this work is to propose the new alloy system with the addition of a component that improves the bone tissue growth process. The most appropriate component in this way can be gallium.

METHODS: Five alloys with different Zn and Ga contents were prepared. In order to improve the mechanical and corrosion properties, Mg-Zn-Ga alloys were produced by hot extrusion. For all alloys, the microstructure was studied and the mechanical properties were determined. In addition, the corrosion rate was determined for all alloys from the hydrogen evolution in Hank's solution.

RESULTS: Typical engineering tensile stress-strain curves obtained for large standard cylindrical specimens of the Mg-Zn-Ga-(Y) alloys after hot extrusion at 150 or 200 °C are shown in Figure 1. The high-alloy alloys exhibited higher TYS and UTS than their low-alloy counterparts, but the El curves were very similar for the alloys studied. The YS and El of Mg-Zn-Ga alloys after extrusion are higher than their binary Mg-Zn and Mg-Ga counterparts [1]. This indicates that the addition of both Ga and Zn has a positive effect on the strength of magnesium alloys.

It has been found that the corrosion rate in Hank's solution depends on the chemical composition of the alloys.

DISCUSSION & CONCLUSIONS: Five Mg-Zn-Ga-(Y) alloys with different Zn and Ga contents were prepared and subjected to hot extrusion. Increasing the alloying element content resulted in higher strength of the alloys. For example, when the Zn and Ga contents in the alloy extruded at

200 °C increased from 2 to 4 wt%, the TYS and UTS increased by 115 and 71 MPa, respectively, but El decreased from 13.9 to 7.6 %.

It was found that the corrosion rate in Hank's solution depends on the chemical composition of the alloys. As the content of zinc and gallium in the alloys increases, the corrosion rate increases. For example, the MgZn2Ga2 alloy has a corrosion rate of 0.2 mm/g after extrusion at a temperature of 150°C, which is required for medical devices. This alloy also has a therapeutic effect due to the presence of gallium.

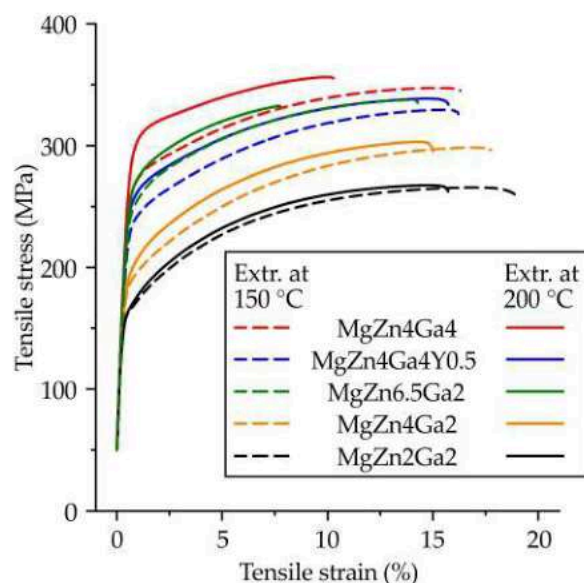


Fig. 1: Engineering tensile stress-strain curves for the Mg-Zn-Ga-(Y) alloys extruded at 200 or 150 °C.

REFERENCES: ¹ Y. Chen, Z. Xu, C. Smith, J. Sankar *Acta Biomater.* 2014, 10, 4561–4573.

ACKNOWLEDGEMENTS: The authors are grateful to the Ministry of Science and Higher Education of the Russian Federation for financial support under the Megagrant (No. 075-15-2022-1133).



Additively manufactured Zn-2Mg alloy porous scaffolds with customizable biodegradable performance and enhanced osteogenic ability

Aobo Liu¹, Peng Wen¹

¹ *State Key Laboratory of Clean and Efficient Turbomachinery Power Equipment, Department of Mechanical Engineering, Tsinghua University, Beijing, China*

INTRODUCTION: Ideal Zn-based biodegradable metal bone implants necessitate customizable biodegradable behaviours and improved osteogenic ability, conforming to the individual requirements of specific patients. Although design of implant material composition is a prevalent strategy, its efficacy in modulating the implant's performance is notably restricted [1]. Structure design has shown efficacy in regulating the performance of bio-inert metal implants, like Ti alloy scaffolds [2]. However, no study has been systematically conducted on the impact of structure design on the performance of biodegradable Zn-based metal scaffolds. The mechanism that how structure design controls the biodegradable performance and osteogenic ability of scaffolds remains unclear. Hence, in this study, Zn-2Mg alloy scaffolds with different porosities and different unit sizes were designed and fabricated to study the influence and the underlying influencing mechanism of structure design on the in vitro and in vivo behaviour of Zn alloy scaffolds.

METHODS: Gyroid unit cells were generated with different unit sizes and porosities. Scaffolds with a unit size of 2 mm and porosities of 40%, 60%, and 80% were denoted as G-40-2, G-60-2, and G-80-2. Scaffolds with a porosity of 60% and unit sizes of 1.5 mm, 2 mm, and 2.5 mm were denoted as G-60-1.5, G-60-2, and G-60-2.5 (Fig. 1).

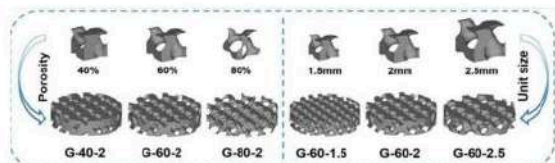


Fig. 1: Structure design of Zn-2Mg scaffolds.

RESULTS: Compressive strength (CS) and elastic modulus (EM) of scaffolds substantially decreased with increasing porosities. CS and EM just slightly decreased with increasing unit sizes (Fig. 2). Weight loss after degradation increased with increasing porosities and decreasing unit sizes (Fig. 3). Scaffolds with lower porosities and smaller unit sizes had better osteogenesis (Fig. 4).

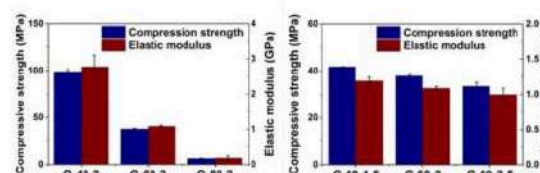


Fig. 2: Compressive properties of scaffolds.

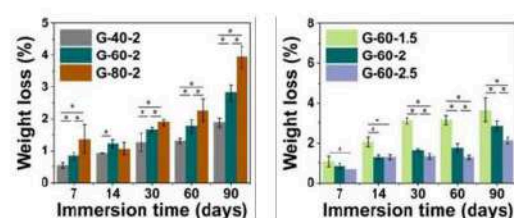


Fig. 3: Weight loss of scaffolds after immersion.

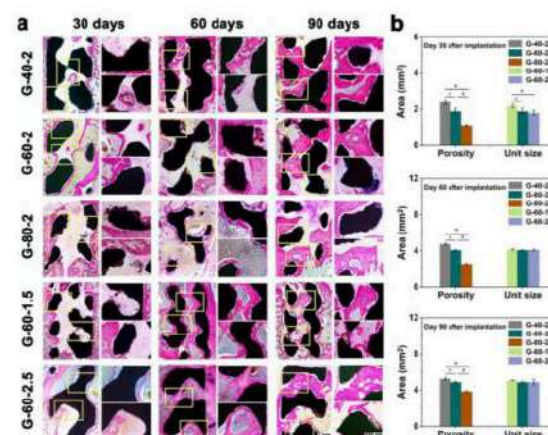


Fig. 4: In vivo osteogenic ability analysis.

DISCUSSION & CONCLUSIONS: The biodegradable performance of scaffolds can be accurately regulated on a large scale by structure design and the additively manufactured Zn-2Mg alloy scaffolds have improved osteogenic ability for treating bone defects.

REFERENCES: ¹Y. Qin, H. Yang, A. Liu, et al. (2022) *Acta Biomater.* **142**: 388-401. ²Y. Zhang, N. Sun, M. Zhu, et al. (2022) *Biomater. Adv.* **133**: 112651.

ACKNOWLEDGEMENTS: This template was modified with kind permission from eCM Journal.



3D-printing of bioresorbable Zinc-Magnesium for critical-size bone defects

M. Voshage¹, F. Fischer¹, L. Jauer¹, S. Pöstges², A. Kopp², J.H. Schleifenbaum¹

¹Chair for Digital Additive Production DAP, RWTH University, Aachen, Germany,

²Meotec GmbH, Aachen, Germany

INTRODUCTION: In this work, bioresorbable zinc-magnesium alloys are 3D-printed by Powder Bed Fusion of Metals using a Laser Beam (PBF-LB/M). The goal is to manufacture load-bearing implants (e.g. patient-specific scaffolds or cages) with suitable degradation properties without damage to the surrounding tissue.

METHODS: For the experiments, Zn0.5Mg and Zn1Mg powder-mixes from *Nanoval* are used. Test specimens are manufactured using a modified PBF-LB/M machine from *Aconity3D*. Scaffold structures are designed with respect to size and load capacity depending on the medical indication using *Rhino 7.3* and *Grasshopper* plugin. Compression tests are conducted according to DIN 50134. Test specimens are based on f_{ccz} unit cells with 10x10x15 cells in XYZ and a strut diameter of 200 μm with a pore width of 800 μm . EBSD analyses are carried out to determine the phase constituents as well as grain size and grain orientation in the manufactured test specimens.

RESULTS: Scaffold structures with a strut diameter of 200 μm are manufactured as shown in fig. 1-top. By combining a tailored exposure strategy with abrasive post-processing, sintered particles are removed, achieving dimensional accuracy of approx. $\pm 20 \mu\text{m}$ in the scaffold structures. Mechanical properties are analysed using compression tests (fig. 1-center). The max. compressive force for Zn0.5Mg is 2046 N, while for Zn1Mg it is 1927 N. The compressive stress Re_H can be calculated as 19.57 MPa for Zn0.5Mg and 18.26 MPa for Zn1Mg. The strain at this point is $\epsilon_{\text{max}} = 8.42\%$ for Zn0.5Mg and $\epsilon_{\text{max}} = 6.57\%$ for Zn1Mg. Decreased strength with increased ductility is demonstrated for Zn0.5Mg compared to Zn1Mg and can be explained by different microstructures. Fig. 1-bottom shows the results of EBSD analyses of Zn1Mg and Zn0.5Mg specimen. The mean area-weighted α -Zn grain size of the Zn1Mg specimens is $3.39 \pm 1.58 \mu\text{m}$ and $6.00 \pm 3.38 \mu\text{m}$ for Zn0.5Mg.

DISCUSSION & CONCLUSIONS: A decrease in grain size with increasing Mg content is consistent with the results from the literature¹. According to the Hall-Petch relation, grain refinement is expected to increase strength. Furthermore, a decrease in strain and compression

is attributed to rise in intermetallic $\text{Mg}_2\text{Zn}_{11}$ phases. The compressive stress depends not only on the material properties but also on geometry and porosity. Additive manufacturing of complex structures made from bioresorbable ZnMg with load-bearing properties suitable for bone replacement has been demonstrated. The process chain for tailored implants includes a customized design with data preparation, a tailored PBF-LB/M process, and abrasive post-processing.

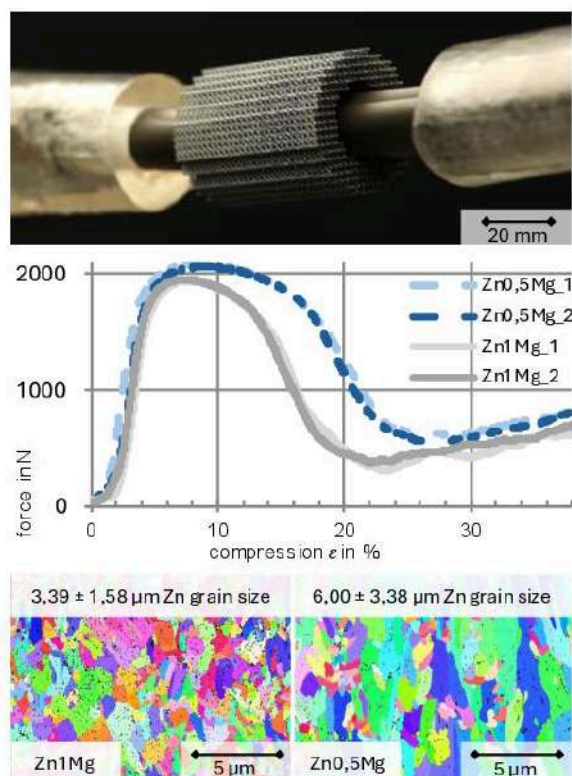


Fig. 1: (top) PBF-LB/M manufactured scaffold², (center) Results of compression tests according to DIN 50134, (bottom) EBSD analysis²

REFERENCES: ¹Y. Yang et al. (2018) *A combined strategy to enhance the properties of Zn by laser rapid solidification and laser alloying*, doi.org/10.1016/j.jmbbm.2018.03.018

²M. Voshage (2024) *Additive manufacturing of Zinc Magnesium alloys*, ISBN 978-3-98555-199-6

ACKNOWLEDGEMENTS: Parts of this work were funded by the German Federal Ministry of Education (13GW0404D & 03RU1U173C)



Combination of biodegradable Zn- and Mg-based alloys using multi-material Additive Manufacturing: challenges and opportunities

S Pöstges¹, T Poel¹, J Molina², J Llorca², A Kopp¹

¹ Meotec GmbH, Aachen, Germany.

² IMDEA Materials Institute, Getafe, Spain.

INTRODUCTION: Biodegradable metals, particularly zinc (Zn) and magnesium (Mg) alloys, offer significant potential for biomedical applications, especially in temporary implants that gradually degrade within the body. Recent studies demonstrate the feasibility of additive manufacturing (AM) of both materials to address patient-specific solutions with high geometric complexity^{1,2}. This study explores the innovative combination of Zn- and Mg-based alloys using multi-material AM techniques, aiming to synergize the unique properties of these materials for optimized performance in medical devices.

METHODS: Gas atomized, pre-alloyed Zn1Mg and WE43MEO powder is used to carry out the tests. All specimens are manufactured using a modified Laser Powder Bed Fusion system from Aconity 3D GmbH with the option to integrate a drum-based recoating module from Schaeffler Aerosint S4 allowing a layer wise combination of two different powder materials. To identify the optimum build plate material a total of 48 cuboid specimens with different volume energy density as well as support structure geometries are fabricated. In a next step, both materials are printed on top of each other by variation of the bonding parameters between both materials targeting to produce samples with a crack free interface. Additionally, the deposition accuracy of the recoating module is studied by varying the parameters of the recoating unit.

RESULTS: In the context of this study, Zn1Mg cuboid test specimens are reproducibly manufactured on a WE43 build plate with a relative density greater than 99.5 % and a support structure geometry of 300 µm. Additionally, a crack free interface between Zn1Mg and WE43MEO is achieved when combining the materials in printing direction as shown in Fig. 1 exemplary. For the layer wise multi-material 3D printing, parameters for the ejection and suction pressure of the drum-based recoating module are found to obtain a layer thickness of 30 µm for both materials.

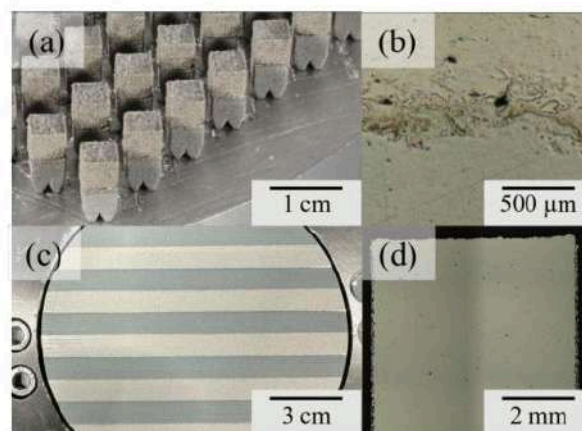


Fig. 1: (a) Multi-material cuboid specimens with Zn1Mg base part and WE43MEO top part, (b) cross section image of the fusion zone with crack free interface, (c) layer-wise combination of both powder materials with optimized parameters of the recoating unit, (d) exemplary cross section image of Zn1Mg cuboid specimen printed on a WE43 build plate with a relative density of 99.74 %

DISCUSSION & CONCLUSIONS: A sufficient build plate material was found as both materials were manufactured with a reproducible relative density > 99.5 % on a WE43 plate. Moreover, the general feasibility of combining both powder materials in printing direction was shown. In further investigations the mechanical and degradation properties will be determined. The parameter optimization of the drum-based recoating unit led to a layer wise combination of both powders representing the basis of the processing within one layer which will be studied.

REFERENCES: ¹M. Li et al (2021) Microstructure, mechanical properties, corrosion resistance and cytocompatibility of WE43 Mg alloy scaffolds fabricated by laser powder bed fusion for biomedical applications, *Materials Science & Engineering C* **119**: 1-17. ²M Voshage et al (2022) Additive Manufacturing of biodegradable Zn-xMg alloys: Effect of Mg content on manufacturability, microstructure and mechanical properties, *Materials Today Communications* **32**: 1-9.



Effect of PEO-coatings in hybrid Zn-Mg alloys processed through high-pressure torsion

J Salinas¹, N Mollae², C.J. Boehlert¹, J Llorca, *M Echeverry-Rendón*²

¹Michigan State University, USA; ²IMDEA Materials Institute, Spain

INTRODUCTION: Metals such as Fe, Mg, and Zn are the most reported for degradable metallic implants¹. All of them are considered essential elements for the human body and are necessary to perform the basic systemic functions of cells, tissues, and organs. Zn shows intermediate corrosion rates between Fe and Mg (≈ 0.1 mm/year), but it is the least studied to date, and the *in vivo* effects in the medium/long term are not yet fully understood. Studies so far have shown that Zn has good corrosion resistance and acceptable biocompatibility. Still, significant concerns have been raised due to its poor mechanical strength, aging at room temperature, creep effects, and high sensitivity to strain rate.

Consequently, there are currently numerous studies aimed at improving the mechanical properties of Zn alloys by adding other biodegradable metals, such as Mg, Ca, Sr, etc.² Conversely, plasma electrolytic oxidation (PEO) is an electrochemical surface treatment that results in a natural ceramic-like coating that can improve the corrosion resistance and biological behavior of Zn³. This study aims to determine if the quantity of Mg of Zn-Mg-based alloys in hybrid samples processed through high-pressure torsion alters the effectiveness of PEO. The goal is to achieve a suitable product to implement as a biodegradable orthopedic implant.

RESULTS: Hybrid samples of Zn-3Mg, Zn-10Mg, and Zn-30Mg processed through high-pressure torsion were successfully coated using PEO treatment in a phosphate-based electrolyte. The optimum voltage for the coating in the different materials was defined between 250 and 270 V, and the current density was in the range of 600 and 650 mA/cm². The thickness of the coatings obtained was in the order of 40-50 μ m. Samples were characterized from the surface and cross-section using SEM and EDS. The porous-like coating was obtained with a uniform distribution. Degradation results and cytocompatibility through indirect and direct test experiments showed an increase in the improvement of the PEO-treated Zn.

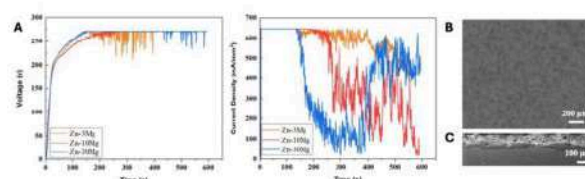


Fig.1: Curves of PEO coatings obtained for continuous voltage (A) PEO surface of the Zn-Mg coating (B). The rest of the parameters (C) Cross-section of the sample

DISCUSSION & CONCLUSIONS: Through the PEO technique, it was possible to obtain uniform and optimized coatings based on ZnO and Zn(OH) to improve the biological properties of Zn mainly. The Mg content in Zn alloys has a direct relationship with the microstructure and the formation process of the coating, which defines critical characteristics of the material, such as corrosion resistance and biocompatibility. This study concluded that aspects such as the techniques for obtaining the alloy, composition, and coatings could synergistically promote the degradation behavior and biocompatibility of materials used as biodegradable implants.

REFERENCES: ¹ M Heide, E Walker, L Stanciu (2015) Mg, Fe and Zn Alloys, the Trifecta of Bioresorbable Orthopaedic and Vascular Implantation. *J Biotechnol Biomater* 5:178. ² X. Liu, J Sun, K Qiu, Y Yang, Z Pu, L Li, Y Zheng (2016). Effects of alloying elements (Ca and Sr) on microstructure, mechanical property and in vitro corrosion behavior of biodegradable Zn-1.5Mg alloy. *J. Alloys Compd.* 664, 444-452. ³ J. Joseph, S. Corrujeira, R. Catubig, K. Wang, A. Sommers, P. Howlett, D. Fabijanic (2020) Formation of a corrosion-resistant coating by a duplex PEO and conversion surface treatment, *Surface & Coatings Technology*, 395 125918.

ACKNOWLEDGEMENTS: The National Science Foundation Division of Material Research (Grant No. DMR2153316), and the "Ayudas de atracción de talento investigador "César Nombela" 2023" of the Regional Government of Madrid (2023-T1/TEC-29099).



Customization of the property profile of Mg-Zn-Ca for medical applications

Björn Wiese¹, Maria J. Nienaber², Monika Luczak¹, Jan Bohlen²

¹ *Helmholtz-Zentrum Hereon, Institute of Metallic Biomaterials, Geesthacht, D.*

² *Helmholtz-Zentrum Hereon, Institute of Material and Process Design, Geesthacht, D.*

INTRODUCTION: For revealing the impact of Zn in extruded Mg-Zn-Ca alloys, the Zn content and the extrusion speed were varied. The microstructure development and the influence on the mechanical properties were analysed to reveal the impact of developing microstructure to a potential property profile for specific applications. Ultra-pure Mg is often used for medical applications, but the present study shows that this is not necessary. Enormous potential savings could be achieved by using conventional pure Mg.

METHODS: The alloys were composed from pure magnesium (99.97 %), pure Ca (99.90 %) and Zn (99.90 %) as raw material for casting. Mg was melted and pure Zn and Ca were alloyed at 720 °C. The alloyed melt was stirred for 20 min. Preheated steel moulds with a diameter of 70 mm at the top and a total height of 230 mm were filled with the melts^{1,2}. Direct chill casting was carried out under a protective atmosphere. The obtained chemical composition is listed in Tab. 1 for the final material.

Tab. 1: Chemical composition of all three alloys. Measured with atomic absorption spectroscopy for Fe and Cu, and inductively coupled plasma optical emission spectrometry for Ni and Ca and Zn.

	Ca wt. %	Zn wt. %	Fe wt. %	Cu wt. %	Ni wt. %
Mg-0.2Zn-0.3Ca	0.24	0.20	0.0019	0.0014	0.0012
Mg-0.3Zn-0.3Ca	0.25	0.30	0.0018	0.0014	0.0011
Mg-0.5Zn-0.3Ca	0.28	0.51	0.0021	0.0013	0.0011

Bars with a diameter of 10 mm were extruded from homogenized billets (500 °C /24 h and water quenched) with an extrusion ratio of 1:25 at 350 °C and a ram speed of 0.6, 2.2 and 4.4 mm/s. Grain size, texture, hardness, uniaxial tensile and compressive properties as well as the degradation rate (DR) in DMEM + Glutamax + 10% FBS were analysed.

RESULTS: As the extrusion speed increases, the grain size increases, and the texture becomes less pronounced. The variation in Zn content shows little influence on microstructure and texture development. The hardness increased with the Zn content as well as with the respective grain sizes (Fig. 1).

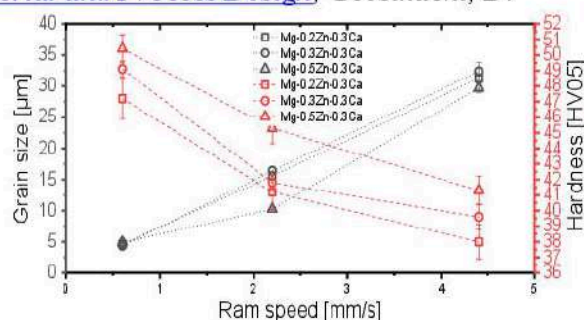


Fig. 1: Grain size and hardness of the three alloys vs. ram speed.

The strengths in the compression and tensile tests show a similar trend to hardness. Comparable DRs are achieved for all alloys and ram speeds (Fig. 2). Only Mg-0.2Zn-0.3Ca at 4.4 mm/min stands out, but there is an outlier in the 6 DR samples, which explains the higher standard deviation and the average value.

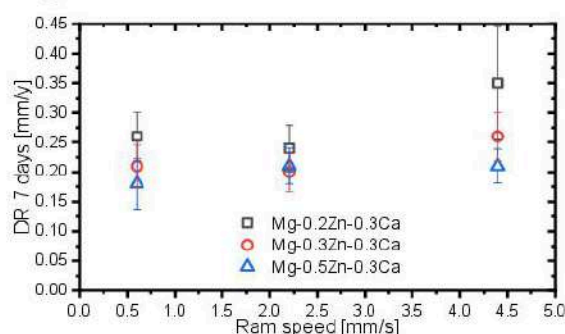


Fig. 2: DR of the three alloys vs. ram speed.

DISCUSSION & CONCLUSIONS: The variation in Zn content reveals only a minor influence on the grain size and texture development, as Zn has only a minor influence on recrystallization. More Zn leads to increased hardness and strength, a result of solid solution strengthening. As the ram speed increases, the grain size increases and the hardness and strength decline, as the proportion of fine grain hardening decreases, like for other systems^{1,2}. The degradation is unaffected by the alloy and the process parameters, which achieved low DR despite technically pure Mg for production.

REFERENCES: ¹J. Harmuth et al. (2019) *Frontiers in Materials* 6:201. ²B. Wiese et al. (2021) *Journal of Magnesium and Alloys* 9-1:112-122.



The effect of adding manganese on the deformation behaviour and properties of zinc alloys

M. Bieda¹, E. Rusinek¹, W. Gozdur¹, M. Gieleciak¹, A. Jarzębska¹, L. Maj¹, L. Rogal¹, J. Skiba²

¹*Institute of Metallurgy and Materials Science of Polish Academy of Sciences, Krakow, Poland*

²*Institute of High Pressure Physics, Polish Academy of Sciences, Warsaw, Poland*

INTRODUCTION: Research on biodegradable zinc alloys involves the addition of various alloy additives and using the deformation methods to meet the requirements for implants. However, the results are not optimal; it has been shown that alloy additions such as Li or Mg are beneficial for strengthening the material, and at the same time, Mn and Cu are beneficial for their plasticity [1,2]. This work aimed to investigate the influence of hydrostatic extrusion and manganese alloying on the microstructure and mechanical properties of zinc and compared it to previous magnesium studies [3].

METHODS: Materials for investigations were prepared by gravity casting in an argon atmosphere from pure zinc with various manganese contents (0.5 and 1% wt., respectively) and then deformed using hydrostatic extrusion (HE). Deformed material was subjected to a microstructure investigation using XRD (X-ray Diffraction), SEM (scanning electron microscope), and TEM (transmission electron microscope), and its thermal stability was checked. Mechanical properties using static tensile tests and microhardness measurements were analyzed. Additionally, immersion tests were carried out in Hanks' solution under conditions mimicking a human body (temperature = 37 °C, pH = 7.4) for 14 days. The corrosion rate was calculated based on the weight loss of the samples after removing the corrosion products, and SEM observations were performed.

RESULTS: The mechanical properties obtained for the Zn with 0.5 % wt. and 1 % wt. of Mn after casting and two passes of HE were lower than obtained for zinc alloyed with magnesium [3], and UTS reached 285 MPa and YS 208 MPa for higher addition of Mn. However, a significant improvement in elongation E was observed, reaching about 40 %. In Fig 1, it is visible that the size and shape of the grains are different for pure zinc and alloys. Additionally, the grain refinement of Zn α grains and intermetallic phases Mg_2Zn_{11} and $MnZn_{13}$ were noticed.

The observation of materials after immersion tests shows the corrosion pits in $MnZn_{13}$ intermetallic phases.

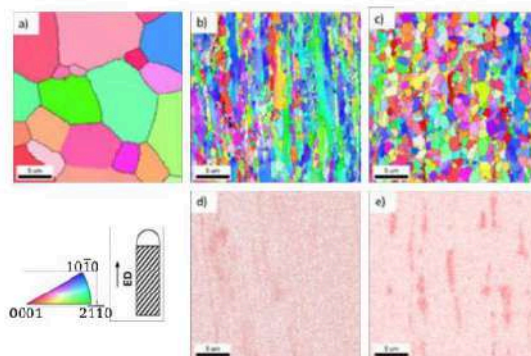


Fig. 1: SEM/EBSD orientation maps of pure zinc a), zinc alloy with 1 % wt. of Mn b), zinc alloy with 0.5 % wt. of Mg c) after HE and corresponding elemental distribution maps for Mn d) and Mg e) where darker red areas are correlated with intermetallic phases (Mg_2Zn_{11} , $MnZn_{13}$).

DISCUSSION & CONCLUSIONS: Alloying and hydrostatic extrusion are beneficial for the mechanical properties of zinc manganese alloys. It was noticed that different Mg and Mn additions could modulate both microstructure formation, strength, and ductility, where even a small amount of Mg was beneficial for strength and a small amount of Mn for ductility of zinc alloys. The intermetallic phase formation is additionally essential for the thermal stability of the material in elevated temperatures and the behaviour of the material during corrosion.

REFERENCES: ¹Kabir K. et. al, Recent research and progress of biodegradable zinc alloys and composites for biomedical applications: Biomechanical and biocorrosion perspectives, *Bioactive Materials*, 6, 3, 836-879, (2021), ²Huang, H. et. al, Recent advances on the mechanical behavior of zinc based biodegradable metals focusing on the strain softening phenomenon, *Acta Biomaterialia*, 152, 1-18(2022), ³Pachla W et. al, Structural and mechanical aspects of hypoeutectic Zn-Mg alloys for biodegradable vascular stent applications, *Bioactive Materials* 6, 1, 26-44, (2021).

ACKNOWLEDGEMENTS: This work was supported by the Institute of Metallurgy and Materials Science, Polish Academy of Sciences, within a statutory work.



Functional coatings on biodegradable magnesium alloys for orthopedic applications

M. Karaś¹, S. Boczek¹, Ł. Maj², J. Skiba³, D. Kapinos¹, K. Limanówka¹, A. Jarzębska², M. Bieda²

¹ *Lukasiewicz Research Network – Institute of Non-Ferrous Metals, Light Metals Division, Poland*

² *Institute of Metallurgy and Materials science Polish Academy of Science, Cracow, Poland*

³ *Institute of High Pressure Physics, Polish Academy of Sciences, Warsaw, Poland*

INTRODUCTION: The process of manufacturing biodegradable magnesium implants is complex, combining the requirements of materials engineering, surface engineering, corrosion engineering and medical engineering [1, 2]. For this study, only the protective coatings will be considered. Conversion coatings have multiple functions: they slow down the dissolution rate of magnesium in physiological environments, reduce the amount of hydrogen released from the raw material and increase the adhesion of biological coatings to magnesium surfaces by increasing the surface roughness. This study describes anodic oxidation conversion coatings on biodegradable MgZn1Ca0.2Li1 and MgZn1Ca1Li1 alloys after hydrostatic extrusion.

METHODS: To characterize the protective coatings synthesized on biodegradable magnesium alloys a comprehensive analysis was conducted using scanning electron microscopy (SEM), transmission electron microscopy (TEM), and X-ray diffraction (XRD). Additionally, a hydrogen release station was used to determine the corrosion rate. The study meticulously examined the influence of various parameters in the coating manufacturing process (such as: process time and current density) in KOH+KF solution.

RESULTS: The chemical composition of biodegradable magnesium alloys plays an important role. Higher calcium content in magnesium alloys increases hydrogen release, indicating a higher corrosion rate. Simultaneously, the hydrostatic extrusion reduces the grain size from above 300 to 1.8-4 microns, depending on the material and sample. Grain reduction affects the strength and corrosion properties of biodegradable magnesium alloys. Hydrostatic extrusion significantly enhances the strength properties of biodegradable magnesium alloys, it also increases hydrogen release. Conversion coatings produced in a KOH+KF solution consist of potassium, fluorine, oxygen, and magnesium, with dominant phases being MgF₂ and KMgF₃ and significantly reduce the dissolution kinetics of the magnesium alloy. Results from immersion corrosion tests revealed a

significant positive impact of the investigated coatings on reducing hydrogen evolution, underscoring their potential to enhance the performance and biocompatibility of magnesium alloys in biomedical applications.

DISCUSSION & CONCLUSIONS: In conclusion, magnesium alloys with alloying additives such as calcium, zinc and lithium are promising materials for medical applications due to their similar properties to bone tissue, biodegradability and potential biocompatibility. Anodizing is a promising method of producing a protective coating due to relatively low cost of producing coatings, high adhesion of coatings to substrates and reasonable control over their properties obtained by optimizing process parameters, such as electrolyte used, current density, or duration of surface treatment.

REFERENCES:

- [¹] M. Salahshoor and Y. Guo (2012) *Biodegradable Orthopedic Magnesium-Calcium (MgCa) Alloys*, Processing, and Corrosion Performance, *Materials* **5**, pp 135-155; [²] J.F.Nie, B.C. Muddle (1997) *Precipitation hardening of Mg-Ca(Zn) alloys*, *Scripta Materialia*, Vol **37**, No, 10, pp 1475

ACKNOWLEDGEMENTS: Research was carried out as part of the "Implementation Doctorate" program of the Ministry of Education and Science in Poland project No DWD/5/0007/2021



Biodegradable zinc and zinc-magnesium alloys from a microstructural and mechanical perspective.

M. Gieleciak¹, A. Jarzębska¹, Ł. Maj¹, P. Petrzak¹, M. Kulczyk², M. Bieda¹

¹ *Institute of Metallurgy and Materials Science, Polish Academy of Sciences, Krakow, Poland*

² *Institute of High Pressure Physics, Polish Academy of Sciences, Warsaw, Poland*

INTRODUCTION: Despite much research focusing on zinc and its alloys, some unresolved issues remain. It seems that the in-depth analysis of the relationship between microstructure and mechanical properties still differs from that regarding corrosion or biological aspects. However, it is equally important, taking into account the differences between ambient and human body temperature and the problem of low recrystallization temperature of zinc.

METHODS: Pure zinc and zinc-magnesium alloys with 0.6 and 1.2 wt % of alloying additives were used in this study. Materials were prepared by casting and two-step plastic deformation. i.e. hot extrusion (HE) and hydrostatic extrusion (HSE) in 4 passes. The phase composition was measured by XRD, and the microstructure was characterized by SEM/EBSD and TEM. Additionally, mechanical properties were tested using the static compression test. Then the samples were heated at 50°C and the tests were repeated to assess the changes occurring in the materials. A long-term heating experiment was also performed to evaluate the behaviour of individual crystallographic orientations.

RESULTS: Based on XRD analysis, the microstructure of pure zinc consists of α -Zn, while zinc-magnesium alloys of α -Zn and $\text{Mg}_{12}\text{Zn}_{11}$ intermetallic phase which is consistent with the Zn-Mg phase diagram. Characterization by SEM/EBSD revealed, that hydrostatic extrusion led to composite-like microstructure where $\text{Mg}_{12}\text{Zn}_{11}$ is creating bands along the extrusion direction. Moreover, HSE creates preferential dominant orientation - for pure Zn it is the direction $\langle 2-1-10 \rangle$, for the ZnMg1.2 alloy $\langle 0001 \rangle$, and for ZnMg0.6 both $\langle 2-1-10 \rangle$ and $\langle 10-10 \rangle$. Differences in the number of dislocations depending on the material were also observed. Heating at 50°C positively affects mechanical properties while changing only the substructure. Long-term heating shows that the initially dominant orientations do not change, but in addition to static recrystallization, diffusion of magnesium from the intermetallic phase was also observed in the case of alloys.

DISCUSSION & CONCLUSIONS: During HSE process, hydrostatic pressure needed for deformation varies depending on the material. As a result, dynamic recrystallization occurs to a various extent, leaving the highest amount of dislocations in the ZnMg0.6 alloy and the least in pure zinc. In the heated materials after compression test an improvement in the yield strength was observed in each case, attributing this to the recovery processes before static recrystallization. Existed dislocations transformed into low-angle grain boundaries, while LAGB into high-angle grain boundaries. Long-term heating revealed, that magnesium addition has a beneficial effect of inhibiting static recrystallization and the lowest changes in the average grain size were noted for ZnMg1.2 . Moreover, higher temperatures and longer time led to the deforming of Zn-grains in pure metal, while in the case of alloys, magnesium location in the Zn-grain boundaries was observed.

REFERENCES: ¹E.Mostaed et.al (2018) *Zinc-based alloys for degradable vascular stent applications* Acta Biomaterialia, **71**:1-23.

²J. Čapek et.al (2020) *ZnMg0.8Ca0.2 (wt%) biodegradable alloy – The influence of thermal treatment and extrusion on microstructural and mechanical characteristics* Materials Characterization **162**:110230.

³ L.Ye et.al (2022) *Evolution of grain size and texture of Zn-0.5Cu ECAP alloy during annealing at 200 °C and its impact on mechanical properties* Journal of Alloys and Compounds **919**:165871

ACKNOWLEDGEMENTS: This research was partially funded by the National Science Centre Polish UMO-2020/39/O/ST5/02692.



Development of bioresorbable Mg-Zn-Ca-Mn and Mg-Zn-Ga alloys for bone implants

A Komissarov^{1,3}, V Bazhenov², S Rogachev³, A Li³, D Ten³, N Redko¹, A Drobyshev¹, KS Shin^{1,4}

¹ Laboratory of Bioresorption and Bioresistance, Department of Maxillofacial and Plastic Surgery, Moscow State University of Medicine and Dentistry A.I. Evdokimova, Moscow, Russia ² Casting Department, National University of Science and Technology MISIS, Moscow, Russia ³ Laboratory of Hybrid Nanostructured Materials, National University of Science and Technology MISIS, Moscow, Russia ⁴ Magnesium Technology Innovation Center, Seoul National University, Seoul, Republic of Korea

INTRODUCTION: Magnesium alloys are promising materials for temporary fixation devices in osteosynthesis due to their favorable biocompatibility, mechanical properties, and an acceptable biodegradation rate. This study aims to develop bioresorbable Mg-Zn-Ca-Mn and Mg-Zn-Ga alloys for bone implants, with the objective of enhancing the bone tissue growth process [1].

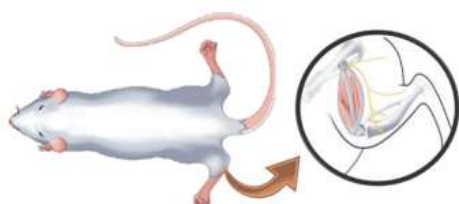
METHODS: To enhance the mechanical properties and corrosion resistance, MgZn2Ca0.7Mn1 and MgZn2Ga2 alloys were manufactured through hot extrusion. The microstructure and mechanical properties were examined, and the corrosion rate was determined in Hank's solution. The assessment of alloy resorption parameters was also conducted at one, three-, and six-months post-surgery.

RESULTS: The necessary strength properties for the medical alloys used in osteosynthesis can be achieved through the use of hot extrusion for MgZn2Ca0.7Mn1 and MgZn2Ga2 alloys as shown in the Table.

Material	YS (MPa)	UTS (MPa)	EI (%)
Mg-Zn-Ca-Mn	229	278	10
Mg-Zn-Ga	159	265	18

The corrosion tests demonstrate that the Mg-Zn-Ga alloy exhibits the lowest corrosion rate, at 0.2 mm per year, in comparison to the Mg-Zn-Mn-Ca alloy, which displays a corrosion rate of 0.3 mm per year.

The preclinical trials *in vivo* were carried out as shown below.



The assessment of alloy resorption parameters was conducted at one, three-, and six-months post-surgery and the results are shown in the Table 1.

Table 1. Change in dimension after installation.

	Diameter, mm	Length, mm	Resorption, %
Before installation	1,7; 1,7; 1,7	5,0; 5,0; 5,0	---
1 month after	1,46; 1,40; 1,36	4,6; 4,0; 4,0	17
3 months after	0,7; 1,0; 0,8	3,9; 3,7; 3,4	49
6 months after	Not rendered	Not rendered	100

DISCUSSION & CONCLUSIONS: Ingots of MgZn2Ca0.7Mn1 and MgZn2Ga2 alloys were prepared and subjected to hot extrusion. It was found that the desirable strength properties for the implant can be achieved by hot extrusion process using appropriate extrusion process parameters such as extrusion temperature and speed.

It was found that the corrosion rate in Hank's solution depends on the chemical composition of the alloys. The MgZn2Ga2 alloy shows the desired corrosion rate of 0.2 mm per year for the implant.

Assessment of alloy resorption parameters was performed postoperatively. The biodegradation process was characterized by the systematic development of newly formed bone tissue. The results indicated that magnesium alloys are suitable for clinical use and showed complete resorption within six months.

REFERENCES: ¹ Y. Chen, Z. Xu, C. Smith, J. Sankar *Acta Biomater.* 2014, 10, 4561–4573.

ACKNOWLEDGEMENTS: The authors are grateful to the Ministry of Science and Higher Education of the Russian Federation for financial support under the Megagrant (No. 075-15-2022-1133).



From Corrosion to Mechanics: Evaluating Novel Magnesium Alloys for Biodegradable Wire Applications

Beril Ulugun¹, Sneha Raj¹, Nana Barimah Osei-Owusu¹, Sreenivas Raguraman¹, Adam Griebel², Timothy P. Weihs¹

¹ Whiting School of Engineering, Johns Hopkins University, Baltimore, MD. ² Fort Wayne Metals, Fort Wayne, IN

INTRODUCTION: Magnesium alloys are emerging as promising candidates for temporary, wire-based implants due to their desirable combination of strength, biocompatibility, and biodegradability. Here we study the corrosion-induced degradation of mechanical properties of two novel magnesium alloys, WE43MEO and ZX10. To assess their potential for applications such as stents, sternal cables, staples, and sutures, we investigate how corrosion affects the wires' mechanical properties along with their initial microstructural features and susceptibility to pitting.

METHODS: We first analyze microstructural features of annealed, 300- μ m, ZX10 and WE43MEO wires through SEM-EB SD and perform bio-immersion testing in DMEM solution with 5% CO₂ environment. Wire samples were removed periodically at 1, 3, 5, and 7 days and analysed to calculate their mass loss and corrosion rate. Additionally, micro-CT scans were performed to assess pitting behaviour by quantifying parameters like pitting factor, pitting density, and maximum pit depth¹.

Finally, the mechanical properties of the wires were evaluated after exposure to the corrosive environment. Quasi-static testing with custom-made 3D-printed cartridges in an MTS Criterion C43 testing machine was used to determine changes in strength and ductility. Furthermore, a heated bath attached to a Test Resources 840 testing system was employed to assess the fatigue behaviour of the wires under uniaxial cyclic loading within the corrosive media at 37°C.

RESULTS: The analysis revealed microstructural differences between the alloys. WE43MEO exhibited smaller elongated grains (2.4 μ m) with large, elongated precipitates, while ZX10 displayed larger equiaxed grains (3.2 μ m) with a non-uniform distribution of larger precipitates.

In terms of corrosion, WE43MEO suffered a higher corrosion rate and greater mass loss compared to ZX10. The corrosion morphology of WE43MEO showed extensive formation of large, wide pits along its length (Fig 1). Conversely, ZX10 exhibited smaller, interconnected pits.

Micro-CT analysis corroborated these findings, demonstrating a larger pitting factor for WE43MEO but a lower pitting density.

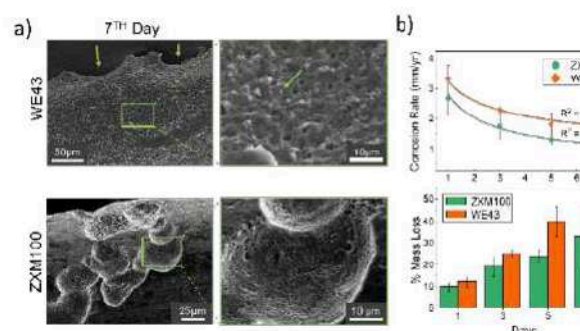


Fig. 1: a) Corrosion morphology for both wires after 7 days b) The corrosion rate and mass loss results for both wires.

Furthermore, WE43MEO's mechanical strength and ductility drops below ZX10 after 5th day of corrosion even though it starts higher.

DISCUSSION & CONCLUSIONS: The observed corrosion dependence on microstructure directly impacts the suitability of these alloys for specific applications. While WE43MEO initially offers superior strength, its rapid mechanical degradation makes it less ideal for long-term implants. However, its early strength advantage suggests potential for shorter-term applications where higher initial load bearing is crucial. Conversely, ZX10's more corrosion-resistant microstructure translates to slower mechanical decline, making it a promising candidate for longer-term implants. Future work should aim to refine the relevant microstructures for improved performance, possibly by achieving a more uniform distribution of smaller precipitates.

REFERENCES: ¹van Gaalen K., Gremse F., Bemm F, et al. *Bioactive Materials*. 2022; (8): 545–558. Automated ex-situ detection of pitting corrosion and its effect on the mechanical integrity of rare earth magnesium alloy - WE43.

ACKNOWLEDGMENTS: Thanks to Fort Wayne Metals for providing the wire and Meotec for providing the WE43MEO wire precursor.



Stress corrosion cracking testing as an assessment tool for novel biodegradable Mg alloys

Sochima S. Ezenwajiaku¹, Michele V. Manuel¹

¹ *Department of Materials Science and Engineering, University of Florida, Gainesville, USA*

INTRODUCTION: Despite breakthroughs and advances in research of novel magnesium (Mg) biodegradable implants there is still a misalignment of *in vitro* and *in vivo* material performance. This is partially due to the limitations of current evaluation methods. There are few *in vitro* strategies and experimental frameworks that can mimic the complex dynamic process in the body. Mechanical properties, particularly during the degradation process, are a performance parameter that requires an improved assessment technique. As our field expands, it is appropriate to review and propose enhanced testing techniques for novel biodegradable metals.

CURRENT STATE OF ART: The majority of studies assessing new Mg biodegradable materials (BMs) tend to concentrate on mechanical properties before implantation/degradation and corrosion resistance as distinct factors¹. Ideal samples with tensile, yield, and elongations of > 300 MPa, 230MPa, and 15-18% respectively, are acceptable for orthopaedic fixation applications². However, when evaluating the effectiveness and applicability of BMs, sustaining mechanical support during the tissue healing process is critical. The change of residual strength during degradation has been coined as mechanical integrity. Recent shifts in the field have begun to add mechanical integrity as an evaluation criterion, currently *pseudo in-situ* mechanical testing is commonly employed as a standard practice. Nonetheless, there is a lack of standardization, and this method is subject to several limitations. However, an alternative approach to assessing mechanical properties during degradation is through stress corrosion cracking (SCC) testing. The evaluation of SCC has the potential to become a more reliable indicator of *in vivo* mechanical performance³.

STRESS CORROSION CRACKING TESTING: Magnesium (Mg) based alloys have shown significant promise among the various BMs, however, its poor chemical stability in corrosive environments, like the human body, is a challenge. This poor stability can lead to SCC, a failure mechanism that combines a harsh corrosive environment and applied stress, potentially leading to premature catastrophic failure. Factors such as, microstructure, alloy composition, pH, solution

constituents, temperature, and test conditions significantly affect the SC sensitivity of Mg alloys. The alloys' structural and compositional characteristics can mitigate the cracking sensitivity. It is widely recognized that robust passivation, which is the capability to form a protective layer on the surface, can decrease the susceptibility to SCC, but very few studies focus on the SCC resistance. Utilizing SCC test techniques like slow strain rate testing (SSRT) enables the extraction of both qualitative and quantitative data, including SC susceptibility indices for ultimate tensile strength and elongation to failure, critical stress intensity factor, as well as crack propagation patterns. These test methods can provide extensive information for evaluating mechanical properties/integrity during degradation in a shortened experimental timeframe.

DISCUSSION & CONCLUSIONS: Overall, effectiveness of biodegradable metals relies heavily on sustained mechanical support during tissue healing. However, current evaluation methods are primarily limited to corrosion resistance and pre-implantation mechanical testing. SSRT and other SCC testing methods have the potential to serve as a more reliable indicator of the mechanical performance of materials *in vivo*. Furthermore, these methods can aid in the establishment of new metrics and evaluation standards for the design of novel biodegradable materials and prediction of failure mechanisms.

REFERENCES: 1. Mei D, Zhang Q, Li Y, et al. The misalignment between degradation rate and mechanical integrity of Mg-Zn-Y-Nd alloy during the degradation evaluation in modified Hanks' solutions. *J Magnes Alloys*. Published online May 20, 2023. doi:10.1016/j.jma.2023.04.006
2. Khan AR, Grewal NS, Zhou C, Yuan K, Zhang HJ, Jun Z. Recent advances in biodegradable metals for implant applications: Exploring *in vivo* and *in vitro* responses. *Results Eng*. 2023;20:101526.doi:10.1016/j.rineng.2023.101526
3. Jiang J, Geng X, Zhang X. Stress corrosion cracking of magnesium alloys: A review. *J Magnes Alloys*. 2023;11(6):1906-1930. doi:10.1016/j.jma.2023.05.011



Microstructural characterisation and evaluation of mechanical properties of additively manufactured biodegradable Zn-xMg alloys

H Abenayake¹, C Persson¹, F D'Elia¹

¹ Division of Biomedical Engineering, Department of Materials Science and Engineering, Uppsala University, Sweden

INTRODUCTION: Among the three main families of biodegradable metals (Fe, Mg, and Zn)¹, biomedical Zn-alloys have recently garnered significant attention as promising materials for biodegradable implants. Compared to Mg-alloys that degrade too fast and Fe-alloys that degrade too slow, Zn-alloys have an intermediate biodegradation rate, resulting in optimal biocompatibility². However, numerous mechanical aspects of Zn-alloys such as strength, ductility, and static recrystallisation do not yet meet the required mechanical characteristics of natural bone structures, hindering their implementation as biodegradable implants². Due to the favourable mechanical properties induced by Mg alloying, Zn-Mg alloys have attracted increased interest in recent years³. Based on experimental evaluations in the literature³ and thermodynamic calculations, a Mg alloying content of less than 1 wt.% has been identified as ideal for improving tensile strength while minimally compromising ductility. Furthermore, the complexity of natural bone makes Additive Manufacturing (AM) a promising method for bone replacement due to its superior design flexibility, along with its unique ability to tailor microstructure and mechanical properties. Thus, the purpose of this study was to evaluate the mechanical behaviour of three additively manufactured Zn-xMg alloys (x=0.06, 0.5, and 1 wt.%) in relation to their microstructure, influenced by Mg content.

METHODS: Alloys were prepared by mixing powders of pure Zn and pure Mg. Laser powder bed fusion (L-PBF), a metal AM technology, was employed. As a measure of print quality, bulk density of as-printed samples was primarily quantified using image analysis of light optical microscopy (LOM) images. Phase analysis was performed using a combination of X-ray diffraction and energy dispersive X-ray spectroscopy. The microstructure was characterised using scanning electron microscopy and LOM. Mechanical properties were preliminarily assessed through microhardness measurements.

RESULTS: Relative densities > 99.5% were achieved for all three alloys under different processing windows (laser power, scanning speed, and hatch distance). As shown in Fig 1a, a

hierarchical microstructure featuring melt pool boundaries (dashed white lines), columnar (dashed red circle), dendritic (dashed yellow square), or combined structures (dashed green circle) was observed. Homogeneous distribution of Mg₂Zn₁₁ intermetallic (framed image) was identified as one of the primary strengthening mechanisms. This is evidenced by gradual increase in microhardness with increasing Mg content (due to increased amount of intermetallic) as depicted in Fig 1b.

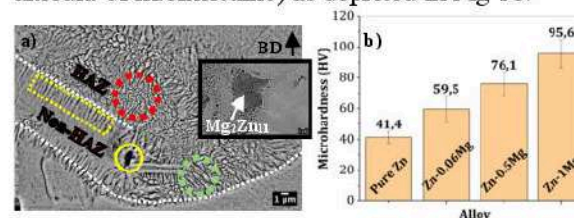


Fig. 1. a) An SEM image of as-printed Zn-0.5Mg, framed SEM image showing Mg₂Zn₁₁ intermetallic; b) Microhardness w.r.t Mg content

DISCUSSION & CONCLUSIONS: Although dense parts could be produced, porosity (Fig. 1a - yellow circle) originating from MgO-rich regions was observed, attributed to oxidised Mg powder particles. Heat-affected zones (HAZ) subjected to thermal cycling mainly consist of columnar structures due to the reduced net cooling rate, while non-HAZ consist of dendritic microstructures. Besides intermetallic strengthening, solid solution strengthening also contributes to the increased microhardness with higher Mg content. In conclusion, Mg alloying is a promising approach to addressing the poor mechanical properties of Zn, and future works aims to characterise tensile properties and recrystallisation effects.

REFERENCES: ¹H. Hermawan, Prog Biomater, 2018, 7, 93–110. ²G. Li et al., Acta Biomater, 2019, 97, 23–45. ³M. Voshage et al., Mater Today Commun, 2022, 32, 103805.

ACKNOWLEDGEMENTS: This work is conducted within the Additive Manufacturing for the Life Sciences Competence Centre (AM4Life). The authors acknowledge financial support from Sweden's VINNOVA (Grant no: 2019-00029), as well as the Swedish Research Council (2021-04708) and EU (grant no. 101110609; AMMagScaff).



The effect of powder preparation on mechanical properties and degradation behavior of biodegradable Fe-Mn-C sintered alloys for biomedical applications

Abdelhakim Cherqaoui¹, Carlo Paternoster¹, Simon Gélinas², Carl Blais², Diego Mantovani¹

¹: Laboratory for Biomaterials and Bioengineering, Research Center of CHU de Quebec, Quebec City, G1L 3L5, Canada;

²: Department of Min-Met-Materials Engineering, Laval University, Quebec City, G1V 0A6, Canada.

INTRODUCTION: Fe-Mn-C alloys have recently raised interest for temporary biodegradable implants, thanks to their outstanding mechanical properties and good biocompatibility [1]. However, the control of their degradation rate could open their applicability to several applications [2]. Therefore, this study aims to develop a powder metallurgy Fe-Mn-C steel with porosity features suitable for a range of biomedical applications. The effects of powder preparation on the microstructure, the degradation rate, and the mechanical performances of Fe-Mn-C were investigated.

METHODS: Mixed (MX) and mechanically milled (MM) FeMnC powders were used to produce four groups of sintered FeMnC samples. The number in the condition name specifies the weight amount of milled powder. Particle size, chemical composition, and powder morphology were investigated using a laser particle size analyzer, microwave plasma atomic emission spectroscopy (MP-AES), energy dispersive spectroscopy (EDS), and scanning electron microscopy (SEM). Mixtures of MX and MM powders ranging from 55 μm to 75 μm were compacted in a uniaxial press (600 MPa) to obtain green compacts. They were sintered later at 1200 °C under an Ar-10%H₂ atmosphere for 3 h, followed by furnace cooling. Microstructural and mechanical characterization of sintered samples were carried out using SEM, x-ray diffraction (XRD), and transverse rupture tests. The degradation behavior was investigated through static immersion tests (up to 14 days) in Hanks' solution (pH 7.4) at 37 °C.

RESULTS: Chemical analysis of the starting powders and the sintered samples revealed variations in the amounts of Mn, C, and O. The MM powder exhibited a higher oxygen content of approximately 0.85 ± 0.04 wt.% compared to the MX powder, which had 0.06 ± 0.01 wt.%. In the final sintered samples, the amounts of Mn, C, and O were approximately 17 wt.%, 0.4 wt.%, and 0.15 wt.%, respectively. Fig. 1 shows that a network of interconnected pores was successfully formed especially for MX, 25MX, and 50MX. Porosity decreased with increasing amount of MM powder. The highest density was achieved with the 75MM sample, which had a relative density of $RD_{75MM} = 81.18 \pm 0.52$ %. This later exhibited a

tensile rupture strength of 777 ± 23 MPa. Degradation rates (DRs) were in the range 0.04 ± 0.01 (MX) to 0.12 ± 0.02 mm/year (25MM). SEM/EDS analysis carried out on degraded surfaces revealed the presence of degradation product layers containing mainly Fe, Mn, C, and O. This result suggests that the degradation products formed on the sample surfaces during the static immersion degradation tests were mainly in the form of Fe and Mn carbonates.

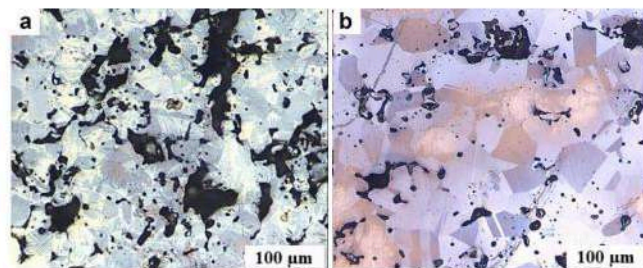


Figure 1. Nital 2% OM images of sintered samples for a) MX, b) 75MM conditions.

DISCUSSION & CONCLUSION: The preparation method of the starting powder significantly influenced the final microstructure, mechanical performance, and degradation behavior of the sintered alloy. The addition of MM powder up to 50 wt. % resulted in complex microstructures composed of ferrite, austenite, and martensite. In contrast, 75MM exhibited a dual-phase microstructure with 61 wt.% austenite and 39 wt.% martensite. These microstructural variations, along with the densification levels of each sample group, led to differences in DRs and mechanical properties. Notably, the 75MM sample exhibited the highest mechanical performances ($TRS_{75MM} = 777 \pm 23$ MPa) but had low degradability ($DR_{75MM} = 0.06$ mm/year). In contrast, the 25MM sample demonstrated an optimal balance of improved DR ($DR_{25MM} = 0.12$ mm/year) and satisfactory mechanical strength ($TRS_{25MM} = 691 \pm 34$ MPa), making it suitable for biodegradable implant applications such as suture anchors [3].

REFERENCES: [1] Gambaro S. et al., *Mat Tod Comm* 27 (2021) 102250, [2] Schinhammer M. et al., *Acta Bio* 6 (2010) 1705, [3] Nagra N. et al., *Bone Joint Res* 6 (2017) 82

ACKNOWLEDGEMENTS: This work was funded by NSERC-Canada under the Alliance program.



Effect of medium renewal mode on the degradation behavior of Mg alloys for biomedical applications during the long-term in vitro test

MY Liu^{1,2}, QY Zhang¹, XH Tang¹, CX Liu¹, D Mei¹, LG Wang¹, SJ Zhu¹, ML Zheludkevich², SV Lamaka², SK Guan¹

¹ School of Materials Science and Engineering & Henan Key Laboratory of Advanced Light Alloys, Zhengzhou University, China. ² Institute of Surface Science, Helmholtz-Zentrum Hereon, Germany.

INTRODUCTION: In vitro testing environment closely mimicking in vivo condition and representative of degradation behavior of magnesium alloy is yet to be achieved. For example, the effects of medium renewal mode are still vague. In this study, we investigated the influence of the specific ratio of medium volume to surface area and the disposable medium real-time renewal mode (flow-through) on Mg corrosion based on three representative test protocols. It is found that in flow-through medium renewal mode, the composition of the medium is maintained quasi-constant which is essential for corrosion tests. This work is beneficial for ultimately establishing the representative in vitro testing protocols for Mg bioabsorbable materials.

METHODS: The immersion tests were performed at 37°C, either in HBSS (pH=7.42 ± 0.02) or isotonic 0.9 wt.% aqueous NaCl (pH=6.8). Three medium renewal modes were selected in this work: a) According to ISO 10993-121, 1.25 mL of stagnant medium per 1 cm² of sample surface area was used, called 1:1.25 in the following text; b) According to ASTM-G31-722, 20 mL of stagnant medium per 1 cm² of sample surface area was used, called 1:20 in the following text; c) Referring to the new test approach, the initial volume of 20 mL per 1 cm² sample surface area and the disposable media was renewed with the rate of 1 mL·min⁻¹, which is provided by a peristaltic pump.

RESULTS: (a) In the HBSS medium, the morphology and thickness of corrosion products on the Mg surface are affected by medium renewal modes, which influence the corrosion rate of both Mg materials. (b) The weight loss results of pure Mg in the NaCl solution under the three medium renewal modes are significantly different from the trends when tested in the HBSS solution. Moreover, the corrosion rates also show the difference between ZE21B alloy and pure Mg at the early stage of corrosion.

DISCUSSION & CONCLUSIONS: Compared with the 1:1.25 and 1:20 renewal modes, the flow-

through medium renewal provides the most stable ionic and pH environment, which is similar to the in vivo service environment of Mg implants. By comparing the corrosion behavior of Mg-based materials under the three medium renewal modes, it is found that the influence of medium renewal modes on the corrosion behavior of Mg can be weakened by using the large ratio of medium volume to surface area.

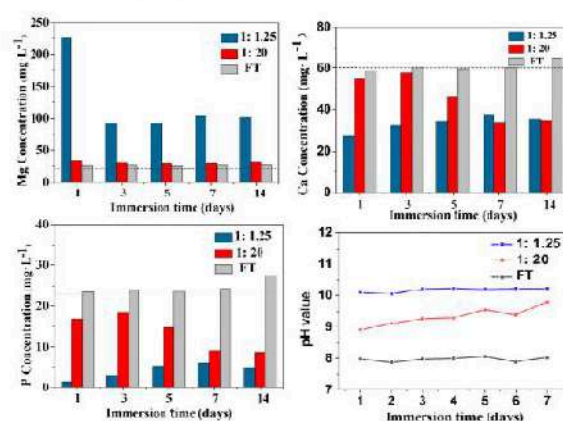


Fig. 1: The main ion concentration and pH value change under various HBSS renewal modes.

REFERENCES: ¹ International Organization for Standardization (2012), ISO 10993-12:2012, Biological evaluation of medical devices—Part 12: sample preparation and reference materials. ISO, Geneva, Switzerland. ² ASTM International (2004), ASTM-G31-72: standard practice for laboratory immersion corrosion testing of metals, Annual book of ASTM standards. American Society for Testing and Materials, Philadelphia, PA, USA. ³ C. Wang, C. Song, D. Mei, et al. (2022), Corros. Sci. 197 (2022) 110059.

ACKNOWLEDGEMENTS: The authors thank the Henan Province High-end Foreign Experts Introduction Program (HNGD2022037), the financial support from the National Key Research and Development Program of China (2021YFC2400703), and the National Natural Science Foundation of China (52301107).



Micro-Arc Oxidation of NiTi and Mg1.2Zn0.5Ca0.5Mn Skeletal Fixation Device

LH Olivas-Alanis¹, D Cho¹, B Panton¹, T Avey¹, Chmielewska², M Sanguedolce⁴, A Luo¹, David Dean^{1,4}

¹ Department of Material Science and Engineering, The Ohio State University, Columbus, OH, US

² Multidisciplinary Research Center, Cardinal Stefan Wyszyński University, Warsaw, Poland

³ Department of Mechanical, Energy and Management Engineering, University of Calabria, Rende, CS, Italy

⁴ Department of Plastic and Reconstructive Surgery, The Ohio State University, Columbus, OH, US

INTRODUCTION: Stress shielding-induced bone loss is often attributed to the high stiffness of Ti6Al4V, the standard-of-care material used in skeletal fixation and replacement devices [1]. Hence, the development and application of stiffness-matched devices is of great importance. In addition to “debulking” strategies, the use of new, safe materials may improve device performance. We present here a test of a multimaterial mandibular graft fixation device. The two materials are a Mg alloy we developed and have studied Mg1.2Zn0.5Ca0.5Mn; and a Ni-rich Nickel-Titanium (NiTi) alloy. Both materials are less than half as stiff as Ti6Al4V in their dense forms. The Mg alloy will degrade. At that point, the device will be incapable of stress-shielding. We have developed a coating strategy that uses Micro-Arc Oxidation (MAO) and sol-gel deposition of CaP. The surface treatment and coating is designed to ensure that the Mg alloy component will not begin to degrade until after bone healing is sufficiently complete.

METHODS: Our multi-material device comprises a Laser Based (PBF-LB) 3D printed NiTi shell and a cast-heat treated Mg1.2Zn0.5Ca0.5Mn machined and solid insert (Fig. 1). The cylindrical Mg alloy insert is cut via electro-discharge machining (EDM). To prohibit accelerated galvanic corrosion, a Zn interlayer is placed between the two components. Once joined, the MAO of the Mg alloy surface is conducted under a current-controlled process with 2.5 A current for 15 minutes. A Stainless-Steel bucket, containing the electrolyte, acted as a counter-electrode. The alkaline phosphate electrolyte composition is 3g/L (NaPO₃)₆ + 8g/L KF·2H₂O [2]. The sample was connected to the power source with a Ti wire fitted to the NiTi shell and exposed to the electrolyte. A polymeric coating was placed over the NiTi surface, to direct the current toward the Mg insert, and removed with acetone after the MAO process is complete. The resulting surface was evaluated via SEM and EDS (Fig. 2). The newly treated Mg alloy surface was subsequently deep coated, with

several layers, with a CaP via a previously published sol-gel process [2].

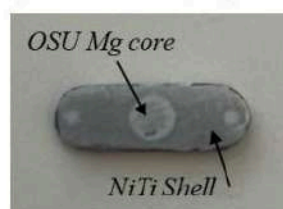


Fig. 1. MAO-treated multimaterial device showing the NiTi shell and Mg core.

RESULTS: Fig. 2 shows the resulting MAO-coated surface on the Mg insert. The process was conducted with a maximum current of 2.5A, and the output process voltage varied between 66 to 160V. The SEM image and EDS analysis show a dense, porous MAO surface layer on the Mg insert with a thickness of up to 50 μm. This porous surface is needed to strongly bind the CaP layer to the Mg alloy surface.

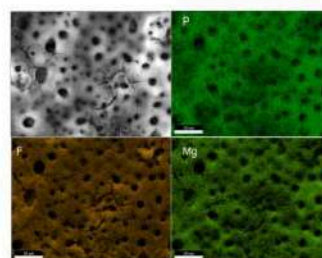


Fig. 2: SEM images Showing the presence of P, F, and Mg in the coating (MAO electrolyte).

DISCUSSION & CONCLUSIONS: This is the first attempt that we are aware of to achieve an MAO treatment on a Mg surface when joined to a NiTi component. This is a significant achievement given the conductivity difference between the materials. Moreover, the current tends to flow through more conductive NiTi rather than through Mg alloy. Hence, treating the Mg surface is challenging, but achievable. The next steps consider the application of this coating to highly complex surfaces.

REFERENCES: ¹ A. Chmielewska and D. Dean (2024) *Acta Biomaterialia* 173(1):51-65. ² H. Ibrahim et al., (2019) *Thin Solid Films* 687, 137456.

ACKNOWLEDGEMENTS: Partial funding was provided by OSU James Comprehensive Cancer Center Biomedical Device Initiative.



New insights into the microstructure of Mg-0.6Ca alloys using electron microscopy and Raman spectroscopy - A correlative characterization.

E Nidadavolu¹, M Mikulics², M Wolff¹, T Ebel¹, R Willumeit-Römer¹, J Mayer^{2,3}, H. Hardtdegen²

¹ *Institute Metallic Biomaterials, Helmholtz-Zentrum Hereon, Geesthacht, Germany*

² *Ernst-Ruska-Centre (ER-C-2), Forschungszentrum Jülich, Jülich, Germany*

³ *Central Facility for Electron Microscopy (GFE), RWTH Aachen University, Aachen, Germany*

INTRODUCTION: Powder processed Mg-Ca alloys are often reported to show homogeneous degradation due to their homogeneous microstructures [1].

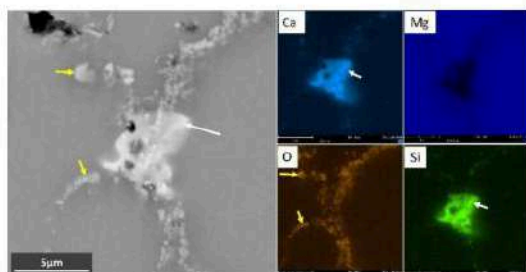


Fig. 1: Representative EDX map of MIM Mg-0.6Ca at a grain boundary.

However, ambiguity in the preliminary cell adhesion studies indicate the necessity to check surface contaminations due to carbon (C) residuals. This is probable as polymeric binders are used in additive manufacturing (AM) technologies like metal injection molding (MIM) and 3D printing [2]. In this regard, Raman spectroscopy was utilized to reveal carbonaceous residuals in the MIM Mg-0.6Ca microstructures.

METHODS: Mg-0.6Ca alloy feedstock was produced by mixing polymeric binder materials (waxes and backbone polymer) with the Mg-0.6Ca powder. Sintering was carried out under argon at 635 °C for 64 h. Later, a specimen of dimensions 6 mm x 6 mm (diameter x height) was machined for both SEM (coupled with EDX detector) and Raman spectroscopy. Raman spectra were collected with a confocal Raman microscope between 100 and 4000 cm⁻¹ wavenumbers.

RESULTS: EDX analysis revealed the presence of numerous fine precipitates located adjacent to each other along the grain boundaries (Fig.1). Predominantly, oxygen (O), calcium (Ca) and silicon (Si) intensities were observed. Certain precipitates comprised only O intensities whereas Ca and Si intensities coexist at random. In the range where carbon related Raman modes are detected (between ~1200 and ~2000 cm⁻¹), modes at nearly

1370 cm⁻¹ and 1560 cm⁻¹ are present which are ascribed to the presence of elemental C and a mode at 1865 cm⁻¹ is probably due to the C=C stretching mode. Grain interiors are mostly free of any precipitation giving rise to noisy signal in Raman due to the specimen's metallic nature (Fig.2 green spectra).

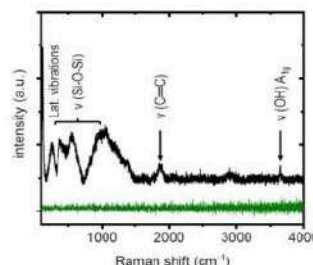


Fig. 2: Representative Raman spectra of MIM Mg-0.6Ca at a grain boundary (black spectra) and grain interior (green spectra).

DISCUSSION & CONCLUSIONS: The results indicate that Raman is a viable option to characterize carbon impurities on metallic biomaterial surfaces. The hydrocarbon cracking during the thermal debinding process (400-550 °C) releases C that might interact with Mg to form metastable carbides. The C=C in Fig. 2 can therefore be related to MgC₂ type carbides. Additionally, free C radicals are probable due to accelerated vacuum thermal decomposition of the hydrocarbons seen at wavenumbers 1370 cm⁻¹ and 1560 cm⁻¹ [2]. The exact nature of the stoichiometry with respect to Ca and Si still needs evaluation, however, the presence of C impurities might be important for future cell culture studies.

REFERENCES: ¹ E. Nidadavolu et al (2021), *Journal of Magnesium and Alloys* 9(2):686-703. ² J.G. Schaper et al (2018), *Advanced Engineering Materials* 26(11):1-9.

ACKNOWLEDGEMENTS: This research was funded by BMBF under the VIP+ project BioMag3D (Code: 03VP09852) and by the Joint Lab for Integrated Model and DataDriven Material Characterization (MDMC) of the Helmholtz Association.



Corrosion study of Fe₂₀Mn_{0.5}C parts obtained through additive manufacturing

I. Limón¹, D. Valdés¹, C. Paternoster², M. Multigner¹, M.D. Escalera¹, M. Muñoz¹, B. Torres^{1,3}, D. Mantovani², J. Rams^{1,3}

¹ Dpto. Ciencia e Ing. de Materiales, ESCET, Universidad Rey Juan Carlos, Madrid, Spain

² Laboratory for Biomaterials and Bioengineering, CRC-I, Dept Min-Met-Materials Eng. & CHU de Quebec Research Center, Regenerative Medicine, Laval University, Canada

³ Inst. de Inv. en Tecnologías para la Sostenibilidad, Universidad Rey Juan Carlos, Madrid, Spain

INTRODUCTION: Additive manufacturing (AM) offers unique opportunities to satisfy the complex design requirements of implants like stents. On the other hand, research on Fe-based biodegradable alloys for stent applications has increased considerably over the past decade due to their suitable mechanical properties like ductility and high ultimate strength¹. In this work, the effect of Laser Powder Bed Fusion (LPBF) parameters on the corrosion of Fe₂₀Mn_{0.5}C has been studied using potentiodynamic polarisation and Electrochemical Impedance Spectroscopy (EIS).

METHODS: An optimization of LPBF parameters (7×14×3 mm) was carried out varying the laser power (160-240 W) and the scan speed (340-640mm/s) (Fig. 1) in Renishaw equipment attending to the volumetric energy density (VED), which allows for quantitative comparison between parts manufactured by different laser parameters, and porosity of the samples. Three conditions were selected for the electrochemical tests: P160V640, P200V440 and P240V340. The electrochemical tests were carried out on at least three samples (15×15×3 mm) for each condition (one sample in each test) to guarantee the reproducibility of the results. The corrosion tests were performed using Hanks' modified solution. An Autolab PGSTAT 302N potentiostat was employed for electrochemical measurements. These measurements were conducted at room temperature in a three-electrode inert polymeric cell. The working electrode was the Fe₂₀Mn_{0.5}C sample, while the reference and counter electrodes were silver/silver chloride (Ag/AgCl) and graphite, respectively. Anodic polarization measurements were carried out at a 0.00166 V/s scan rate from -10 to 10 mV around the open circuit potential (OCP). The EIS tests were conducted at a frequency range from 10⁶ Hz to 1 mHz with 10 points per decade and a sinusoidal power amplitude of 0.01 V, after 1, 24, 48, 72, 96 and 168 hours immersion times.

RESULTS: The OCP values (Fig. 2) showed an increase from 1 hour to 24 hours of immersion,

with all three specimens reaching very similar OCP values (~ -0.73 V), after which they stabilized for all three conditions. The *R_p* values at the first 24 hours of the immersion period) were very similar for all conditions, around ~ 500 Ω·cm². After 24 hours, the P240V340 specimen gradually increased its resistance until 96 hours of immersion, reaching a value of ~ 16900 Ω·cm². The differences observed could be related to the different porosity of the samples.



Fig. 1. Additively manufactured samples still attached to the building platform.

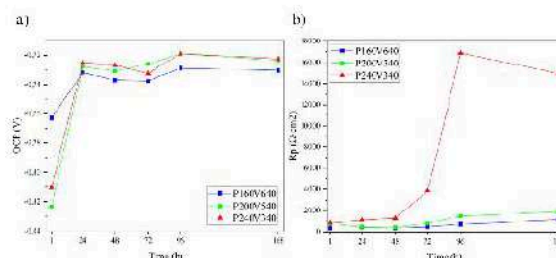


Fig. 2: Polarization results: a) open circuit potential (OCP), b) polarization resistance (*R_p*).

DISCUSSION & CONCLUSIONS: The corrosion rate strongly correlates with the porosity which in turn depends on the VED of the LPBF system during the manufacturing process.

REFERENCES: ¹ M. Schinhammer, C. M. Pecnik, F. Rechberger, A. C. Hânzi, J. F. Löffler, and P. J. Uggowitzer, "Acta Mater.", vol. 60, no. 6–7, pp. 2746–2756, Apr. 2012.

ACKNOWLEDGEMENTS: Financial support (AEI) PID2021-123891OB-I00, PID2021-124341OB-C21 and URJC -CI-PREDOC2020.



Partially bioresorbable Ti-Mg composite dental implant (BIACOM[®])

M Balog¹, P Križik¹, A M H Ibrahim¹, M Takáčová², M M de Castro¹, M Stamborska¹, A Catic³, Z Schauperl⁴, J Skiba⁵

¹*Institute of Materials and Machine Mechanics, SAS, Slovakia.* ²*Biomedical Research Center, Institute of Virology, SAS, Slovakia.* ³*School of dental medicine, University of Zagreb, Croatia.*

⁴*Faculty of mechanical engineering and naval architecture, University of Zagreb, Croatia.*

⁵*Institute of High Pressure Physics, PAS, Poland.*

INTRODUCTION: A high rate of adentia along with growing demand for cosmetic dentistry drive the dental implant (DI) market. Owing to their excellent biocompatibility, mechanical properties and corrosion resistance the commercial purity TiGr4, and TiGr5 alloy, are widely preferred in orthopedics and dentistry. Although Ti-based implants show good clinical performance, there are two issues that have not been fully addressed: i) the stress-shielding effect of implant over underlying bone structure, and ii) the insufficient bioactivity of the implants with surrounding bone in as-processed condition. We introduced a novel Ti-Mg composite, named BIACOM[®], tailored for the application of DI [1]. BIACOM[®] features highly strained ultrafine-grained pure Ti matrix embedded with interconnected Mg filaments skeleton. BIACOM[®] exploits the advantages of both biometals: a permanent Ti matrix provides the requested mechanical properties, a bioresorbable Mg component acts as beneficiary modulator for generating an osseoconductive surface via spontaneous dilution in body environment as well as bone formation stimulant. Mg, which has Young's modulus (E) much lower to that of Ti, gives rise to a reduction of the stress-shielding effect and has very good biodegradation potential. Owing to the porosity, which forms as a result of the selective Mg dilution, E of BIACOM[®] decreases and the bonding interface strength improves further. Concurrently BIACOM[®] maintains the mechanical performance and fatigue endurance, which complies with the minimum values specified in the ISO 22674 standard for the Type 4 biomedical material [2]. The BIACOM[®] specimens with the optimized surface yield acceptable corrosion rates of Mg [3]. Furthermore, they show a desirable *in-vitro* response, that is comparable to that of the TiGr4 reference. Preliminary implantation assays, which utilized large animal models and Ti12vol%Mg specimens, resulted in a positive response *in vivo* [4].

METHODS: The raw BIACOM[®] material rods, with Ti17vol%Mg composition, were produced from a plasma atomized TiGr1 and a gas atomized Mg99.8wt.% powders by a powder metallurgy

hydro-extrusion compaction. Two different DI designs: conventional and integrated, and two surface finishes: as-machined and HBSS prewashed were evaluated. The DI were CNC machined from as-extruded BIACOM[®]. Mechanical performance was modelled by FEA and experimentally verified in compliance with the ISO14801 standard for the fatigue testing of endosseous DI. The corrosion of Mg from the surface of the implants was evaluated by H₂ evolution volumetric method. *In-vitro* cytotoxicity biological response was assessed by the indirect contact MTT assay using DMEM extracts of DI and L929 cell line according to the ISO 10993-5. The TiGr4 DI were used as a reference.

RESULTS&DISCUSSION&CONCLUSIONS:

The present paper concisely reports the development of BIACOM[®] DI, which were designed in a way to reflect the peculiar properties of this novel partially bioresorbable material. The results confirmed that the integrated design BIACOM[®] DI with a prewashed surface meets the relevant mechanical and biological standards requested for endosseous DI, with an advantage of reduced stress-shielding effect and osseoconductive surface.

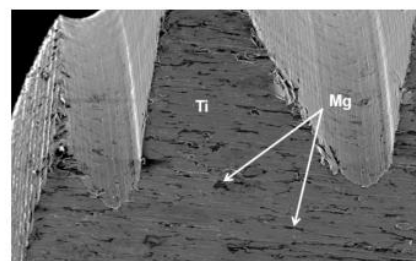


Fig. 1 The tip of the integrated BIACOM[®] DI.

REFERENCES: ¹ M Balog et al. (2019) *J. Mech. Behav. Biomed. Mater.* **90**: 45. ² A M H Ibrahim et al. (2020) *J. All. Compd.* **839**: 155663. ³ A M H Ibrahim et al. (2021) *Mater. Sci. Eng., C.* **127**: 112259. ⁴ A Catic et al. (2019) *Clin. Oral Implants Res.* **30(S19)**: 163.

ACKNOWLEDGEMENTS: Supported by the APVV-20-0417, VEGA-2-0157-24 and ITMS 313021T081 projects and the Stefan Schwarz Fund.



Extruding Low-Profile Semi-Finished Products from Bioabsorbable Magnesium Alloys for Cardiovascular Implants – Influence of Process Parameters

N Hoevelmann¹, Prof. Dr.-Ing. Kristian Arntz², A Kopp¹, M Muether¹

¹Meotec GmbH, Aachen DE; ²Univ. of Applied Science Aachen, DE

INTRODUCTION: The use of biodegradable magnesium alloys in cardiovascular applications is highly attractive to follow the “leave nothing behind” strategy, that is widely followed by industry and clinics. [1] Therefore is necessary to form tubes or wires with high tensile strength, high elongation and small grain sizes.

METHODS: Three biodegradable magnesium alloys (WE43, ZX00, and AZ31) were casted, extruded to a diameter of 9.5 mm and heat treated to form billets for succeeding low-profile extrusion. Wires of a diameter 1.5 - 2.5 mm from 9 mm billets were pressed in a custom vertical low-profile extrusion line. Input variables for the low-profile extrusion process were temperature, speed, method (direct/indirect) and extrusion-ratio. The investigated influence on mechanical properties, microstructure, and surface quality were analysed by tensile testing, sectioning, etching and laser-microscopy.

RESULTS: Press speed and press temperature are interconnected, as the block temperature increases with rising press speed. A strong interaction between these parameters was expected but not confirmed. The lack of significance in speed could be due to the narrow range of speed values used in the experiments. At lower process temperatures, higher forces are required for forming, as shown in the process window diagram. The WE43 experiments demonstrate this, with three out of four presses at 460°C requiring maximum force. Temperature and speed are closely linked, increasing press speed raises forming temperature due to increased friction and adiabatic heating. Comparing the results from this study with those from literature on various magnesium alloys, there is no clear indication that higher temperatures or speeds result in lower tensile strengths. For WE43 samples, the highest tensile strength of 415 MPa was achieved at low temperature and high speed. No clear trend is observed for elongation; higher tensile strengths often correspond to lower ductility, but higher elongations are also seen with high strengths. Recrystallization mechanisms result in a finer grain structure during and after forming. Higher deformation degrees lead to smaller newly formed grains. This relationship is confirmed by comparing the grain sizes of 1.5 mm and 2.5 mm

wires across all alloys. The pressing method significantly impacts the target properties in the experiments conducted. Contrary to Zhang et al.'s [2] thesis that higher temperatures negatively affect tensile strength, higher tensile strengths were achieved with direct pressing for all alloys. Direct pressing likely involves higher forming temperatures due to increased friction heating the material. The advantages of indirect pressing, such as faster pressing with lower temperature development, were not utilized in this study for direct comparison.

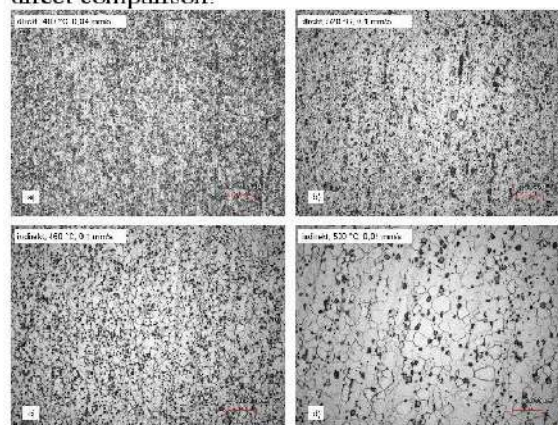


Fig. 1: Micrographs of the Ø 1.5 mm WE43 longitudinal samples at 1500x magnification.

DISCUSSION & CONCLUSIONS: The results indicate that in alloys WE43 and ZX00, only tensile strength is significantly influenced by the process parameters, with press method having a positive effect and temperature having a negative effect. Moreover, the interaction between press method and temperature negatively impacts tensile strength in ZX00 with increased process settings. Maximum tensile strengths exceeding 400 MPa, maximum elongations of 20%, grain sizes below 1 µm, and surface roughness depths smaller than 2 µm can be achieved.

REFERENCES:

- Gregory A. Stanley, MD *A Tale of Two Legs: Putting Patients Ahead by Leaving Nothing Behind* Endovascular today, April 2017
- Zhang, B. P.; Geng, L., et al. *Enhanced mechanical properties in finegrained Mg-1.0Zn-0.5Ca alloys prepared by extrusion at different temperatures* Scripta Materialia (Bd. 63), H. 10, S. 1024–1027



Influence of laser power and scanning speed on performances of LPBF Fe-16Mn-0.7C for bioabsorbable stent applications

Maria Laura Gatto¹, Paolo Mengucci¹, Marcello Cabibbo¹, Carlo Paternoster², Diego Mantovani²

¹ *Università Politecnica delle Marche, Ancona, Italy.* ² *Laval University, Quebec City, Canada;*

INTRODUCTION: Fe-Mn-C alloys have significant applications in developing temporary implants like bioabsorbable stents [1]. Laser powder bed fusion (LPBF), a promising additive-manufacturing technique, allows tailoring the microstructure by adjusting laser process parameters, expected to improve the degradation rate and mechanical properties of Fe-Mn alloys [2].

METHODS: In this study, we produced Fe-16Mn-0.7C bulk samples by varying laser power (50÷70 W) and scanning speed (700÷1000 mm/s), while maintaining a constant volumetric energy density (VED) of approximately 88 J/mm³ (Table 1), to understand the effect of printing parameters on the alloy's performances.

Table 1. Printing parameters used for producing Fe-16Mn-0.7C samples by LPBF technology.

Sample	Laser power [W]	Scanning speed [mm/s]	VED [J/mm ³]
P70v1000	70	1000	87.5
P60v855	60	855	87.7
P50v715	50	715	87.6

RESULTS: Fully austenitic microstructure, Fe and Mn amount in wt.%, and mechanical properties (microhardness approximately of 300 HV) appear comparable among the samples fabricated with different conditions. However, the defect analysis via X-ray micro-computed tomography (Fig. 1) allows to identify an operational window for producing fully dense Fe-16Mn-0.7C bulk samples using LPBF. Ongoing corrosion tests are being conducted to validate the obtained results further.

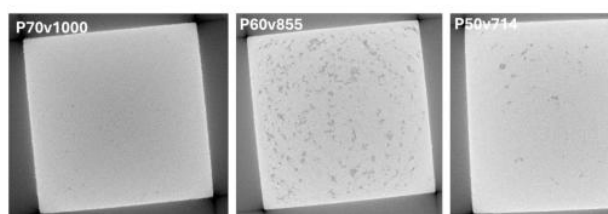


Fig. 1: 2D Cross-sectional slices of Fe-Mn-C samples produced by LPBF.

DISCUSSION & CONCLUSIONS: This operational window resulted in laser parameters (power and scanning speed) much lower than those reported in the literature [2].

REFERENCES:

- [1] Schinhammer, M., Hânzi, A. C., Löffler, J. F., & Uggowitzer, P. J. (2010). Design strategy for biodegradable Fe-based alloys for medical applications. *Acta biomaterialia*, 6(5), 1705-1713.
- [2] Liu, P., Wu, H., Liang, L., Song, D., Liu, J., Ma, X., & Baker, I. (2022). Microstructure, mechanical properties and corrosion behavior of additively-manufactured Fe-Mn alloys. *Materials Science and Engineering: A*, 852, 143585.



Towards an accurate prediction of magnesium biocorrosion by closer mimicking the in-vivo environment

M Yalcinkaya, A Bruinink, M Cihova, P Schmutz

Laboratory for Joining Technologies and Corrosion, Empa - Swiss Federal Laboratories for Materials Science and Technology, Dübendorf CH-8600, Switzerland

INTRODUCTION: Magnesium (Mg) has attracted great interest as a biodegradable metallic implant due to the formation of bioresorbable corrosion products during its degradation in the body. Yet, a challenge in the reliable prediction of degradation mechanism is that currently performed in-vitro experiments typically induce the formation of corrosion products with different chemical structures and transport properties than those observed in animal studies (in-vivo) [1].

From a materials perspective, another complexity level is generated by the low solubility of alloying and impurity elements in magnesium, resulting in the formation of cathodic secondary phases [2]. As the majority of published in-vitro studies involved such heterogeneous Mg surfaces, it remains unclear, if the corrosion product layer actually limits magnesium's anodic oxidation or decreases the cathodic reactivity of secondary phases.

To investigate the influence of these cathodic secondary phases on the Mg corrosion behavior in a physiological mimicking environment, an experimental setup was developed to include often overlooked in-vivo aspects such as solution flow, physiological pH buffering on the implant surface. Two very different materials were compared: low-purity Mg (99.9 wt% Mg; Fe >200 ppm), which contains a high amount of Fe-rich intermetallic phases, and ultra-high purity magnesium (XHP) (>99.999 wt% Mg; Fe <1 ppm) as a homogenous substrate without any secondary phase.

METHODS: Samples were exposed to our new formulation of a simulated interstitial body fluid (SIBF) that mimics the composition of human interstitial body fluid, based on an extensive literature review of the real measured values of inorganic ions and organic species [3]. The pH of SIBF is regulated with dynamic bicarbonate buffering and flown over Mg. The electrochemical reactivity of Mg samples was then evaluated by performing Electrochemical Impedance Spectroscopy (EIS). The samples were subsequently characterized using Scanning Electron Microscopy/Energy Dispersive X-ray Spectroscopy (SEM/EDS).

RESULTS: Fig.1 shows that the precipitation of corrosion products forms a porous intermediate layer on the Mg matrix and intermetallic phases.

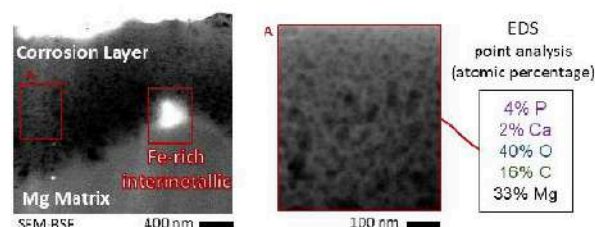


Fig. 1: Ion-milled cross-section of low-purity Mg, after 24 h in SIBF (37 °C, 1 µl/sec, pH 7.4)

EIS and SEM/EDS results indicated significantly reduced cathodic reactivity of the intermetallic phases, where the obtained values became comparable to those of ultra-high purity Mg.

Furthermore, corrosion products formed in solutions with different ions were studied on both purity degrees to assess the ionic diffusion barrier effect of Mg-hydroxide, Mg-phosphate, and Ca-phosphate formed on a heterogeneous or homogeneous surface.

DISCUSSION & CONCLUSIONS:

The levels of free Ca^{2+} , PO_4^{3-} and CO_3^{2-} ions have completely opposite effects on the electrochemical reactivity of Mg depending on the presence of Fe-rich intermetallic phases. Non-physiological concentrations of these ions in test solutions might be responsible for microstructure-dependent variations seen between in-vivo and in-vitro studies. We further aim to understand how organic compounds and inflammatory pH levels affect specific corrosion products to provide a more accurate Mg biocorrosion mechanism.

REFERENCES: ¹ J Walker, S Shadanbaz, N Kirkland, et al (2012) *J Biomed Mater Res B Appl Biomater* 100:1134-41. ² D Höche, C Blawert, S V Lamaka, et al (2016) *Phys. Chem. Chem. Phys.* 18:1279-91. ³ A Bruinink, *Handbook of Biomaterials* RSC (in press)

ACKNOWLEDGEMENTS: The authors would like to acknowledge the Metrohm Foundation for the financial support of this research.



cryo-atom probe tomography; quasi-'in situ' analysis of the reactive liquid-solid interface during Mg corrosion

Tim M. Schwarz¹, Leonardo S. Aota¹, Eric Woods¹, Xuyang Zhou¹, Ingrid McCarroll¹, Baptiste Gault^{1,2}

¹ Max-Planck-Institute for Sustainable Materials, Germany, ² Imperial College London, UK

INTRODUCTION: Corrosion reactions at liquid-solid interfaces critically impact infrastructure degradation and sustainability¹, and in medicine for biodegradable body implants². For the latter, Mg, is a promising candidate thanks to its biocompatibility and biodegradability, making it an excellent replacement for temporary implants made of Ti or steel³. However Mg alloys corrode rapidly and uncontrollably, through mechanisms not fully understood, i.e. there remain open questions regarding the influence of different alloying elements, their distribution, as well as different electrolytes, on the corrosion processes.

Understanding the corrosion processes at the reactive liquid-solid interface requires analytical methods with high local and chemical analysis capability and ideally to measure these reactions *in-situ*, on an atomic length scale, which is currently lacking. Atom probe tomography (APT) provides analytical imaging in 3D with equal chemical sensitivity across the periodic table even for light elements such as hydrogen and with comparable spatial resolution⁴ and can therefore close the gap.

transferred into a cryo-FIB using an ultrahigh-vacuum, cryo-transfer shuttle. A newly developed cryo-lift-out method was used to prepare APT specimens⁶.

RESULTS: By correlating cryo-APT and TEM, we observed outward growth of Mg hydroxide and inward growth of an intermediate corrosion layer of hydr/-oxides with different compositions. The high chemical sensitivity of APT revealed that instead of a MgO layer between the hydroxide and MgCa alloy, a Mg(OH) layer was formed, into which Ca partitions.

DISCUSSION & CONCLUSIONS: With the demonstrated approach it is possible to quasi-"in-situ" analyse the reactive solid-liquid interface by cryo-APT and investigate the early corrosion mechanisms of a Mg0.1Ca alloy. These metastable defect phases at the reactive interface could only be observed by quasi-"in-situ" cryo-APT analyses of the corrosion process, yet these early reaction products are highly reactive and must play a critical role in accelerating the corrosion. However, a better understanding of these early stages of corrosion and their products is necessary to advance the understanding of corrosion processes and their modeling, and consequently for higher level of control over the biodegradation rate of future implant material.

REFERENCES: ¹Bender, R. *et al.* Corrosion challenges towards a sustainable society. *Mater. Corros.* **73**, 1730–1751 (2022). ²Witte, F. The history of biodegradable magnesium implants: A review☆. *Acta Biomater.* **6**, 1680–1692 (2010). ³Niranjan, C. A. *et al.* Magnesium alloys as extremely promising alternatives for temporary orthopedic implants – A review. *J. Magnes. Alloys* **11**, 2688–2718 (2023) ⁴Gault, B. *et al.* Atom probe tomography. *Nat. Rev. Methods Primer* **1**, 51 (2021) ⁵Schwarz et al. Quasi-"in-situ" analysis of the reactive liquid-solid interface during magnesium corrosion using cryo-atom probe tomography submitted (2024) ⁶Woods, E. V. *et al.* A Versatile and Reproducible Cryo-sample Preparation Methodology for Atom Probe Studies. *Microsc. Microanal.* **29**, 120 (2023).

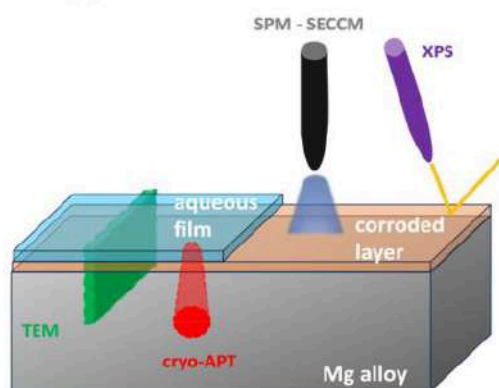


Fig. 1: Schematic overview of different methods to analyze the liquid-solid interface⁵.

METHODS: A binary Mg0.1Ca alloy was corroded using Deionized (DI) water in a glove box under an N₂ atmosphere. The corrosion process was started by pipetting a droplet of 20 µl DI water on a polished surface. Afterwards, the corrosion state was fixed by plunge-freezing the sample in liq. N₂ and solidifies the aqueous phase within a porous network. The frozen sample was



***In vitro* degradation analysis of 3D printed Mg-5Gd alloy scaffolds**

K Pérez Zapata¹, E Nidadavolu¹, M Wolff¹, T Ebel¹, R Willumeit-Römer¹

¹*Institute of Metallic Biomaterials, Helmholtz-Zentrum Hereon GmbH, Germany*

INTRODUCTION: Magnesium (Mg) alloys have been potentially classified as candidates for use as tissue implants due to their biocompatibility, biodegradability, and mechanical properties. These alloys have been extensively investigated in orthopedic implants, and additive manufacturing (AM) of scaffolds has been seen as one of the most attractive alternatives for bone repair [1]. Within these emerging areas, tissue engineering enables the customization of porous implants to facilitate patient adaptation and bone growth. This requires scaffolds to have good degradability, interconnected structure to promote bone growth, and degradation control to withstand physical loads during healing [2]. The AM of magnesium alloys allows the production of structures similar to natural bone tissue with pore size ranging from 100 till 1000 μm . In this study, the results of scaffolds produced with different pore sizes and their influence on degradation behavior are reported.

METHODS: Three gyroid structures with different pore sizes and cell wall thickness were generated using Creo 7.0 software. Mg-5Gd feedstock comprised of the raw powder and polymer binder materials. Fused granular fabrication (FGF) technique was used to 3D print these scaffolds (AIM3D, ExAM255, Germany). Green parts were sintered under argon at 648 °C for 32h. *In vitro* degradation was carried out under physiological cell culture conditions (37 °C, 5% CO₂, 20% O₂, 95% rel humidity) using DMEM + Glutamax (Life Technologies, Darmstadt, Germany) supplemented with 10% FBS (PAA Laboratories, Linz, Austria). Scaffolds were characterized using micro-Tomography (μCT) and degraded specimens were analyzed using scanning electron microscopy (SEM) technique.

RESULTS: μCT analysis revealed the cell wall thickness of 650 μm , 790 μm , and 1000 μm , corresponding to 1250 μm , 1080 μm and 720 μm pore sizes, respectively in the produced structures. SEM analysis revealed scaffolds that were completely covered with degradation products (see Fig. 1). A homogeneous layer on the surface containing nodular morphologies and some needle-like crystals were found. Due to the different pore sizes of the scaffolds, different degradation rates were observed. As shown in table 1, the highest DR is associated with the sample with the smallest

pore size, which may be caused by an increase in surface area.

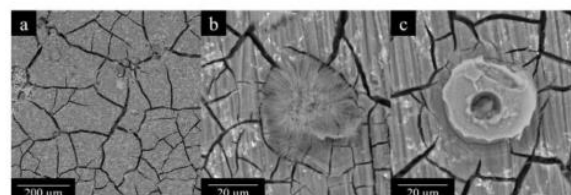


Fig. 1: Degradation products on Mg-5Gd scaffold structures a) homogeneous layer, b) needle, c) nodules. **Table 1.** DR values of Mg-5Gd scaffolds over a duration of 7 days.

Scaffold	Wall thickness (μm)	DR (mm/year)
P1250	650	5.4
P1080	790	3.9
P720	1000	1

DISCUSSION & CONCLUSIONS: It was found that the smaller pore sized P1000 scaffold showed a lower DR compared to others. With higher surface area a higher release of Mg ions upon contact with the cell culture medium is envisioned. Hence, pore size is significantly influential in modulating degradation behavior. Additionally, to maintain the mechanical stability of the scaffolds during degradation, a thicker strut i.e. smaller pore size can be beneficial. In this regard, compression tests on the produced scaffolds will be carried out. These preliminary results show that sinter-based 3D printing technology is a viable alternative to mass produce tailor-made Mg biomaterials. Using smaller nozzle diameters <200 μm during 3D printing further facilitates production of scaffold pore sizes < 720 μm reported here, which might potentially reduce the DR to <1 mm/year.

REFERENCES: ¹ N. Sezer (2021) *Additive manufacturing of biodegradable magnesium implants and scaffolds: Review of the recent advances and research trends*, JMA. ² I. Marco, (2017) *In vivo and in vitro degradations comparison of pure Mg, Mg-10Gd and Mg-2Ag: a short term study*, European Cells and Materials.

ACKNOWLEDGEMENTS: This research was carried out in the framework of BioMag3D project (code Nr. 03VP09852) financed by the BMBF. The authors acknowledge H Lüneburg, M Luczak and A Schuster for their expertise in methodology and technical assistance.



Advanced biodegradation imaging with novel correlative 3D X-ray and electron microscopy workflow - ZX00 case study

T. Akhmetshina¹, R.E. Schäublin^{1,2}, A.M. Rich¹, L. Berger¹, P. Zeng², I. Rodriguez-Fernandez^{3,4}, N.W. Phillips^{3,7}, J.F. Löffler¹

¹Laboratory of Metal Physics and Technology, Department of Materials, ETH Zurich, Switzerland

²Scientific Center for Optical and Electron Microscopy (ScopeM), ETH Zurich, Switzerland

³Paul Scherrer Institute, Villigen PSI, Switzerland

⁴Institute for Biomedical Engineering, University and ETH Zurich, Switzerland

⁷Present address: Mineral Resources, CSIRO, Australia

INTRODUCTION: This work presents a new correlative microscopy workflow that combines quantitative 3D X-ray ptychography (PXCT) with high-resolution electron microscopy. The combination allowed us to successfully investigate corrosion in a medical Mg alloy (ZX00) with minimal damage to the sample while still closely approximating *in situ* conditions.

METHODS: The ZX00 (Mg-0.45Zn-0.45Ca, wt.%) extruded alloy was prepared as described previously¹. A 5- μ m diameter pillar for PXCT was created with a focused ion beam (FIB). The measurements were performed at the cSAXS (X12SA) beamline of the Swiss Light Source (SLS) at the Paul Scherrer Institute. The sample was scanned before and immediately after 1 hour of immersion in simulated body fluid (SBF) at 37 °C and pH 7.4. The same sample was imaged using a FIB-SEM slice-and-view procedure. A lamella was extracted from the middle of the scanned pillar and investigated with scanning transmission electron microscopy (STEM).

RESULTS: The PXCT reconstructions provided 3D electron density maps of the pillar with nanoscale resolution (83 nm for the pristine and 123 nm for the corroded state). The high contrast efficiency of PXCT enabled a clear distinction of nanoscale Mg₂Ca precipitates from the Mg matrix, and their location was further confirmed with FIB-SEM. Moreover, it revealed the complex structure of the corrosion products where four different layers could be distinguished based on their electron density difference (Fig.1a). Electron microscopy with energy dispersive X-ray spectrometry (EDX) mapping allowed correlation of the electron densities to the precise chemical composition of the corrosion products. The results illustrate that the corrosion layer morphology is dense and defect-free, and the corrosion of the material is grain-orientation sensitive (Fig.1b,d). High-resolution STEM-EDX mapping (Fig.1c) revealed Zn redistribution and clustering at the metal-corrosion products interface.

DISCUSSION & CONCLUSIONS: Directly comparing the pristine and corroded states of the same sample enabled us to establish the influence of chemical heterogeneities and microstructure on corrosion resistance. The developed workflow paves the way for more advanced corrosion studies of bioactive materials.

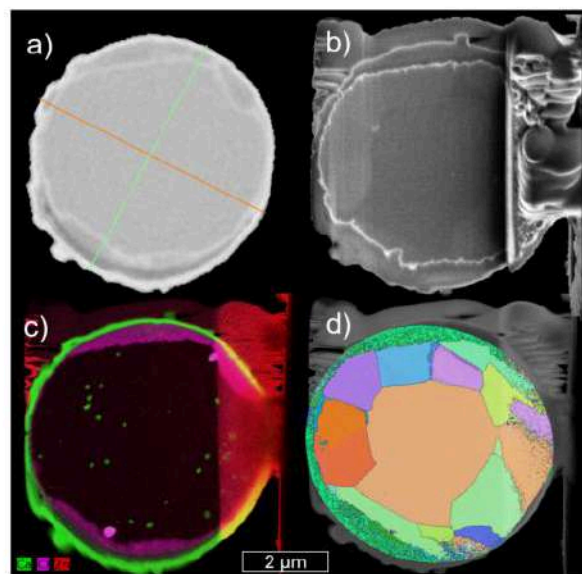


Fig. 1: Same ROI of the corroded pillar (cross-section) imaged with a) PXCT b) SEM c) STEM-EDX and d) TEM grain orientation map.

REFERENCES: ¹P. Holweg, L. Berger, M. Cihova, N. Donohue, B. Clement, U. Schwarze, N. G. Sommer, G. Hohenberger, J. J. J. P. van den Beucken, F. Seibert, A. Leithner, J. F. Löffler, A. M. Weinberg, *Acta Biomater.* 2020, 113, 646.

ACKNOWLEDGEMENTS: The authors gratefully acknowledge financial support from the Swiss National Science Foundation (SNF Sinergia, Grant No. CRSII5-180367). They thank the Paul Scherrer Institute for the allocation of beamtime at the SLS, ScopeM at ETH Zurich and CIME at EPFL, Lausanne for the access to its facilities.



Properties and characterization of magnetron sputtering coatings for biomedical resorbable applications

M Shekargoftar¹, S Ravanbakhsh¹, VS Oliveira¹, G Barucca², P Mengucci², M Cabibbo³, SS Parapari⁴, S Šturm⁴, A Sarkissian⁵, F Witte⁶, C Paternoster¹ and D Mantovani¹

¹ *Laboratory for Biomaterials and Bioengineering, CRC-I, Department of Min-Met-Materials Eng., & University Hospital Research Center, Regenerative Medicine, Laval University, QC, Canada;* ² *Department of Materials, Environmental Sciences and Urban Planning, Università Politecnica delle Marche, Ancona, Italy;* ³ *Department of Industrial Engineering and Mathematical Sciences, Università Politecnica delle Marche, Ancona, Italy;* ⁴ *Jozef Stefan Institute, Ljubljana, Slovenia;* ⁵ *Plasmionique Inc, QC, Canada;* ⁶ *Department of Prosthodontics, Geriatric Dentistry and Cranio-mandibular Disorders, Charité Universitätsmedizin, Berlin, Germany*

INTRODUCTION: Physical vapor deposition (PVD), allowing the condensation of material from the vapor of a solid target, is a widely-used thin film deposition technique already employed in several industries, from microelectronics to biomedical engineering^{1,2}. PVD systems differ according to the way the vapor is produced: one of them is called *magnetron sputtering*. It involves bombarding a target material, ejecting its atoms and directing it toward the substrate through appropriate magnetic fields, that leads to the formation of thin films on the substrate³. Magnetron sputtering (MS) can be used to obtain coatings through a controlled deposition rate, offering a fine tuning of the properties of the condensed material. This is needed especially for those applications in which a strict property control is needed, like for biomedical ones^{4,5}. The technique allows the deposition of pure elements, alloys, ceramic and other compounds, with or without the use of reactive gases. In this work, MS was used for deposition of several biodegradable coatings containing Fe- and Mg- for different applications. The effects of working gases and deposition parameters such as power and substrate temperature on the properties of the coatings were analyzed.

METHODS: The coatings were deposited using a MS system (Plasmionique MS300, QC, Canada). Coatings were deposited on a silicon substrate for preliminary process analysis, and then on functional substrates, for example Mg. The sputtering gas was Ar. The properties of the coatings were characterized using scanning and transmission electron microscopy (SEM and TEM), X-ray diffraction (XRD), X-ray photoelectron spectroscopy (XPS), and other complementary techniques to assess physical, electrochemical and mechanical properties; in particular, the corrosion behavior was studied in Hanks' solution.

RESULTS: Fig. 1 presents the cross-section micrographs of two Fe-Mn-based coatings enriched with W. The chemical composition was related to the different power applied respectively to the Fe-

Mn-C target, and to the W one; for example, the thickness for $P_W = 100$ W was $t = 0.8$ μm , while for $P_W = 400$ W to the thickness was $t = 1.8$ μm , with subsequent W increase, because of the increased sputtering rate of W. The corrosion rates associated with powers of 100 W and 400 W were 0.26 mm/y and 59.06 mm/y, respectively. In addition, it was found that increasing the substrate temperatures produced more homogeneous surfaces, decreased corrosion rates, and increased mechanical properties.

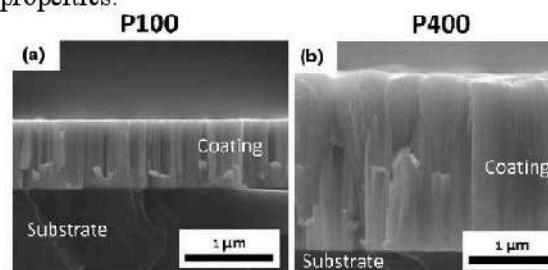


Fig 1. Cross-sections of Fe-Mn-C-W films deposited with a) $P_W = 100$ W and b) $P_W = 400$ W for 1 h

Mg-containing coatings showed a morphology, and corrosion properties related to the microstructure and to the presence of Mg.

DISCUSSION & CONCLUSIONS: Investigating various parameters and working gases in this work provides a template for design and optimization of coatings for diverse applications. Overall, the results contributed to increase the knowledge about magnetron sputtering coatings as a valid technique for deposition of resorbable coatings with controlled properties.

REFERENCES: ¹ Deng Y, *et al.* (2020). *Ceram Int* 46:18373–18390; ² Gupta G, *et al.* (2020). *Mater Today Proc* 38:259–264; ³ Heimann RB (2021). *Surf Coat Tech* 405:126521; ⁴ Li J, *et al.* (2022). *JOM* 74:3069–3081; ⁵ Nilawar S, *et al.* (2021). *Mater Adv* 2:7820–7841.

ACKNOWLEDGEMENTS: This work was supported by NSERC-Canada-Alliance. DM holds a Canada Research Chair Tier I (2012-2026).



Investigating Biocompatibility and Cell Growth on the Surface of additively manufactured Zn1Mg Specimens

F. Fischer¹, Qun Zhao², M. Voshage¹, M. Praster², L. Jauer¹, A. Kopp³, E. Balmayor², J. Greven⁴, J.H. Schleifenbaum¹

¹Chair for Digital Additive Production DAP, RWTH University, Aachen, Germany, ²Experimental Orthopaedics and Trauma Surgery, Department of Orthopaedics, Trauma and Reconstructive Surgery, University Hospital RWTH Aachen, Aachen, Germany, ³Meotec GmbH, Aachen, Germany, ⁴Department of Thoracic and Cardiovascular Surgery, Medical Faculty, RWTH Aachen, University Hospital Aachen, Aachen, Germany

INTRODUCTION: The growing need for alternatives to autologous bone grafts when treating bone defects leads to the development of bioresorbable materials like zinc-magnesium¹. This work investigates the biocompatibility, cytotoxicity, and osteoblast cell growth of additively manufactured (AM) zinc-magnesium specimens to assess this alloy for clinical application (e.g. patient specific, load-bearing implants).

METHODS: Zn1Mg alloy cylinders from *Nanoval GmbH & Co. KG* were fabricated using a modified laser powder bed fusion machine from *Aconity 3D* with a diameter of 6 mm and a thickness of 1 mm. The specimens are “as-manufactured” (i.e. no further post-processing) for all tests. Osteoblasts were cultured in DMEM (Pan Biotech, Aidenbach, Germany, catalog number: P04-05550, 37°C, 5% CO₂) with the cylinders for up to 14 days to determine first aspects of biocompatibility and growth properties of the alloy. Cell viability, cytotoxicity, and proliferation were assessed using Live/Dead staining with calcein, DAPI staining, with subsequent fluorescence microscopy, and flow cytometry (FACS). Additionally, cellular morphology was examined using Phalloidin/DAPI staining and scanning electron microscopy (SEM).

RESULTS: Live/Dead staining shows high osteoblasts viability and proliferation on Zn1Mg after 7 days. FACS analysis confirms a 99.1% survival rate out of 40k cells (fig. 1, top). Fluorescence microscopy of DAPI-stained cells indicates an increase in nuclei over 3, 7, and 14 days. Furthermore, the phalloidin/DAPI staining (fig. 1 (center)) reveals a pronounced development of the cytoskeleton after 14 days. SEM images of the Zn1Mg cylinder surface after contact with the cells for 14 days (fig. 1 (bottom)) display the typical texture of additively manufactured parts, characterized by unmelted particles sintered to the surface. Embedded in this texture, osteoblasts can be seen.

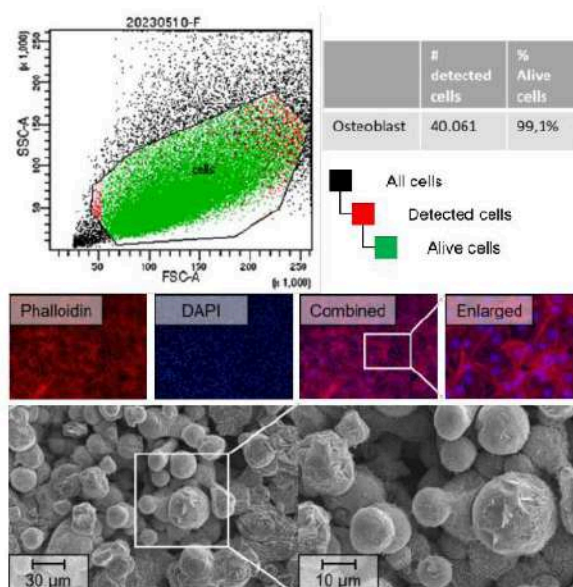


Fig. 1: (top) FACS analysis after contact with Zn1Mg (center) Phalloidin/DAPI staining of osteoblasts after 14 days (bottom) SEM images of cylinder surfaces after 14 days²

DISCUSSION & CONCLUSIONS: The 99.1% survival rate significantly exceeds the 70% minimum requirement of DIN EN ISO 10993-5, classifying Zn1Mg alloy as non-toxic. Cell viability and proliferation show positive responses to the alloy and its degradation products. Surface roughness does not hinder cell attachment, as indicated by observed filopodia suggesting cell migration. These findings support future use of AM Zn1Mg for patient-specific implants and scaffolds enhancing cell ingrowth.

REFERENCES: ¹C. Shuai et al. (2019) Biodegradable metallic bone implants, DOI: 10.1039/C8QM00507A ²M. Voshage (2024) Additive manufacturing of Zink Magnesium alloys, ISBN 978-3-98555-199-6

ACKNOWLEDGEMENTS: Parts of this work were funded by the German Federal Ministry of Education (13GW0404D & 03RU1U173C)



Characterisation and assessment of corrosion rate of HfO₂-PDLGA coated WE43 produced by atomic layer deposition for cardiovascular stent applications

CG Hynes¹, Z Ghaferi², S Malinov¹, A Flanagan², F Buchanan¹, A Lennon¹

¹School of Mechanical and Aerospace Engineering, Queen's University Belfast, UK.

²Boston Scientific Ltd., Galway, Ireland

INTRODUCTION: Atomic layer deposition (ALD) as a coating technique has several potential advantages for the development of magnesium (Mg) based bioresorbable cardiovascular stents and the control of Mg's rapid corrosion rates: ALD eliminates issues related to line-of-sight coating methods and can produce conformal coatings with tuneable, nanoscale thicknesses¹, that do not deleteriously impact on the overall stent geometry from an overall strut thickness perspective². Hafnium dioxide (HfO₂) is commonly produced by ALD and there is an emerging interest in its use as a suitable biomaterial. This study aims to investigate the potential of HfO₂ coatings, deposited via ALD, in conjunction with poly lactic co glycolic acid (PDLGA) – a common drug eluting polymer employed for cardiovascular stents – to regulate the degradation rates of WE43 magnesium alloy for stent applications.

METHODS: HfO₂ coatings were grown at 150°C by ALD on WE43 Mg coin components to produce HfO₂ layers with a thickness of 5 nm, 50 nm and 100 nm. XPS was conducted to assess coating composition. SEM studies evaluated the structure and morphology of the coating. Degradation studies were conducted in simulated body fluid (SBF) to measure hydrogen (H₂) evolution. Additionally, 0.3 mm dia. WE43 wires were coated with 50 nm HfO₂ and subsequently dip coated with PDLGA. Wires were immersed in SBF to assess the corrosion resistance of the HfO₂-PDLGA coatings and tensile testing was conducted before and after immersion for 40 hrs.

RESULTS: SEM images (Fig. 1a,b) revealed a uniform HfO₂ coating on the Mg surface. XPS analysis revealed an atomic concentration of O and Hf at a ratio of 2:1, indicating an adequate coating process (Fig.1c). H₂ evolution studies (Fig. 1d) revealed a thickness-based reduction in H₂ evolution across HfO₂ coated samples in a 21-day period. Tensile tests (Fig. 2 a,b) of the coated wires demonstrated improved retention of yield strength of HfO₂ coated wire specimens after immersion in SBF.

DISCUSSION & CONCLUSIONS: HfO₂ coatings demonstrated improved corrosion resistance of Mg, which was tuneable with respect to the coating thickness.

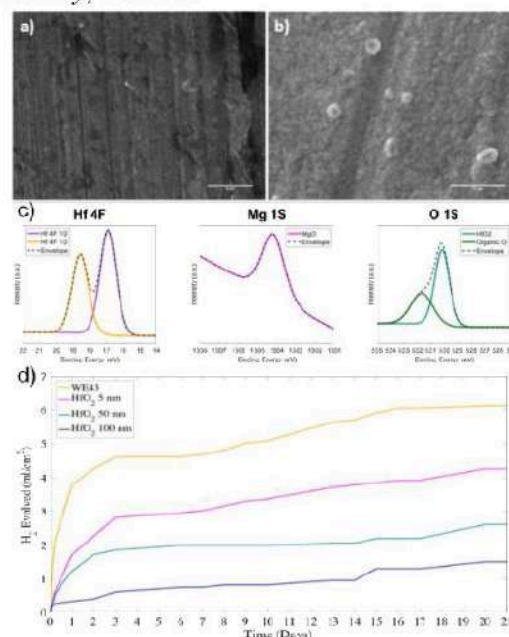


Fig. 1: SEM images of a) WE43 and b) HfO₂ 50 nm coating, c) XPS of 50 nm HfO₂ and d) H₂ evolution measures of WE43, 5 nm, 50 nm and 100 nm HfO₂ coatings.

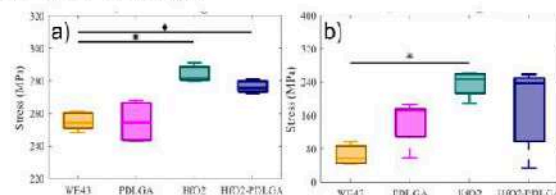


Fig. 2: Yield strength of WE43 wire, PDLGA, HfO₂ and HfO₂-PDLGA coating a) before immersion and b) after immersion in SBF.

Tensile testing of the coated wires demonstrated improved strength retention of the HfO₂ coated wires after immersion in SBF, although the addition of PDLGA-coating increased variability considerably (Fig. 2b). This study provides interesting preliminary insights into the potential role of HfO₂ as a coating material for controlling Mg degradation.

REFERENCES: ¹ Johnson, R. *et al. Materials Today*. 17, 236-246 (2014). ² Basiaga, *et al., Arch. Civil Mech Eng.* 17, 32-42 (2017)

ACKNOWLEDGEMENTS: This project has received funding from the EU's H2020 Research and Innovation Programme under the Marie Skłodowska-Curie grant agreement no 813869.



Surface characterization and biocompatibility evaluation of electropolished pure magnesium for biomedical applications

J Kloiber^{1,2}, H Helmholz³, R Willumeit-Römer³, H Hornberger^{1,2}

¹ Biomaterials Laboratory, Faculty of Mechanical Engineering, Ostbayerische Technische Hochschule (OTH), Regensburg, Germany. ² Regensburg Center of Biomedical Engineering (RCBE), Ostbayerische Technische Hochschule (OTH) and University of Regensburg, Regensburg, Germany. ³ Institute of Metallic Biomaterials, Helmholtz Zentrum Hereon, Geesthacht, Germany

INTRODUCTION: Magnesium (Mg) materials are interesting for use in guided bone and tissue regeneration. However, Mg-based material carry the risk of inhomogeneous degradation in aqueous environment [1]. Electropolishing is an attractive surface treatment to improve the corrosion behaviour of Mg [2], but it is not well known how the modified surface affects the biocompatibility of this resorbable metal. The aim of this study was to investigate the degradation and biocompatible behaviour of electropolished Mg to assess the effects of corrosion and surface treatment on tissue regeneration under physiological conditions.

METHODS: Extruded pure Mg discs (99.94 wt% Mg; Helmholtz Zentrum Hereon, Geesthacht) with a diameter of 10 mm and a height of 2 mm served as working material. The samples were electropolished in a mixture of phosphoric acid and ethanol for 5 min at a current density of 0.08 A/cm². The degradation behaviour was observed in Dulbecco's Modified Eagle's Medium (DMEM) + 10% fetal bovine serum (FBS) and the wetting behaviour was determined by measuring the contact angle. The investigation of the biocompatibility of the Mg samples included a live dead staining of human mesenchymal stem cells incubated at the material surface for 5 days.

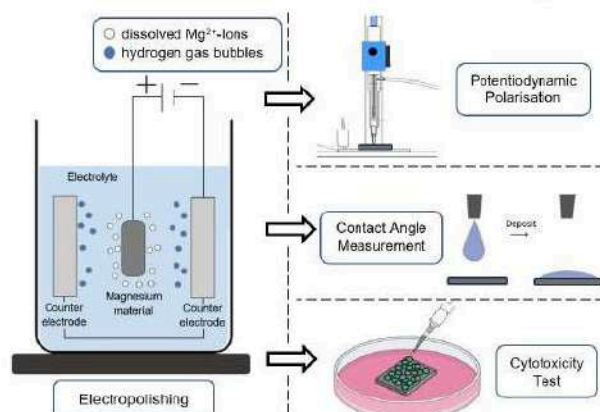


Fig. 1: Schematic illustration of the electropolishing setup and in vitro testing of the degradation and biocompatible behaviour of surface-treated Mg.

RESULTS: The degradation rate of electropolished Mg samples was, compared to mechanically polished surfaces, more than 15 times lower with values of about 0.08 mm/year. With a contact angle of approx. 30° in DMEM + 10% FBS, electropolished Mg surfaces exhibit optimized wettability. After electropolishing, cells could adhere to the Mg surface, but to a smaller extent.

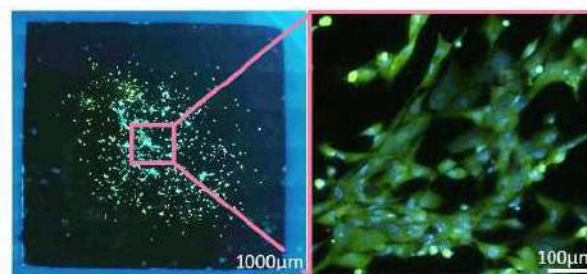


Fig. 2: Extent of cell adhesion and proliferation on electropolished pure Mg surfaces.

DISCUSSION & CONCLUSIONS: The electrochemical treatment can give an important contribution to the corrosion control of Mg materials, without having a cytotoxic effect on cells. However, the extremely smooth surface after the post-treatment restricts their adhesion. Moreover, it can be assumed that a wettable surface leads to a more even distribution of body fluids on the Mg component, so that the corrosive attack can also occur more uniform. The fact that Mg implants are designed to degrade means that the material surface and therefore its surface properties are constantly changing during the lifetime of an implant. This requires further in vitro investigation methods to be optimized and evaluated.

REFERENCES: ¹ A.H. Martinez Sanchez (2015) *Acta. Biomater.* **13**:16-31. ² J. Kloiber et al. (2023) *Mater. Today Commun.* **38**:107983.

ACKNOWLEDGEMENTS: We gratefully thank Regensburg Center of Biomedical Engineering (RCBE) for the support of laboratory consumables.



Exploring the biocompatibility and corrosion properties of a novel Mg-Ca-Zn-Y-Mn alloy for orthopedic implant materials

DC. Martinez¹, A Dobkowska¹, A Paradiso¹, D Drozdenko², A Farkas², K Mathis², K Pucia³, A Kaminski³, Y Kawamura⁴, W Swieszkowski¹

¹*Biomaterials Group, Faculty of Materials Science and Engineering, Warsaw University of Technology, Poland*

²*Department of Physics of Materials, Faculty of Mathematics and Physics, Charles University, Czech Republic.*

³*Laboratory of Experimental Animals, Medical University of Warsaw, Poland.* ⁴*Magnesium Research Center, Kumamoto University, Japan.*

INTRODUCTION: Mg-1Ca-0.5Zn-0.1Y-0.03Mn (at.%) alloy containing the long-period stacking ordered (LPSO) phases are characterized by high mechanical properties when compared to traditional Mg-based alloys [1]. This allows for considering it as temporary material for their potential use in biomedical applications. The present study investigates the biocompatibility and resistance to corrosion of the Mg-1Ca-0.5Zn-0.1Y-0.03Mn (at.%) alloy under physiological conditions.

METHODS: Rapidly solidified (RS) ribbons made of the Mg-1Ca-0.5Zn-0.1Y-0.03Mn (at.%) alloy were manufactured by single-roller melt-spinning, consolidated, and extruded [1]. SEM/EDX and EBSD were used to characterize the microstructure. The corrosion behavior was assessed using both *in vitro* and *in vivo* tests. Under cell culture conditions, electrochemical measurements and immersion tests were performed in supplemented Dulbecco's modified eagle medium. EDX and FTIR were used to determine the chemical composition of the corrosion products. The Mg-Ca-Zn-Y-Mn alloy's cytotoxicity and biocorrosion behavior was assessed through indirect and direct cell culture using murine fibroblast (L929) and osteosarcoma MG-63 cells. Finally, Mg-1Ca-0.5Zn-0.1Y-0.03Mn (at.%) (and pure Mg as a control) in the form of discs were surgically implanted in a calvaria bone defect on male Wistar rats (Permission nr. WAW/031/2024) for 7 and 28 days. The *in vivo* corrosion rate from the Mg retrieved implants will be calculated, and the corroded surfaces will be characterized by SEM/FIB/EDX.

RESULTS: When analyzing *in vitro* findings, the pH rose after 3d from ~7.9 to ~8.3 was observed, with a decrease after 7d to ~8.1. The osmolality of the supernatants increased (0.331 ± 0.01 Osmol/Kg) compared to the control medium (0.304 ± 0.001 Osmol/Kg) after 3 d of immersion. It was stabilized after 5 d to 0.384 ± 0.02 Osmol/Kg. The calculated corrosion rate by the mass loss method was 0.38 ± 0.21 mm/year. L929 cells were over 90% viable in 100%, 50%, and 25% Mg extracts in indirect cell culture (Fig 1a, b). Similarly, viable MG63 cells were observed on the Mg alloy surface after 7d of cell culture (Fig 1b, c), where the filopodia and cytoplasmic prolongations of the MG63 cells denoted the cell attachment and cell-cell communication. In addition, higher P and Ca content were observed in the

corrosion layer near the cells. These results allowed us to move forward with *in vivo* implantation to assess the Mg alloy using multimodal analysis (OCT, μ CT, and qualitative histology) when it encounters soft and bone structures (Fig. 1e).

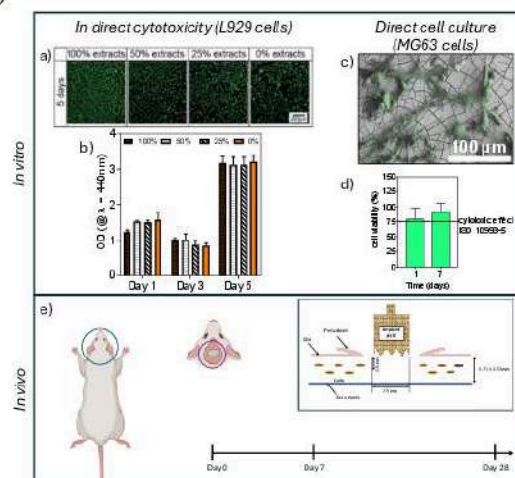


Figure 1: Representative images of the *in vitro* assessment (a-d) and the *in vivo* experimental design (e) to investigate the corrosion behavior of the Mg-1Ca-0.5Zn-0.1Y-0.03Mn (at.%) alloy.

DISCUSSION & CONCLUSIONS: The Mg-1Ca-0.5Zn-0.1Y-0.03Mn (at.%) alloy exhibited promising biocompatibility and corrosion resistance, with L929 and MG63 cells showing high viability and cell attachment. These properties, combined with the corrosion rate lower than 0.5 mm/year, indicate the alloy's potential for use as orthopedic implant material.

REFERENCES: [1] Y. Kawamura, F. Shimada, K. Hamada, S. Ueno, S. Inoue, Development of Biomedical Mg-1.0Ca-0.5Zn-0.1Y-0.03Mn (at.%) Alloy by Rapidly Solidified Powder Metallurgy Processing, *Mater. Trans.* 64 (2023) 2333-2336.

ACKNOWLEDGEMENTS: This research was conducted under the project "Development of Advanced Magnesium Alloys for Multifunctional Applications in Extreme Environments" No. V4-JAPAN/2/15/MagMAX/2022 financed by the National Centre for Research and Development in Poland in the framework of Visegrad Group (V4)-Japan Joint Research Program—Advanced Materials.



Long-term *in vivo* assessment of magnesium-based biodegradable screw-plate implants in a large-animal cranio-maxillofacial defect model

W Rubin¹, T Akhmetshina¹, AM Rich¹, J Ross², D Toneatti³, K Nuss², B Schaller³, JF Löffler¹

¹ *Laboratory of Metal Physics and Technology, Department of Materials, ETH Zurich, Switzerland*

² *Musculoskeletal Research Unit (MSRU), University of Zurich, Switzerland*

³ *Department of Cranio-Maxillofacial Surgery, University Hospital, Inselspital Bern, Switzerland*

INTRODUCTION: Lean magnesium–calcium based biodegradable metallic alloys (BMAs) have been studied in various pre-clinical settings¹⁻³ and present a promising alternative to permanent metallic implant materials for potential clinical use in traumatology. To further explore the efficiency of osteotomy stabilization using BMA-based screw-plate implants, a large-animal study with a cranio-maxillofacial defect model is being conducted over an extended time duration of 42 months. The study covers four different timepoints of sacrifice, ranging from two, six, and 24 months until complete material biodegradation. Initial results for the two- and six-months groups demonstrated promising outcomes for the Mg-based implants⁴. Here, complementary and extending data are presented up to its currently latest observation timepoint of 30 months.

METHODS: As described in Ref. [4], each animal received osteotomies with fully mobilized bone fragments located at the calvarial (CD) and zygomatic arc (ZAD) regions, representing mechanically non- and moderately loaded cranio-maxillofacial areas. The fragments were refixedated by screw-plate implants of (i) specifically designed plasma electrolytic oxidation (PEO)-coated ultra-high-purity Mg–Ca (UHP-X0) alloy implants, and (ii) standard titanium-based implants as a reference. Radiographic data on implant-volume loss, gas-cavity formation, and bone response was evaluated up to the latest time point.

RESULTS: All animals continued to show normal mastication behavior and remained healthy until sacrifice. The implants' volume loss was constant between 6 and 18 months with an average monthly loss of about 3.2% for both implantation sites. Volume-loss rates differed mainly within the first months and at later times for the non-loaded implantation site. Within the Mg group, the gas-cavity volumes peaked initially in weeks two and four and again at six to ten months. Both implantation sites yielded similar gas-cavity volumes when normalized to the implant surfaces. Gas cavities formed near the degrading implants and were also found in later degradation stages up to 30 months. Based on histology, the Mg group yielded bone-implant contact (BIC) at least as high as titanium in both defect areas (*Fig. 1*). Furthermore, new bone formation was higher in the Mg group, which peaked for both materials four weeks after implantation. The

moderately loaded osteotomies exhibited generally higher bone formation. Bone-density reduction near the Mg screws was found radiographically from the second week on and was confirmed by histomorphometry.

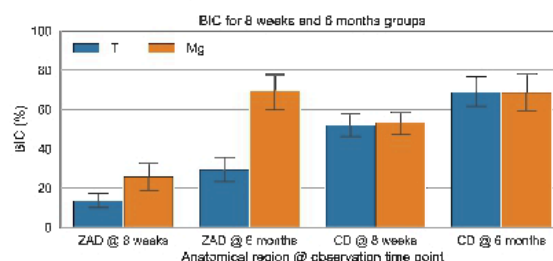


Fig. 1: BIC results for both materials and locations, for the 8-weeks and 6-months animal groups.

DISCUSSION & CONCLUSIONS: Implant volume loss was found to be nearly linear. The gas evolution fluctuations of the PEO-coated Mg samples within the first two months coincided with higher implant-volume losses. In contrast, the later gas-cavity volume increase was not reflected by respective degradation-rate variations. Around the Mg implants, signs of osteostimulative effects were seen, but bone resorption was also observed to some extent. First signs of bone-tissue resorption were observed around the Mg-based material in week two, when increased gas-volume formation was also measured. On the other hand, new bone deposition was found to start equally for both material groups from week four on and was consistently higher for the Mg group. The BIC was considerably higher for the Mg group than for the Ti reference for the moderately loaded osteotomies, possibly due to an induced mechanical stimulus. There are also various indications that the Mg-based material positively affects the local bone metabolism upon continuous implant degradation.

REFERENCES: ¹R. Marek et al. (2023) *Biomater. Adv.* 150:213417. ²L. Berger, et al., 14th Biometal Conf. (Aug. 2022), *Europ. Cells and Materials*, in press. ³P. Holweg et al. (2020) *Acta Biomater.* 113:646-659. ⁴W. Rubin et al., 15th Biometal Conf. (Aug. 2023), *Europ. Cells and Materials*, in press

ACKNOWLEDGEMENTS: The authors gratefully acknowledge financial support by the Swiss National Science Foundation (SNF Sinergia, Grant No. CRSII5-180367), and thank D-HEST at ETH Zurich for its support with the radiography measurements.



Evaluation of iron based bioresorbable flow diverters in the rabbit elastase induced aneurysm model

AA Oliver^{1,2}, C Bilgin¹, J Cortese¹, EA Bayraktar¹, YH Ding¹, D Dai¹, M Connon³, KD Carlson², AJ Griebel⁴, JE Schaffer⁴, D Dragomir-Daescu², R Kadirvel⁵, RJ Guillory II³, DF Kallmes¹

¹Radiology, ²Physiology and Biomedical Engineering, ⁵Neurosurgery, Mayo Clinic, Rochester, MN.

³Biomedical Engineering, Medical College of Wisconsin, Milwaukee, WI. ⁴Fort Wayne Metals, Fort Wayne, IN

INTRODUCTION: Flow diverters (FDs) are miniature braided stents used to treat intracranial aneurysms. Bioresorbable flow diverters (BRFDs) aim to serve their temporary function of occluding and healing the aneurysm before safely absorbing into the body. This may mitigate complications associated with the permanent presence of conventional FDs such as device induced thromboembolism, stenosis, and side branch occlusion [1]. In this work, we evaluate an iron based BRFD in the rabbit elastase induced aneurysm model.

METHODS: BRFDs and control FDs were 4.75mm diameter and 7mm length and were constructed from 48 braided, 25 μ m diameter wires. The BRFDs contained 36 bioresorbable FeMnN alloy (35% Mn, 0.15% N, balance Fe, by wt%) wires and 12 polyimide coated Ta wires to impart radiopacity. The control FDs were composed entirely of permanent 35NLT/Pt DFT wires. All wire components were manufactured by Fort Wayne Metals. BRFDs were deployed for 3 months (n = 7 rabbits) to treat aneurysms induced in the rabbit elastase model [2]. Digital subtraction angiography (DSA) and gross dissection microscopy were used to assess aneurysm occlusion. BRFDs and control FDs were deployed in the abdominal aorta for 3 (n = 7 rabbits) or 6 (n = 3 rabbits) months. MicroCT and hematoxylin & eosin (H&E) staining were used to assess the resorption rate and biological response, respectively, of the aortic implants.

RESULTS: The BRFDs failed to completely occlude the aneurysm in 6 rabbits (Figure 1). The BRFD completely thrombosed in one of the rabbits, resulting in the occlusion of both the parent artery and the aneurysm. MicroCT analysis determined that the volume of FeMnN alloy wires in BRFDs deployed within the aorta lost 61 \pm 14% and 83 \pm 13% (mean \pm standard error) of their initial volume after 3 and 6 months, respectively. H&E staining demonstrated that there was minimal stenosis in the control FDs and BRFDs at 3 and 6 months. No adverse tissue reactions were observed in any of the BRFDs in response to notable corrosion.

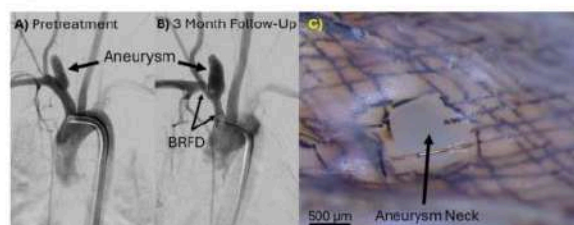


Fig. 1: DSA of the elastase induced aneurysm before (A) and 3 months after (B) BRFD deployment. (C) Gross dissection microscope image of the unoccluded aneurysm neck.

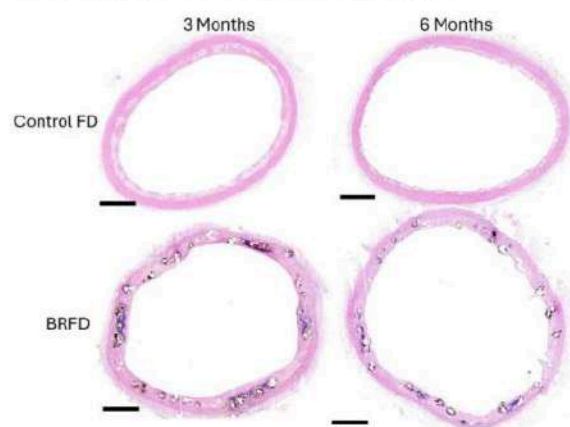


Fig. 2: Representative H&E stains of control FDs and BRFDs implanted in the rabbit aorta for 3 or 6 months. Scale bars are 500 μ m.

DISCUSSION & CONCLUSIONS: We believe rapid and localized corrosion resulted in BRFD wires fragmenting away from the aneurysm neck before they could become covered with neointima and occlude the aneurysm. The FeMnN wires corroded faster than anticipated, but their corrosion did not appear to elicit any adverse tissue responses. In conclusion, the FeMnN alloy appears to be safe in terms of localized toxicity in the arterial environment, but future work should focus on bioresorbable materials with slower, more uniform corrosion for the BRFD application.

REFERENCES: ¹A. Oliver, K. Carlson, C. Bilgin, et al (2023) *J Neurointerv Surg* **15.2**: 178-182. ²T. Altes, H. Cloft, J. Short, et al (2000) *Am J Roentgenol* **174.2**: 349-354.

ACKNOWLEDGEMENTS: Alexander Oliver is supported by the American Heart Association grant # 23PRE1012781.